dASPP and Boa regulate C-terminal Src kinase activity to control epithelial proliferation and integrity

Paul Francis Langton

Apoptosis and Proliferation Control Laboratory

London Research Institute

Cancer Research UK, London

A thesis submitted for the degree of

Doctor of Philosophy at the University of London

June 2008

ProQuest LLC
789 East Eisenhower Parkway
P.O. Box 1346
Ann Arbor, MI 48106-1346

Declaration by candidate:

I, Paul Francis Langton, declare that the work presented in this thesis is my own, except where acknowledged. I have acknowledged all quotations and results from the published or unpublished work of others.

ABSTRACT

Src-family kinases (SFKs) control a wide variety of biological processes, from cell proliferation and differentiation to cytoskeletal rearrangements. Abnormal SFK activation has been implicated in a wide variety of cancers and is associated with metastatic behaviour. SFKs are maintained in an inactive state by inhibitory phosphorylation of their C-terminal region by C-terminal Src kinase (CSK). In this study, *Drosophila* ASPP (dASPP) has been characterized and identified as a regulator of dCsk activity. dASPP is the homolog of the mammalian ASPP proteins, which are known to bind to and specifically stimulate the pro-apoptotic function of p53. dASPP is a positive dCsk regulator. Firstly, *dASPP* mutants show similar phenotypes to *dCsk* mutants, which are partially rescued by *dSrc64B* loss of function. Secondly, *dASPP* loss of function enhances the specific phenotypes of *dCsk* mutants in wing epithelial cells. Thirdly, dASPP physically interacts with dCsk to potentiate the inhibitory phosphorylation of dSrc42A. Taken together, these results suggest that dASPP has a role in maintaining epithelial integrity through dCsk regulation (Langton et al., 2007).

This work also provides the initial characterization of Boa (Binder of dASPP). Boa physically interacts with dASPP and is important for maintaining high levels of dASPP at the apical membrane. This may be achieved by regulating the stability or localization of dASPP. The data suggests that Boa is important for dASPP function as it also genetically interacts with dCsk. dASPP or Boa loss of function results in similar phenotypes, although there are important differences indicating that Boa has other roles besides dASPP regulation.

In another project, I have examined the transcriptional control of DIAP1 (*Drosophila* Inhibitor of Apoptosis 1) by the Ras pathway. Preliminary results suggest that the Ras pathway up-regulates DIAP1 transcription and this may be mediated by the Ttk69 transcription factor.

ACKNOWLEDGEMENTS

Firstly, I would like to thank my supervisor, Nic Tapon, for giving me the opportunity to work on such an interesting project, and for his expert guidance and support throughout my Ph.D. I would like to especially thank Julien Colombani for his invaluable collaboration on the dASPP project, for many helpful discussions and for critically reading my thesis. I would like to thank all of the members of the Tapon lab, past and present, for being fantastic colleagues and making my time at Cancer Research UK so enjoyable. In particular, thanks to Birgit Aerne, Ditte Andersen, Ruhena Begum, Alice Genevet, Filipe Josué and Cédric Polesello, whom I have known for the longest and have been great people to know. Thanks also to the new members of the lab, Eunice Chan, Tobias Maile and Michael Wehr, whom I am looking forward to working with over the following 6 months. Many thanks to my second supervisors Sally Leevers and David Ish Horowicz for useful discussions and advice; to Anne Weston of the E.M facility at Cancer Research UK; to Terrence Gilbank, Steve Murray and Frances Earl of the *Drosophila* facility at Cancer Research UK and to Peter Jordan of Light Microscopy.

Many thanks to my family and friends for their much-appreciated love and support. Finally, I would like to thank my love Taemi, she is the most special person I know and has always been there for me.

This work was funded by Cancer Research UK.

TABLE OF CONTENTS

LIST OF FIGURES

LIST OF ABBREVIATIONS

APF	After puparium formation
ASPP	Apoptosis-stimulating protein of p53
ATP	Adenosine triphosphate
Boa	Binder of dASPP
Bsk	Basket
Btk	Bruton's tyrosine kinase
C3	Caspase 3
CAS	CRK associated substrate
Cbp	CSK binding protein
Cdk	Cyclin dependent kinase
CHK	CSK homologous kinase
CRC	Colorectal cancer
CSK	C-terminal SRC kinase
Dlg	Discs-large
Dpp	Decapentaplegic
dCsk	*Drosophila* C-terminal SRC kinase
ECM	Extra-cellular matrix
EGF	Epidermal growth factor
EMS	Ethylmethane sulfonate
EMT	Epithelial to mesenchymal transition
EST	Expressed sequence tag
FAK	Focal adhesion kinase
FLP	FLPase
FRT	FLP recombination target
GFP	Green fluorescent protein
GMR	Glass multimer reporter
GST	Glutathione S Transferase
GTP	Guanosine triphosphate
Hid	Head involution defective
Hpo	Hippo
IAP	Inhibitor of apoptosis protein
IP	Immuno-precipitation
JNK	Jun N-terminal kinase
LATS	Large tumour suppressor
LOF	Loss of function
MAPK	Mitogen activated protein kinase

MARCM	Mosaic analysis with a repressible marker
Mats	Mob as tumour suppressor
MF	Morphogenetic furrow
MMP	Matrix metalloprotease
mw	mini-white
Nf2	Neurofibramatosis type-2
PBS	Phosphate buffered solution
PCR	Polymerase chain reaction
Phly	Phyllopod
PI3K	Phosphoinositide 3-kinase
PLP	Periodate-lysine-paraformaldehyde
Pnt	Pointed
Ptc	Patched
Puc	Puckered
RTK	Receptor tyrosine kinase
Sav	Salvador
SEM	Scanning electron microscopy
Sev	Sevenless
SFK	SRC family kinase
SH	SRC homology
Shg	Shotgun
Sina	Seven in absentia
SMW	Second mitotic wave
TNF	Tumour necrosis factor
Ttk	Tramtrack
UAS	Upstream activating sequence
UTR	Untranslated region
w	white
Wg	Wingless
Wts	Warts
Yap	Yes-associated protein
Yki	Yorkie

CHAPTER 1 Introduction

1.1 Introduction overview

As several broad topics are covered in this introduction I give here a brief overview to orient the reader and explain why each topic is being introduced. Firstly, I start out with a general introduction to *Drosophila* as a model system and discuss some of the techniques available to researchers. Secondly, I include a section about the control of growth (accumulation of mass) in *Drosophila,* as this is the main research interest of the lab. Thirdly, I provide a comprehensive introduction to the Hippo pathway. The majority of work in our lab is focused on understanding the Hippo pathway, which is a potent growth regulatory network in *Drosophila* and mammals. The Hippo pathway was the starting point for my project as I carried out a screen for novel components. Fourthly, I introduce Src-family kinases (SFKs) and their regulation in *Drosophila* and mammals. SFKs are introduced because I subsequently found that dASPP, which was identified in my screen, is likely to function upstream of SFKs rather than in the Hippo pathway. This is followed by an introduction to what is currently known about ASPP family proteins in mammals, which have been described as p53 regulators. Finally, I finish with a brief introduction to the Ras pathway in *Drosophila*, as I carried out a separate project investigating the transcriptional regulation of DIAP1 by the Ras pathway.

1.2 An introduction to *Drosophila melanogaster*

1.2.1 *Drosophila* as a model organism

Drosophila melanogaster, commonly known as the fruit fly, is small two-winged flies of the order diptera. *Drosophila melanogaster* is one of the major model organisms in biological research and has been studied for over a hundred years, yielding many advances in our understanding of genetics, disease, immunity, development and evolution. There are several reasons why *Drosophila* is such a valuable organism to

biologists. Firstly, they are small, easy and relatively inexpensive to maintain in the laboratory. Secondly, the generation time is short (10 days at 25°C), which allows for comparatively rapid genetic experiments. Thirdly, *Drosophila* has only 4 pairs of chromosomes, comprising one sex chromosome and three autosomes, facilitating mapping of loci of interest. Finally, recombination does not occur in males, this greatly facilitated the generation of early genomic maps as recombination events could be easily scored in females.

Further facilitating *Drosophila* research is the abundance of available resources including several large stock centres, online databases, and established protocols covering many techniques. The sequencing of the genome in 2000 has greatly advanced all aspects of research including comparative genomics and the identification of homologs of human disease related genes. *Drosophila* is a suitable system for the analysis of human disease related genes in a genetically tractable organism as 62% of such genes are conserved in the fly (Rubin et al., 2000). In addition *Drosophila* genetic transformation is now routine allowing the introduction of transgenes, and the development of many subsequent techniques.

1.2.2 The life cycle of *Drosophila melanogaster*

The *Drosophila melanogaster* life cycle (see figure 1) at 25°C is about 10 days from egg to adult, although this varies considerably with temperature, for example the life cycle at 18°C is about 19 days. Fertilised females can lay hundreds of eggs per day and in the wild they are laid onto rotting vegetation such as decaying fruit or fungus. The embryos develop over a period of 12-15 hours at 25°C before hatching as first-instar larvae. The larvae feed on the food source and increase in mass by about 400X during the 4-day larval growth phase. Moulting occurs at 24h and 48h after hatching, defining the second and third larval instars respectively, which are easily identified by the morphology of the mouth hooks. Roughly 5 days after egg laying (AEL) third-instar larvae leave the food source (the 'wandering' phase) in response to a pulse of the steroid hormone Ecdysone, and pupate. The pupal stage lasts a further 4.5-5 days and during this time the majority of larval tissues are broken down, one exception being the imaginal discs, which undergo extensive morphological changes and develop into adult

Figure 1: The *Drosophila melanogaster* life cycle. The life cycle of *Drosophila melanogaster* lasts about 10 days at 25°C. Embryos laid by fertilised females develop over a period of 12-15 hours before hatching. The larval phase of the life cycle lasts 4 days during which time larvae increase in mass by 400x. Moulting occurs at 24h and 48h, defining the second and third instar phases. Roughly 5 days after egg laying, larvae leave the food source and pupate. The pupal stage of the life cycle lasts another 4-5 days and during this time extensive morphological changes occur. After emerging from the pupal case female flies are receptive to mating attempts after about 8 hours. Image taken from Flymove: http://flymove.uni-muenster.de.

structures such as legs and wings. Upon completion of pupariation adult flies emerge and females are receptive to male mating attempts after about 8 hours.

1.3 Imaginal disc development

Imaginal discs are epithelial sheets that develop during the larval and pupal stages of the life cycle and undergo extensive morphological changes during pupariation to give rise to the adult organs. The eye-antennal disc and the wing disc (see figure 2) are the most frequently studied tissues and provide a system for the interrogation of many biological processes including tissue patterning, cell growth, proliferation, apoptosis, cell polarity and differentiation.

The eye-antennal disc develops from a group of roughly 20 cells allocated during embryonic development. The eye disc cells divide during the first and second larval instars giving rise to the majority of the cells that will form the adult eye. A differentiation front known as the morphogenetic furrow (MF) passes from posterior to anterior during the third larval instar (Held, 2002). Cells anterior to the MF actively and asynchronously proliferate, and those within the furrow are arrested in G1. Patterning begins as cells exit the MF with groups of cells forming evenly spaced preclusters, which will differentiate into photoreceptor cells (see figure 2 A). Non precluster cells posterior to the MF undergo a final, synchronous round of entry into S-phase, followed by staggered divisions, a phenomenon known as the second mitotic wave (SMW) (see figure 2 B). This precise temporal and spatial control of proliferation and differentiation makes the eye a good system in which to study these processes.

The wing imaginal disc initially contains roughly 40 cells, which actively proliferate during the larval stages to produce a tissue of about 50,000 cells. Cell division stops at the onset of pupariation, and adult structures such as the longitudinal veins and notum bristles differentiate. Wing discs are divided into discrete anterior and posterior compartments and signalling initiated at the boundary sets up a gradient of the Decapentaplegic (Dpp) morphogen, which promotes proliferation and is involved in patterning the disc. Cellular interactions initiated at the dorsal / ventral boundary establishes a perpendicular Wingless (Wg) gradient that is also crucial for wing

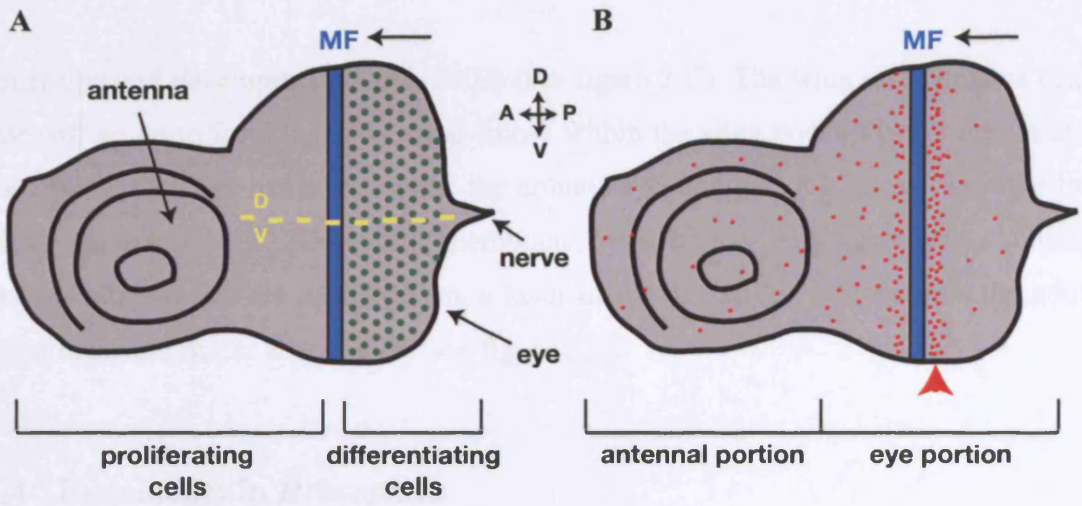

Figure 2: *Drosophila* eye and wing imaginal discs. (A and B) Schematics of third larval instar eye-antennal imaginal discs. During the third instar a wave of differentiation known as the morphogenetic furrow (MF) (blue region, arrow indicates direction of progression) sweeps across the eye disc from posterior to anterior. (A) Differentiation begins as cells exit the MF; groups of cells form evenly spaced preclusters, which will differentiate into photoreceptors (photoreceptor clusters in green). The position of the dorsal / ventral boundary is indicated. (B) A schematic showing the pattern of mitoses (dividing cells in red). Anterior to the MF, cells actively and asynchronously proliferate. Cells within the MF are arrested in G1. Uncommitted cells posterior to the MF undergo one final, synchronous round of S-phases, followed by staggered divisions, this is known as the second mitotic wave (SMW) (red arrowhead). (C and D) Schematics of third instar wing imaginal discs. Images taken and modified from (Butler, 2003). (C) Cells within the wing pouch (green) will form the adult wing. The hinge region (yellow) will form a structure that connects the wing to the body wall (blue). The anterior / posterior and dorsal / ventral boundaries are indicated. Signalling initiated at these boundaries has important roles in wing patterning. (D) A cross section through a wing disc along the anterior / posterior boundary indicating the three layers of cells: the peripodial membrane, the columnar epithelium, and the adepithelium.

patterning and development (Held, 2002) (see figure 2 C). The wing disc contains cells that will go on to form the adult wing (those within the wing pouch), hinge region and the notum. The disc has three layers: the columnar epithelium, which will become the adult epidermis; the peripodial membrane, which has important roles during metamorphosis, and the adepithelium, a layer of myoblasts that will become the adult flight muscles (Butler et al., 2003) (see figure 2 D).

1.4 P-elements in *Drosophila*

Transposable elements are pieces of DNA that can integrate into genomic DNA and have the ability to move around the genome by 'jumping' from location to location (Engels, 1992). Transposable elements are thought to constitute 10-20% of the *Drosophila melanogaster* genome. P-elements are just one family of transposable element found in *Drosophila*, they are roughly 2.9kb in length and consist of a four exon gene encoding the transposase enzyme and 31bp perfect inverted terminal repeats.

Interestingly, it is believed that P-elements have only recently become part of the *Drosophila* genome and were acquired by a horizontal transmission event from another *Drosophila* species. This is thought to have occurred less than 100 years ago as only laboratory stocks established in the early 1900s have escaped P-element invasion. In the wild, P-elements are ubiquitous and are thought to have rapidly spread through heredity and transposition (Engels, 1992). When P-elements jump to new genomic sites they leave behind a double strand DNA break, which is usually repaired by homologous recombination using the sister chromatid as a template. This replaces the original P-element with a copy form the sister chromatid, meaning that after transposition, one extra P-element copy is present in the genome. This is thought to be responsible for the rapid increase in P-element number observed when P-elements are introduced to M strains (those without P-elements) under experimental conditions (Good et al., 1989).

1.5 Genetic techniques in *Drosophila*

The identification of P-elements has allowed the development of many molecular and genetic techniques including the generation of transgenics, mutagenesis, analysis of gene expression patterns, clonal analysis and gene replacement.

1.5.1 Germline transformation using P-element vectors

One of the most important *Drosophila* genetic techniques developed is the generation of transgenic animals using P-elements as vectors (Rubin and Spradling, 1982; Spradling and Rubin, 1982). The gene of interest is inserted into the P-element sequence within a plasmid, which is microinjected into pre-blastoderm embryos in the presence of functional transposase. The P-element then transposes from the plasmid to a random chromosomal site. If the P-element integrates into the germline then a percentage of the progeny of the injected flies will be transformants. Screening for transformants is possible if a second gene containing a dominant marker, such as an eye colour marker, is also inserted into the P-element sequence prior to injection (Rubin and Spradling, 1982). The source of transposase may be genetically supplied by another transgenic insertion or supplied by co-injection of a transposase expressing helper plasmid. The ability to transform *Drosophila* allows the development of many subsequent techniques based on integration of DNA, some of which are described below.

1.5.2 Mutagenesis by P-element insertion

P-elements have been particularly useful tools for generating mutants; the insertion of a P-element into the region of a gene can result in a loss of function (LOF) phenotype. A sufficient number of single insertion P-element lines have been generated and are available such that one can obtain a P-element insertion near a gene of interest for most *Drosophila* genes (Bellen et al., 2004).

These collections were created by crossing a P-element bearing line to a transposase expressing line. The P-element is mobilised in the germline of the F1 progeny and the F2 generation is screened for flies with new insertions, and which lack the transposase-

expressing chromosome. The engineered transposase gene used to mobilize P-elements lacks the 2-3 intron (Δ 2-3), as the presence of this intron is known to be inhibitory to mobilization. The Δ 2-3 transposase is inserted within an element, which cannot itself transpose due to deletion of the terminal repeats (Robertson et al., 1988). The transposase-expressing chromosome is often also marked with a dominant marker such as *stubble* to allow it to be selected against in the F2 generation.

New insertions are identifiable if the P-element being mobilized contains an eye colour marker; the intensity of eye colour will depend on the local chromatin status and P-element copy number. New insertions may be mapped by inverse PCR whereby the genomic DNA is digested, circularised and sequenced using P-element specific primers (Sentry and Kaiser, 1994). This allows identification of the sequence flanking new P-element insertions and the identification of the disrupted gene.

1.5.3 Mutagenesis by imprecise P-element excision

Once a P-element near a gene of interest has been obtained it is possible to create further mutations in that gene by re-supplying transposase (Δ2-3) (Salz et al., 1987; Tsubota and Schedl, 1986). P-element stocks are normally generated in a *white (w)* mutant background and P-elements are marked with the *mini-white (mw)* gene, which gives an orange eye colour. When crossed to the transposase expressing line the F1 flies show an orange/white mosaic eye phenotype as the P-element is mobilising in the somatic and germ cells. The F1 flies are crossed to balancer stocks, which are chromosomes with large inversions to prevent homologous recombination and contain lethal mutations that prevent them from overtaking a stock. The F2 generation will contain mutant flies as a result of mobilisation of the P-element; males are crossed to balancer stocks to retain putative mutant chromosomes and then extracted from the cross and screened.

The F2 generation will contain various genotypes. Progeny that have orange eyes and thus retained the P-element insertion are discarded. Progeny that have white eyes have lost the P-element are kept for PCR screening. The majority of the white-eyed F2 generation will be the result of precise excision of the P-element where the surrounding

DNA is left in tact. However, a small proportion (roughly 2%, depending on the insertion site) will have deletions of the genomic DNA on either one or both sides of the insertion site. Using genomic primers that generate a PCR product spanning the P-element insertion site it is possible to recognise these imprecise excisions.

Precise excision events will give the expected PCR product size, as a deletion was not generated at the locus. Imprecise excision events will give one band of the expected size (from the balancer chromosome) and one band of reduced size corresponding to the size of the deletion. This band can then be extracted from the gel and sequenced to define the exact breakpoints. Imprecise excisions will only be recognisable using this method if the deletion breakpoints are within the range of the PCR primers used for screening. For technical reasons this limits the size of deletions that can be obtained by PCR screening to about 3kb, however P-elements have preferential insertion sites including in the promoters of genes, so often one needs only a small deletion to disrupt a gene. Once a mutant male has been identified by PCR, the cross to the balancer stock is kept and the offspring are mated *inter se* to obtain the mutant stock. It is also possible to generate large deficiencies between two P-elements located in *cis* on the same chromosome (Cooley et al., 1990).

1.5.4 Enhancer trapping to visualise expression patterns

Enhancer trapping is another technique that takes advantage of *Drosophila* transformation techniques. This involves mobilizing a P-element containing the LacZ gene under the control of a weak promoter and selecting single re-insertion lines. Enhancer elements present in the local chromatin near the reintegration site affect expression of the *LacZ* gene. Therefore this technique can be used to identify genes with interesting expression patterns during development (O'Kane and Gehring, 1987). One is example of an enhancer trap line is the *DIAP-LacZ* line used in this work (see figure 16), which contains a *P(lacZ)* insertion in the first intron of the *thread (th)* gene.

1.5.5 Generating mosaics in *Drosophila* tissues

Genetic mosaic techniques are widely used in *Drosophila* research and are highly useful in the analysis of genes during development. These techniques are particularly useful for studying the function of genes that result in embryonic or larval lethality when mutated. Inducing LOF of such genes in small areas (clones) bypasses the early lethality and the phenotype can be assessed (Perrimon, 1998). Genetic mosaics have also been used to answer questions about the cell autonomy of gene function and to trace cell lineages in tissues (Blair, 2003).

A commonly used method for generating mosaic flies relies on the site-specific recombination between FRTs (FLPase recombination targets) catalysed by expression of the yeast FLP recombinase (FLPase) (see figure 3). It was first shown that this system could be used in *Drosophila* in 1989; expression of FLP from one transgene could induce recombination between two FRTs flanking the *white* gene on another transgene, leading to mosaic eyes (Golic and Lindquist, 1989). P-elements containing FRTs have been inserted at the base of all major chromosomal arms to allow clonal analysis of about 95% of *Drosophila* genes (Xu and Rubin, 1993). A cell automomous marker is present distally to the FRT site to allow identification of clonal tissue (Xu and Rubin, 1993).

In order to generate clones of a mutation of interest one must first recombine the mutation onto a chromosome bearing an FRT site at the base of the chromosome arm. This recombinant is then crossed to a line containing the same FRT site and a distal cell marker (typically GFP or LacZ), as well as a transgene expressing FLP under the control of a heat shock promoter (Xu and Rubin, 1993). When a heat shock is applied to developing F1 animals, a mitotic recombination event occurs between the FRT sites in a small percentage of cells. This event can result (depending on chromosome segregation) in the production of one daughter cell, which is homozygous for the mutation and one daughter cell, which is homozygous for the cell marker (see figure 3). Therefore the homozygous mutant cells are marked by the absence of the cell marker. The surrounding cells that have not undergone recombination also express the marker, as they are heterozygous for both mutation and marker. Provided that the mutation is not cell lethal, the unmarked mutant cell divides and produces a clone, the phenotype of

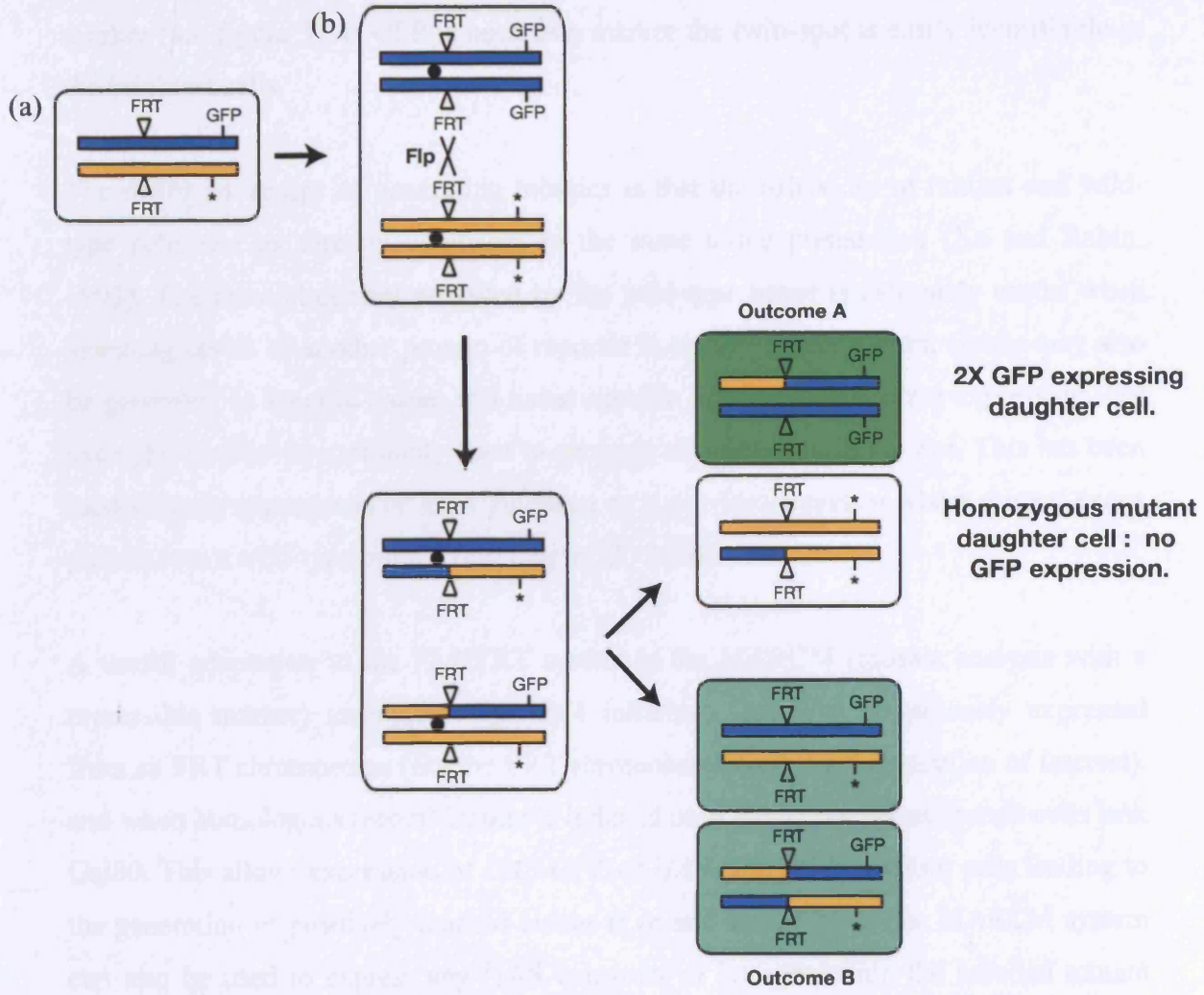

Figure 3: Generating mosaics by homologous recombination. Animals are generated that have the same FRT site on homologous chromosomes (a). One chromosome carries a ubiquitously expressed marker (such as GFP) distal to the FRT site. The other chromosome carries the mutation of interest (*) distal to the FRT site. Expression of *Flipase* (*Flp*) is induced by heat-shock or is under the control of a tissue specific promoter. Flp catalyses recombination between FRT sites on homologous chromosomes during interphase in a small percentage of cells (b). Following recombination, mitosis may lead to the generation of two homozygous daughter cells (outcome A). One daughter cell is homozygous for the marker; the progeny of this cell give rise to a clone called the twinspot that expresses 2X GFP. The progeny of the other daughter cell produces a mutant clone that is homozygous for the mutation of interest and does not express GFP.

which can be analysed at a later developmental stage. The marked sibling cell also divides to produce a clone known as the twin-spot, which expresses two copies of the marker (see figure 3). If GFP is used as a marker the twin-spot is easily identifiable as the brightest cells.

The major advantage of generating mosaics is that the behaviour of mutant and wild-type cells can be directly compared in the same tissue preparation (Xu and Rubin, 1993). The internal control provided by the wild-type tissue is extremely useful when assessing levels of another protein or reporter in mutant tissue. Mutant clones may also be generated in specific tissues if a tissue specific driver drives FLPase expression. For example, *ey-FLP* is commonly used to generate mosaics only in the eye. This has been used to study photoreceptor axon guidance as it provides a system where mutant axons project into a wild-type brain (Newsome et al., 2000).

A useful adaptation to the FLP/FRT system is the MARCM (mosaic analysis with a repressible marker) technique. The Gal4 inhibitor, Gal80, is ubiquitously expressed from an FRT chromosome (not the FRT chromosome carrying the mutation of interest), and when homologous recombination is induced only the homozygous mutant cells lack Gal80. This allows expression of *UAS-GFP* or *UAS-LacZ* in the mutant cells leading to the generation of positively marked clones (Lee and Luo, 1999). The MARCM system can also be used to express any UAS construct of interest within the labelled mutant clones (Blair, 2003).

1.5.6 The Gal4-UAS system for gain or loss of function analysis

Another *Drosophila* tool adapted from yeast is the Gal4-UAS system (see figure 4), which has been extensively used to study both over-expression phenotypes and LOF phenotypes. The Gal4-UAS system is a two-part system. One transgene expresses the Gal4 transcription factor under the control of specific promoters. Another transgene contains UAS (upstream activating sequences) sequences upstream of the gene of interest. When the two are bought together, Gal4 is expressed in a specific pattern and binds to the UAS sequences to drive expression of the genes of interest (see figure 4).

Figure 4: The Gal4-UAS system and the FLPout technique. (A) The Gal4-UAS system. Gal4 is expressed from one transgene. Gal4 expression may be under the control of endogenous enhancer elements or a specific promoter that is cloned upstream of the Gal4 coding sequence in a transposon vector. A second transgene contains UAS sequences placed upstream of *gene X*. Gal4 binds to the UAS sequences and drives expression of *gene X* wherever Gal4 is expressed. Figure adapted from (Perrimon, 1998). (B) The Flp-out technique: This method of mosaic analysis combines the Gal4-UAS system and the Flp-FRT system and is used to make positively marked clones that may be either loss of function or gain of function. The *Gal4* gene is separated from a constitutive promoter by two FRT sites and a 'stuffer' containing a transcription termination signal. Flp expression is usually induced by heatshock and catalyses recombination between the FRT sites in a small percentage of cells. This removes the 'stuffer' and Gal4 is expressed. Gal4 drives transcription of *gene X* and *GFP* and the descendants of these cells become the positively labelled gain of function clones. Loss of function clones may also be generated using this system by replacing *gene X* with an RNAi construct. Figure adapted from (Blair, 2003).

If a *UAS-GFP* or *UAS-LacZ* transgene is also present areas of gene expression can be marked (Brand and Perrimon, 1993).

Placing Gal4 under the control of different promoters allows for tissue specific expression of genes. This may be achieved by cloning the promoters of genes with known expression patterns upstream of the *Gal4* sequence or by enhancer trapping to place the *Gal4* transgene under the control of endogenous promoters. The Gal4-UAS system may also be used for LOF analysis either by expressing dominant negatives or by expressing RNAi constructs. The recent availability of a genome-wide library of transgenic stocks containing RNAi constructs under UAS control provides a novel platform for the analysis of gene function in specific tissues (Dietzl et al., 2007).

1.5.7 The FLPout technique can be used to positively mark clones

The FLPout technique combines the FLP/FRT system and the Gal4-UAS system and can be used to generate positively marked clones. FLPout constructs have been generated; the *Gal4* gene is separated from a constitutive promoter by a 'stuffer' comprising two FRT sites and a transcription termination codon (see figure 4). *Flp* expression is usually under the control of a heatshock promoter. When induced Flp catalyses recombination between the FRT sites leading to removal of the 'stuffer' in a small percentage of cells. This allows heritable *Gal4* expression in the descendants of these cells and expression of transgenes under the control of UAS sequences (see figure 4). *UAS-GFP* is usually present on the same chromosome as the FLPout construct allowing clones to be positively marked (Blair, 2003).

1.6 Control of growth in *Drosophila*

How the size of an animal or organ is determined is a fundamental question in developmental biology. For example, our arms develop independently but reach a near identical final size. This suggests that mechanisms exist to sense the size of organs during development and instruct them when to stop growing when appropriate. The size of an organ or animal is controlled by the relative contributions of three cell behaviours: cell proliferation, cell growth and cell death (Conlon and Raff, 1999). These processes

may be regulated by systemic or intrinsic cues and the importance of these different types of growth cues varies from organ to organ (Conlon and Raff, 1999).

1.6.1 Humoral control of growth

Drosophila growth (accumulation of mass) is controlled at both the humoral and intrinsic level. Humoral growth is regulated by a network of secretory tissues including the larval fat body, which is an endoreplicating tissue involved in fat and glycogen storage, the oenocytes, the ring gland and various neuronal populations The fat body senses nutrient availability using amino acid transporters (for example, Slimfast) and accordingly governs global insulin signalling and the growth rate of peripheral tissues (Colombani et al., 2003). This positive regulation of humoral growth by insulin signalling is antagonized by 20-hydroxyecdysone (ecdysone) signalling. Peaks of ecdysone levels are known to determine transitions between developmental stages. It was shown that ecdysone signalling also negatively regulates growth by affecting the localization of dFOXO, a negative regulator of translation that responds to levels of insulin signalling (Colombani et al., 2005). Interestingly, inhibiting Slimfast in the fat body results in a larval growth defect and a reduction in the size of endoreplicating tissues. However, the size of the mitotic imaginal discs is largely unaffected due to an extension of larval development time, suggesting that the growth of these tissues is less sensitive to nutrient conditions (Colombani et al., 2003).

1.6.2 Intrinsic control of growth

Similar to most mammalian organs, the growth of *Drosophila* imaginal discs is controlled largely by intrinsic signals from within the discs themselves. Several signalling pathways are implicated in controlling imaginal disc growth including the Decapentaplegic (Dpp), Wingless (Wg), Notch (N), Phosphoinositide 3-kinase (PI3K), Mitogen-activated protein kinase (MAPK), and Hippo (Hpo) pathways. Final disc size is determined by the combined action of these pathways and there is considerable crosstalk between them.

These pathways may regulate cell proliferation, cell growth, cell death or a combination of these processes to exert control over final disc size. Evidence supporting the existence of a sensor of organ size comes from studies showing that perturbation of one of these processes is not sufficient to alter final organ size. For example, accelerating proliferation in one compartment of the wing disc by expressing the cell cycle regulators *cyclinE* and *cdc25/string* does not lead to an increase in final compartment or wing size, rather the compartment contains more cells of a smaller size (Neufeld et al., 1998). In another example, cell death in the wing disc can be compensated for by increased proliferation, allowing apoptosis to be tolerated without affecting final disc size. It is thought that dying cells secrete the Wg and Dpp morphogens to induce compensatory proliferation of neighbouring cells (Huh et al., 2004; Perez-Garijo et al., 2004; Ryoo et al., 2004). If cell death pathways are stimulated but cells are simultaneously prevented from dying (by expression of the Caspase inhibitor p35) then considerable non-autonomous proliferation is observed (Huh et al., 2004; Perez-Garijo et al., 2004; Ryoo et al., 2004). These results show that proliferation, cell growth and cell death are tightly linked processes in developing organs and perturbation of one of these processes can be compensated for by the actions of another to maintain constant tissue size.

The organ size sensing mechanism can however be overridden by modulating pathways that control more than one of the processes affecting organ growth. For example, expression of activated Ras (Ras^{V12}) overrides size control mechanisms as Ras simultaneously drives cell division and cell growth, through regulation of dMyc and activation of PI3K signalling (Prober and Edgar, 2002). Ras also promotes cell survival by inhibiting the pro-apoptotic protein, Hid (Head Involution Defective) (Bergmann et al., 1998; Kurada and White, 1998). Additionally, loss of some members of the Hippo pathway, including Hippo itself, results in a dramatic increase in organ size. This occurs because Hippo signalling regulates proliferation, growth and apoptosis (Harvey and Tapon, 2007). Below, a general introduction to the cellular behaviours regulating organ growth will be given, with the exception of cellular growth, which is not relevant to the genes characterized in this work. In a later section (section 1.7) the effects of the Hippo pathway on these processes will be discussed, with emphasis on how the pathway may be part of the organ size sensing mechanism.

1.6.3 Proliferation

Cell division is the mechanism by which a mother cell gives rise to two daughter cells. For cell division to succeed, a cell must faithfully replicate its DNA and transmit a copy of the genome to each of the two daughter cells. Following division the daughter cells enter a growth phase, which must be completed before they can divide again. The cycle of growth, duplication and division is known as the cell cycle and the amount of time taken to complete the cell cycle varies from organism to organism. Eukaryotic cells have developed complex regulatory mechanisms dictating progression through the cell cycle. This ensures faithful replication as one stage of the cell cycle cannot proceed until the previous stages are complete (Malumbres and Barbacid, 2001). The same mechanisms can also prevent cells from dividing if they are damaged, thus ensuring that potentially harmful mutations are not passed on to daughter cells. The cell cycle regulation machinery enables cells to respond to extracellular signals (mitogens and nutrients) and divide accordingly, this is crucial for controlling cell numbers within tissues. Importantly, deregulation of cell cycle control is a necessary step for tumourigenesis.

1.6.3.1 The cell cycle and its regulators

The cell cycle consists of four main phases, G1 phase, S phase, G2 phase and M phase (see figure 5 A). During S phase the DNA is replicated, this phase lasts about 10-12 hours for a typical mammalian cell. M phase is much shorter, lasting about an hour, during which time the cellular contents are partitioned between the daughter cells, followed by cytokinesis. The G1 and G2 phases that separate S phase and M phase allow time for cell growth so that cell size within a population in constant (Malumbres and Barbacid, 2001). These phases also allow time for cells to assess whether intracellular and extracellular conditions are suitable before committing to division. During G1 the cell will receive both positive and negative inputs from cell cycle control pathways and the balance of these inputs determines whether it divides. If conditions are unfavourable, cells can delay entry into S phase or even enter a quiescent state (G0) and resume the cell cycle some time later (see figure 5 A). Cells can also arrest in G1 or G2 in response to DNA damage, allowing DNA repair to take place and preventing

Figure 5: Cyclin-Cdk complexes regulate the cell cycle. (A) A simplified schematic of a typical eukaryotic cell cycle and some of its regulators. The cell cycle can be divided into four stages. During S-phase, the cell replicates its DNA content. During M-phase the cellular components are partitioned between two daughter cells and cytokinesis occurs. S-phase and M-phase are separated by two 'gap' phases, G1 and G2, during which time cells receive both extracellular and intracellular signals that regulate progression to the next stage. Many such signals determine the activity of Cyclin-Cdk complexes, central players in the cell cycle control machinery. The G1 to S-phase transition is highly regulated and progression requires the activities of CyclinD-Cdk4/6 and CyclinE-Cdk2 complexes. Entry into M-phase requires the activity of CyclinB-Cdk1 complexes, which are positively regulated by the Cdc25 (String in *Drosophila*) phosphatase. Schematic modified from (Malumbres, 2005). (B) An example of how extracellular growth factors (mitogens) influence the cell cycle. The proto-oncogene, c-Myc, is a target of the EGFR/Ras pathway and promotes entry into S-phase by several mechanisms. c-Myc ultimately leads to increased CyclinD-Cdk4/6 and CyclinE-Cdk2 activity, which phosphorylate pRb and promote E2F release. Liberated E2F then upregulates expression of genes required for DNA replication. Schematic adapted from (Zornig, 1996).

potentially harmful mutations from being passed on to their progeny. Another checkpoint exists in M phase and prevents cytokinesis if chromosome segregation has not been completed.

Central players in the cell cycle control system are the Cyclin-dependent kinases (Cdks) (Malumbres and Barbacid, 2005) (see figure 5A). When active, Cdks phosphorylate target proteins involved in controlling crucial cell cycle steps such as DNA replication or mitosis. Cdks only become activated at the relevant stage of the cell cycle and this activity is regulated by the abundance of their binding partners, the Cyclins (Morgan, 1997). Expression of Cyclins oscillates during the cell cycle ensuring that Cdks are only active at the relevant stage. For example, the expression of S phase specific Cyclins, such as Cyclin E, is induced during late G1. This allows for the assembly and activation of Cdk-Cyclin complexes, which act on proteins controlling entry into S phase. Once S phase is initiated these Cyclin molecules are degraded. Similar cyclic expression and degradation is observed for the M phase-specific Cyclins.

In addition to their regulation by the abundance of Cyclins, Cdks are regulated by phosphorylation and by binding of other proteins. For example, the Wee1 kinase and the Cdc25 phosphatase regulate Cdks that control entry into M phase, through inhibitory Cdk phosphorylation. The binding of proteins such as p21 and p27 inhibits the Cdk-Cyclin complexes controlling entry into S phase (Morgan, 1997) (see figure 5 A). The activity of Cdks is highly regulated, allowing inputs from several different signalling pathways to be processed and ensuring that cells only divide when necessary.

Complex regulatory mechanisms exist to control the activity of Cdk4/6-CyclinD complexes and Cdk2-CyclinE complexes, which promote progression from G1 to S phase (Malumbres and Barbacid, 2005). These Cdk-Cyclin complexes act to relieve inhibition of a transcription factor called E2F, which transcribes genes required for S phase entry. In non-dividing cells E2F is bound to Retinoblastoma protein (Rb) and inactive. When cells are instructed to divide, Cdk4/6-CyclinD and Cdk2-CyclinE complexes are activated and hyperphosphorylate Rb; E2F is released and can transcribe target genes (Morgan, 1997). Several positive feedback mechanisms exist to ensure that S phase is robustly initiated once E2F is liberated, for example E2F activates its own transcription and that of CyclinE (see figure 5 B).

1.6.3.2 Mitogens regulate cell cycle progression

One important pathway positively regulating cell division is the MAPK (Mitogen activated protein kinase) pathway. This pathway responds to extracellular signals (mitogens), and transmits signals to the nucleus that regulate the cell cycle control machinery. Typically, mitogen signalling promotes cell cycle progression by regulating the G1 to S phase transition. Certain mitogens, such as Platelet-derived growth factor (PDGF) and Epidermal growth factor (EGF), can stimulate proliferation of a wide variety of cell types, whereas others are more specific. Mitogens bind to receptor tyrosine kinases (RTKs) leading to their activation and the initiation of downstream signalling events. The small GTPase Ras proteins are heavily implicated in the signalling events downstream of RTK activation. When GTP bound, Ras proteins activate a MAP kinase cascade that ultimately leads to MAPK activation, which enters the nucleus and phosphorylates target genes. Several transcription factors are targeted by MAPK and this affects the transcription of genes that regulate entry into S-phase.

One consequence of mitogen stimulation is increased transcription of *c-Myc* proto-oncogene. c-Myc can promote entry into G1 by several mechanisms (see figure 5 B). Firstly, it increases transcription of *CyclinD* leading to formation of Cdk4/6-CyclinD complexes (Daksis et al., 1994), a necessary step in the G1 to S phase transition. Secondly, c-Myc increases transcription of *cul-1*, a gene encoding a subunit of the SCF ubiquitin ligase (O'Hagan et al., 2000). SCF is responsible for degrading the Cdk2-CyclinE inhibitory protein p27, and thus promotes S phase entry. Lastly, c-Myc directly regulates the transcription of the *cdc25* gene, which produces a phosphatase that activates Cdk2 and Cdk4 (Zornig and Evan, 1996). This example illustrates how mitogens can influence cell division, though the complete picture is vastly more complex. Cell division is also regulated by intracellular signals including by adhesion molecules, damage sensing pathways and metabolic pathways. A more detailed description of the EGFR-Ras mitogenic signalling pathway in *Drosophila* is given in a later section (section 1.11).

1.6.4 Apoptosis

Apoptosis is a type of cell death, which plays vital roles during both the development and adult life of animals (Hay et al., 2004). Apoptosis may be triggered by intracellular or extracellular cues, which ultimately lead to the activation of proteases called Caspases. Caspase activation beyond a certain threshold leads to the irreversible death of a cell. Several morphological changes occur during apoptosis, including cell shrinkage, loss of contact with neighbouring cells, chromatin condensation and membrane blebbing. These features are a consequence of the cleavage of Caspase targets including proteins involved in DNA fragmentation (for example, Inhibitor of Caspase activated DNase) (Nagata, 2005) and cytoskeletal regulation (for example, beta-catenin) (Van de Craen et al., 1999). Eventually apoptotic cells form compact structures known as apoptotic bodies, which are subsequently engulfed by phagocytes or neighbouring cells. Consumption by other cells prevents the damage to surrounding cells and inflammation associated with necrosis, another form of cell death.

One function of apoptosis during development is to shape organs, for example cell death is responsible for creating the gaps between the digits of vertebrate limbs (Zuzarte-Luis and Hurle, 2002). Another function is to remove excess cells such as the supplementary neurons generated during development of the vertebrate nervous system. Tissues that are no longer needed may also be destroyed by apoptosis, such as the amphibian tadpole tail (Meier et al., 2000a).

In adults, the balance between cell division and apoptosis is instrumental in regulating organ size (Hay et al., 2004). Apoptosis also provides a protection mechanism that prevents the propagation of abnormal or damaged cells. For example, cells infected by pathogens or those with damaged DNA are eliminated and tissue integrity is maintained. Apoptosis is tightly linked to the cell cycle and can be utilised to remove cells that are dividing aberrantly. This is an important cellular defence against cancer and suppression of cell death is a necessary step for oncogenic transformation. Conversely, inappropriate apoptosis can lead to disease; it is a feature of neurodegenerative disorders and compromises the immune system in patients with AIDS (Hay et al., 2004).

1.6.4.1 The cell death machinery

Many of the molecules required for cell death were identified in the nematode, *C.elegans*. Of the 1090 cells generated during *C.elegans* development, invariably 131 are eliminated by apoptosis. Screening for mutations that alter the number of cells dying during development identified the *C.elegans* Caspase (CED-3), its adaptor (CED-4) and the CED-4 inhibitor (CED-9) (Meier et al., 2000a).

The cell death machinery is conserved in *Drosophila* but is more complex, with 7 identified Caspases. When the apical Caspase DRONC becomes activated, it cleaves and activates effector Caspases such as DRICE, which execute the apoptotic program (Hay et al., 2004) (see figure 6). In mammals 14 Caspases have been identified and include the apical Caspases 8 and 9, and the effector Caspases 3 and 7 (Hay et al., 2004). Apoptosis can occur in the absence of gene transcription and is controlled by the post-translational regulation of Caspases. Caspases are expressed as inactive precursors, which become activated following death stimuli. Active Caspases cleave substrates, including other Caspases, at aspartic acid residues, leading to an amplification of the cell death signal.

In *Drosophila* and mammals Caspase activity is kept low by IAPs (Inhibitor of Apoptosis Proteins), which bind to and inhibit both apical and effector Caspases by several mechanisms (Hay et al., 2004). Expression of DIAP1 (*Drosophila* Inhibitor of Apoptosis 1) is able to block cell death phenotypes induced by expression of Caspases (Meier et al., 2000b). Furthermore, loss of DIAP1 induces cell death in many different contexts, highlighting its crucial role as an apoptosis inhibitor (Hay and Guo, 2006). The mechanisms by which DIAP1 inhibits Caspases are complex and still under investigation. DIAP1 has been shown to bind to the apical Caspase DRONC, and mediate DRONC ubiquitination and inactivation (Wilson et al., 2002). DIAP1 also ubiquitinates itself, leading to its proteasome-mediated degradation. DIAP1 stability is also controlled by the Caspases themselves via and N-terminal cleavage event, which exposes an asparaginyl (Asn) residue targeted by the 'N-end rule' degradative pathway (Ditzel et al., 2003). Paradoxically, the short half life of DIAP1 (~30 minutes) appears to be crucial to its ability to block cell death, leading to the hypothesis that DIAP1 degradation concurrently leads to degradation of bound Caspases such as DRONC

Figure 6: Caspase dependent cell death in *Drosophila*. Pro-apoptotic proteins are in red/orange and anti-apoptotic proteins are in blue. DIAP1 is crucial for keeping Caspase activity low and does so by inhibiting both apical Caspases such as Dronc and effector Caspases such as Drice (the Caspase 3 homolog). The pro-apoptotic Hid, Grim and Rpr proteins bind to and inhibit DIAP1. Binding of Rpr to DIAP1 also leads to dTraf1 stabilization, and subsequent activation of the JNK pathway. Rpr and Grim can also promote apoptosis independently of DIAP1 though global inhibition of translation. Hid pro-apoptotic activity is negatively regulated by the EGF/Ras pathway and positively regulated by the Hippo signalling via Yki and the microRNA *bantam*. Rpr induces cell death in response to Ecdysone and cellular stresses such as DNA damage - the Rpr promoter contains a p53-binding site. Figure adapted from (Hay, 2006).

(Ditzel et al., 2003). DIAP1 can also prevent apoptosis by inhibiting TRAF1, which functions upstream of the JNK signalling pathway (Hay et al., 2004) (see figure 6).

Apoptosis in *Drosophila* is commonly induced by the Hid, Grim, Reaper proteins, which can bind to DIAP1 and displace bound Caspases thus relieving their inhibition (Hay et al., 2004) (see figure 6). It seems that Hid, Grim and Rpr can also reduce DIAP1 protein levels through distinct alternative mechanisms. Hid binding stimulates DIAP1 self-ubiquitination and degradation, whereas Rpr and Grim induce DIAP1 downregulation by another mechanism. This activity does not require DIAP1 ubiquitin ligase activity and in the case of Grim may be through a general suppression of translation (Yoo et al., 2002). A deficiency (H99) removing the *hid*, *grim* and *rpr* genes blocks nearly all cell death in the *Drosophila* embryo, suggesting the proteins they encode are essential death regulators (White et al., 1994). Hid, Grim and Rpr themselves are subject to regulation by several different signalling pathways. For example, their translation is subject to control by micro-RNAs including the Hippo pathway target *bantam*, which represses Hid translation (Brennecke et al., 2003; Nolo et al., 2006; Thompson and Cohen, 2006). Further, Hid is negatively regulated by the MAPK signalling pathway via phosphorylation and transcriptional control (Bergmann et al., 1998; Kurada and White, 1998) (see figure 6).

1.6.4.2 The intrinsic cell death pathway

In mammals, the apical Caspase 9 (functionally equivalent to *Drosophila* DRONC) is positively regulated by its adaptor protein APAF-1. Activation of APAF-1 and Caspase 9 is regulated by the actions of pro-apoptotic Bcl2 family members such as Bax and Bak. Death-inducing signals can lead to Bax and Bak mediated mitochondrial membrane permeabalization and release of Cytochrome c. Cytochrome c then associates with APAF-1 and promotes the aggregation and activation of Caspase 9 molecules, leading to the formation of a complex known as the apoptosome (Hay et al., 2004). This pathway is sometimes referred to as the intrinsic pathway as it is mediated by signals from within the cell. The intrinsic pathway may be activated following cellular stresses, which compromise the integrity of the mitochondrial membrane. For example, DNA

damage leads to p53 activation and subsequent transcriptional upregulation of the Bcl2 family member Bax (Samuels-Lev et al., 2001).

Although some of the components of the intrinsic pathway are conserved in *Drosophila*, the relationship between them is far from understood. *Drosophila* has an APAF-1 homolog called dARK, which functions in an analogous manner as an adaptor of DRONC. *Drosophila* also has Bcl2 family members, DEBCL and Buffy, but it is not clear whether they function to activate dARK (Hay et al., 2004) (see figure 6). The role of Cytochrome c in *Drosophila* apoptosis remains controversial. Cytochrome c was shown to be dispensable for Caspase function and apoptosis in *Drosophila* cells and *in vivo* (Dorstyn et al., 2004). However, it is also reported that one of the *Drosophila* Cytochrome c genes, *cyt-c-d*, is required for Caspase activation during spermatid differentiation (Arama et al., 2006) and for developmental apoptosis in the pupal retina (Mendes et al., 2006). Taken together, the data suggests that an intrinsic pathway does exist in *Drosophila*. In support of a mitochondrial role in *Drosophila* apoptosis it was recently shown that Hid and Reaper localize to the mitochondria and bring about membrane permeabalization (Abdelwahid et al., 2007).

1.6.4.3 The extrinsic cell death pathway

Mammalian and *Drosophila* cell death may also be induced by the extrinsic pathway, which responds to death stimuli coming from outside the cell. For example, mammalian lymphocytes can kill cells by expressing the TNF ligand, Fas, which binds to tumour necrosis factor (TNF) receptors on the target cell. Ligand binding causes the recruitment and aggregation of various intracellular adaptor proteins and inactive pro-Caspase 8 molecules. Following recruitment, Caspase 8 molecules are cleaved and go on to initiate the Caspase cascade in the target cell. *Drosophila* possesses a single TNF ligand homolog, Eiger, which is a potent inducer of cell death. In contrast to the mammalian extrinsic pathway Eiger does not induce apoptosis through the Caspase 8 homolog, DREDD, but instead activates the Jun-N-terminal kinase (JNK) pathway to induce apoptosis (Moreno et al., 2002).

1.7 An introduction the Hippo signalling pathway

1.7.1 Discovery of a novel pathway controlling *Drosophila* growth

During development, cell proliferation, apoptosis and cell size must be tightly regulated in a coordinated manner to ensure that organisms reach the correct final adult size. A fundamental question in developmental biology is: how do organs stop growing when they reach the appropriate size? *Drosophila* adult organs such as the eyes, wings and legs are derived from imaginal discs; small epithelial sacs, which develop during the larval and pupal stages of the life cycle. The Hippo signalling pathway (see figure 7), recently identified in *Drosophila melanogaster*, acts to restrict the size of imaginal discs and organs by carrying out the dual functions of promoting apoptosis and exit from the cell cycle (Harvey and Tapon, 2007). LOF mutations in upstream 'core' Hippo pathway components lead to severely overgrown adult structures, therefore the Hippo pathway is part of the mechanism that limits the size organs can reach.

The Hippo pathway was first identified in clonal screens for overgrowth phenotypes, which were carried out by several different groups. These screens involved randomly mutagenising chromosomes carrying FRT recombination sites, generating homozygous mutant clones in the eye and screening F1 adults visually for aberrations that give mutant tissue (marked white) a growth advantage over wild-type tissue (marked red). One benefit of screening for overgrowth genes in this way is that mutations in tumour suppressor genes are often lethal at an early stage, precluding analysis of the phenotype in adults. This lethality is bypassed by generating clones of mutant tissue in a non-essential organ such as the eye.

1.7.2 The 'core' components of the Hippo pathway

1.7.2.1 Warts / Lats (Wts)

The first member of the Hippo pathway to be identified was Warts / LATS (Wts) (see figure 7), which was recovered in a screen for overgrowth phenotypes in mosaic animals with clones of X-ray or P-element induced mutations (Justice et al., 1995; Xu et

al., 1995). Loss of *wts* in clones causes severe overgrowth phenotypes in imaginal discs and epithelial tumours in the corresponding adult structures (Justice et al., 1995; Xu et al., 1995). In *Drosophila* Wts and Tricornered (Trc) are members of the nuclear DBF2-related (NDR) family of serine/threonine kinases. Trc is not a growth regulator but instead functions to regulate Furry (Fry) and this interaction is required for normal wing hair development (He et al., 2005) and dendritic tiling (Emoto et al., 2004). Much of what is known about NDR kinases comes from studies in yeast, which show that NDR kinases, including the Wts homolog Dbf2, play roles in the mitotic exit network and cytokinesis (Hergovich et al., 2006). The human genome encodes 4 NDR family kinases; NDR1, NDR2, LATS1 and LATS2. The functions of mammalian NDR1 and NDR2 are not clear but mammalian LATS1 functions analogously to Wts as a tumour suppressor; LATS1 deficient mice develop ovarian and soft tissue tumours (St John et al., 1999).

1.7.2.2 Salvador / Shar-pei (Sav)

Several years later Salvador (Sav) / Shar-pei (Shrp) was identified in clonal screens for EMS induced mutations that cause overgrowth of mutant tissue in the eye (Kango-Singh et al., 2002; Tapon et al., 2002) (see figure 7). The main findings of these studies will be summarized below, as they were the first comprehensive analysis of the characteristic Hippo pathway phenotype.

sav clones induced in the eye, notum or haltere display tumour-like outgrowths of tissue. Interestingly, it was shown that clones of *sav* cells in the eye contain many more inter-ommatidial cells than wild-type tissue and this abnormal cell number results from both delayed cell cycle exit and reduced apoptosis (Kango-Singh et al., 2002; Tapon et al., 2002).

In wild-type discs, a synchronous, final round of S-phases followed by staggered divisions occurs posterior to the MF. This is known as the second mitotic wave (SMW) and very little proliferation occurs posterior to the SMW. In *sav* mutant cells ectopic cell division is visualised posterior to the SMW using BrdU labelling to mark cells in S-phase. This data suggests that *sav* mutant cells do not exit from the cell cycle in a timely

Figure 7: The *Drosophila* Hippo signalling pathway. The Hippo pathway was identified in *Drosophila* and is an important regulator of tissue size. The Hippo pathway negatively regulates the size of organs by carrying out the dual functions of promoting apoptosis and exit from the cell cycle. The 'core' components of the pathway are in red and consist of the kinases Hpo and Wts, their adaptor proteins Sav and MATS, and the transcriptional co-activator Yki. Hpo phosphorylates Wts, which in turn phosphorylates Yki leading to its exclusion from the nucleus. Yki binds to as yet unidentified transcription factor(s) (X) to promote the expression of *cyclinE*, *DIAP1*, *bantam*, *merlin* and *expanded*. Expanded and Merlin function upstream of Hpo but the mechanism by which Hpo is activated remains elusive. The atypical Cadherin Fat functions in the Hippo pathway, it is thought that Fat is required for Expanded membrane localization. Fat has also been proposed to regulate Wts protein levels by inhibiting Dachs. RASSF antagonizes the pathway by competing with Sav for binding to Hpo. Figure adapted from (Harvey, 2007).

fashion leading to ectopic cell divisions. Furthermore *sav* mutant cells were found to contain elevated levels of cyclinE, a critical regulator of entry into S-phase (Kango-Singh et al., 2002; Tapon et al., 2002).

In wild-type eyes, an excess of inter-ommatidial cells are generated during development and these are eliminated by a burst of apoptosis between 24 and 40 hours APF (after puparium formation). In pupal retinas containing *sav* clones, apoptosis is largely confined to the wild-type tissue suggesting that *sav* is required for developmental apoptosis (Kango-Singh et al., 2002; Tapon et al., 2002). In agreement with *sav* acting as a pro-apoptotic gene, levels of DIAP1, the *Drosophila* Inhibitor of Apoptosis, are elevated in *sav* clones (Tapon et al., 2002). Taken together this suggests that the excess inter-ommatidial cell number in *sav* mutant cells is due to both delay in exit from cell cycle and reduced apoptosis.

Tapon et al. also made a connection between *sav* and *wts*, two genes now known to encode members of the Hippo pathway. Further analysis of *wts* mutant cells showed that, like *sav* mutant cells, *wts* clones show excess inter-ommatidial cells, BrdU incorporation posterior to the furrow and reduced apoptosis at 38h APF. Additionally, co-expression of *sav* and *wts* gives a stronger phenotype than expression of each alone. A physical interaction between Sav and Wts was also observed; the WW domain of Sav is capable of binding to Wts (Tapon et al., 2002).

1.7.2.3 Hippo (Hpo)

Hippo (Hpo) (see figure 7) was also identified in mosaic screens and *hpo* mutant clones have similar phenotypes to *wts* or *sav* clones, namely, excess inter-ommatidial cells, increased cyclin E and DIAP1 levels and proliferative advantage over wild-type cells (Harvey et al., 2003; Pantalacci et al., 2003; Udan et al., 2003; Wu et al., 2003). Hpo is a serine/threonine kinase of the Sterile-20 group and the *Drosophila* ortholog of human Mst1 and Mst2. Mammalian Mst1 and Mst2 have been shown to have roles in promoting apoptosis through phosphorylation of histone H2B (Cheung et al., 2003) and FOXO transcription factors (Lehtinen et al., 2006). Recently a role for Mst1 and Mst2

in the mammalian Hippo pathway has been confirmed (Chan et al., 2005; Dong et al., 2007).

Hpo shows strong binding to Sav by co-immunoprecipitation and yeast two-hybrid (Pantalacci et al., 2003; Udan et al., 2003; Wu et al., 2003) suggesting that Hpo can complex with Sav. Hpo and Sav interact via their C-terminal regions; in two-hybrid studies the C-terminus of Hpo binds to the C-terminus of Sav (Wu et al., 2003). Moreover, in-vitro translated C-terminal domains of Sav and Hpo can bind by co-immunoprecipitation (Udan et al., 2003). It is now known that the C-terminal region of Hpo and Sav contains a unique 30-40 amino acid coiled-coil domain known as the SARAH domain (Scheel and Hofmann, 2003), which is crucial for binding of Hpo to either Sav or RASSF (Polesello et al., 2006) (See below).

When Hpo and Sav are co-expressed, a Sav mobility shift is observed suggesting that Sav is a phosphorylation target of Hpo. In support of this notion the mobility shift can be suppressed by phosphatase treatment (Pantalacci et al., 2003; Wu et al., 2003). Binding to Hpo stabilises Sav protein levels but this is not a consequence of phosphorylation as kinase-dead Hpo also stabilizes Sav (Pantalacci et al., 2003).

Hpo is also able to phosphorylate Wts in kinase assays and co-transfection of Hpo and Wts in S2 cells leads to a Wts bandshift. Interestingly this bandshift is greater in the presence of Sav suggesting that Sav functions to enhance Hpo kinase activity (Wu et al., 2003). Therefore, Sav and Hpo function upstream of Wts; Sav binds to Hpo and this interaction promotes signalling to Wts.

Hpo also phosphorylates DIAP1 in *in-vitro* kinase assays presumably leading to downregulation of DIAP1 protein levels (Harvey et al., 2003; Pantalacci et al., 2003). However, another group provided evidence that regulation of DIAP1 by Hpo is also transcriptional by examining the response of a DIAP1 transcriptional reporter (*DIAP-LacZ*) in *hpo* mutant tissue (Wu et al., 2003).

1.7.2.4 Mob as tumour suppressor (Mats)

Mob as tumour suppressor (Mats) (see figure 7) also functions in growth regulation and Mats mutant clones show characteristic Hippo pathway phenotypes. Mats is able to physically associate with Wts and this increases the kinase activity of Wts (Lai et al., 2005). It was recently shown that Mats functions downstream of Hpo genetically. Mats is a phosphorylation target of Hpo and that this phosphorylation increases its affinity for Wts (Wei et al., 2007). The *S.cerevisiae* homolog of Mats (Mob1p) is an important regulator of the mitotic exit network kinase Dbf2p, the homolog of Wts, suggesting that the interaction between Mats and Wts is evolutionarily conserved (Hergovich et al., 2006).

In summary, these findings indicate that Wts, Sav, Hpo and Mats function in the same signalling pathway and are required to limit organ growth. Hpo binds to its adapter Sav and this interaction promotes the phosphorylation of Wts and Mats. Wts phosphorylates target proteins. As Wts is downstream of Hpo and Sav it could integrate signals from other pathways, which offers an explanation for its stronger LOF phenotype.

1.7.2.5 Yorkie (Yki)

Yorkie (Yki) (see figure 7) is a transcriptional co-activator and functions downstream of Wts in the Hippo pathway (Huang et al., 2005). The discovery of Yki was important in the field as it provided a link between Hpo signalling and transcriptional control and is to date the most downstream 'core' component of the pathway. Yki was identified in a yeast 2-hybrid screen for Wts interactors and is homologous to the mammalian Yes-associated proteins (YAP1 and YAP2). Interestingly *yki* has the opposite phenotype to *wts*, *sav*, *hpo* or *mats* in that over-expression of *yki* results in similar overgrowth phenotypes to LOF of other Hippo pathway components (Huang et al., 2005). Conversely, only small *yki* LOF clones can be recovered and these clones are negative for *DIAP-LacZ*. This provides further evidence that the Hippo pathway can regulate DIAP1 at the transcriptional level (Huang et al., 2005).

Several lines of evidence place Yki downstream of Hpo and Wts. Firstly, in a cell-based assay, the activity of Yki as a transcriptional co-activator is suppressed by co-expression of Hpo, Sav and Wts. Secondly, Yki is epistatic to Hippo pathway components. For example, *yki hpo* double mutant clones are phenotypically similar to *yki* clones (small) rather than *hpo* clones (large). Thirdly, Yki is phosporylated by Wts and the observed Yki mobility shift is enhanced in the presence of Hpo and Sav (Huang et al., 2005). This is an inhibitory phosphorylation as signalling from Wts reduces Yki activity in the transcription assay. As Yki does not contain DNA binding sequences it is thought that Yki binds to an as yet unidentified transcription factor to activate Hippo pathway targets.

Recently, S168 was identified as the critical Yki residue targeted by Wts for growth inhibition and its phosphorylation leads to exclusion of Yki from the nucleus, an event mediated by the 14-3-3 proteins (Dong et al., 2007). The translocation of Yki to the cytoplasm in the presence of Hippo signalling is visualized in S2 cells by immunofluorescence and cell fractionation, and *in vivo* using a Yki antibody (Dong et al., 2007). Mutation of this residue alleviates inhibition by Hippo signalling and leads to constitutive Yki activation; inducible expression under the control of the tubulin promoter of mutant but not wild-type *yki* drives overgrowth (Dong et al., 2007). Moreover, it was shown that the equivalent YAP residue, S127, is targeted by the mammalian Hippo pathway and relocalizes YAP to the cytoplasm (Dong et al., 2007). Yki is believed to be a co-activator and would therefore need to interact with a DNA-binding transcription factor. The identity of such factor(s) remains unknown, therefore none of the Hippo pathway targets have been formally demonstrated to be directly under Yki transcriptional control.

1.7.3 Other components of the Hippo pathway

1.7.3.1 *bantam* – a transcriptional target of the Hippo pathway

The first identified Hippo pathway targets, CyclinE and DIAP1, although important regulators of cell division and apoptosis could not account for the extreme severity of Hippo pathway mutations; the discovery of the microRNA *bantam* as a target of Hippo

signalling helped to reconcile this. Over-expression of *bantam* in the eye causes an increase in the number of inter-ommatidial cells (Nolo et al., 2006; Thompson and Cohen, 2006) and this phenotype is more severe than over-expression of cyclinE or DIAP1 (Nolo et al., 2006).

A GFP sensor containing *bantam* target sites was used as a measure of *bantam* expression, wherever *bantam* is expressed GFP expression is inhibited (Brennecke et al., 2003). The *bantam* sensor responds to changes in Hpo signalling and the fact that *yki* expression can affect the sensor provides evidence that *bantam* is a target of the Hippo pathway (Nolo et al., 2006; Thompson and Cohen, 2006). Importantly, *bantam* is required for Yki to induce overproliferation; *yki* over-expression clones are much larger than controls but if *bantam* is absent these clones are not overgrown (Thompson and Cohen, 2006). Conversely, over-expression of *bantam* is able to rescue the small size of *yki* mutant clones (Nolo et al., 2006; Thompson and Cohen, 2006). This suggests that *bantam* is a target of the Hippo pathway and acts to promote cell division. It is likely that *bantam* also mediates some of the pro-apoptotic effects of the Hippo pathway as Hid is known to be a *bantam* target (Brennecke et al., 2003). The mRNA(s) *bantam* binds to for cell cycle control have yet to be identified and unlike many other Hippo pathway members there are no clear mammalian *bantam* homologs.

1.7.3.2 Expanded (Ex) and Merlin (Mer) function upstream of Hippo

Merlin is a FERM domain containing protein homologous to Neurofibramatosis type-2 gene (NF2). NF2 is a tumour suppressor gene and mutations in NF2 are the cause of a familial form of cancer associated with the development of tumours of the skin and the nervous system. Merlin has been shown to have tumour suppressor roles in flies and functions redundantly with a related FERM domain containing protein, Expanded, to regulate tissue growth and differentiation (McCartney et al., 2000). A role in the Hippo pathway was proposed due to *merlin, expanded* double mutant phenotypic similarities; clones show many excess inter-ommatidial cells in the pupal retina and tissue outgrowths (Hamaratoglu et al., 2006). Mutations in *merlin* or *expanded* alone cause only mild overgrowth phenotypes suggesting that they can at least partially replace each other.

Merlin and Expanded were the first reported examples of proteins functioning upstream of Hpo (see figure 7) and several key experiments suggest that this is the case. Firstly, over-expression of *expanded* is rescued by loss of *wts* but over-expression of *hpo* is not rescued by loss of *expanded* and *merlin*. Secondly, transcriptional upregulation elicited by loss of *expanded* is suppressed by over-expression of *hpo*. It was also shown that Merlin and Expanded are able to act together to induce Wts phosphorylation (Hamaratoglu et al., 2006). Interestingly, Merlin and Expanded are also transcriptional targets of the Hippo pathway and this may provide a negative feedback control mechanism to regulate the pathway (Hamaratoglu et al., 2006). The mechanism by which Merlin and Expanded regulate the Hippo pathway is still unclear but may involve transducing a signal from an as yet unknown receptor. Alternatively, since Merlin has been reported to mediate contact inhibition in mammals, Merlin/Expanded signalling may respond to cell-cell contacts (Zhao et al., 2007).

Another group reported that Merlin and Expanded are required for the efficient membrane clearance of several different transmembrane receptors. *merlin expanded* double mutant clones show elevated levels of EGF receptor, Notch, Patched, Smoothened, Fat and DE-Cadherin (Maitra et al., 2006). Pulse-chase experiments using an extracellular Notch antibody showed that Notch is removed form the cell surface more quickly in wild-type than *expanded/merlin* mutant cells, suggesting a role for Merlin and Expanded in endocytosis of membrane receptors (Maitra et al., 2006). This data raises the possibility that Merlin and Expanded only indirectly regulate the Hippo pathway as a consequence of their effects on other signalling pathways.

1.7.3.3 Fat (Ft) functions upstream of Hippo

One putative receptor for the Hippo pathway is the atypical cadherin Fat. Fat is known to play important roles in the generation of planar cell polarity (PCP) and control of organ growth. Fat had long been known to function as a tumour suppressor in *Drosophila* but the pathways downstream of Fat were elusive. Closer examination revealed that *fat* mutant cells upregulate Hippo pathway targets such as *cyclin E*, *DIAP-LacZ* and *expanded-LacZ* (Bennett and Harvey, 2006; Silva et al., 2006; Willecke et al., 2006). Genetic experiments suggest that Fat functions apically in the Hippo pathway

upstream of Expanded, for example, *fat* mutations fail to rescue the small eye caused by over-expression of *expanded* (Bennett and Harvey, 2006; Willecke et al., 2006). Since Fat is a transmembrane protein and functions upstream of Expanded, it has been proposed that Fat functions as a receptor for the Hippo pathway. However, *fat* mutant phenotypes are significantly weaker than Hippo pathway phenotypes suggesting that, like Expanded and Merlin, Fat may function redundantly. In agreement with this, Fat is required for the apical localization of Expanded but not Merlin (Bennett and Harvey, 2006; Silva et al., 2006; Willecke et al., 2006). As Fat is required for Expanded localization/function, it also acts redundantly with Merlin. *fat expanded* double mutant clones do not show many excess inter-ommatidial cells whereas *fat merlin* double mutant clones show the characteristic Hippo pathway phenotype (Silva et al., 2006; Willecke et al., 2006).

An alternative and not mutually exclusive model of the role of Fat in the Hippo pathway has been proposed whereby Fat acts through the unconventional myosin Dachs to regulate the levels of Wts protein. Epistasis experiments suggest that Fat functions upstream of Dachs and Dachs functions upstream of Wts (Cho et al., 2006). In agreement with a role for Dachs in Hippo signalling it was shown that DIAP1 levels are elevated in *dachs* overexpressing cells (Cho et al., 2006). Interestingly, in *fat* mutant clones levels of Wts protein (but not levels of other Hippo pathway members) are downregulated, and in *dachs fat* double mutant clones Wts levels are unaffected (Cho et al., 2006). This suggests that Fat acts to inhibit the function of Dachs, which itself is required to reduce levels of Wts. This work provided an alternative mechanism for the regulation of the Hippo pathway by Fat, which is independent of Expanded and Hpo. Fat activity is known to be positively regulated by another protocadherin, Dachsous (Ds), raising the possibility that Ds is a ligand for the Hippo pathway. In support of this view *ds* over-expression clones show upregulation of the Hippo pathway target DIAP1 within the clones and also in surrounding wild-type cells (Cho et al., 2006).

1.7.3.4 dRASSF antagonises Hippo signalling

Several upstream positive regulators of Hpo and Wts have now been described however the only known antagonists are Dachs and dRASSF, the *Drosophila* ortholog of the

mammalian RASSF proteins. There are 8 RASSF family members in humans (RASSF1-8), which have been proposed to function as tumour suppressors. Silencing of RASSF1A by promoter methylation is one of the most frequent alterations in human tumours (van der Weyden and Adams, 2007). RASSF proteins are characterized by an RA domain and RASSF1-6, which are the most closely related to dRASSF, also possess a SARAH domain.

dRASSF or Sav are able to physically interact with Hpo via their SARAH domains, a unique domain found in all three proteins. It is thought that dRASSF and Sav compete for binding to the Hpo SARAH domain as in cells dRASSF and Sav are never detected in the same Hpo complex. Also, adding increasing amounts of Sav disrupts the binding of Hpo and dRASSF (Polesello et al., 2006). Therefore dRASSF can inhibit Hippo signalling by binding to Hpo and sequestering it away from its adapter and positive regulator, Sav. dRASSF is also thought to have a tumour suppressor function aside from its oncogenic role in the Hippo pathway as *dRASSF* mutation can partially rescue the poor growth of *ras* clones (Polesello et al., 2006).

1.7.4 The Hippo pathway has other functions besides growth regulation

Aside from its crucial role in the control of organ growth the Hippo pathway has been shown to have other functions during development. For example, Wts has been shown to antagonize another growth regulator, Melted, to control the fates of R8 photoreceptors in the developing eye (Mikeladze-Dvali et al., 2005). Colour vision in *Drosophila* is achieved by a random distribution of p and y sub-types of ommatidia, which respond to different wavelengths of light by expressing different rhodopsins. Wts and Melted are required to respond to signals from the R7 photoreceptor that specify which rhodopsin is expressed in the R8 (Mikeladze-Dvali et al., 2005).

In addition to this post-mitotic role in photoreceptor development the Hippo pathway has been shown to be required for neurogenesis during the larval stages. In *wts*, *hpo* or *sav* mutants the number and length of dendritic branches is greatly reduced (Emoto et al., 2006). This is a late defect as initially *wts* mutant neurons have similar dendritic arbors to wild-type neurons but at later developmental stages the complexity of *wts*

mutant arbours is reduced suggesting a role for Hpo and Wts in the maintenance of dendrites (Emoto et al., 2006).

The Hippo pathway also has a role in responding to DNA damage by mediating apoptosis downstream of Dmp53. Ionizing radiation induces an apoptotic response to DNA damage, which is dependent on Dmp53, the *Drosophila* ortholog of the mammalian p53 tumour suppressor. This response also requires Hippo signalling as *hpo*, *sav* or *wts* mutant clones contain fewer apoptotic cells than the surrounding tissue (Colombani et al., 2006). Additionally Hpo phosphorylation is induced in response to ionizing radiation in wild-type but not *Dmp53* mutant ovaries suggesting that Dmp53 activates the Hippo pathway in response to DNA damage (Colombani et al., 2006).

Recently the Hippo pathway has been shown to have an early developmental role in establishing oocyte polarity. During mid-oogenesis *gurken* (*grk*) mRNA becomes localized to a region between the oocyte nucleus and the membrane of the presumptive posterior follicle cells (PFCs). Grk is an EGFR ligand and provides a signal that specifies the PFCs. The PFCs are then thought to signal back to the oocyte which reorganizes the microtubule network and establishes anterior-posterior polarity via an unknown signal. If the PFCs are mutant for 'core' Hippo pathway components, then the posterior determinants Staufen and Oskar do not localize to the posterior end of the egg chamber. This only occurs when the PFCs, rather than other follicle cells, are mutant, suggesting that Hippo signalling is specifically required in the PFCs to control anterior posterior body axis formation (Meignin et al., 2007; Polesello and Tapon, 2007).

1.7.5 The Hippo pathway and cancer

Given that most of the Hippo pathway members discussed above have clear mammalian homologs and that they carry out such potent growth regulatory functions in *Drosophila*, it is reasonable to expect that a similar pathway plays a role in human tumourigenesis. Strong evidence for functional conservation is provided by the data showing that the human *MATS1*, *MST2* and *YAP* genes can rescue the corresponding *Drosophila* mutants *in vivo* (Huang et al., 2005; Lai et al., 2005; Wu et al., 2003). The homolog of *sav*, *hWW45*, is deleted in renal cancer cell lines (Tapon et al., 2002) and a

MATS homolog is disrupted in cell lines derived from human melanomas (Lai et al., 2005). Studies in mice have identified LATS1 (one of two Wts homolgs) as a tumour suppressor; knockout mice developed soft tissue sarcomas and ovarian cancer and are extremely sensitive to carcinogenic treatments (St John et al., 1999).

The homologue of *yki* (known as *YAP*) has oncogenic properties and has also been implicated in cancer. The genomic locus 9qA1 contains the mouse equivalents of *yki* and *DIAP1* (*YAP* and *cIAP*) and is often duplicated in a mouse model of hepatocellular carcinoma (Zender et al., 2006) and in mouse mammary tumours (Overholtzer et al., 2006). It was further shown that YAP and cIAP1 act synergistically and are the driving force behind tumourigenesis associated with this genomic amplification (Zender et al., 2006). Importantly, the genomic region containing *YAP* is also amplified in some human hepatocellular carcinoma samples and esophageal cancers (Zender et al., 2006). Over-expression of *YAP* results in cellular changes required for tumourigenesis such as epithelial to mesenchymal transitions, increased proliferation and resistance to apoptosis (Overholtzer et al., 2006). The fact that the *merlin* homolog *NF2* is a known mammalian tumour suppressor and its deletion is the cause of neurofibromatosis type 2, also strongly implicates the Hippo pathway in human cancer.

Despite the links between many Hippo pathway orthologs and tumourigenesis a clearly defined mammalian Hippo pathway has only recently been described to regulate tissue growth. The characterization of a mammalian Hippo pathway benefited from the identification of S127 as the YAP phosphorylation site. Using phospho-specific antibodies it was demonstrated that YAP is targeted by Mst1/2 and Lats1/2 in mammalian cells leading to its exclusion from the nucleus (Dong et al., 2007; Zhao et al., 2007). Furthermore, conditional activation of YAP in mouse livers leads to a dramatic increase in organ size as a result of increased cell numbers, much like the phenotypes seen when *yki* is expressed in *Drosophila* organs (Dong et al., 2007). RT-PCR analysis of transgenic livers revealed that both cell cycle regulators and apoptosis inhibitors are upregulated by YAP. The cell-death inhibitor BIRC5/survivin was strongly induced and shown to be functionally important as BIRC5 RNAi inhibited the transforming capability of YAP (Dong et al., 2007). It has also been recently shown that the Hippo pathway inhibits YAP via S127 phosphorylation to achieve contact inhibition of growth in mammalian cells. Inhibition of YAP rescues the contact inhibition defect

in a WW45 (Sav) deleted cancer cell line (Zhao et al., 2007). This suggests that the Hippo pathway can respond to the density of cells within a tissue and regulate growth accordingly. Thus, it seems that the Hippo pathway functions analogously in *Drosophila* and mammals to restrict organ growth by inhibiting Yki/YAP dependent transcription of genes involved in the control of proliferation and apoptosis. Therefore, although much work still needs to be done to assess the role of the Hippo pathway in mammalian systems, there are clear indications that this conserved signalling cassette contributes to tumourigenesis.

1.8 An introduction to the regulation and function of SFKs

1.8.1 Mammalian SRC family kinases

Cellular SRC (c-SRC) is a member of the SRC family kinases (SFKs), which include SRC, FYN and YES. c-SRC is heavily implicated in cancer and in the progression of the disease leading to metastasis. c-SRC is either overexpressed or activated in a wide variety of tumours and this reflects its roles in promoting proliferation, loss of adhesion and increased cell motility and invasiveness (Yeatman, 2004) (see figure 8). Intensive research is currently underway to understand the cellular consequences of c-SRC activation and to develop c-SRC inhibitors for cancer treatment. c-SRC is a tyrosine kinase and contains a C-terminal regulatory region and four SH (SRC homology) domains. The SH1 domain is the kinase domain. The SH2 and SH3 domains bind to other proteins and are involved in the intramolecular interaction that inactivates c-SRC. The SH4 domain contains a myristoylation site, which allows c-SRC to dock to the plasma membrane (Cole et al., 2003).

1.8.2 Regulation of c-SRC

Viral SRC (v-SRC) of the avian Rous sarcoma virus (RSV) was the first viral oncogene to be identified and, unlike c-SRC, is capable of transforming infected cells. It was subsequently discovered that v-SRC is derived from vertebrate c-SRC and was incorporated by the virus by recombination. v-SRC transformed fibroblasts have a visibly altered morphology, they disaggregate from each other and float in the medium as a consequence of loss of cell-cell and cell-substratum adhesions. The cells have increased motility and are able to invade a basement matrix. v-SRC transformed cells also exhibit increased proliferation rates and nutrient requirements (Yeatman, 2004).

v-SRC differs from c-SRC in that it contains several activating point mutations and lacks vital C-terminal regulatory sequences. The C-terminal region of c-SRC and other SFKs is targeted by CSK (C-terminal SRC kinase) (Okada et al., 1991) and its homolog CHK (CSK homologous kinase) (Klages et al., 1994), which negatively regulate c-SRC

Figure 8: Cellular consequences of c-SRC activation. c-SRC regulates cell-cell adhesions (adherens junctions) and cell-matrix adhesions (focal adhesions) and c-SRC activation leads to decreased adhesion, increased motility and invasiveness. Active c-SRC disrupts adherens junctions by promoting E-Cadherin internalisation. Active SRC-FAK complexes regulate focal adhesion turnover through R-Ras, which inhibits integrin function. The focal adhesion components Paxillin and Cas and the cytoskeletal regulator RhoA are also targeted by SRC-FAK complexes. SRC-FAK association leads to JNK activation and transcription of matrix-metalloprotease genes, *mmp2* and *mmp9*. c-SRC activation also promotes angiogenesis and proliferation by increasing levels of STAT3. Figure adapted from (Yeatman, 2004).

by phosphorylating a conserved tyrosine residue (Tyr527 in avian c-SRC). This inactivates c-SRC by causing an intramolecular interaction between the phosphorylated tyrosine and its SH2 domain, reducing the ability of substrates to access the kinase domain and also blocking access to the SH2 and SH3 protein-protein interaction domains (Pawson, 1997). Unexpectedly, the crystal structure of inactive c-SRC revealed another interesting feature; in the inactive conformation, the SH3 domain contacts a region within the SH2-kinase domain linker region. This interaction is thought to force a crucial residue (Glu310) away from the active site, thus inhibiting activity. Functional data showing that the binding surface of the SH3 domain is essential for kinase inhibition supports this idea (Pawson, 1997). A similar intramolecular interaction was observed when the crystal structure of Hck, a closely related SFK was determined (Pawson, 1997) suggesting that switching between the open active conformation and the closed conformation is important for regulation of other SFK members. The v-SRC C-terminal truncation produces an activated SRC molecule resistant to inhibition by CSK and CHK. The transforming capabilities of v-SRC highlight the importance of Tyr527 phosphorylation in preventing inappropriate c-SRC activation.

In addition c-SRC is negatively regulated by ubiquitylation followed by proteasome-mediated degradation, for example, expression of the ubiquitin ligase CBL-3 inhibits v-SRC transformation (Kim et al., 2004a). CBL-3 binds specifically to fully active c-SRC (Tyr419 phosphorylated, see below) and promotes its ubiquitination and downregulation (Kim et al., 2004a).

c-SRC can be activated by removal of the Tyr527 phosphorylation by phosphatases such as PTP1 and SHP2, which allow c-SRC to adopt an open, active conformation (Jung and Kim, 2002; Zheng et al., 1992). Full activation of c-SRC also requires an auto-phosphorylation of a tyrosine (Tyr419) within the kinase domain. Binding of other proteins to c-SRC can also regulate its activity, for example, focal-adhesion kinase (FAK) and CRK-associated substrate (CAS) can bind to the SH2 and SH3 domains of c-SRC and this can prevent the inactive conformation from forming (Burnham et al., 2000; Schaller et al., 1994; Thomas et al., 1998). c-SRC can also be activated in response to extracellular cues via interaction with activated receptor tyrosine kinases such as the EGF receptor (Tice et al., 1999) and the FGF receptor (Landgren et al., 1995). Co-transfection of c-SRC and EGFR into fibroblasts results in a synergistic

potentiation of transformation, c-SRC associates directly with EGFR and phosphorylates tyrosine residues (Tyr-854 and Tyr-1101), an event necessary for the mitogenic response (Tice et al., 1999).

c-SRC activity is also regulated by its sub-cellular localization; activated c-SRC is translocated to the plasma membrane to which it binds via its myristoylated SH4 domain, allowing full activation through auto-phosphorylation of Tyr419 (Kmiecik and Shalloway, 1987; Yeatman, 2004). The membrane localization allows c-SRC to gain access to target proteins including RTKs and components of focal adhesions.

1.8.3 Downstream effectors of c-SRC

Many of the downstream targets of c-SRC (see figure 8) were identified using phospho-tyrosine antibodies and these include transcription factors, adaptor proteins and focal adhesion components (Yeatman, 2004). The numerous c-SRC targets identified indicate that there are probably also many indirect targets contributing to the activated c-SRC transformation phenotype. Gene expression profiling of SRC-transformed rat fibroblasts uncovered a SRC 'transformation footprint'. Interestingly, the homologs of many of the genes identified were also mis-expressed in colon tumour samples where c-SRC is known to be activated (Malek et al., 2002).

1.8.3.1 c-SRC regulates STAT3 to promote proliferation and angiogenesis

The STAT family of proteins are believed to be important targets of c-SRC. In v-SRC transformed cells, levels of STAT3 are increased and dominant negative STAT3 expression can inhibit transformation (Bromberg et al., 1998). The role of STAT3 in v-SRC transformation is probably to increase proliferation via transcription of cell cycle regulators such as *cyclinE* and *c-Myc*. However, STAT3 upregulation may also contribute to angiogenesis as it regulates the expression of vascular endothelial growth factor (VEGF) (Frame, 2004).

1.8.3.2 Regulation of focal adhesions by c-SRC

Focal adhesions are large complexes of over 50 proteins, including c-SRC, FAK, CAS, paxillin, tensin and α-catenin, which bind to integrins. Integrins are the proteins that link the actin cytoskeleton to the extracellular matrix (ECM). Focal adhesions are dynamic structures with a rapid turnover in migrating cells. Migrating cells extend protrusions and form new adhesions near the leading edge, followed by disruption of old adhesions at the rear. It is thought that c-SRC facilitates the disruption of focal adhesions partly through phosphorylating two cytoplasmic tyrosines of β1A integrin subunits. Mutation of one of these residues (Tyr-783) inhibits the ability of v-SRC to transform mouse fibroblasts and focal adhesions are maintained in the presence of v-SRC (Sakai et al., 2001). v-SRC induced phosphorylation of another integrin subunit, β3, has also been reported to contribute to decreased adhesion (Datta et al., 2002). This suggests that phosphorylation of integrins by v-SRC reduces interaction between the actin cytoskeleton and the ECM, thus reducing adhesion. v-SRC is also thought to regulate integrins indirectly through tyrosine phosphorylation of an intermediate protein, R-Ras, a RAS family small GTPase. v-SRC has been shown to phosphorylate R-Ras at Tyr-66 leading to inhibition of integrin activity and reduced adhesion (Zou et al., 2002). v-SRC can also regulate focal adhesions by inhibiting RHOA, a small GTPase absolutely required for their assembly. v-SRC phosphorylates and activates p190 RHOGAP leading to inhibition of RHOA activity and to focal adhesion disruption (Chang et al., 1995; Fincham et al., 1999).

In addition to their role as adhesion molecules integrins can also affect cellular processes by recruiting and activating signalling molecules, including the tyrosine kinase FAK. FAK is recruited to integrin β-subunits via its C-terminal region and becomes activated by an unknown mechanism, leading to phosphorylation of Tyr-397. This provides a binding site for the SH2 domain of SFKs leading to the formation of active c-SRC-FAK complexes and subsequent phosphorylation of numerous target proteins with roles in cell motility, invasion and adhesion (Mitra and Schlaepfer, 2006).

Targets of c-SRC-FAK complexes include the focal adhesion adaptor proteins Paxillin and CAS, which recruit other molecules to focal adhesions upon activation. Active c-

SRC-FAK complexes are believed to be important for rapid turnover of focal adhesions and hence affect cell motility.

Active c-SRC-FAK complexes also can lead to increased invasiveness by localising to invadopodia, which are integrin enriched cytoplasmic extensions formed by invasive cells. Expression of FRNK, a FAK inhibitor, is sufficient to inhibit v-SRC mediated invasion through matrigel, suggesting that c-SRC-FAK complexes can promote invasion (Hauck et al., 2002). This idea is supported by data showing that expression of v-SRC in FAK-/- fibroblasts does not lead to invasive phenotypes (Hsia et al., 2003). Additionally, activation of FAK leads to stimulation of the JNK signalling pathway and concurrent expression of matrix-metalloproteases MMP2 and MMP9, which promote ECM breakdown and facilitate invasion (Hauck et al., 2002; Hsia et al., 2003) (see figure 8).

1.8.3.3 Regulation of cell-cell adhesions by c-SRC

Activated SRC not only regulates adhesion to the ECM via interactions with focal adhesion components but also regulates cell-cell adhesions via regulation of adherens junctions. Cell-cell adhesion is achieved through homotypic E-cadherin interactions between neighbouring cells. Adherens junction components also include β-catenin and α-catenin, which provide a link to the actin cytoskeleton, and the adherens junction regulator p120 catenin. c-SRC inhibits adherens junctions by reducing E-cadherin localization and function and by promoting its internalization by the endocytic pathway (Palacios et al., 2005) (see figure 8). Translocation of E-cadherin to the membrane is blocked by v-SRC expression when cells are supplied with calcium and attempt to form cell-cell contacts. Therefore activated SRC can affect the sub-cellular localization of E-Cadherin (Frame, 2004). p120-catenin is thought to both stabilise and disrupt adherens junctions depending on the context. It has been proposed that p120-catenin binds to E-Cadherin and this facilitates its phosphorylation by v-SRC, in turn leading to reduced Cadherin function (Frame, 2004). With respect to E-cadherin internalization, it was shown that activated c-SRC leads to tyrosine phosphorylation, ubiquitination and internalization of E-Cadherin in a process requiring the E3 ubiquitin ligase, Hakai (Fujita et al., 2002). The loss of E-Cadherin from the surface of cells results in loss of

cell-cell contacts and epithelial to mesenchymal transition (EMT) (Frame, 2004). Cancer cells that have undergone EMT show a switch in adhesion from cell-cell contacts to cell-matrix contacts and are considered to be more prone to metastasis. Therefore the suppression of E-Cadherin function by activated c-SRC may partly account for the correlation between tumours with activated c-SRC and metastasis such as in the case of advanced colon cancers.

In summary, activated c-SRC regulates both cell-cell contact (adherens junction) and cell-ECM contact (focal adhesion) components to achieve its dramatic effects on cell adhesion, motility and invasiveness. Loss of adherens junctions promotes EMT, leading to loss of cell-cell adhesion and increased motility. The actions of activated c-SRC at focal adhesions increase motility and promote invasiveness. It is probably for these reasons that activated c-SRC is so often associated with metastasis. The kinase FAK plays a pivotal role in several of the processes occurring downstream of activated c-SRC, particularly in promoting invasion. Activated c-SRC can also increase proliferation rates and induce angiogenesis.

1.8.4 c-SRC and cancer

Activated c-SRC is known to increase fibroblast proliferation rates but whether this effect has any consequences during tumourigenesis is not clear. For example, c-SRC activity in colon cancer cells does not correlate with proliferation rates or with tumour growth rates *in vivo* (Yeatman, 2004). However, it is well documented that gastrointestinal-tract tumours show increasing levels of c-SRC activity as the disease progresses with the highest levels of activity observed in metastatic growths (Talamonti et al., 1993). The link between activated c-SRC and metastasis is supported by data showing that expression of CSK, the c-SRC inhibitor, suppresses metastasis in murine models (Nakagawa et al., 2000). Several other cancer types have been reported to show increased c-SRC activity, such as pancreatic, oesophageal, breast and lung cancers (Irby and Yeatman, 2000). Interestingly, some colon cancers simultaneously have high levels of c-SRC and low levels of CSK, a combination causing further increases in c-SRC activity (Cam et al., 2001). Surprisingly, despite the increases in c-SRC activity observed in various tumours, there has been only one report of naturally occurring c-

SRC mutations in human cancer; it was shown that a small proportion of colon cancers have an activating mutation at residue 530 (Irby and Yeatman, 2000). However, the fact that c-SRC can be activated by other means than mutation, such as by the EGF receptor, provides an explanation for the apparent lack of c-SRC mutations described. Work is currently underway to develop inhibitors of c-SRC activation as new drugs for cancer treatment and several compounds are now entering clinical trials (Yeatman, 2004). Depletion of c-SRC only has mild cellular consequences meaning that c-SRC inhibitors may be relatively non-toxic compounds.

1.8.5 Functions of other SFKs

Of the nine SFK members identified, c-SRC, Yes and Fyn are considered to be ubiquitously expressed and show a broad expression pattern throughout mouse development. These three SFKs are also the only members identified as viral transforming oncogenes. The study of mutants lacking various combinations of these SFKs revealed that they have partially overlapping functions during development. LOF of any one of these genes gives rise to either restricted phenotypes in the case of c-SRC (mutant mice are viable but die after a few weeks due to bone remodelling defects) (Soriano et al., 1991) or no phenotype in the case of Fyn or Yes (Stein et al., 1994). However, *c-SRC / Fyn* double mutants or *c-SRC / Yes* double mutants commonly die before birth and the number of offspring is considerably lower than expected. This suggests that these SFKs function redundantly and can compensate for LOF of another (Stein et al., 1994). A proportion of *Fyn / Yes* double mutants do survive to adulthood but these mice commonly develop renal diseases. This is unexpected as Fyn is not thought to be expressed in mouse kidneys. However, Fyn and Yes are both expressed in T-cells suggesting that the renal disease may be a consequence of an autoimmune disorder (Stein et al., 1994). Therefore it is possible that Fyn and Yes play redundant roles in T-cells.

Aside from their roles in controlling proliferation and adhesion, the main other described function for SFKs is regulation of immune cell function. The role of SFKs in the immune system is well documented but will be discussed only briefly here as this function is largely irrelevant when studying *Drosophila* SFKs as insects do not possess

and adaptive immune system. Several SFK members have important roles in the immune system and those members that are not ubiquitously expressed show specific expression in hematopoetic lineages. For example, myeloid lineages express Hck, Fgr and Lyn; B cells express Fyn, Lyn and Blk; T cells primarily express Fyn and Lck (Palacios and Weiss, 2004).

Lck and Fyn are crucial for T-cell function and are involved in the transmission of signals from proximal T-cell antigen receptors (TCRs). Lck and Fyn are recruited to TCRs and phosphorylate intracellular tyrosine residues to which members of the Syk family kinases bind. Syk family kinases, particularly ZAP-70, are phosphorylated and activated by Lck and Fyn and mediate the propagation of signalling (Palacios and Weiss, 2004). TCR signalling, and thus Lck and Fyn activity, is required at multiple stages during T-cell development and also in mature T-cells for proliferation following antigen recognition and survival signalling (Palacios and Weiss, 2004). With the exception of T-cell survival, which requires both Lck and Fyn, the major contributor to TCR signalling is Lck. In an analogous manner, SFKs are also required for signal transduction from B-cell antigen receptors. CSK is required to inhibit SFKs in T-cells and B-cells and loss of CSK prevents T-cell and B-cell maturation (Thomas and Brugge, 1997).

1.9 CSK and CHK - endogenous SFK inhibitors

1.9.1 An introduction to CSK and CHK

Carboxy-terminal SRC kinase (CSK) and Csk-homologous kinase (CHK) are endogenous inhibitors of SFKs, which phosphorylate SFKs at a conserved tyrosine residue in the C-terminal regulatory tail. Evidence supporting a biologically functional role for CSK as a c-SRC inhibitor comes from studies of knockout mice. *CSK* knockout mice die at an early embryonic stage, in contrast, *CSK* / c-*SRC* double mutants die shortly before birth and show less severe neural tube defects (Thomas et al., 1995). Additionally, cells derived from *CSK* mutant embryos show high c-SRC and Fyn activity and reduced c-SRC C-terminal phosphorylation (Imamoto and Soriano, 1993). In contrast to SFKs, CSK is a highly specific tyrosine kinase. This is thought to be because long range three dimensional interactions occurring specifically between CSK and c-SRC are required for phosphorylation (Cole et al., 2003).

CSK and CHK are related to SFKs (CSK and c-SRC showing 40% overall sequence identity) and have similar domain architecture, including a tyrosine kinase domain and SH2 and SH3 domains. CSK and CHK differ from SFKs in that they lack the N-terminal myristoylation domain involved in membrane anchoring and also lack the C-terminal regulatory tail (Cole et al., 2003). It appears that the SH2 and SH3 domains of CSK are important for the catalytic activity of the kinase domain rather than negatively regulating it, as is the case for c-SRC. When the SH2 and SH3 domains are deleted from purified CSK enzyme, a 100-fold reduction in catalytic activity is observed suggesting that these domains are involved in an intramolecular interaction (Sondhi and Cole, 1999). It was further shown that only the SH3 domain is important for catalytic activity as it, but not the SH2 domain, could partially rescue the activity of the isolated kinase domain (Sondhi and Cole, 1999). However, the SH3 domain only rescued the catalytic activity of the isolated kinase domain to 5% of that of full length CSK indicating that other interactions are involved. The crystal structure of full length CSK, determined in 2002, has indicated that the intramolecular interaction that is required for catalytic activity is between the SH2-SH3 linker region and the catalytic domain (Ogawa et al., 2002). This is a distinct mode of regulation to that used by c-SRC and Hck.

1.9.2 Regulation of CSK

Whereas the localization of c-SRC is largely membranal, CSK is found throughout the cytoplasm. However, expression of activated c-SRC causes a re-localization of CSK to regions of high c-SRC activity, in particular, actin rich structures called podosomes (Howell and Cooper, 1994). Kinase-dead CSK protein also co-localized with activated c-SRC at podosomes but CSK mutants lacking either the SH2 domain or SH3 domain did not. This suggests that the SH2 and SH3 domains of CSK are important in controlling its sub-cellular localization to efficiently inhibit c-SRC (Howell and Cooper, 1994).

It is now thought that the localization of CSK is controlled by its interaction with a transmembrane phosphoprotein called Cbp (CSK-binding protein). Cbp was identified as a tyrosine phosphorylated protein that co-precipitates with CSK following immunoprecipitation of CSK from neonatal rat brain lysates (Kawabuchi et al., 2000). Cbp is ubiquitously expressed but enriched in a detergent insoluble membrane fraction also enriched for CSK and the SFK Fyn. Immunoprecipitation of proteins in this fraction revealed that Cbp specifically binds to CSK but not c-SRC or Fyn and that binding requires the SH2 domain of CSK (Kawabuchi et al., 2000). This agrees with previous studies showing that the SH2 domain of CSK is important for its relocalization to areas of high c-SRC activity. SFK inhibitors partially prevented phosphorylation of Cbp, suggesting that SFKs contribute to Cbp phosphorylation and association with CSK. An important Cbp phosphorylation site was identified as Tyr-314. Mutation of this residue prevented association with CSK and its subsequent relocalization as visualised by immunofluorescence (Kawabuchi et al., 2000). Cbp not only regulates the membrane recruitment of CSK but also seems to positively regulate its activity. Addition of phosphorylated Cbp was shown to increase the ability of CSK to phosphorylate c-SRC in kinase assays (Takeuchi et al., 2000). Therefore the identification of Cbp provides a new mechanism by which SFKs are regulated that involves negative feedback; high SFK activity leads to Cbp phosphorylation and recruitment of the SFK inhibitor CSK to the membrane.

1.9.3 CSK co-operates with other proteins to inhibit SFKs

Inhibition of active SFKs by CSK may also require the action of various phosphatases as fully active, autophosphorylated (Tyr-419 in c-SRC) c-SRC and Yes proteins are resistant to inhibition. However, dephosphorylation of Tyr-419 by protein tyrosine phosphatase 1B (PTP1B) allows for inhibition of c-SRC by CSK (Sun et al., 1998), suggesting that CSK and PTP1B co-operate in SFK inhibiton. Shp2 is another phosphatase regulating CSK function as it has been shown to control the phosphorylation status of Cbp. Shp2 dephosphorylates Cbp leading to reduced recruitment of CSK to SFKs. Shp2-deficient cells show increased phosphorylation of SFK C-terminal regions, implying that Shp2 is a positive regulator of SFK signalling (Zhang et al., 2004). Therefore, the inhibition of SFKs by CSK is a complex process involving the contribution of other proteins, including Cbp and PTP1B, and the antagonistic effects of Shp2.

1.9.4 *In vivo* studies of CSK

In vivo studies of CSK function support its role as an SFK inhibitor and reveal important roles for CSK in epithelial development. Conditional inactivation of CSK in mouse squamous epithelia using a keratin-5 promoter and the Cre-lox system results in skin defects leading to hyperplasia and inflammation (Yagi et al., 2007). Analysis of CSK deficient epidermis showed that epidermal basal cells overproliferate and show a delay in differentiation. Additionally, β-catenin staining of basal epidermal cells is abnormal and is observed in a diffuse cytoplasmic pattern instead of at cell-cell contacts. Therefore loss of CSK affects epidermal cell-cell adhesion (Yagi et al., 2007). Keratinocytes cultured from mutant mice show high levels of tyrosine phosphorylation of c-SRC targets involved in focal adhesion regulation such as FAK and Paxillin. This implies a switch in the adhesion properties of CSK mutant cells from cell-cell adhesion to cell-substrate adhesion, a hallmark of EMT. Mutant keratinocytes showed high levels of the c-SRC targets MMP2 and MMP9, which have roles in both EMT and inflammation, and high levels of TNF-α, a trigger for inflammatory responses. Treatment of areas of the mutant skin displaying dermatitis with the anti-inflammatory agent FK506 reduced the thickness of the epidermis and decreased basal proliferation

(Yagi et al., 2007). This suggests that CSK inactivation leads to an inflammatory response, which causes hyperplasia in the conditional knockout mice.

1.9.5 CSK and tumourigenesis

Whereas there are many examples in the literature of increased SFK activity in cancers, there are relatively few examples of the association of loss of CSK and tumourigenesis. This may reflect the fact that, despite its restricted expression pattern under normal conditions (see below), CHK may be able to compensate for loss of CSK in tumour suppression. However, reduced CSK levels have been reported in early colorectal cancer (CRC) during the pre-malignant, hyperproliferative phase. Further, knockdown of CSK in colon cancer cell lines results in increased proliferation via the MAPK signalling pathway (Kunte et al., 2005), suggesting that loss of CSK may contribute to the aberrant proliferation during early stages of CRC. CSK also inhibits the ability of SFKs to influence integrin mediated signalling during advanced stages of CRC. Expression of wild-type CSK in human colon cancer cell lines reversed some of the defects associated with SFK overactivation including decreased cell-cell adhesion, increased focal contacts and increased motility and invasiveness (Rengifo-Cam et al., 2004). This result does not imply that loss of CSK is responsible for the metastatic phenotypes but suggests that agents with the ability to recapitulate the function of CSK may be useful in preventing CRC metastasis.

1.9.6 An introduction to CHK (CSK homologous kinase)

CHK is homologous to CSK (mouse CSK and CHK share 53% identity), has a similar domain architecture and is also able to inhibit SFKs by phosphorylation of the C-terminal region (Klages et al., 1994). However, CSK is ubiquitously expressed whereas CHK expression is restricted to neurons and haematopoietic cells. Another difference between CSK and CHK seems to be the mode of SFK inhibition employed. Both proteins inactivate SFKs by phosphorylation of C-terminal tyrosine residues but CHK also inhibits SFKs by a novel non-catalytic mechanism involving binding and the formation of stable complexes. For example, CHK can bind to and inhibit the function of Hck even when the C-terminal tyrosine is mutated (Chong et al., 2004) suggesting

that phosphorylation of Hck by CHK is not required for inhibition. A further report by the same group showed that CHK binds to and inhibits multiple active conformations of the SFK Hck. For example, CHK is able to bind and inhibit the activity of Hck molecules lacking the SH2 and SH3 domains. This mechanism is specific to CHK as CSK is not able to inhibit these forms of Hck. Interestingly CHK does not form stable complexes with SFK proteins (Lyn was tested) in the inactive, 'closed' conformation (Chong et al., 2006). This mode of regulation may act to control events downstream of SFKs involving SFK mediated tyrosine phosphorylation but also those involving binding of targets to SFKs. Downregulation of CHK has been reported in human brain tumours (neuroblastoma and glioblastoma) and in transformed neuroblastoma and astrocytoma derived cell lines (Kim et al., 2004b). The specific loss of CHK in these cancers probably reflects its restricted neuronal expression.

1.10 *Drosophila* SFKs and Csk

1.10.1 Identification of dCsk as a negative regulator of growth

While SFK inhibition by phosphorylation of the C-terminal region is carried out by CSK and CHK in mammals, *Drosophila* has a single CSK/CHK ortholog. *dCsk* was first identified in a genetic screen for modifiers of a small, rough eye phenotype resulting from over-expression of the *wts/LATS* tumour suppressor. *dCsk* mutations dominantly suppress the small eye phenotype implying that *dCsk*, like *wts*, is a tumour suppressor gene and functions in the same cellular processes (Stewart et al., 2003). dCsk shows high homology to hCsk within the kinase and SH2 domains (62% and 73% amino acid identity respectively) although the SH3 domain is not conserved.

Analysis of *dCsk* mutant phenotypes revealed that *dCsk* is indeed a negative regulator of tissue growth, *dCsk* mutants typically die as giant pupae and imaginal discs from homozygotes are larger than controls (Read et al., 2004; Stewart et al., 2003). This increase in tissue size was attributed to a proliferation defect as cells posterior to the MF fail to exit the cell cycle in a timely fashion in mutant discs, much like the phenotype seen in *hpo* or *wts* clones (Read et al., 2004; Stewart et al., 2003).

Wts contains a C-terminal tyrosine (Y1098), which is within a motif similar to the motif surrounding the CSK tyrosine phosphorylation target site of SFKs (Stewart et al., 2003). In kinase assays GST-dCsk phosphorylated its known target dSrc42A using GST-Src42^{K267R} as a substrate (this dSrc42A mutant is incapable of autophosphorylation). GST-dCsk also phosphorylated GST-Wts but not GST-Wts^{Y1098F}, indicating that Wts is a target of dCsk and specifically phosphorylates a C-terminal tyrosine residue (Stewart et al., 2003). Over-expression of *wts* rescues the lethality of *dCsk* mutants but over-expression of *dCsk* does not rescue the lethality of a weak *wts* mutant indicating that dCsk functions upstream of Wts in the control of tissue size (Stewart et al., 2003). However, this rescue is incomplete potentially due to the fact that dCsk regulates other targets besides Wts including dSrc42A and dSrc64B, the two *Drosophila* c-SRC orthologs.

1.10.2 Pathways functioning downstream of dCsk

Using genetic approaches the signalling pathways functioning downstream of dCsk were examined. Reducing the gene dosage of *dSrc64B* by 50 % partially rescued the pupal stage lethality of *dCsk* mutant animals (26% of adults eclosed) supporting a role for dCsk upstream of *Drosophila* SFKs. Interestingly, heterozygosity for *dSrc42A* suppressed *dCsk* lethality to a lesser extent (4% of adults eclosed), which could reflect different requirements for dCsk inhibition between dSrc42A and dSrc64B (Read et al., 2004). Tec29A/Btk (Btk) is another Src family kinase and functions downstream of dSrc42A and dSrc64B in *Drosophila* and downstream of c-SRC in mammals (Guarnieri et al., 1998; Roulier et al., 1998; Saouaf et al., 1994; Tateno et al., 2000). *btk* mutations dominantly suppress the lethality of *dCsk* mutant flies (70% of adults eclosed), this suppression is stronger than that by *dSrc42A* or *dSrc64B* mutations possibly due to redundancy between the *Drosophila Src* genes and because Btk functions downstream of both SFKs (Read et al., 2004).

The JNK signalling pathway mediates events downstream of c-SRC in mammals (Dolfi et al., 1998; Hauck et al., 2002; Hsia et al., 2003) and accordingly, heterozygosity for *basket* (*bsk*), a member of the *Drosophila* JNK signalling pathway, suppresses *dCsk* lethality (60% of adults eclosed). This implicates the JNK pathway in mediating signalling downstream of dCsk in *Drosophila* (Read et al., 2004). Activated c-SRC up-regulates STAT3 and this is known to be important for its transforming capabilities (Bromberg et al., 1998). STAT also seems to function downstream of dCsk; *dCsk* mutations enhance the eye phenotype elicited by over-expression of the Jak/STAT ligand Unpaired (Upd), and levels of STAT protein are increased in *dCsk* mutant cells. This indicates that dCsk negatively regulates Jak/STAT signalling (Read et al., 2004). Taken together this data confirms that dCsk regulates *Drosophila* SFKs, which target a similar set of signalling pathways to human c-SRC.

1.10.3 The relationship between dCsk and *Drosophila* SFKs

Further proof that dCsk is a regulator of *Drosophila* SFKs (dSrc42A and dSrc64B) was provided by *in vivo* analysis of SFK over-expression, which gives rise to similar

phenotypes to dCsk LOF. Mild over-expression of either SFK, achieved using weakly expressing transgenes, results in delayed cell cycle exit posterior to the MF and moderate overgrowth of adult eyes (Pedraza et al., 2004). This is highly similar to the phenotype of hypomorphic *dCsk* alleles. Strong over-expression of either SFK, achieved using strongly expressing transgenes, results in eye ablation by apoptosis (Pedraza et al., 2004). *dCsk* LOF can also lead to apoptosis. Complete removal of dCsk in the eye using a recently generated null allele ($dCsk^{Q156stop}$) leads to eye ablation (Vidal et al., 2007) and *dCsk* mutant cells at boundaries are susceptible to apoptosis (Vidal et al., 2006) (see below). These results suggest that the *dCsk* phenotype is indeed due to increased SFK signalling and that the intensity of SFK signalling governs the phenotype observed. Furthermore, the SFK over-expression phenotype is highly sensitive to dCsk levels. Removing one copy of *dCsk* enhances the weak *SFK* expression phenotype leading to partial ablation of the eye. Moreover, *dCsk* expression is sufficient to rescue the eye ablation phenotype resulting from strong *SFK* expression (Pedraza et al., 2004). This data provides *in vivo* evidence that dCsk is a critical regulator of *Drosophila* SFKs.

Combining the weakly expressing SFK transgenes (which cause overgrowth) with expression of the cell cycle inhibitor *p21*, results in almost ablated eyes without altering the levels of apoptosis. This suggests that the pathways promoting proliferation and apoptosis downstream of SFKs are separable and the balance between them determines the phenotype observed (Pedraza et al., 2004).

It has been shown that dCsk phosphorylates *Drosophila* SFKs using *in vitro* kinase assays. dCsk phosphorylates dSrc42A and dSrc64B at Tyr511 and Tyr547 respectively and when these residues are mutated dCsk no longer phosphorylates either fusion protein. The biological significance of these sites was confirmed *in vivo* by expressing constitutively active SFKs lacking the tyrosine targeted by dCsk. Whereas dCsk expression rescues the eye ablation resulting from strong expression of wild-type SFKs, it fails to rescue the eye ablation resulting from expression of constitutively active SFKs (Pedraza et al., 2004). This provides further evidence that dCsk regulates SFKs and shows that this is achieved through an inhibitory C-terminal phosphorylation.

As strong expression of SFKs leads to apoptosis, it is expected that loss of dCsk also results in apoptosis. However, it has been suggested that dCsk actually protects cells from apoptosis, for example dCsk knockdown on the eye using RNAi largely blocks the wave of apoptosis occurring at 29h APF in the developing pupal retina (Vidal et al., 2006). Conversely, it is reported that complete removal of dCsk using a null allele does result in apoptosis, leading to eye ablation. These differences in phenotype can be explained if there is a threshold level of SFK activation above which apoptosis is triggered. For example, mild SFK activation induced by dCsk RNAi may protect cells from apoptosis whereas strong SFK activation resulting from complete loss of dCsk induces apoptosis.

1.10.4 Phenotypes of dCsk boundary cells

Although broad loss of dCsk has not been reported to induce cell death in wing imaginal discs, loss of dCsk in discrete patches results in apoptosis of mutant cells at the interface between mutant and wild-type cells (Vidal et al., 2006). For example, if the *EGUF/hid* (*ey-Gal4/UAS-FLP/GMR-hid*) technique (Stowers and Schwarz, 1999) is used to generate eyes composed only of *dCsk* mutant cells, the resulting eye is overgrown and mispatterned due to excess proliferation, inhibition of apoptosis and reduced cell adhesion. However, if *dCsk* clones are generated using conventional FLP/FRT methods, they are eliminated within developing tissues such as the eye and wing and replaced by wild-type cells. Additionally, if dCsk is depleted by RNAi in the Patched (Ptc) domain, which forms a stripe down the anterior-posterior boundary of the wing disc, mutant cells juxtaposing wild-type cells move to a basal position within the epithelium, migrate away from the Ptc domain and apoptose (Vidal et al., 2006). The different outcomes of loss of dCsk in whole tissues versus discrete patches is proposed to be due to specific interactions between mutant and wild-type cells at boundaries.

The exclusion and migration of dCsk mutant cells at boundaries is highly reminiscent of epithelial to mesenchymal transition (EMT) and metastasis of tumour cells, two processes that are thought to involve c-SRC activation. Furthermore, the phenotype of dCsk boundary cells requires the cell adhesion mediators dE-Cadherin and p120-catenin, the cytoskeletal regulator Rho1, the JNK pathway and MMP2, a matrix

metalloprotease (Vidal et al., 2006). These have all been implicated in SFK signalling in mammals, particularly in c-SRC mediated control of cell adhesion and migration. Data from mammalian cell culture indicates that phosphorylation of Cadherins by c-SRC can promote weakened adhesion between cells, a crucial step in progression towards metastasis (Takeda et al., 1995). p120-catenin has also been named as a c-SRC substrate. It directly interacts with Cadherin molecules and is thought to promote adhesion by preventing their endocytosis. p120-catenin also directly interacts with and inhibits RhoGTPase to increase cell motility (Fox and Peifer, 2007). Therefore it appears that SFKs target a similar repertoire of cell adhesion and motility regulators in *Drosophila* and mammals. Interestingly, reducing Rho1 and dp120-catenin function can rescue loss of dCsk in discrete areas but does not suppress broad loss of dCsk suggesting that these factors are specifically required in the response at boundaries (Vidal et al., 2006). Rho1 over-expression in discrete patches can phenocopy loss of dCsk highlighting its importance in removal of dCsk boundary cells (Vidal et al., 2006).

Small GTPases of the Rho family can promote JNK pathway activity and activation of the JNK pathway promotes apoptosis in *Drosophila* wing discs (Adachi-Yamada et al., 1999). The death of dCsk boundary cells is JNK pathway dependent and is highly sensitive to alterations in JNK pathway activity. For example, heterozygosity for the JNK phosphatase *puckered (puc)* dramatically enhances the levels of apoptosis at dCsk boundaries (Vidal et al., 2006). Interestingly the migratory behaviour of these cells is also sensitive to JNK pathway alterations. This may not be surprising, as the JNK pathway has been implicated in the cell movements required for dorsal closure in *Drosophila* (Tateno et al., 2000). Additionally JNK signalling is required for expression of *MMP2* in mammalian cells expressing v-SRC (Hauck et al., 2002). In fact, increased expression of matrix metalloproteases such as *MMP2* is highly characteristic of metastatic tumour cells and allows for degradation of the extracellular matrix, a step necessary for metastasis. Accordingly, the migration of *dCsk* mutant cells away from the *ptc* domain is suppressed by *MMP2* mutation (Vidal et al., 2006). Therefore the apoptosis and migration of *dCsk* mutant boundary cells requires JNK signalling.

Taken together the *Drosophila* and human data point towards an attractive model whereby activated SFKs affect multiple adherens junction components ultimately leading to decreased adhesion and increased motility and apoptosis mediated by

downstream events. The fact that this effect seems to be specific to boundary cells implies that cells at the periphery of tumours, which contact wild-type cells may be more prone to metastasis (Vidal et al., 2006). However, one major difference between dCsk boundary cells and metastatic cells or those undergoing EMTs is that most if not all excluded dCsk cells undergo apoptosis. This suggests that a second mutation that prevents apoptosis would be minimally required for *dCsk* LOF cells to become metastatic. Co-operation between the adhesion regulator Scribble and Ras^{V12} has been shown to induce metastatic-like behaviour in *Drosophila* (Pagliarini and Xu, 2003). It has recently been shown that loss of dCsk can indeed lead to metastasis in *Drosophila* when combined with Ras^{V12} expression. Generating such clones in the eye imaginal disc leads to the formation of secondary tumours throughout the larval body (Vidal et al., 2007).

Besides a clear role for *Drosophila* SFKs in regulating tissue growth and epithelial integrity, several other developmental processes requires SFKs including formation of nurse cell ring canals, packaging during oogenesis, dorsal closure and regulation of receptor tyrosine kinase signalling. The roles of *Drosophila* SFKs in ring canal formation and dorsal closure will be discussed below as it is relevant to this work.

1.10.5 *Drosophila* SFK function in nurse cell ring canal formation

At the start of *Drosophila* oogenesis, a cystoblast divides four times, to give rise to a sixteen-cell germline cyst. However, these divisions are incomplete and the intercellular bridges that connect the cells are stabilized by actin and form ring canals. One of the germline cyst cells becomes the oocyte and is supplied with maternally derived products via the ring canals, which increase in size during oogenesis to reach a final size of about 10μm (Cooley, 1998). Prior to the addition of actin filaments, ring canals are identifiable by phospho-tyrosine labelling. In *dSrc64B* or *Tec29/btk* (*btk*) mutants ring canals form but are unusually small and show a reduction in phospho-tyrosine staining (Guarnieri et al., 1998; Roulier et al., 1998). These reports also noted that dSrc64B is required for the localization of Btk to the ring canals. One proposed model suggests that Btk is recruited to the ring canals by interacting with PIP3 where it is activated by dSrc64B phosphorylation (Lu et al., 2004). The role for dSrc64B in Btk localization is

explained by the fact that Btk activity is necessary for its own localization (Lu et al., 2004). It has been shown that a dSrc64B-dependent pathway leads to phosphorylation of the actin bundling protein Kelch at Y627, providing a mechanism for how dSrc64B and Btk regulate ring canal growth (Kelso et al., 2002). Interestingly regulation by dCsk does not seem to be important for dSrc64B in ring canal formation; loss of dCsk does not affect ring canal size and *dCsk* mutants do not rescue the ring canal defects associated with hypomorphic *dSrc64B* alleles (O'Reilly et al., 2006).

1.10.6 *Drosophila* SFKs are involved in dorsal closure

Dorsal closure during embryogenesis and the thoracic epidermal closure during metamorphosis require dynamic cell shape changes. Members of the JNK signalling cascade are heavily implicated in these processes and pathway mutants show embryonic dorsal open and adult thoracic cleft phenotypes. Weak *dSrc42A* mutants that survive to adulthood show thoracic cleft phenotypes, which are enhanced by reducing Bsk activity (Tateno et al., 2000). Strong *dSrc42A* mutants are embryonic lethal and do not show embryonic dorsal open phenotypes but do have deformed mouthparts, a phenotype shared with *btk* mutants. However either *dSrc42A / btk* or *dSrc42A / dSrc64B* double mutants exhibit a dorsal closure phenotype indicating that, at least for this process, dSrc42A and dSrc64B function redundantly and that Btk is also involved in dorsal closure (Tateno et al., 2000). Importantly, the dorsal open phenotype of *dSrc42A / btk* mutants is rescued by activated *dJun* expression, implying that dSrc42A and Btk function upstream of the JNK pathway during development (Tateno et al., 2000). The expression of the JNK phosphatase *puc*, is regulated by the JNK pathway to provide a negative feedback loop and can therefore be used as a readout of pathway activity. *puc* is expressed in the midline of the notum in wild-type third-instar wing discs but not *dSrc42A* mutant discs and expression of activated *dSrc42A* can induce ectopic *puc* expression (Tateno et al., 2000). Therefore, *Drosophila* SFKs function upstream of the JNK pathway during dorsal closure.

dSrc42A has been reported to mediate regulation of adherens junction components necessary for dorsal closure. Mutations in *shotgun* (*shg*), the *Drosophila* homolog of E-Cadherin, or *armadillo* (*arm*), which links E-Cadherin to the cytoskeleton via α-catenin,

can give rise to dorsal closure phenotypes when combined with *dSrc42A* mutants (Takahashi et al., 2005). dSrc42A forms a ternary complex with E-cadherin and Armadillo at the membrane and a 14 amino acid dSrc42A peptide containing the autophosphorylation site binds Armadillo. Additionally, *dSrc42A; dSrc64B/+* embryos, which exhibit dorsal open phenotypes have reduced E-Cadherin and F-actin accumulation at the leading edge suggesting that SFKs are required to stabilize adherens junctions during dorsal closure (Takahashi et al., 2005).

1.11 An introduction to ASPP family proteins

1.11.1 The p53 tumour suppressor

Members of the ASPP (Apoptosis Stimulating Protein of p53) family of proteins have been described as important regulators of p53, which specifically mediate the apoptotic function of p53.

Mutations in the *p53* tumour suppressor gene are frequent in a wide variety of human cancers underlying the importance of p53 in regulating cellular homeostasis. For example *p53* is mutated in 50% of all human tumours and it is inactivated by other means, such as increased expression of inhibitors, in most other cases (Vogelstein et al., 2000). p53 essentially acts as a damage sensor and is capable of inducing cell cycle arrest and/or apoptosis in response to cellular stresses such as DNA damage caused by ionizing radiation, reactive oxygen species, and inappropriate growth signalling as a result of oncogene activity (Vogelstein et al., 2000). In the absence of functional p53, abnormal cells are able to continue dividing unchecked and to evade cell death. For this reason p53 is regulated by a complex network of proteins and by an array of mechanisms including phosphorylation, ubiquitylation and nuclear translocation.

p53 is a transcription factor and exerts most of its effects via transcriptional control of target genes. Many known apoptosis regulators are targets of p53, including death receptors such as CD95 and DR5 and other molecules such as BAX, PUMA and NOXA (Trigiante and Lu, 2006). The pro-apoptotic function of p53 is thought to be particularly important for its tumour suppressor function and involves both the receptor and mitochondrial mediated apoptotic pathways (Haupt et al., 2003). Post-transcriptional regulation by p53 has also been described whereby p53 is able to activate BAX to induce mitochondrial membrane permeabalization and apoptosis. p53 is able to induce BAX-dependent apoptosis even when nuclear import is blocked, suggesting that p53 co-operates with BAX to induce apoptosis (Chipuk et al., 2004). p53 is thought to induce cell cycle arrest via another target, the cyclinE/cdk2 inhibitor p21, which blocks entry into S-phase. It has been proposed that different post-transcriptional modifications on

p53 and binding of different co-factors can determine whether p53 induces apoptosis or cell cycle arrest (Trigiante and Lu, 2006).

1.11.2 Introduction to ASPP family

The ASPP family of proteins are regulators of p53, which specifically mediate the apoptotic response and their identification gave insights into how p53 makes the decision between inducing apoptosis and cell cycle arrest. ASPP proteins are characterized by a conserved C-terminal portion containing ankyrin repeats, an SH3 domain and a proline rich region. The ASPP proteins were first identified following a yeast two-hybrid screen for mouse p53 interacting proteins that identified a p53-binding molecule, which was named p53BP2 (Iwabuchi et al., 1994). In other reports p53BP2 was identified as an interactor of several other proteins in yeast two-hybrid experiments including BCL-2 (Naumovski and Cleary, 1996), protein phosphatase 1 (PP1) (Helps et al., 1995) and YES-associated protein (YAP) (Espanel and Sudol, 2001). Interestingly, like for p53, all of these interactions occur via the conserved ankyrin repeat and SH3 domains of p53BP2. Although these studies highlight the importance of the p53BP2 ankyrin and SH3 domains, the biological significance the interactions described, with the exception of p53, is not known.

p53BP2 has since been shown to represent a truncated splice variant of full length ASPP2, a protein of 1128 amino acids (Samuels-Lev et al., 2001). Searches for ASPP2 homologous proteins revealed that there are 2 other ASPP family members, ASPP1 and iASPP, proteins of 1091 and 828 amino acids respectively, which both contain the characteristic C-terminal proline rich region and SH3 and ankyrin domains (Trigiante and Lu, 2006). Therefore the ASPP protein family consists of three members on different chromosomes; ASPP1 and ASPP2 are more similar to each other than either are to iASPP because the N-terminal portion of iASPP is not homologous to the other family members.

1.11.3 ASPP1 and ASPP2

Endogenous, full length ASPP1 and ASPP2 were shown to bind to endogenous p53 and this interaction is increased upon UV treatment indicating that ASPP proteins may regulate p53 in response to DNA damage (Samuels-Lev et al., 2001). Co-expression of *ASPP1* or *ASPP2* with *p53* results in a marked increase in the number of apoptotic cells within a population compared to *p53* expression alone. Furthermore, co-expression of *ASPP1* or *ASPP2* with *p53* did not affect the number of cells in G1 as analysed by FACS suggesting that the ASPP proteins specifically stimulate the apoptotic but not cell cycle checkpoint function of p53 (Samuels-Lev et al., 2001). In support of this notion a chromatin immunoprecipitation (CHIP) experiment using a p53 antibody showed that expression of ASPP2 is able to enhance the binding of p53 to the *bax* promoter by 3 fold but has no effect on the binding of p53 to the *p21* promoter. Using cell-based luciferase reporters it was shown that ASPP1 and ASPP2 are able to stimulate p53-mediated expression of pro-apoptotic genes *bax* and *PIG-3* but have little effect on other reporters such as *p21*, *mdm2* and *cyclinG* (Samuels-Lev et al., 2001).

A truncated form of ASPP1 and p53BP2, the truncated form of ASPP2, which both lack the N-terminal sequences, were not as efficient at stimulating the apoptotic function of p53 as the full-length proteins. This suggests that although the ASPP C-terminus binds to p53, there are N-terminal sequences important for ASPP function. Interestingly, ASPP1 or ASPP2 did not stimulate *bax* expression and apoptosis when co-expressed with mutant forms of p53 derived from tumours, offering an explanation for the inability of these forms of p53 to induce apoptosis. Furthermore *ASPP* expression was shown to be downregulated in several wild-type p53-expressing breast tumours; this result provides an insight into how some tumours may tolerate wild-type p53 (Samuels-Lev et al., 2001).

Mdm2 and Mdmx are important endogenous p53 inhibitors, which bind to the N-terminal region of p53 and prevent p53 transcriptional activation. Mdm2 possesses E3 ligase activity and also regulates p53 via proteasome-mediated degradation (Coutts and La Thangue, 2005). It has been demonstrated that Mdm2 and Mdmx can prevent ASPP1 and ASPP2 from enhancing the transactivation functions of p53. Importantly this is not achieved simply through p53 degradation, as Mdmx and Mdm2 (Δ222-437),

which do not target p53 for degradation, are still able to abrogate apoptosis induced by *p53* and *ASPP* expression (Bergamaschi et al., 2005).

Another report from the same group showed that ASPP proteins regulate all p53 family members including p63 and p73 and in this manner can induce apoptosis independently of p53. ASPP1 and ASPP2 are able to bind to p63 and p73 *in vivo* and *in vitro* and can enhance p63 and p73 expression of apoptotic target genes such as *bax* and *PIG-3* but not the cell cycle regulating target *p21* (Bergamaschi et al., 2004). Expression of either *ASPP1* or *ASPP2* in p53-deficient Soas-2 cells induces a modest apoptotic response. This is prevented by p63 or p73 RNAi but not p53 RNAi (control), suggesting that the apoptotic response induced by *ASPP* expression in the absence of p53 is mediated via p63 and p73 (Bergamaschi et al., 2004).

ASPP proteins may also contribute to the p53-dependent cell death that results from aberrant E2F activation since *ASPP1* and *ASPP2* were reported to be transcriptional targets of E2F. Therefore ASPP proteins may constitute a novel mechanism linking the cell cycle to apoptosis, which protects against over-proliferating cells (Fogal et al., 2005).

1.11.4 iASPP

iASPP shares significant C-terminal homology to ASPP1 and ASPP2 and is also able to bind to and regulate p53. However iASPP has an opposing role to that of ASPP1 and ASPP2 in that it acts to inhibit the p53 apoptotic response rather than enhance it (Bergamaschi et al., 2003). iASPP was first identified as a protein of 351 amino acids, which binds to the RelA/p65 subunit of NF-κB and inhibits its transcriptional activity (Yang et al., 1999). This protein was named RAI (RelA associated inhibitor) due its described function. In conflict with subsequent data on iASPP/RAI this group found no interaction with p53 by yeast two-hybrid and showed that *iASPP/RAI* expression does not affect levels of p53 induced *PIG-3* reporter expression (Yang et al., 1999).

Knockdown of iASPP/RAI in human cell lines induces apoptosis and knockdown of *C.elegans* iASPP (Ce-iASPP) by RNA interference induces germ cell apoptosis

(Bergamaschi et al., 2003). This increase in germ cell apoptosis was prevented when worms were mutant for *Ce-p53* suggesting that iASPP functions to inhibit p53 *in vivo* (Bergamaschi et al., 2003). The 4 critical ASPP residues required for binding to p53 are conserved in iASPP, indicating that iASPP may function by competing with ASPP1 and ASPP2 for binding to p53. Indeed expression of *iASPP* or *Ce-iASPP* is able to abrogate the *bax* reporter induction observed when *p53* and *ASPP1* or *ASPP2* are expressed (Bergamaschi et al., 2003). iASPP is also able to co-operate with oncogenes such as Ras to transform cells *in vitro*; this oncogenic role likely reflects the ability of iASPP to inhibit p53-mediated apoptosis (Bergamaschi et al., 2003).

Further searches identified a longer form of iASPP. Full-length iASPP is protein of 828 amino acids and has exactly the same C-terminal sequences as the shorter RAI form previously studied but has extra N-terminal sequence. The N-terminal region of iASPP is thought to be important for its sub-cellular localization as full-length iASPP is largely cytoplasmic and iASPP/RAI is nuclear (Slee et al., 2004).

In vivo evidence for a link between ASPP and p53 was provided by studies on *ASPP2* null mice. *ASPP2* null mice are recovered a lower than expected frequency following crosses between heterozygotes and those that do survive birth die within 30 days displaying heart defects and hydrocephalus. The lethality of *ASPP2* null mice is further increased by heterozygosity or homozygosity for *p53* indicating that p53 and ASPP2 function in a common process *in vivo* (Vives et al., 2006). Furthermore, *ASPP2* heterozygous mice are prone to the development of spontaneous tumours compared to wild-type mice; 40% of *ASPP2* knockout mice developed B-cell lymphomas compared to 22% of wild-type mice and 15% of *ASPP2* mutant mice developed sarcomas (Vives et al., 2006). Mice doubly heterozygous for *p53* and *ASPP2* developed lymphomas more quickly than single heterozygotes. This data provides evidence that ASPP2 functions as a tumour suppressor *in vivo*.

1.11.5 ASPP proteins and cancer

Several lines of evidence indicate a role for ASPP family proteins in tumourigenesis. Firstly, all of the residues in p53 required for ASPP binding (His^{178}, Arg^{181}, Met^{243} and

Arg^{247}) are commonly mutated in human cancers (Gorina and Pavletich, 1996). Importantly, mutation of Arg^{181}, detected in breast and cervical tumour cells, renders p53 defective in apoptosis induction but still capable of arresting the cell cycle (Ludwig et al., 1996). This supports the *in vitro* data showing that ASPP specifically regulates p53-mediated apoptosis and suggests that this function of ASPP is physiologically significant. Secondly, reduced *ASPP1* and *ASPP2* expression is observed in roughly 60% of breast tumours that express wild-type *p53*. In some tumour samples with no change in ASPP1 or ASPP2 levels, an increase in iASPP levels was detected (Bergamaschi et al., 2003; Samuels-Lev et al., 2001). Reduced *ASPP1* expression is also detected in leukaemia cell lines (Liu et al., 2004) and is a feature of acute lymphoblastic leukaemia (ALL) (Agirre et al., 2006). *ASPP1* promoter methylation was detected in 25% of ALL patients with reduced *ASPP1* mRNA levels and correlates with a poor prognosis (Agirre et al., 2006). Thirdly, *ASPP2* heterozygous mice are susceptible to tumour development and the tumours often retain the remaining *ASPP2* allele suggesting that ASPP2 is a haploinsufficient tumour suppressor.

ASPP proteins function as p53 regulators and hence are obvious targets for the development of therapeutic agents for cancer treatment, however there are no such molecules currently in use presumably owing to the relatively recent discovery of this family of proteins. One promising agent is a short peptide derived from ASPP2, called CBP3, which is able to restore DNA binding and killing capabilities to a p53 mutant defective in apoptosis induction (Friedler et al., 2002).

1.12 The Ras signalling pathway in *Drosophila*

1.12.1 Overview of the Ras pathway

The EGFR/Ras/MAPK signalling pathway (the Ras pathway) carries out several important functions in the developing *Drosophila* eye. The Ras pathway promotes cell proliferation and cell survival and is re-iteratively utilised to control the differentiation of ommatidial cell types posterior to the MF (Dickson, 1998). Much of what we know about the Ras pathway comes from studies into its function in photoreceptor differentiation in *Drosophila.*

In a greatly simplified view of the pathway, RTK activation leads to tyrosine phosphorylation of cytoplasmic residues that act as docking sites for Drk (downstream of receptor kinases). Drk functions as an adapter protein to link RTKs (EGFR and Sev) to Sos, the guanine nucleotide exchange factor (GEF) for Ras1 (Olivier et al., 1993; Simon et al., 1993). Ras1 is a small GTPase and the ratio between active (GTP bound) and inactive (GDP bound) Ras is controlled by the activities of Sos and the GTPase activity of Ras itself, which is stimulated by various GTPase activating proteins (GAPs). Active Ras1 initiates a kinase cascade that transmits the signal to the nucleus via dRaf1 (RAF), dSor1 (MEK) and Rolled (MAPK). Active MAPK enters the nucleus and phophorylates target transcription factors, including Pnt, Yan and Jun, to regulate transcription of pathway targets (Raabe, 2000).

1.12.2 EGFR and Sev are required to specify ommatidial cell fates

In the *Drosophila* eye, photoreceptors and other ommatidial cells are sequentially recruited in the order R8, R2/R5, R3/R4, R1/R6, R7 (Raabe, 2000), cone cells, and lastly the pigment cells (Freeman, 1996). Using cell lineage studies it was shown that the different photoreceptor cells are not clonally related, suggesting a model whereby photoreceptors are recruited from a population of naïve cells (Lawrence and Green, 1979). Photoreceptors that have differentiated secrete the EGFR ligand, Spitz, which acts over a short range to recruit subsequent photoreceptors by activating the Ras pathway in presumptive cells. The final photoreceptor to differentiate, the R7 cell,

requires additional input from another RTK, Sevenless (Sev) that also functions upstream of the Ras pathway (Dickson, 1998). Sev is activated in the R7 precursor following interaction with Bride of Sevenless, which is a transmembrane ligand expressed in the R8 cell (Reinke and Zipursky, 1988).

Inducing knockdown of EGFR function at specific time points by using a *hs-Gal4* driver to express *UAS-EGFR-DN* (dominant negative EGFR), prevents formation of ommatidial cell types that are differentiating at the time of heat shock. For example if *EGFR-DN* is expressed in late third instar larvae then ommatidia with missing cone cells are observed. These ommatidia however contain the full complement of photoreceptors as these cell types differentiate before the cone cells (Freeman, 1996). By knocking down EGFR function at different time points it was shown that EGFR is required for the differentiation of all ommatidial cell types. Signalling via EGFR is also sufficient to induce differentiation as ectopic expression of Spitz can lead to the recruitment of extra photoreceptors or cone cells (Freeman, 1996). Although EGFR is required for the formation of all photoreceptors and Sev is required specifically in the R7 photoreceptor, these two RTKs are interchangeable. For example, EGFR expression can rescue R7 formation in a Sev mutant background and conversely Sev ectopic expression can lead to recruitment of extra cone cells (Freeman, 1996).

Over-expression of activated Sev in *sev*-expressing cells (R1/R6, R3/R4, R7, cone cells) leads to rough eye phenotype as supernumerary R7 cells are specified (Basler et al., 1991). This phenotype is highly sensitive to modulations in Ras signalling and was used a sensitized background to identify components acting downstream of Sev. This and other similar screens led to the identification of several proteins functioning downstream of Sev including Ras1 and Raf (Raabe, 2000). Ras and Raf over-expression phenotypes were then used in subsequent genetic modifier screens leading to the identification of further Ras pathway components (Dickson et al., 1996; Karim et al., 1996). These screens corroborated data on the Ras pathway from mammalian studies and helped to define a conserved pathway transducing signals from RTKs to the nucleus.

1.12.3 Pointed and Yan - transcription factors functioning downstream of MAPK

How does activation of Ras signalling induce photoreceptor differentiation ? The first clue to answering this question came with the identification of the ETS domain containing transcriptional repressor, Yan. *yan* LOF results in the production of excess photoreceptors. Yan is expressed exclusively in undifferentiated cells in the eye imaginal disc (Lai and Rubin, 1992) suggesting that it functions as an inhibitor of photoreceptor differentiation. It was subsequently shown that Yan is a phosphorylation target of MAPK, a downstream component of the Ras pathway. Activation of the Ras signalling pathway in presumptive photoreceptor cells leads to Yan phosphorylation and exclusion from the nucleus, thus permitting differentiation (Rebay and Rubin, 1995). Mutating the putative MAPK phosphorylation sites in Yan results in a constitutively active protein and its expression completely blocks differentiation. Furthermore, it was shown that Yan functions as a general inhibitor of differentiation as activated Yan blocks mesoderm development in embryos (Rebay and Rubin, 1995). Therefore, Ras signalling promotes differentiation, at least in part, by inhibiting the function of Yan, a general inhibitor of differentiation.

Another ETS domain transcription factor playing important roles in photoreceptor determination downstream of Ras is Pointed (Pnt). The *pnt* gene encodes two isoforms PntP1 and PntP2, which function as transcriptional activators. MAPK has been shown to phosphorylate Thr151 of PntP2, which increases its activity as a transcritiptional activator. PntP1 activity is thought to be constitutive (Brunner et al., 1994; O'Neill et al., 1994). Unlike Yan, PntP2 plays a positive role in photoreceptor differentiation and loss of PntP2 blocks differentiation of all photoreceptors. In one model it is suggested that Pnt and Yan constitute a cellular 'switch' involved in the control of differentiation. The default state is inhibition of differentiation by Yan; when Ras signalling is induced in presumptive photoreceptors Yan becomes inactivated and PntP2 becomes activated leading to transcription of target genes (Raabe, 2000).

1.12.4 Tramtrack functions downstream of MAPK and represses neuronal fates

Inhibition of Yan is a prerequisite for differentiation, however, another barrier to differentiation must be overcome by Ras signalling. The transcriptional repressor Tramtrack (Ttk) functions as an inhibitor of neuronal differentiation and is regulated by the Ras pathway. The *ttk* locus encodes two different proteins, Ttk69 and Ttk88. Expression of Ttk88 in photoreceptor precursors prevents neuronal differentiation and loss of Ttk88 leads to ectopic R7 production. Phyllopod (Phyl) is an early target of the Ras pathway and acts along with Seven in Absentia (Sina) to degrade Ttk88. This was shown genetically and using Ttk88 specific antibodies. The *ttk88* over-expression eye phenotype is rescued by over-expression of *phyl* and vice versa, but not in a *sina* mutant background (Tang et al., 1997). Furthermore, *phyl* over-expression leads to loss of Ttk88 protein staining in third instar eye discs but not in a *sina* mutant background (Tang et al., 1997). Taken together these results support a model whereby Phyl functions to downregulate Ttk88 by a Sina dependent mechanism. This model is supported by *in vitro* binding assays showing that Phyl, Sina and Ttk88 physically interact (Tang et al., 1997). Sina also physically interacts with UbcD1, a ubiquitin conjugating enzyme providing a mechanism linking the complex to the proteasome degradation pathway. Therefore, the Ras pathway promotes differentiation by inducing Phyl expression, which acts along with Sina to degrade Ttk88. However, this is not the complete picture since, although Ttk88 degradation is required for all photoreceptors to differentiate, Phyl is only expressed in R1/R6 and R7 photoreceptors and Sina is only required for R7 development (Dickson, 1998). This suggests that other factors must exist that function to inhibit Ttk88 in the remaining photoreceptors.

Ttk69 also functions as an inhibitor of neuronal differentiation and is targeted for degradation by Phyl and Sina (Li et al., 1997) suggesting that the Ttk proteins are functionally similar. However Ttk69 plays additional roles in eye development, for instance, *ttk69* has also been shown to promote cone cell differentiation (Wen et al., 2000). Furthermore, Ttk69 is proposed to have both negative and positive effects on photoreceptor development. In the larval eye disc Ttk69 functions as a repressor of differentiation, and must be degraded by Phyl and Sina. However, in the pupal retina Ttk69 functions to maintain photoreceptors in a differentiated state. Ttk69 (but not Ttk88) is detected in all photoreceptor cells in the pupal retina and *ttk69* mutant clones

in the adult eye lack photoreceptors (Lai and Li, 1999). This suggests that Ttk69 plays both positive and negative roles in photoreceptor development.

1.12.5 Control of proliferation by Pnt and Ttk

Ttk69 has also been shown to have roles in the control of cell division in response to Ras signalling. In the third instar eye disc, uncommitted cells posterior to the MF enter S-phase and arrest in G2. Only those cells that receive the Spitz signal from neighbouring precluster cells enter mitosis (Baker and Yu, 2001). This final, synchronous round of division is known as the second mitotic wave (SMW) and provides a sufficient population of cells to complete eye development. The Spitz signal from the precluster also provides a survival signal to the neighbouring uncommitted cells. This helps to adjust the number of uncommitted cells to the number of ommatidia as cells that don't receive the signal are susceptible to apoptosis (Baker and Yu, 2001). The transcription factors PntP2 and Ttk69 regulate entry into mitosis in the SMW by oppositely affecting the transcription of *cdc25/string*, a crucial regulator of mitosis. Over-expression of *ttk69* of loss of PntP2 (in clones) blocks the SMW; cells posterior to the furrow incorporate BrdU suggesting that they enter S-phase but fail to stain for phospho-histone 3 (PH3) indicating that mitosis is blocked (Baonza et al., 2002). It was further shown that PntP2 and Ttk69 compete for binding to the *cdc25/string* promoter and that if both *ttk69* and *cdc25/string* are overexpressed the SMW is rescued (Baonza et al., 2002). It is proposed that control of *cdc25/string* levels by Ras signalling via PntP2 and Ttk69 is not restricted to the SMW but is important for cell cycle control in other contexts.

1.12.6 Ras signalling promotes cell survival

The Ras signalling pathway is known to promote cell survival in *Drosophila* by specifically inhibiting the activity of the pro-apoptotic protein, Hid (Bergmann et al., 1998; Kurada and White, 1998). Hid is believed to be a phosphorylation target of MAPK/ERK and contains several MAPK consensus phosphorylation sites (Bergmann et al., 1998). Hid induces apoptosis by promoting the polyubiquitination and degradation of DIAP1, consequently relieving inhibition of Caspases (Yoo et al., 2002).

Therefore Ras signalling promotes cell survival in *Drosophila* by indirectly increasing DIAP1 protein levels via Hid inhibition. In addition, the Ras pathway likely has other effects on cell survival, mediated via its inputs to other signalling pathways.

This introduction to the Ras pathway in *Drosophila* has focused mainly on eye imaginal disc development but the pathway regulates proliferation, survival and differentiation in a wide variety of contexts during development.

CHAPTER 2 Materials and methods

2.1 Genetics and immuno-histochemistry

2.1.1 General immunofluorescence protocol

3rd instar 'wandering' larvae of the relevant genotype were collected from vials and placed in a drop of 1xPBS (see solutions) on a silicon dissection pad. Eye-antennal or wing imaginal discs were dissected from larvae using micro-dissection tweezers. The eye-antennal discs were dissected and left attached to the mouthparts. Wing imaginal discs were dissected so that they remained attached to the trachea and anterior epidermis. This allowed the tissue to be seen while washing, thus avoiding losing material. Following dissection tissues were fixed with fresh periodate-lysine-paraformaldehyde (PLP) (see solutions) in glass depression wells for 20 minutes in the dark at room temperature. Tissues were then transferred to 1.5 ml eppendorf tubes and washed three times for 10 minutes at room temperature in PBT (PBS + 0.1% triton). Tissues were then permeabilized and pre-blocked by incubating for 1 hour at room temperature in PBT (PBS + 0.3% triton) containing 5% Normal Goat Serum (NGS) (MP Biomedicals). Following one wash in PBT (PBS + 0.1% triton), samples were incubated with primary antibody overnight at 4°C. All washes and antibody incubations were done with agitation on a rotating wheel.

The next day tissues were washed five times in PBT (PBS + 0.1% triton) and incubated with secondary antibodies for 2 hours at room temperature in PBT containing 5% NGS. Tissues were then washed a further five times in PBT and once in PBS for 10 minutes at room temperature. The PBS was then replaced with CitiFluor mounting medium (50% Glycerol, 50 % PBS) and tissues were transferred by pipette to a 1mm glass slide. Samples were then transferred using micro-dissection tweezers to a 15µl drop of Vectashield mounting medium (Vector Laboratories) on another 1mm glass slide. Eye-antennal discs and wing discs were then dissected away from the other remaining tissue and a coverslip was placed onto the slide. Imaging was done on an upright Zeiss

LSM510 Laser Scanning Microscope using 25x or 40x objectives and LSM510 software. Images were treated with Adobe Photoshop CS2.

2.1.2 Pupal retina immunofluorescence protocol

Pupal retina-brain complexes were dissected and immuno-labelled using a modified version of the Rubin Lab protocol (http://www.bio.com/protocolstools/protocol.jhtml?id = p19). Animals at the white pre-pupal stage were collected from crosses and transferred to new vials. The pupae were incubated at 25°C for 40-42 hours. Pupae were then transferred onto a silicon dissection pad where they were stuck to a piece of double sided sticky-tape such that the anterior end was secured and the posterior end accessible for dissection. Roughly one-third of the hard exterior cuticle was removed from the posterior end using micro-dissection tweezers. The pupae were then removed from the pupal case by pulling them out from the posterior end with micro-dissection tweezers. Dissected pupae were transferred immediately to a drop of PBS on the pad. A small dorsal to ventral incision was made in the soft cuticle at the anterior end using a fine razor blade. The retina-brain complexes were pushed out through this incision by pressing down on the middle of the pupae with micro-dissection tweezers to 'squeeze' out the contents. Soft tissue was washed away from the retina-brain complexes using a 20µl pipette, and complexes were transferred by 20 µl pipette to ice cold PBS in a glass depression well until the remaining pupae were dissected.

Pupal retina-brain complexes were immuno-labelled in much the same way as eye-antennal or wing imaginal discs (see General antibody staining protocol) except washes and antibody incubations were done in glass depression wells and liquid was removed from samples using a syringe. Following antibody staining pupal retina-brain complexes were transferred to 15µl Vectashield drops on 1mm glass slides and the retinas were dissected away from the brain.

2.1.3 Scanning electron microscopy (SEM)

Adult female flies of the relevant genotype were collected and transferred to fresh vials for 6 hours. They were then submerged in 10% ethanol for 30 minutes followed by

further 30 minute incubations in ethanol solutions of increasing concentration (30%, 50%, 70%, 90% and 100%). Samples were prepared and imaged by Anne Weston of the Cancer Research UK EM facility using a Jeol JSM 6700F Scanning electron microscope.

2.1.4 Mutagenesis by imprecise P-element excision

Shown below are cross schemes used to generate *dASPP* mutants by imprecise excision of second chromosome P-element insertions; *GE13722* was excised to generate the $dASPP^{d}$, $dASPP^{e}$ and $dASPP^{precise}$ lines (cross scheme A) and $P(XP)CG4302^{d03020}$ was excised to generate the $dASPP^{8}$ and $dASPP^{ctrl}$ lines (cross scheme B).

Cross scheme A:

P_0 ♂♂ *w ; GE13722(mw) / CyO* **X** *w ; Sp / CyO ; Δ2-3, Sb / TM6B* ♀♀

↓

F_1 ♂♂ *w ; GE13722(mw) / CyO ; Δ2-3, Sb / +* **X** *w ; Sp / CyO* ♀♀

↙

F_2 Single ♂ *w ; GE13722* / CyO* **X** *w ; Sp / CyO* ♀♀

Cross scheme B:

P_0 ♂♂ *w ; P(XP)CG4302*^{d03020} *(mw) / CyO* **X** *w ; Sp / CyO ; Δ2-3, Sb / TM6B* ♀♀

↓

F_1 ♂♂ *w ; P(XP)CG4302*^{d03020} *(mw) / CyO ; Δ2-3, Sb / +* **X** *w ; Sp / CyO* ♀♀

↙

F_2 Single ♂ *w ; P(XP)CG4302*^{d03020} ** / CyO* **X** *w ; dASPP*^{d} */ CyO* ♀♀

In cross scheme A, the P-element line (*GE13722*) is crossed to the transposase source (*Δ2-3*). Hybrid males (mosaic orange and white eyes) are selected from the F1 and crossed *en masse* to second chromosome balancer virgins (*Sp / CyO*). In the F2 generation, white-eyed excision males (*GE13722**) are selected and crossed individually to *Sp / CyO* virgins. Males are 'lifted' from this cross after 4 days and

screened for deletions by PCR. Once mutant chromosomes had been identified the relevant crosses to *Sp / CyO* were kept and progeny were mated *inter se* to obtain balanced mutant stocks. Cross scheme B is similar to cross scheme A except the F2 generation, white-eyed males (*P(XP)CG4302*^{d03020} *) were crossed to *dASPP*^{d} / *Cyo* and new deletions were recovered by screening for the *dASPP* phenotype.

2.1.5 Creating recombinant chromosomes

Shown below is a cross scheme that was used to generate recombinant chromosomes. The example shown is the generation of a recombinant second chromosome that has both an FRT site (*FRT,42D*) near the base of the 2R chromosome arm and the *dASPP*^{8} mutation, which is at a more distal location on 2R. This chromosome was used to generate *dASPP*^{8} LOF clones. A similar cross scheme was used to generate all recombinant chromosomes used in this work.

P_0 ♂♂ *dASPP*^{8} / *CyO* **X** *FRT,42D / FRT,42D* ♀♀

↘

F_1 ♂♂ *w ; Sp / CyO* **X** *dASPP*^{8} / *FRT,42D* ♀♀

↓

F_2 ♂♂ *FRT,42D(?), dASPP*^{8}*(?) / CyO* **X** *w ; Sp / CyO* ♀♀

In the first cross *FRT42D* and *dASPP*^{8} are bought together. Virgin females are selected in the F1 that have both *FRT42D* and *dASPP*^{8} in *trans* on the second chromosome and are identified by the absence of the dominantly marked *CyO* chromosome. These females are crossed *en masse* to *Sp/CyO* males and the meiotic recombination event occurs in the female germline. The F2 generation contains putative recombinant flies. F2 males are crossed to second chromosome balancer virgins, then 'lifted' after 4 days and screened for presence of both *FRT42D* and *dASPP8* by PCR. Crosses from recombinant males were kept and progeny were mated *inter se* to obtain recombinant stocks.

2.1.6 Density-controlled wing measurements

Crosses to obtain the relevant genotypes were initiated. Once the females were laying eggs (1-2 days), the flies were transferred to a container, which was inverted over an agar and apple juice substrate. Eggs were collected for 4-6 hours before the flies were removed. The embryos were kept at 25°C for 24 hours and then first instar larvae were collected. 30-50 (depending on the experiment) larvae were transferred to each yeasted vial and cultured at 25°C until eclosion. For some genotypes it was necessary to collect enough larvae for up to 8 vials (400 larvae) due the low expected frequency of that genotype in the F1. When the flies eclosed from the density-controlled crosses, the relevant genotype was collected and either put into 100% ethanol (for wing measurements) or anaesthetised (for weighing). Males were used for wing area and body weight measurements.

When it came to mounting the wings, flies were put into a glass depression well in ethanol and 'right hand' wings were removed with micro-dissection tweezers. Wings were dried on a piece of tissue then placed into a drop of Euparal (Sigma-Aldrich) on a slide. A coverslip was placed over the wings and the slides were dried overnight on a 65°C hotplate. Wings were digitally photographed using a LeicaDC200 camera on an MFIII dissection microscope. Wings were then measured using the Polygonal Lasso tool on Adobe Photoshop. Generally, the area of 20 male wings from different flies was measured for each genotype and the average wing size, standard deviation and Student's T-test p values were calculated using Excel.

2.1.7 Alignment of dASPP and Boa with homologs from other species

The alignment of dASPP-PA and Boa-PA with human, *A.gambiae* and *C.elegans* homologous proteins were done using SMART (http://smart.embl-heidelberg.de/) and blastp 2 sequences (http://www.ncbi.nlm.nih.gov/blast/bl2seq/wblast2.cgi)

2.2 Molecular biology and Biochemistry

2.2.1 DNA extraction protocol

Genomic DNA was prepared from adult flies either by using the DNeasy kit (Qiagen) and following manufacturers directions or by using a 'rapid' DNA extraction protocol. The latter involves homogenizing flies in 49 µl of SB buffer (see solutions) in 1.5ml eppendorf tubes using the handles of plastic inoculation loops. Samples were then transferred to a 200µl PCR tube and 1µl of 10µM Proteinase K (Invitrogen) was added. Samples were then run on the following PCR program:

1) 30 minutes at 37°C
2) 2 minutes at 95°C (to denature the proteinase K enzyme.)

2.2.2 PCR – Polymerase chain reaction

PCR products were amplified using Taq PCR Master-mix kit (Qiagen) and a PTC-200 peltier thermal cycler (MJ Research). For cloning PWO master-mix (Roche) was used due to its high fidelity. A typical PCR reaction of 50µl was composed of the following ingredients:

25µl Master-mix
1µl 5'-primer (20µM)
1µl 3'-primer (20µM)
1µl Template DNA (10-50ng)
22µl distilled H_2O

A typical PCR reaction was run on the following PCR program:

1) 95°C for 5 minutes.
2) 95°C for 40 seconds.
3) 60°C for 30 seconds.
4) 72°C for 1 minute per kb of product.
5) Go to step (2) - 32 cycles.
6) 72°C for 10 minutes.
7) 4°C forever.

PCR products were run on 1% Agarose Gels (TAE + 1% Agarose (Invitrogen) + 1μl of Ethidium Bromide (Roche)) and gels were photographed using an IMAGO compact imaging system (B and L systems).

2.2.3 DNA sequencing

DNA was sequenced by the Sequencing Service at Cancer Research UK using a 3730 DNA Analyzer (Applied Biosystems). Extension products were amplified and purified using the DyeEx Spin kit (Qiagen). Purified extension products were handed to the Sequencing Service for sequencing.

2.2.4 RNA extraction and RT-PCR

dASPP, *boa*, *tankyrase* and *actin* transcript analysis was done on total adult fly RNA isolated using the RNeasy mini kit (Qiagen) and following manufacturers instructions. RNA samples were quantified using a Nanodrop (Nanodrop). For each sample 0.5μg of RNA was reverse transcribed using the First Strand cDNA Synthesis System (Roche). 1μl of the cDNA template was used for RT-PCR using primers specific to the relevant transcripts. PCRs were run for 28 cycles and bands were resolved on 1% agarose gels.

2.2.5 *Drosophila* cell-culture

Drosophila Kc167 cells were cultured at 25°C in Schneiders medium (Gibco) + 10% FCS (foetal calf serum) (Gibco). Cells were split (1/6) every 3 days in fresh medium.

2.2.6 Cloning of dASPP, dCsk and Boa

dASPP-RA, dCsk-RB and Boa-RA were cloned using the Gateway system (Invitrogen). dASPP-RA cDNA was amplified using an EST (RE13301) as a template and the primers dASPP-5' RA and dASPP-3' no stop (see primers table). dCsk-RB cDNA was amplified using an EST (LP09923) as a template and the primers dCsk-5' RB and dCsk-3' RB (see primers table). Boa-RA was amplified using an EST (GH01133) as a

template and the primers Boa-5' and Boa-3' (see primers table). PCR products were then purified using a QIAquick PCR Purification kit (Qiagen) and ligated into the pENTR-topo vector (Invitrogen). The resulting plasmids were transformed into One-shot Top10 cells (Invitrogen) according to the manufacturers instructions, and plated onto Kanamycin (100ng/μl) selection plates, which were placed at 37°C overnight. Colonies were picked the following day and cultured in 5ml of L-broth (see solutions) overnight at 37°C with agitation. Mini-preps were done using the QIAquick Spin Mini-prep kit (Qiagen) and plasmid DNA was sequenced (see DNA sequencing) using primers supplied with the Gateway system (Invitrogen).

dASPP-RA, dCsk-RB or Boa-RA were then transferred from pENTR-TOPO to multiple Gateway expression vectors by the LR reaction. These included pActin 3xHA and pActin 6xMyc for the expression of tagged proteins in Kc167 cells, and pUASP for *UAS-dASPP* and *UAS-boa* transgenic generation. Following the LR reaction the resulting plasmids were transfected into One-shot Top10 cells (Invitrogen), which were plated on Ampicillin (100ng/μl) plates and placed at 37°C overnight. Colonies were picked and cultured for 8 hours at 37°C in 2ml L-broth. This 2ml culture was poured into 50ml of L-broth and placed at 37°C overnight with agitation. The following day midi-preps were performed using the High-speed Plasmid Midi and Maxi kit (Qiagen). The resulting plasmid DNA was quantified using the Nanodrop (Nanodrop), sequenced and stored at minus 20°C. All Gateway vectors were obtained from the Gateway Drosophila Vector Collection (Murphy lab, Carnegie Institution)

2.2.7 Immunoprecipitations (IPs) and Western blotting

The relevant plasmids were transfected into *Drosophila* Kc167 cells in 6 well plates using Effectene reagent (Qiagen) according to the manufacturers instructions, and cells were cultured at 25°C for three days. Cells were collected and lysed in 200μl of IP buffer (see solutions) for 20 minutes on ice. Samples were cleared by centrifugation at 14,0000 rpm at 4°C for 10 minutes. The supernatant was removed and proteins were quantified on an Eppendorf Biophotometer using Bradford reagent (Biorad). 150μg of protein was used for kinase assays and 500μg of protein was used for co-immunoprecipitations. $1/10^{th}$ of the total input was loaded on the gel to check

expression levels of tagged proteins (labelled input in figure 23 A and C). All the following steps were carried out at 4°C in the cold room.

Samples were pre-cleared by incubating protein samples in 250µl of IP buffer with 60µl of protein A/G sepharose beads for 1 hour with agitation on a spinning wheel. The beads were then spun down by centrifugation for 1 minute at 2000rpm. The supernatant was transferred to a clean 1.5ml eppendorf and 1µl of the relevant IP antibody was added (HA for dASPP or Boa IP, Myc for dASPP or dCsk IP and GFP for control IPs). Samples were then incubated for 1 hour with agitation to allow the antibody to bind to the relevant tagged protein. 80µl of a 50:50 resuspension of protein A/G sepharose beads were added and samples were incubated for 1 hour with agitation to allow the antibody to bind to the beads. The beads were then spun down and the supernatant was removed with a syringe and discarded. The beads were washed 3 times in 1ml of IP buffer for 2 minutes. Following each wash the beads were spun down and the supernatant removed. After the last wash beads were spun down and 15µl of SDS-PAGE sample buffer (Invitrogen) was added.

Samples were boiled at 70°C for 10 minutes and then resolved on SDS-PAGE gels (NuPAGE 4-12% Bis-Tris gels from Invitrogen) and proteins were transferred to PVDF membranes. Proteins were visualised by immunoblotting with the relevant antibodies and chemiluminescence was observed using the ECL-plus Western blotting detection system (Amersham Biosciences).

2.2.8 Kinase assay and quantification of dCsk activity

Cells were transfected with either dCsk-Myc alone (125ng DNA) or co-transfected with dCsk-Myc (125ng plasmid DNA) and dASPP-HA (125ng, 250ng or 375ng plasmid DNA) using Effectene reagent (Qiagen). dCsk-Myc was immunoprecipitated from cell lysates as described above. Following the 3 washes with IP buffer (see above) the beads were washed 3 times with 1ml of kinase assay buffer (see solutions). After the final wash, 10µl of kinase assay buffer, 10µCi of ^{32P}-ATP and 10µg of substrate (GST-Src42A^{K276R}, see below) were added to the beads. The samples were incubated for 20 minutes at 37°C to allow the immunoprecipitated dCsk to phosphorylate the substrate.

Then 15µl of sample buffer was added and samples were boiled at 70°C for 10 minutes to denature proteins. Samples were resolved by SDS-PAGE and gels were stained with coomassie blue to visualise GST-Src42A^{K276R} levels and then exposed for 20 minutes in the phosphorimager (Molecular Dynamics STORM 860) to quantify the radioactive signal, and thus dCsk kinase activity. The phosphorylation signal value was normalized to the efficiency of dCsk-Myc immunoprecipitation (1/5th of IP was kept after final IP buffer wash, see above, labelled 'IP myc' on figure 23 C), which was quantified using fluorescent secondary antibodies (see antibodies) and the Odyssey Infrared Imaging System (Li-COR Biosciences).

2.2.9 Generation of GST fusion proteins

A glutathione-S-transferase (GST)-dCsk fusion protein was produced. dCsk-RB was amplified using an EST template (LP09923) and the primers GST dCsk-5' and GST-dCsk-3' (see primers table). dCsk-RB was cloned into the BglII and XhoI sites of the pGEX4T1 vector (Pharmacia). The plasmid was transfected into BL21 pLysS (protease deficient) cells (Stratagene). 500ml bacterial cultures were grown until they reached the appropriate density (OD600=0.65). The culture flask was chilled on ice for 5 minutes, then 500µl of 1M IPTG was added to induce expression of GST-dCsk. Cultures were grown at 37°C for a further 3 hours to allow production of GST-dCsk. Cells were spun down at 4000rpm for 20 minutes and frozen on liquid nitrogen and thawed on ice. Cells were re-suspended in 10ml of lysis buffer (see solutions) and sonicated 3 times for 40 seconds on ice to break cell membranes. Cells were then spun down at 10,000rpm in a fixed-angle rotor. The supernatant was transferred to a clean 15ml conical flask and 500µl of Glutathione-sepharose beads (Pharmacia) were added. The sample was incubated for 30 minutes at 4°C with agitation to allow GST-dCsk to bind to the beads. The beads were then spun down for 1 minute at 4000rpm at 4°C and then washed 4 times for 5 minutes in lysis buffer. To recover GST-dCsk from the beads they were re-suspended in 500µl of thrombin re-suspension buffer (see solutions) containing 5mM reduced glutathione (which competes with the beads for GST-dCsk binding) and incubated for 5 minutes with agitation at 4°C. The beads were spun down and the supernatant was kept, this elution step was repeated once more and the eluates pooled. Samples were then dialysed overnight at 4°C in 4 litres of PBS. Samples were then

concentrated (Millipore, Centricon), quantified and aliquotted, frozen in liquid nitrogen and placed in a - 80°C freezer for storage.

This method was also used to produce GST-Src42A^{K276R} (the kinase assay substrate). dSrc42A was amplified from an EST (LD35329) using primers GST Src42A-5' and GST Src42A-3' (see primers table). dSrc42A was ligated into the EcoR1 and Xho1 sites of pGEX4T1 (Pharmacia). dSrc42A mutagenesis to generate a non-autophosphorylatable dSrc42A (Src42A^{K276R}, mutation of the ATP binding site) was done using unique restriction sites (Mfe1 and Stu1) and PCR fragments amplified from pGEX4T1-Src42A using the primers Src mut1-5', Src mut1-3', Src mut2-5' and Src mut2-3' (see primers table). The subsequent steps to produce GST-Src42A^{K276R} fusion protein were the same as used to generate GST-dCsk (see above). GST-Src42A^{K276R} was generated for the kinase assays (see above) so that the observed signal is the result of dCsk activity and not autophosphorylation.

2.2.10 GST pulldown

For the GST pull-down (see figure 23 B) *Drosophila* Kc167 cells were transfected with dASPP-HA. Cells were lysed in lysis buffer for 20 minutes and samples were cleared by centrifugation at 14,0000 rpm at 4°C for 10 minutes. Protein concentration was quantified using Bradford reagent (Biorad). 1/10th of the total protein after lysis was kept for the input (labelled input in figure 23 B). 500µg of total protein was incubated with either 10µg GST or 10µg GST-dCsk overnight at 4°C with agitation. Then 40µl of Glutathione-sepharose beads (Pharmacia) were added to the samples and incubated for 4 hours at 4°C with agitation to allow GST to bind. The beads were spun down for 2 minutes at 2000rpm, the supernatant was removed and discarded and the beads were washed 3 times in lysis buffer for 5 minutes at 4°C. Following the last wash, the beads were spun down and 15µl of sample buffer (Invitrogen) was added. Samples were boiled at 70°C for 10 minutes and spun down for 1 minute at 2000rpm. The supernatant was removed and samples were resolved by SDS-PAGE and proteins were transferred to PVDF membranes. Immuno-labelling blots with anti-HA revealed whether dASPP was present in either the GST or GST-dCsk pull-downs.

2.3 Solutions

10x Fly PBS – Phosphate buffered saline (1l).
76.1g NaCl
18.8g Na_2HPO_4 (sodium phosphate dibasic)
4.1g NaH_2PO_4 (sodium phosphate monobasic)
Add ddH2O up to 1l and autoclave.

TAE
40mM Tris Acetate
1mM EDTA

PLP (2% paraformaldehyde) fixative (10ml).
5ml ddH_20
3.75ml 0.2M $NaHPO_4$ pH7.2
1.25ml 0.2M Na_2HPO_4
0.18g lysine
- Remove 2.5ml. To the remaining 7.5ml add:
1.25ml ddH_2O
1.25ml 16% paraformaldehyde
25mg $NaIO_4$ (sodium periodate)
PBS / PBT

SB Buffer (for genomic fly preps).
10mM Tris-Hcl pH 8.2
1mM EDTA
25mM NaCl

IP Buffer.
50mM Tris pH8
150mM 5M NaCl
1% NP40
1mM EGTA
50mM NaF
10mM Vanadate
1% Phosphatase Inhibitor Cocktail II (Sigma)
1 pill / 10ml of Protease Inhibitor Cocktail (Roche)

Kinase Assay buffer
20mM Hepes
20mM $MgCl_2$
4mM NaF
1 pill / 10ml of Phosphatase Inhibitor Cocktail II (Sigma)
2mM DTT

Lysis buffer.
50mM Tris pH7.2
50mM NaCl
5mM $MgCl_2$
1mM DTT

Thrombin resuspension buffer.
50mM Tris pH8
150mM Nacl
2mM $MgCl_2$
1mM DTT

L-Broth (1 litre)
10g tryptone
5g yeast extract
5g NaCl
1ml 1M NaOH

L-agar
L-broth + 1% Agar
add 100mg/ml of appropriate antibiotic.

2.4 Table of genotypes shown in figures

Figure number	Genotype
9 C	*w ; GMRsav,wts / +*
9 C'	*w ; GE13722 / + ; GMRsav,wts / +*
9 C''	*w ; Df(2R)Exel6072 / + ; GMRsav,wts / +*
11 B – B'	*yw, eyFLP ; FRT42D, dASPP^{d} / FRT42D, ubi-GFP*
11 C	See figure for genotypes.
11 C – C'	*yw, eyFLP ; FRT42D, dASPP^{8} / FRT42D, ubi-GFP*
11 D	See figure for genotypes.
12 B	*w* and *w ; dASPP^{d} / CyO*
12 C	*w* and *w ; dASPP^{8} / dASPP^{8}*
12 D	*w ; dASPP^{8} / dASPP^{8}*
13 A – A''	*w ; dASPP^{ctrl} / dASPP^{ctrl}*
13 B – B''	*w ; dASPP^{8} / dASPP^{8}*
14 A	*w ; dASPP^{ctrl}*
14 B	*w ; dASPP^{8}*
14 C	*w ; dASPP^{ctrl}* and *dASPP^{8}*
14 D	Rescue - *w ; dASPP^{8} / dASPP^{8} ; da-Gal4 / UAS-dASPP*
15 A	See figure for genotypes.
15 B	*w ; FRT42D, ASPP^{d} / FRT42D, ASPP^{d}*
15 B'	*w ; FRT42D, ASPP^{d} / FRT42D, ASPP^{d} ; FRT82B, wts^{X1} / +*
15 C	*yw, eyFLP ; FRT42D, dASPP^{d} / FRT42D, ubi-GFP*
15 C'	*yw, eyFLP ; FRT42D, dASPP^{d} / FRT42D, l(2)cl-R11*
15 C''	*yw, eyFLP ; FRT42D, dASPP^{d} / FRT42D, l(2)cl-R11 ; FRT82B, wts^{X1} / +*
16 A – A''	*yw, hsFLP ; FRT42D, hpo$^{42-47}$ / FRT42D ubi-GFP ; DIAP-LacZ / +*
16 B – B''	*yw, hsFLP ; FRT42D, dASPP^{d} / FRT42D ubi-GFP ; DIAP-LacZ / +*
16 C – C''	*yw, hsFLP ; FRT42D, hpo$^{42-47}$ / FRT42D ubi-GFP ; CycE-LacZ / +*
16 D – D''	*yw, hsFLP ; FRT42D, dASPP^{d} / FRT42D ubi-GFP ; CycE-LacZ / +*
17 A – A''	*w ; FRT82B, dCsk^{1jd8} / +*

Figure number	Genotype
17 B – B''	*w ; dASPP^{8} / dASPP^{8}*
17 C – C''	*w ; dASPP^{8} / dASPP^{8} ; FRT82B, dCsk^{1jd8} / +*
17 D – D''	*w ; dASPP^{8}, btk^{KO2006} / dASPP^{8} ; FRT82B, dCsk^{1jd8} / +*
17 E – E'	*w ; FRT82B, dCsk^{1jd8} / FRT82B, dCsk^{1jd8}*
18 A – A''	*w ; dASPP^{d} / dASPP^{d} ; FRT82B, dCsk^{1jd8} / +*
18 B – B''	*w ; dASPP^{8} / dASPP^{8} ; FRT82B, wts^{X1} / +*
19 A – A'''	*w ; dASPP^{8} / + ; puc^{E69} / +*
19 B – B'''	*w ; FRT82B, dCsk^{1jd8} / puc^{E69}*
19 C – C'''	*w ; dASPP8 / + ; FRT82B, dCsk^{1jd8} / puc^{E69}*
19 D – D'''	*w ; dASPP^{8} / dASPP^{8} ; puc^{E69} / +*
20 A – A''	*w ; ptcGal4 / UAS-GFP*
20 B – B''	*w, dCskIR ; ptcGal4 / UAS-GFP*
20 C – C''	*w, dCskIR ; ptcGal4, dASPP^{8} / UAS-GFP, dASPP^{8}*
20 D – D''	*w, dCskIR ; ptcGal4, dASPP^{8} / UAS-GFP, dASPP^{8} ; UASdASPP / +*
20 E – E''	*w, dCskIR ; ptcGal4, dASPP^{8} / UAS-GFP, dASPP^{8} ; UASdASPP / +*
21 A	*w, dCskIR ; ptcGal4 / UAS-GFP*
21 B	*w, dCskIR ; ptcGal4, dASPP^{8} / UAS-GFP, dASPP^{8}*
22 A – A''	*w, dCskIR ; ptcGal4, dASPP^{8} / UAS-GFP, dASPP^{8}*
22 B – B''	*w, dCskIR ; ptcGal4, dASPP^{8} / UAS-GFP, dASPP^{8} ; UAS-DIAP1 / +*
24 A – A''	*yw, eyFLP ; FRT82B, dCsk^{1jd8} / FRT82B, ubi-GFP*
25 A – A'	*w ; dASPP^{ctrl} / dASPP^{ctrl}*
25 B – B'	*w ; dASPP^{8} / dASPP^{8}*
25 C – C'	*w ; dASPP^{8}, btk^{KO2006} / dASPP^{8}*
25 D – D'	*w ; dSrc64B^{KO} / dSrc64B^{KO}*
25 E – E'	*w ; dASPP^{8} / dASPP^{8} ; dSrc64B^{KO} / dSrc64B^{KO}*
28 B – B'	*yw, eyFLP ; FRT82B, boa^{6} / FRT82B, ubi-GFP*
28 C	See figure for genotypes.
29 A – A''	*yw ; boa^{ctrl} / boa^{ctrl}*

Figure number	Genotype
29 B – D	*yw ; boa^6 / boa^6*
30 A	*yw ; boa^{ctrl} / boa^{ctrl}*
30 B	*yw ; boa^6 / boa^6*
30 C	*yw ; boa^{ctrl} / boa^{ctrl} and yw ; boa^6 / boa^6*
30 D	*yw ; boa^{ctrl} / boa^{ctrl} and yw ; boa^6 / boa^6*
31 A- A''	*yw, eyFLP ; FRT82B, boa^6 / FRT82B, ubi-GFP*
32 A – A''	*yw ; boa^6 / boa^6*
32 B – B''	*yw ; FRT82B, $dCsk^{ljd8}$, boa^6 / boa^6*
33 A – A''	*w*
33 B – B''	*yw, hsFLP / UAS-$EGFR^{act}$; act>CD2>Gal4, UAS-GFP* (FLPout) / +
34 A – A''	*yw, hsFLP ; act>CD2>Gal4, UAS-GFP* (FLPout) / + ; *UAS-pntP1* / +
34 B – B''	*yw, hsFLP ; act>CD2>Gal4, UAS-GFP* (FLPout) / + ; *UAS-pntP2* / +
34 C – C''	*yw, hsFLP ; act>CD2>Gal4, UAS-GFP* (FLPout) / + ; *UAS-ttk69* / +
34 D – D''	*yw, hsFLP ; act>CD2>Gal4, UAS-GFP* (FLPout) / + ; *UAS-ttk88* / +
35 A – A''	*yw, eyFLP ; FRT82B, ttk^{1e11} / FRT82B, ubi-GFP*
35 B – B''	*yw, eyFLP ; FRT82B, ttk^1 / FRT82B, ubi-GFP*
35 C – C''	*yw, eyFLP ; FRT42D, yan^{ex1} / FRT42D, ubi-GFP*

2.5 Table of antibodies used

Primary Antibody	Species	Concentration	Source
β-Galactosidase	Mouse	1:1000	Promega
Discs-Large (Dlg)	Mouse	1:500	DSHB
Cleaved Caspase 3	Rabbit	1:500	Cell signalling
DIAP1	Mouse	1:500	Bruce Hay
dASPP38 (a.a 1006-1020)	Rat	1:1000	Eurogentec, Belgium
dASPP39 (a.a 733-746)	Rat	1:1000	Eurogentec, Belgium
Boa803 (a.a 218-232)	Guinea Pig	1:300	Eurogentec, Belgium
c-Myc (9E10): sc-40	Mouse	1:5000 (blot)	Santa Cruz
c-Myc (A-14): sc-789	Rabbit	1:5000 (blot)	Santa Cruz
HA (3F10)	Rat	1:5000 (blot)	Roche
GFP	Mouse	Only used for IPs	Cancer Research UK
Secondary antibody	**Species**	**Concentration**	**Source**
anti-mRRX	Mouse	1:500	Jackson
anti-rbRRX	Rabbit	1:500	Jackson
anti-ratRRX	Rat	1:500	Jackson
anti-gpRRX	Guinea pig	1:500	Jackson
anti-ratAlexa633	Rat	1:500	Molecular probes
anti-mouseFITC	Mouse	1:500	Jackson
IRdye700DX-labelled	Rat	1:6000	Rockland
IRdye800-labelled	Rabbit	1:6000	Rockland

2.6 Table of primers used

Primer Name	Primer sequence	Application
dASPP-3'a	GAACGTGCGACAGAGAGGGCAG	detects *dASPP*^{d}
dASPP-5'a	CGATCGCCAACGCCGCAACAAG	detects *dASPP*^{d}
2.2-5'	CCTTTTGTATTTGGAGGCGGAGGC	detects *dASPP*^{8}
dASPP-3'b	TAGATCGTTTCGTTTGGGCCTCTCTG	detects *dASPP*^{8} and *dASPP*^{ctrl}
dASPP-5'b	GGTCATCAGGTGACCATGGTAACAG	detects *dASPP*^{ctrl}
2.2-3'	CGGAATGTTCTCCTTTGCGAAAGGC	used to define *dASPP*^{8}
2.3-3'	CAACGCTTCGCTTAACGCGAAGG	used to define *dASPP*^{8}
2.3-5'	CGAAAGTCTGTAGTTTTCGCCTGGAC	used to define *dASPP*^{8}
ATG-3'	CCAGTGGATTTTTATGTTCGTGCTGCG	used to define *dASPP*^{8}
ATG-5'	GTTTGTCTGTTTGCTGATTCTGACTTCTC	used to define *dASPP*^{8}
Boa-5'a	GGTTTTACACAAATTTGTGCTTCAGTGTGCAC	detects *boa*^{2}
Boa-5'b	AGGAGAAGCAGAAGCAGAAGAGGAG	detects *boa*^{6}
Boa-3'a	GTTGTGGCTGCTATGCTGATCGTAGTC	detects *boa*^{2} and *boa*^{6}
RT-3'b	CTGCTGATGATGGGTGTTGGCCT	*dASPP* RT-PCR
RT-RA-5'b	GAGCCGACGAACACTTTGGATGAAAT	*dASPP* RT-PCR (RA)
RT-RB-5'b	ATCCTCCGCGTCGTCCTCAACAT	*dASPP* RT-PCR (RB)
BoaRT-5'a	ACCTGGCCCCCAATGAGAATCCA	*boa* RT-PCR
BoaRT-5'b	TGTCAGTGTTGTGCAGAGCCTGGT	*boa* RT-PCR
TankRT-5'a	CTCATCCTTTCGATATTCGCCGGTCAAT	*tankyrase* RT-PCR
TankRT-3'a	AGCTCTTCGAGGCCTGCAAAACG	*tankyrase* RT-PCR
actRT-5'	CACCCTGAAGTACCCCATTGAGCAC	*actin* RT-PCR
actRT-3'	CAGACGCAGGATGGCATGGGGAAGG	*actin* RT-PCR
dASPP-5' RA	CACCATGAAGGAGCCGACGAACACTTTGG	Cloning dASPP-RA
dASPP-3'nostop	ATCGCTGAAGTGCGGCGAATGCGGC	Cloning dASPP-RA
dCsk-5' RB	CACCATGAACAGCCACGCGACTGCC	Cloning dCsk-RB
dCsk-3' RB	CGCCGTGGCATTGTTCAGTAGC	Cloning dCsk-RB
Boa-5'	CACCATGGAGCTGAAAGTTTGGGTCGAGGG	Cloning Boa-RA
Boa-3'	TTAAACCCACACACCATGAGGAT	Cloning Boa-RA
GST Src42A-5'	GGAATTCGGTAACTGCCTCACCACACAGAAGG	Cloning Src42A
GST Src42A-3'	CCGCTCGAGTCAGTTACAGGCTTCTCGATCTGGA	Cloning Src42A
Src mut1-5'	CAATTGGACGAAGGCGGCTTCTTCA	Src42A^{K276R} generation
Src mut1-3'	TTTCAGAGTTCTAATTGCCACAGGT	Src42A^{K276R} generation
Src mut2-5'	ACCTGTGGCAATTAGAACTCTGAAA	Src42A^{K276R} generation

Primer Name	Primer sequence	Application
Src mut2-3'	AGGCCTGCGCCTCTTTGTAGTCGCT	Src42A^{K276R} generation
GST dCsk-5'	GAAGATCTAACAGCCACGCGACTGCCACGCAG	GST-dCsk generation
GST dCsk-3'	CCGCTCGAGTCACGCCGTGGCATTGTTCAGT	GST-dCsk generation

CHAPTER 3 *Drosophila* ASPP

3.1 A screen for novel components of the *Drosophila* Hippo signalling pathway

3.1.1 The basis of the screen

The Hippo signalling pathway was identified using genetic screens in *Drosophila* and has been the focus of intensive research over the past 5 years. The Hippo pathway has potent growth regulatory functions and negatively regulates the size of organs by carrying out dual roles of promoting apoptosis and exit from the cell cycle (Harvey and Tapon, 2007). At least 11 components of the pathway have now been identified (see figure 7). When this project began in 2003, the only known members of the pathway were Hippo (Hpo), Salvador (Sav) and Warts (Wts). For this reason I carried out a candidate-based screen with the aim of identifying novel components of the Hippo pathway.

The *Drosophila* eye is well suited to studying the control of tissue size. Firstly, it is a non-essential organ so phenotypes can be examined in adult flies. Secondly, even minor changes in cell numbers disrupt the lattice to produce visible phenotypes. Over-expression of *sav* and *wts* using the eye-specific *GMR* (Glass Multimer Reporter) driver (*GMRsav,wts*) results in a small, rough eye phenotype as a result of increased cell death (see figure 9 C). *GMRsav,wts* was used a sensitised background for screening for novel components of the Hippo pathway. Candidate alleles (see below) were crossed into this background and tested for their ability to modify the eye phenotype.

Candidates were selected based on their interaction with Hpo, Sav or Wts in a published yeast 2-hybrid screen. A genome-wide yeast 2-hybrid screen performed by Curagen Inc. provides an online protein-protein interaction map for all *Drosophila* proteins (Giot et al., 2003). Using Hpo, Sav or Wts as a starting point, interaction 'webs' were constructed that included primary and secondary interactions (an example is shown in figure 9 A). A 'score' (0-1) is given for each interaction, which represents the

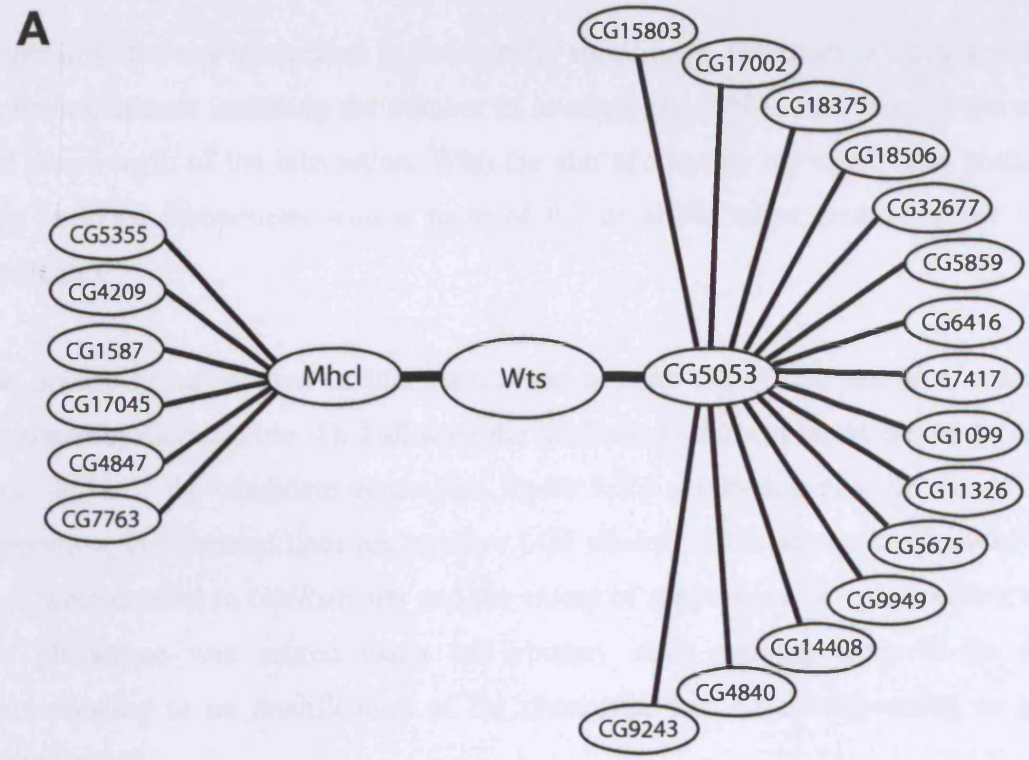

B	no. of genes	genes with EP	suppressors	enhancers
Sav interactors	29	22	6	1
Hpo interactors	32	27	9	2
Wts interactors	23	17	5	0
total	84	66	20	3

Figure 9: A genetic screen for novel components of the Hippo signalling pathway. (A) Candidate genes were selected based on their interaction with either Hpo, Sav or Wts in a published 2-hybrid screen performed by Curagen. Shown are the primary and secondary interactors of Wts, similar interaction 'webs' were constructed for Hpo and Sav (not shown). P-element insertions in the candidate genes were obtained, and tested for their ability to modify a Hpo pathway overexpression phenotype (see C). (B) Summary of the results of the screen. (C) The small, rough eye phenotype resulting from overexpression of *sav* and *wts* (*GMRsav,wts*). (C') An example of a strong suppressor of the *GMRsav,wts* phenotype. *GE13722*, which is a P-element insertion in *CG18375* gene (see A) dominantly suppresses the *GMRsav,wts* phenotype. (C") *Df(2R)Exel6072*, a deficiency for *CG18375* also dominantly suppresses the phenotype.

probability that any interaction is biologically significant. The score is calculated based on several criteria including the number of overlapping cDNAs recovered in the screen and the strength of the interaction. With the aim of filtering out some false positives I only included interactions with a score of 0.3 or above when generating the list of candidates.

The second resource used in this screen was a large transposon insertion collection generated by Genexel Inc. This allowed me to obtain P-element insertions in the loci of about 80% of the candidate genes (see figure 9 B). As P-elements can disrupt gene expression, the Genexel lines are putative LOF alleles for the screen candidates. These lines were crossed to *GMRsav,wts* and the extent of suppression or enhancement of the eye phenotype was scored using an arbitrary scale ranging from -2 to +2 (0 corresponding to no modification of the phenotype and +2 corresponding to strong enhancement).

3.1.2 Results of screen and confirmation of hits

As *GMRsav,wts* gives a phenotype resulting from activation of the Hippo pathway, it is expected that suppressors will be positively involved in the pathway and enhancers will antagonize the pathway. Of the 66 candidates screened, 20 suppressors and 3 enhancers of the phenotype were identified (see figure 9 B). I selected 2 of these genes, *CG18375* and *CG5053* for further analysis. These genes were selected because the *CG18375* insertion was the strongest suppressor of *GMRsav,wts* (see below). The *CG5053* insertion also suppressed *GMRsav,wts* (data not shown) and this gene links *CG18375* to *wts* in the yeast 2-hybrid interaction 'web' (see figure 9 A). The *CG18375* and *CG5053* insertions both suppressed *GMRsav,wts* suggesting that these genes function as negative regulators of tissue size and may do so by regulating the Hippo pathway.

The strongest suppressor of the *GMRsav,wts* phenotype was *GE13722* (see figure 9 C and C'), a P-element insertion upstream of the *CG18375-RA* transcription start site. This insertion dominantly suppressed *GMRsav,wts* and partially rescued both the eye size and morphology. The genetic interaction was confirmed using another *CG18375* allele; *Df(2R)Exel6072* is a deficiency stock that removes *CG18375* and also suppresses the

GMRsav,wts phenotype (see figure 9 C''). However, *Df(2R)Exel6072* suppressed *GMRsav,wts* to a lesser degree than *GE13722*. This was a surprising result as *GE13722* is likely a hypomorphic *CG18375* allele and *Df(2R)Exel6072* is a null allele for the gene. Unfortunately, no deficiency was available for *CG5053* so this interaction could not be confirmed.

The Genexel insertions are EP elements, which are P-elements containing a basal promoter and 14 UAS sequences (Rorth, 1996). By supplying Gal4 one can use EP elements to drive tissue-specific expression of endogenous genes near the insertion site. *en-Gal4* places Gal4 under the control of the *engrailed* promoter and expression in wings is restricted to the posterior compartment. Crossing *en-Gal4* to *GE13722* leads to *CG18375* over-expression, and results in an 11% reduction in the size of the posterior wing compartment (data not shown). This result provides further evidence that *CG18375* is a negative regulator of tissue size.

3.2 Characterization of *CG18375/dASPP*

3.2.1 *CG18375* homologs

CG18375 shows significant homology to the mammalian *ASPP* family genes, which include *ASPP1*, *ASPP2* and *iASPP*. For this reason *CG18375* was named *dASPP (Drosophila ASPP)* and will be referred to as *dASPP* in the following text. Proteins of the ASPP family have been characterised and are implicated in regulation of the tumour suppressor p53 (Trigiante and Lu, 2006). Mammalian ASPP proteins possess a C-terminal region containing an SH3 domain, an ankyrin domain and a proline rich region (see figure 10). The SH3 and ankyrin domains are present in dASPP and show a high degree of conservation with the equivalent ASPP1 and ASPP2 domains (see figure 10). The proline rich region is not conserved. *dASPP* also shows homology to the *C.elegans ASPP* homolog, *ape-1*, and an unnamed *A.gambiae* gene (see figure 10).

Figure 10: Domain structure of dASPP and alignment with homologs from other species. Alignment of dASPP-PA (NP_788423.1) with *A.gambiae* (XP_555930.1), *C.elegans* (NP_505955.1) and human (CAC83011 for hASPP1 and CAC83012 for hASPP2) homologs. dASPP has a conserved C-terminal region containing an SH3 domain and an ankyrin domain. Percentage amino acid identity within the conserved domains is indicated. The alignments and figure were done by Julien Colombani.

3.2.2 *dASPP* mutagenesis, excision of *GE13722*

As *GE13722* is inserted upstream of *dASPP* within the promoter region, it is likely to constitute a weak hypomorphic *dASPP* allele. Indeed, *GE13722* homozygous flies are viable and fertile with no obvious phenotype. Therefore, to analyse the function of *dASPP*, I generated stronger LOF alleles by imprecise excision of *GE13722*.

First, the *GE13722* insertion site was confirmed. This was achieved by amplifying a PCR product from *GE13722* genomic DNA using a P-element specific primer and a genomic primer near the reported insertion site. A band of the expected size was detected (data not shown) and sequenced. This confirmed that the reported insertion site was correct, and *GE13722* is inserted 27bp upstream of the transcription start site of the *dASPP* RA transcript (see figure 11 A).

Once the insertion site was confirmed, I initiated the cross scheme to excise the P-element and generate mutants (see materials and methods for cross scheme). Putative mutant males were crossed individually to second chromosome balancer virgin females (*Sp/CyO*) to retain mutant chromosomes. Once the cross had 'taken' the males were removed and screened by PCR using primers dASPP-5'a and dASPP-3'a (see primers table), which flank the P-element insertion site (see figure 12 A). I screened for a downward band-shift of the PCR product, which indicates that a genomic deletion has occurred during P-element excision.

In the vast majority of cases the expected 2kb band size was seen, this can be the result of four possible events. The first possibility is a precise excision event where the P-element is completely removed without deleting surrounding genomic DNA. The second possibility is an imprecise excision event where the deletion of sequence between the primers is too small to detect by PCR. The third is an imprecise event where a small piece of P-element sequence remains at the insertion site but this is not detectable by PCR. The fourth possibility is an imprecise excision event creating a large deletion. If a large deletion removes one or both of the primer binding sites then no product will be generated from the mutant chromosome. However, a product of the expected size will be amplified from the homologous balancer chromosome. Therefore large deletions are not identified using this method of screening.

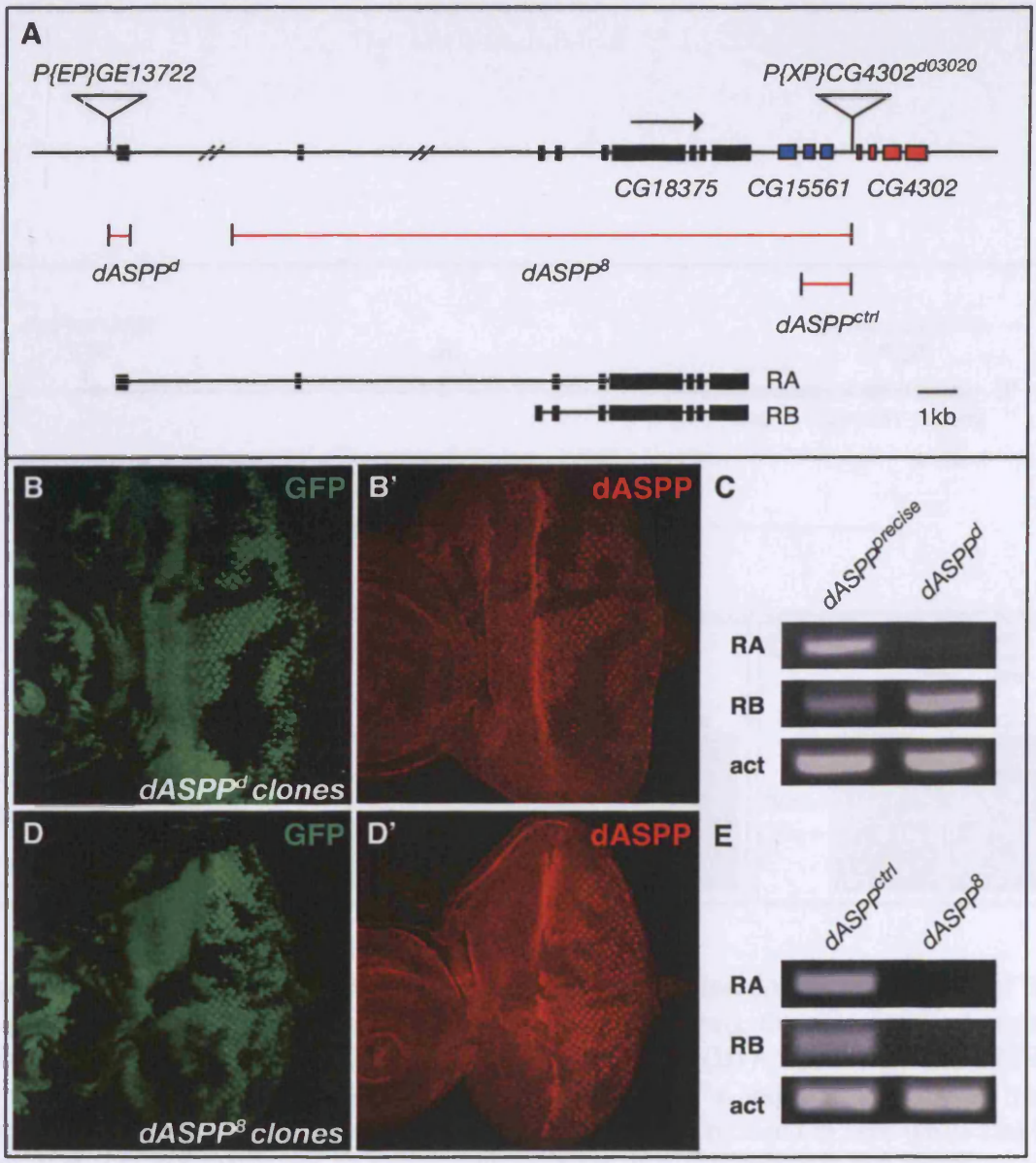

Figure 11: *dASPP* mutagenesis by imprecise P-element excision. (A) A map of the *dASPP* locus showing the two predicted transcripts (RA and RB), the insertion sites of the P-elements used (*P(EP)GE13722* and *P(XP)CG4302^{d03020}*) and the deletions generated (*dASPP^{d}*, *dASPP^{8}* and *dASPP^{ctrl}*). *P(EP)13722* was excised to generate *dASPP^{d}*, which is a 533bp deletion. *P(XP)CG4302^{d03020}* was excised to generate *dASPP^{8}* and *dASPP^{ctrl}*. *dASPP^{8}* is a 29kb deletion that removes *CG15561* and all of the *dASPP* coding sequence. *dASPP^{ctrl}* is a 1.1kb deletion and removes most of *CG15561*. (B-E) Confirmation of the *dASPP* alleles. (B) An eye-antennal imaginal disc bearing *dASPP^{d}* clones, marked by absence of GFP. (B') Note the strong reduction of dASPP antibody staining (red) in *dASPP^{d}* clones. (C) RT-PCR on samples prepared from either control (*P(EP)GE13722* precise excision) or *dASPP^{d}* adult flies. In *dASPP^{d}* samples the RA transcript is not detected but the RB transcript is still expressed. *actin* (act) transcript levels provide a positive control. (D) An eye-antennal imaginal disc bearing *dASPP^{8}* clones, marked by absence of GFP. (D') Note the strong reduction of dASPP antibody staining (red) in *dASPP^{8}* clones. (E) RT-PCR on samples prepared from either *dASPP^{ctrl}* or *dASPP^{8}* adult flies. In *dASPP^{8}* samples neither the RA nor RB transcript is detected.

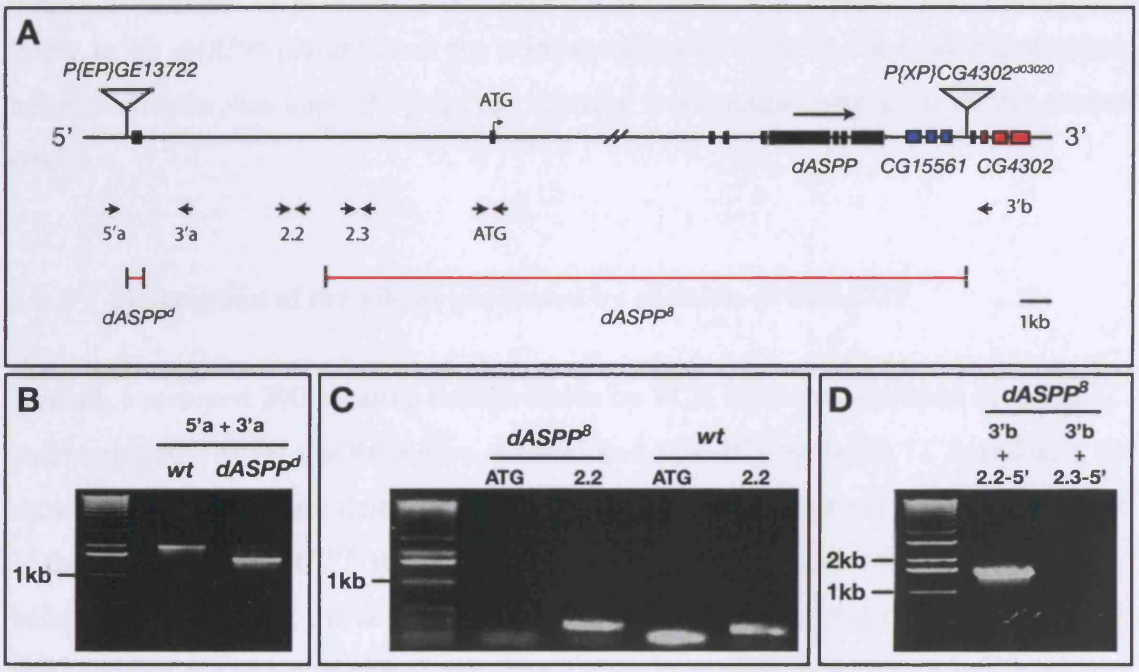

Figure 12: Molecular characterization of the *dASPP* alleles. (A) An illustration of the *dASPP* locus showing the location of the P-elements excised, the primers used (small arrows) and the breakpoints of the *dASPP* alleles generated. (B) A PCR on genomic DNA from either wildtype (wt) or $dASPP^{d}$ flies using primers 5'a and 3'a. This primer pair amplifies a product of ~2kb from wt DNA. This product is reduced in size when amplified from $dASPP^{d}$ DNA due to the 533bp deletion. (C) Determining the limits of the $dASPP^{8}$ deletion. The ATG PCR product fails to be amplified from $dASPP^{8}$ genomic DNA but the 2.2 PCR product is amplified suggesting that the 5' deletion breakpoint is between the 2.2 and ATG primer pairs. (D) Confirmation of the $dASPP^{8}$ allele. Using the 5'primer of the 2.2 primer pair and 3'b (see A) it is possible to amplify a band from $dASPP^{8}$ but not wt (not shown) DNA. No product is amplified when the 3'b primer is used in combination with the 5'-primer of the 2.3 primer pair.

For some of the putative mutant chromosomes screened an upward band-shift was observed, this occurs when the P-element excises imprecisely and part of its sequence remains at the insertion site. In a small percentage of cases (~1%), a downward band shift was observed. This indicates that an imprecise excision event has occurred that results in deletion of genomic DNA between the screening primers. These males are likely to be *dASPP* mutants and the corresponding cross to the second chromosome balancer virgins was kept. Progeny of the cross were mated *inter se* to obtain mutant stocks.

3.2.3 Description of the alleles generated by excision of *GE13722*

Overall, I screened 200 putative mutant males by PCR following excision of *GE13722* and identified 2 novel *dASPP* alleles, $dASPP^{d}$ and $dASPP^{e}$ (see figure 11 A and data not shown). These alleles are deletions of 533bp and 1070bp respectively and remove most of the 5'UTR of the *dASPP* RA transcript. Both of these deletions result in a downward band shift when using the screening primers (see figure 12 B and data not shown). A faint band of the expected size is seen (see figure 12 B) resulting from amplification of the product from the balancer chromosome. The shifted bands were cut out of the gels and sequenced to determine the exact breakpoints. A precise excision ($dASPP^{precise}$) was also recovered to use as a control in genetic experiments. This was identified by sequencing PCR products amplified using the dASPP-5'a and dASPP-3'a primers (see primers table) from homozygous flies obtained from 10 different putative mutant lines and selecting a precise excision line. As expected the precise excision line has no visible phenotype.

Both $dASPP^{d}$ and $dASPP^{e}$ are homozygous viable alleles and the homozygous flies showed visible phenotypes including rough eyes and enlarged wings (see below for phenotypic characterisation). This was the first clear indication that *dASPP* is a regulator of tissue size and the phenotype observed (overgrowth) agrees with the genetic screening data suggesting that *dASPP* is a negative regulator of tissue size.

As $dASPP^{d}$ and $dASPP^{e}$ only affect the sequence of the RA transcript, it was possible that they are not null alleles as the RB transcript is intact. Indeed, the RB transcript can

still be detected by RT-PCR on *dASPP*^{d} flies, whereas the RA transcript was absent (see figure 11 C). To address this question the *dASPP* alleles were crossed to a *dASPP* deficiency (*Df(2R)Exel6072*), which is a null for *dASPP*. However the phenotype of *dASPP*^{d} / *Df(2R)Exel6072* (data not shown) is comparable the phenotype of *dASPP*^{d}/*dASPP*^{d} indicating that *dASPP*^{d} behaves at least like a strong hypomorphic allele or a null. Similar results were obtained for *dASPP*^{e}. However, in order to fully appreciate the *dASPP* mutant phenotype it was important to generate a null allele and ascertain whether removing both *dASPP* transcripts elicits a stronger phenotype. For this reason I undertook another round of P-element excisions.

Initially, *GE13722* was excised again with the aim of generating a larger deletion that removes all the *dASPP* coding sequence. However, the distance from the *GE13722* insertion site to the start of the *dASPP* coding sequence common to both transcripts is roughly 30kb. As deletions this large are not common and cannot be screened for easily by PCR, a different strategy was used when screening for mutant chromosomes.

As the *dASPP*^{d} allele generated is viable over a *dASPP* deficiency (*Df(2R)Exel6072*), it was possible to screen for a *dASPP* null allele by crossing all putative mutant males to *dASPP*^{d}/*CyO* virgins and looking for the distinctive *dASPP* phenotype in the F1 generation. This method of screening is much faster as it does not rely on PCR and I was able to screen 1000 putative mutant chromosomes relatively quickly.

At least 10 new *dASPP* alleles were identified, including 3 new lethal *dASPP* alleles. The lethal alleles were balanced over *CyO-GFP* so that the stage of lethality could be assessed. The lethal *dASPP* alleles generated were all lethal at the first instar larval stage and homozygous mutant embryos (non GFP) were collected for PCR analysis. Disappointingly, the lethal *dASPP* alleles were all very large deletions removing *dASPP* and several neighbouring genes. For example, a PCR product from the *tudor* locus was not amplified from homozygous mutant embryos from the lethal *dASPP* excision stocks (data not shown). As *tudor* is the fifth gene downstream of *dASPP*, these alleles delete several genes and are not useful. Additionally, the new viable *dASPP* alleles were genotyped by PCR but none of the deletions generated were large enough to reach the *dASPP* coding sequence common to both transcripts. Therefore, I was not able to generate a useful *dASPP* null allele by excising *GE13722* as the deletions generated

were either not large enough to fully delete *dASPP* or too large to be useful. Due to this difficulty I decided to excise a different P-element, which is inserted closer to the *dASPP* coding sequence common to both transcripts.

3.2.4 *dASPP* mutagenesis, excision of *P(XP)CG4302^{d03020}*

The nearest available insertion to the *dASPP* coding sequence is *P(XP)CG4302^{d03020}*. This P-element is inserted downstream of *dASPP* and downstream of the neighbouring gene, *CG15561* (see figure 11 A). Having confirmed the insertion site of this transposon, I began the cross scheme to generate excisions (see materials and methods for cross scheme). Roughly 1000 putative mutants were screened for phenotypes when crossed to *dASPP^{d}/CyO* and stocks were established for any deletions recovered. Several of the mutant stocks generated by excision of *P(XP)CG4302^{d03020}* were homozygous viable with phenotypes similar to *dASPP^{d}*. PCR analysis revealed that one of these homozygous viable alleles, *dASPP^{8}*, might remove all of the *dASPP* coding sequence (see figure 12 A). A PCR product near the start codon (amplified using ATG primers, see primers table and figure 12 A) of the RA transcript fails to amplify from *dASPP^{8}* genomic template (see figure 12 C) suggesting that the 5'-breakpoint extends beyond this point. A PCR product roughly 7kb to the 5'-side of the ATG product (amplified using 2.2 primers, see primers table and figure 12 A) does amplify from *dASPP^{8}* genomic DNA (see figure 12 C). This suggests that the *dASPP^{8}* 5'-breakpoint is between the ATG and 2.2 primer pairs. By using a primer to the 3'-side of the *P(XP)CG4302^{d03020}* insertion site (dASPP-3'b primer, see primers table and figure 12 A) in combination with the 5'-primer of the 2.2 primer pair (see primers table and figure 12 A) I was able to amplify a band of roughly 1.5kb from *dASPP^{8}* but not wild-type genomic template (see figure 12 D). This band was purified and sequenced to determine the exact breakpoints of the *dASPP^{8}* deletion.

dASPP^{8} is a 29.5kb deletion to the 5'-side of *P(XP)CG4302^{d03020}* that removes *CG15561* and all of the *dASPP* protein coding sequence. Therefore *dASPP^{8}* is a null *dASPP* allele and as it is homozygous viable I concluded that *dASPP* is not an essential gene. *dASPP^{8}* is a double mutant for *dASPP* and *CG15561*, therefore a single *CG15561* mutant was recovered to use as a control in genetic experiments. *dASPP^{ctrl}* is a 1.1kb

deletion to the 5'-side of *P(XP)CG4302*^{d03020} that removes most of the *CG15561* coding sequence (see figure 11 A). *dASPP*^{ctrl} is a homozygous viable and fertile line with no obvious phenotype suggesting that the *dASPP*^{8} phenotype is due to deletion of *dASPP* rather than *CG15561*.

3.2.5 Confirmation of dASPP mutants

The 2 most useful *dASPP* mutations, *dASPP*^{d} (the RA specific allele) and *dASPP*^{8} (the null allele) were recombined onto the *FRT42D* chromosome, which carries an FRT site near the base of the 2R chromosome arm. *dASPP*^{d} and *dASPP*^{8} clones were generated in eye-antennal imaginal discs and the level of dASPP protein within the clones was examined using a dASPP antibody (dASPP38, see materials and methods). The dASPP38 antibody was generated by Eurogentec and raised in rats against a peptide corresponding to amino acids 1006-1020 of dASPP. In *dASPP*^{d} clones (see figure 11 B-B') and *dASPP*^{8} clones (see figure 11 D-D') a strong reduction in dASPP protein was observed. This result confirms that my alleles are *dASPP* mutants and also confirms that the dASPP38 antibody specifically recognises dASPP. Perhaps surprisingly, the loss of dASPP protein in *dASPP*^{d} and *dASPP*^{8} clones is comparable. The fact that removal of the RA transcript is sufficient to largely abolish dASPP protein expression suggests that the predicted RB transcript may be either not expressed or expressed at very low levels.

The *dASPP* alleles were also confirmed by RT-PCR following generation of cDNA templates from whole fly RNA preps. This confirmed that *dASPP*^{d} is indeed an RA specific mutant as the RA transcript is not detected in *dASPP*^{d} samples (see figure 11 C). The RB transcript is detected in *dASPP*^{precise} and *dASPP*^{d} samples suggesting that this transcript is actually expressed (see figure 11 C). One possibility is that the RB transcript is expressed either at very low levels and this accounts for the strong reduction of dASPP protein observed in *dASPP*^{d} clones. Alternatively, the RB transcript may not be expressed in the eye. Intriguingly, the level of RB transcript appears to be higher in *dASPP*^{d} than *dASPP*^{precise} samples, although the significance of this is not known. As expected, neither the RA nor the RB transcript is detected in *dASPP*^{8} samples (see figure 11 E). Therefore the RT-PCR results confirm that *dASPP*^{d} is an RA specific mutant and that *dASPP*^{8} removes both transcripts.

3.2.6 *dASPP* loss of function results in a large, rough eye phenotype

$dASPP^{d}$ and $dASPP^{8}$ are both viable mutations and homozygous flies show visible phenotypes including large, rough eyes, large wings and excess thoracic macrochetes. Scanning electron micrographs (SEMs) of *dASPP* mutant eyes show that *dASPP* LOF results in a large, rough eye phenotype (see figure 13 A, B and C). Interestingly, the $dASPP^{d}$ eye phenotype appears to be slightly stronger than the $dASPP^{8}$ eye phenotype. I quantified the average number of ommatidia in $dASPP^{ctrl}$ and $dASPP^{8}$ eyes and show that *dASPP* mutant eyes contain more ommatidia than control eyes (see figure 13 A and B). In the developing eye, a differentiation front called the morphogenetic furrow (MF) sweeps across the eye-disc during the third larval instar (Held, 2002). The passage of the MF sets the number of ommatidia, such that increased proliferation before this stage results in an increase in final ommatidia number. $dASPP^{8}$ eyes contain significantly more ommatidia (796 ± 24 per eye, n=7, $p<0.003$) than $dASPP^{ctrl}$ eyes (747 ± 25 per eye, n=7) suggesting that proliferation is accelerated in *dASPP* mutant eyes and that this contributes to the observed increase in eye size. Higher magnification images reveal that *dASPP* mutant eyes show disorganization of the ommatidial lattice and an abnormal arrangement of bristle cells (see figure 13 A', B' and C').

The phenotype of *dASPP* mutant eyes was also examined at the pupal stage using a Discs-large antibody to mark cell membranes in pupal retinas at 40-44h APF (see figure 13 A'' and B''). In wild-type (or $dASPP^{ctrl}$) retinas, the ommatidiae, which are the units of the compound eye, consist of 8 photoreceptor cells (not visible at this apical plane of focus), 4 cone cells and 2 primary pigment cells (Held, 2002). These hexagonal units are separated from each other by 6 secondary pigment cells occupying the sides of the hexagon, 3 tertiary pigment cells occupying three of the vertices, and 3 bristle cells occupy the other three vertices. $dASPP^{8}$ retinas are mis-patterned and clustering of bristle cells is commonly observed (arrow in figure 13 B''). Frequently, bristles are missing from positions near the cluster. This suggests that the clustering phenotype may be the result of cells failing to maintain appropriate cell-cell contacts and moving out of their niche rather than overproduction of bristle cells. Additionally, in wild-type (or $dASPP^{ctrl}$) retinas, each bristle cell always contacts three secondary inter-ommatidial cells (inset in figure 13 A''). In $dASPP^{8}$ mutant retinas bristle cells may contact 4 or more secondary inter-ommatidial cells (inset in figure 13 B''). This disrupts the regular

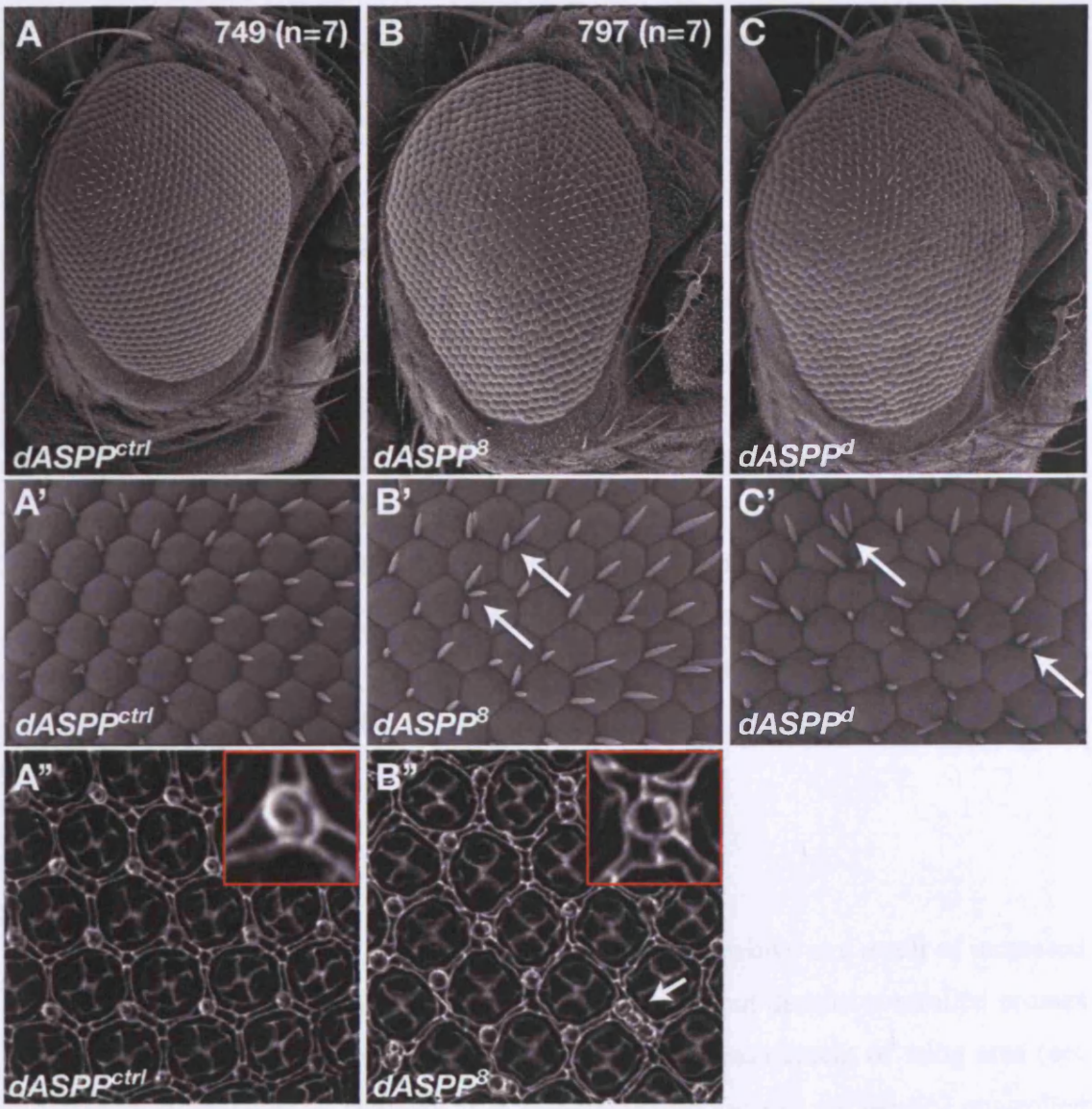

Figure 13: *dASPP* loss of function results in a large, rough eye phenotype. (A) Scanning electron micrograph (SEM) of a $dASPP^{ctrl}$ adult eye (180x). The average number of ommatidia per eye is indicated. (B) SEM of a $dASPP^{8}$ / $dASPP^{8}$ adult eye (180x), note the large size compared to the $dASPP^{ctrl}$ eye and the rough appearance. The average number of ommatidia per $dASPP^{8}$ eye is indicated and is significantly higher ($p<0.01$) than the number of ommatidia per $dASPP^{ctrl}$ eye. (A') High magnification (1000x) SEM of a $dASPP^{ctrl}$ eye to show the regular arrangement of bristles. (B') High magnification (1000x) SEM of a $dASPP^{8}$ eye. Irregularities in the arrangement of bristles are observed and bristles commonly cluster together (arrows). (C and C') The $dASPP^{d}$ eye phenotype is very similar to the $dASPP^{8}$ eye phenotype. (A") $dASPP^{ctrl}$ pupal retina at 40h after puparium formation (APF) stained with a Discs-large (Dlg) antibody to outline cells. The inter-ommatidial cells form a regular hexagonal lattice and bristle cells always contact three secondary inter-ommatidial cells (inset). (B") $dASPP^{8}$ pupal retina at 40h APF stained with anti-Dlg. The regularity of the lattice is disrupted and bristle cells may contact four inter-ommatidial cells (inset). Another phenotype of $dASPP^{8}$ mutant retinas is bristle clustering (arrow).

hexagonal lattice seen in wild-type retinas and ommatidiae in *dASPP*^{8} retinas often have five vertices as opposed to six.

The phenotype observed in *dASPP*^{8} retinas is probably the consequence of several phenomena. There is a minor increase in the number of inter-ommatidial cells (approximately one extra cell per ommatidium). This may be the result of either delayed cell cycle exit or reduced apoptosis of inter-ommatidial cells during the early pupal stages. The effect of *dASPP* LOF on cell cycle exit and inter-ommatidial cell apoptosis was not directly tested as such a minor defect is unlikely to be detectable using BrdU incorporation or TUNEL staining. The increase in inter-ommatidial cell number cannot account for the patterning defects observed. The retinal mis-patterning in *dASPP*^{8} eyes is probably also the result of an adhesion defect as clustering of bristles and abnormal arrangements of cells are observed. As described later dASPP is regulator of *Drosophila* SFKs, which are heavily implicated in cell-cell adhesion processes.

3.2.7 *dASPP* functions as a tumour suppressor gene

dASPP^{d} and *dASPP*^{8} homozygous mutants also have large wings as a result of increased proliferation. This phenotype was quantified by carrying out density-controlled crosses at 25°C to obtain the required genotypes, followed by measurement of wing area (see materials and methods for details). It is important that crosses are density controlled when quantifying organ or animal size as final size is affected by the availability of nutrients during the larval growth phase. In density-controlled experiments carried out by myself, I found that *FRT,dASPP*^{d} wings (n=20) are on average 11.7% larger than control (*dASPP*^{precise}) wings (n=20) (see figure 15 A). In a separate experiment I found that *dASPP*^{8} wings (n=20) are on average 7.8% larger than control (*dASPP*^{ctrl}) wings (n=20). Interestingly, in these experiments the *dASPP*^{d} allele has a stronger phenotype than the *dASPP*^{8} null allele. This difference in strength of phenotype between the alleles is also observed in the eye; *dASPP*^{d} seems to result in a stronger rough eye phenotype (see figure 13 B and C).

The large wing phenotype of *dASPP* mutants was confirmed in density-controlled experiments carried out by Julien Colombani (see figure 14). In this experiment it was

Figure 14: dASPP is a negative regulator of tissue size. Density controlled crosses were performed at 25°C to obtain the genotypes indicated and adult wing area was determined. (A-C) *dASPP* mutant wings (B) are larger than $dASPP^{ctrl}$ wings (A). (D) Quantification of body weight, wing area and wing hair density of $dASPP^{ctrl}$ and $dASPP^{8}$ flies. $dASPP^{8}$ flies are heavier than controls and have larger wings (** indicates that $p<0.01$, using a student's t-test), the hair density is similar to controls suggesting that $dASPP^{8}$ wings contain more cells rather than larger cells. $dASPP^{8}$ overgrowth phenotypes are rescued by ubiquitous *dASPP* expression. The data and figure were generated by Julien Colombani.

found that *dASPP*^{8} wings (n=20) are on average 11.8% larger than *dASPP*^{ctrl} wings (n=20) (see figure 14 A-D). This increase in *dASPP*^{8} wing area is more significant than the increase observed in the previous experiment (7.8%) but different medium was used, which may affect the phenotype. Regardless, each experiment showed independently that *dASPP*^{8} mutant wings are larger than control wings. Little developmental apoptosis occurs in the developing wing disc, therefore an increase in wing size can be attributed to either increased proliferation or increased cellular growth. Each cell in the wing secretes a hair, or trichome, and the density of wing hairs can be used as a measure of cell size. Importantly, the density of wing hairs in *dASPP*^{8} (n=12) and *dASPP*^{ctrl} (n=12) wings is comparable (see figure 14 D) suggesting that the size of cells is not affected by loss of *dASPP*. Therefore, proliferation is increased in *dASPP* mutants, and adult wings contain more cells of normal size. This is in agreement with the result of the ommatidial counts, which indicated that increased proliferation occurs in *dASPP* mutant eyes.

Julien Colombani also quantified the adult body weight and in density-controlled crosses *dASPP*^{8} flies (n=100) are 6.1% heavier than dASPP^{ctrl} flies (n=130) (see figure 14 D). This is in agreement with the eye and wing phenotype characterization suggesting that *dASPP* functions as a negative regulator of tissue and animal size. Both the wing size and body weight are rescued by ubiquitous expression of *dASPP* under the control of the *daughterless* (*da*) promoter using the Gal4-UAS system (see figure 14 D). Ubiquitous expression of *dASPP* in a *dASPP* mutant background results in similar wing size and body weight to control flies. *dASPP* expression also rescues the rough eye phenotype of *dASPP*^{8} mutants (Julien Colombani, personal communication). This confirms that the observed phenotypes are indeed due to loss of *dASPP*.

dASPP mutants have excess thoracic macrochetes, although this phenotype has not been quantified it is observed in *dASPP*^{d} and *dASPP*^{8} homozygous mutants. Wild-type and *dASPP*^{ctrl} have 4 large macrochete bristles towards the posterior end of the thorax. *dASPP* mutants typically have one or two extra macrochetes. Caspases also have non-apoptotic functions, which include controlling the number of macrochetes. In *dark* mutants ectopic macrochetes are observed (Kanuka et al., 2005). Therefore it is possible that dASPP leads to a minor increase in Caspase activity (possibly indirectly via DIAP1

regulation), which is not significant enough to cause cell death but instead affects the number of macrochetes on the scutellum.

3.3 The relationship between dASPP and the Hippo pathway

3.3.1 Genetic interactions between dASPP and Hippo pathway components

As *dASPP* was identified in a screen for novel components of the Hippo signalling pathway, I used the mutant alleles generated to test for genetic interactions with the Hippo pathway. The phenotype of *dASPP* mutants indicate that dASPP, like members of the Hippo pathway, is a negative regulator of tissue size. However, the overgrowth phenotype of *dASPP* mutants is much less severe than the phenotype of *hpo*, *sav* or *wts* mutants. This suggests that if dASPP is a novel component of the Hippo pathway it only plays a minor role in the control of tissue growth by Hippo signalling.

The large wing phenotype of *dASPP* mutants was used to test for genetic interactions with components of the Hippo pathway. LOF of Hippo pathway components in the wing has been shown to cause overgrowth (Harvey and Tapon, 2007). Therefore if dASPP is involved in Hippo signalling then *hpo* or *wts* mutants should enhance the large wing phenotype of *dASPP* mutants. In this experiment the *FRT42D,ASPP^{d}* recombinant chromosome was used and adult *FRT42D,ASPP^{d}* wings were 16.3% larger than *white* (*w*) wings, 18% larger than *FRT42D* wings and 11.7% larger than *dASPP^{precise}* wings (see figure 15 A). *FRT42D,ASPP^{d}* is a recombinant chromosome and the control with the most similar genetic background is *FRT42D* as over half of the *FRT42D,ASPP^{d}* chromosome is derived from the *FRT42D* chromosome. However, *white* (w) and *dASPP^{precise}* were also included as additional controls. All three control genotypes had a comparable wing area although *dASPP^{precise}* wings were slightly larger than *FRT42D* or *white* wings. For the purpose of this experiment it does not matter which control is used so the *white* wing area was taken as the value to which the wing area of other genotypes was normalised (see figure 15 A).

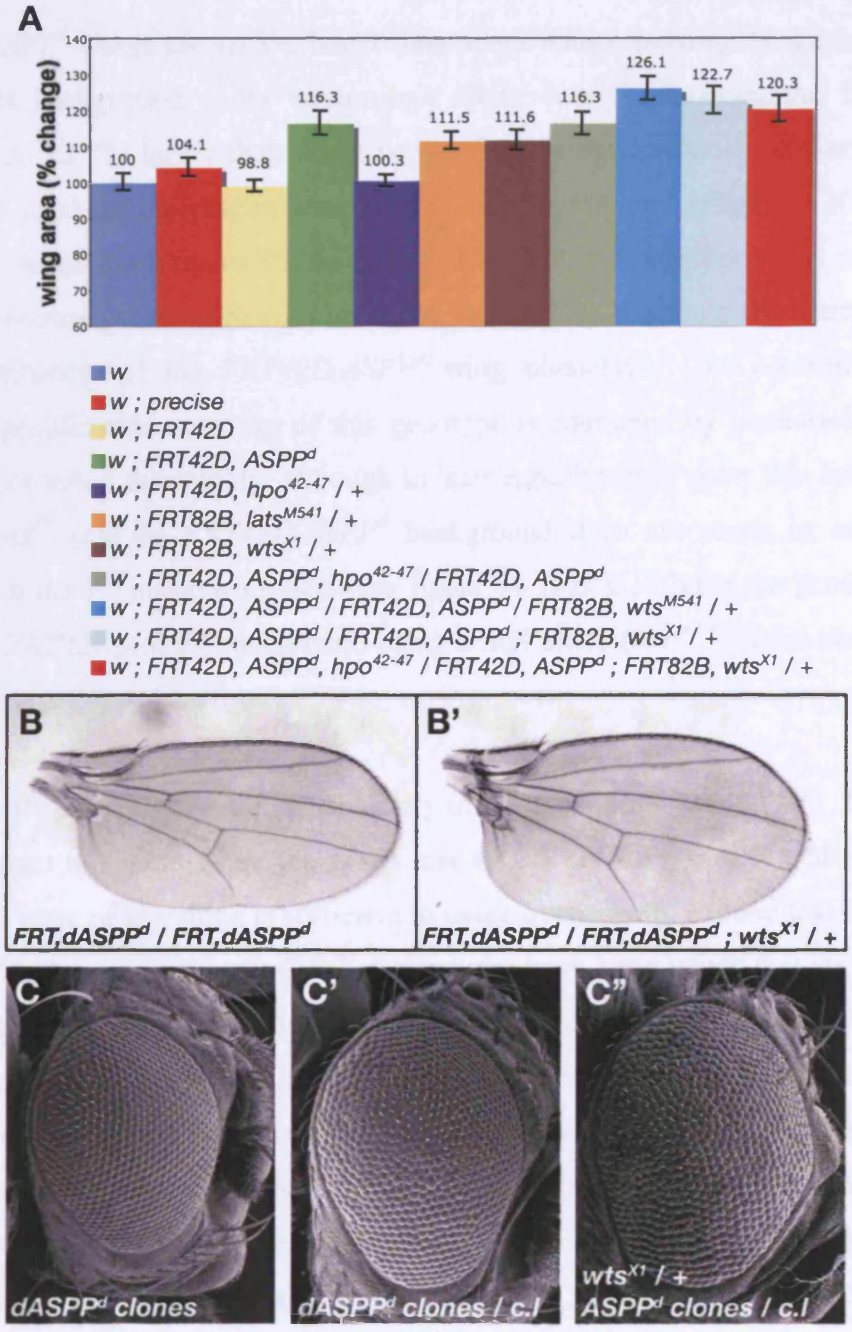

Figure 15: Genetic interactions between *dASPP* and Hippo pathway members. (A) The large wing phenotype of *dASPP*^{d} mutants was used to screen for genetic interactions with the Hippo pathway. The genotypes tested are indicated in the legend. Crosses were carried out in a density controlled manner at 25°C and twenty male wings were measured for each genotype. (B-B') An example of the increase in wing area observed when the gene dosage of *wts* is reduced in a *dASPP*^{d} mutant background. (C-C") *wts* mutations also enhance the rough eye phenotype of *dASPP* mutants. SEMs of adult eyes (180x). (C) Generating *dASPP*^{d} clones in the eye using *eyFLP* does not significantly alter adult eye morphology and only small patches of mutant tissue are observed. (D) However, generating *dASPP*^{d} clones in the eye over a cell lethal (c.l) FRT chromosome disrupts eye morphology and large clones are recovered. (C") This phenotype is clearly enhanced by removing one copy of *wts*.

FRT42D,ASPP^{d} wings are 16.3% larger than *white* wings; halving the gene dosage of *wts* in this background using an amorph allele (*wts*^{X1}) increases the large wing phenotype to 22.7% larger than *white* wings. Surprisingly, when a weaker *wts* allele (*wts*^{M541}) is used the increase in wing area is even greater and wings are 26.1% larger than *white* wings (see figure 15 A, B and B'). This was unexpected as *wts*^{X1} has a considerably stronger overgrowth phenotype the *wts*^{M541}, so should theoretically be the stronger enhancer of the *FRT42D,ASPP*^{d} wing phenotype. One possibility is that excessive proliferation in wings of this genotype is countered by increased apoptosis. This was not tested thoroughly, although in later experiments I show that introducing a copy of *wts*^{X1} into an *FRT42D,ASPP*^{d} background does not result in considerable apoptosis in the 3rd instar wing disc (see figure 18 B-B'). Halving the gene dosage of *hpo* in an *FRT42D,ASPP*^{d} background using a null allele (*hpo*$^{42-47}$) does not affect the large wing phenotype (see figure 15 A).

Therefore, it appears that *dASPP* genetically interacts with *wts* but not *hpo*. However, it was important to also measure the wings size of *wts* heterozygotes to address whether loss of one copy of *wts* alone is sufficient to cause overgrowth. I found that this was the case, *wts*^{X1} heterozygotes or *wts*^{M541} heterozygotes have large wings that are 11.5% and 11.6% larger than *white* wings respectively (see figure 15 A). This result suggests that the enhancement of the *dASPP* large wing phenotype when *wts* is compromised may be due to additive rather than synergistic effects. In the case of *wts*^{M541}, the additional increase in wing area seen when this mutation is introduced into a *dASPP* mutant background can be accounted for by the increase in wing area of *wts*^{M541} heterozygotes. One possibility is that *dASPP* and *wts* regulate wing size by independent mechanisms and when both are compromised the resulting phenotype is the sum of each phenotype. Alternatively, this experiment may not reveal the full extent of the interaction. For example, if excessive proliferation leads to increased apoptosis in *dASPP-wts* compromised discs then the final wing size will be affected. Therefore it is difficult to conclude whether *dASPP* genetically interacts with *wts* from the results of this experiment. The fact that *dASPP* showed no interaction with *hpo* in this experiment suggests that dASPP is not a general regulator of Hippo pathway signalling but may be regulating Wts functions that are independent of Hpo.

Although the interaction between *dASPP* and *wts* in the wing appears to be due to additive effects, a more convincing genetic interaction is observed in the eye (see figure 15 C-C''). Generating $dASPP^{d}$ clones specifically in the eye using *eyFLP* does not significantly alter adult eye morphology and only small patches of clonal tissue are observed (see figure 15 C). However, generating $dASPP^{d}$ clones over a cell lethal FRT chromosome to give the clones a growth advantage disrupts eye morphology and large clones are recovered in adults (see figure 15 C'). If a copy of wts^{X1} is introduced into this genetic background the eye phenotype is noticeably enhanced (see figure 15 C''). The size of the eye is increased and the roughness is enhanced. This is a convincing genetic interaction, as heterozygosity for wts^{X1} does not produce any visible eye phenotype (data not shown). Therefore, in this case, it cannot be argued that the genetic interaction is due to additive effects and I conclude that *dASPP* and *wts* do genetically interact.

3.3.2 dASPP loss of function does not affect Hippo pathway targets

I continued to explore the relationship between dASPP and the Hippo pathway by examining the expression of Hippo pathway transcriptional targets in *dASPP* mutant clones. *DIAP1* (*Drosophila Inhibitor of Apoptosis 1*) and *cyclinE* are both transcriptional targets of Yki (Huang et al., 2005). In *hpo*, *wts*, *sav*, or *MATS* mutant clones, Yki is in the nucleus and drives transcription of target genes including *DIAP1* and *cyclinE*. This can be visualised using transcriptional reporters. *DIAP-LacZ* is an enhancer trap resulting from insertion of a P-element containing the *LacZ* gene into the first intron of the endogenous *DIAP1* gene. *CyclinE-LacZ* is a synthetic construct comprised of 16.4kb of the *cyclinE* promoter placed upstream of the *LacZ* gene (Jones et al., 2000). I confirmed that *hpo* LOF results in transcriptional upregulation of *DIAP1* and *cyclinE* by examining expression of their reporters in hpo^{42-47} clones in the eye. *DIAP-LacZ* (see figure 16 A-A'') and *cyclinE-LacZ* (see figure 16 C-C'') are, as expected, upregulated in hpo^{42-47} clones as visualised by β-Gal staining. These genotypes also provided a positive control for the experiment. Conversely, in $dASPP^{d}$ clones I did not observe any upregulation of either *DIAP-LacZ* (see figure 16 B-B'') or *cyclinE-LacZ* (see figure 16 D-D''). One obvious explanation is that dASPP simply is not a component of the Hippo pathway. An alternative explanation is that dASPP is a

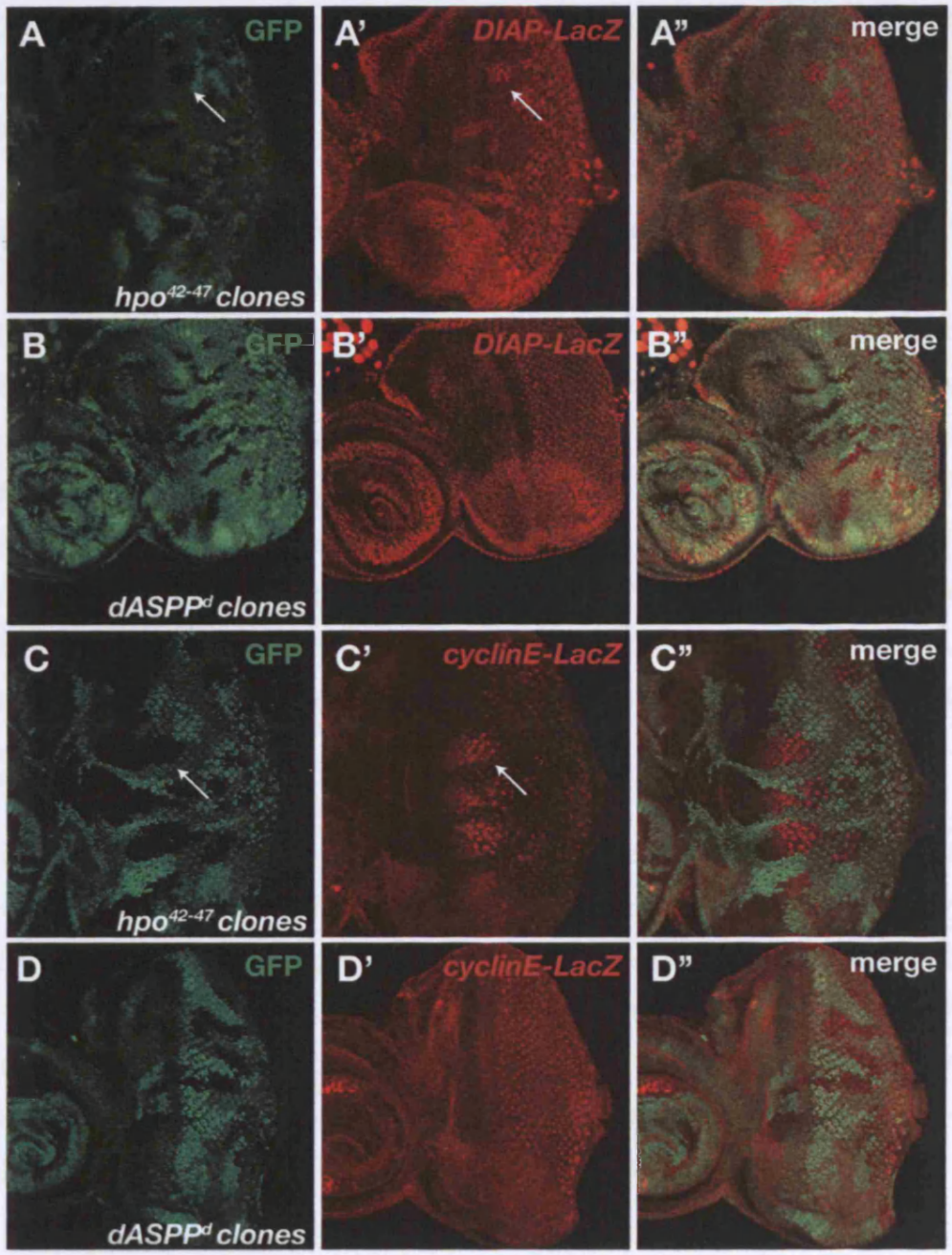

Figure 16: Hippo pathway readouts are not affected by loss of *dASPP*. *DIAP1* is transcriptionally regulated by the Hippo pathway and *DIAP-LacZ* can be used as a read-out of pathway activity. (A-A") Expression of the *DIAP-LacZ* reporter is increased in hpo^{42-47} clones as indicated by Beta-Gal staining (red). (B-B") Expression of the *DIAP-LacZ* reporter is unchanged in $dASPP^{d}$ clones. *cyclinE* is also a transcriptional target of the Hippo pathway. (C-C") Expression of a *cyclinE-LacZ* reporter is increased in hpo^{42-47} clones as indicated by Beta-Gal staining (red). (D-D") *cyclinE-LacZ* is not obviously elevated in $dASPP^{d}$ clones. The fact that Hippo pathway readouts are unaffected in *dASPP* clones suggests that dASPP is not a major contributor to the pathway. In A-D mutant clones are marked by absence of GFP. Arrows in A and C indicate examples of hpo^{42-47} clones with elevated *DIAP-LacZ* and *CyclinE-LacZ* respectively.

component of the Hippo pathway but its LOF phenotype is not strong enough to induce detectable changes in the expression of targets. To address these possibilities a more sensitive readout of pathway activity would be required.

It was surprising to find that the *dASPP* mutants I generated did not show a convincing genetic interaction with the Hippo pathway, because the original P-element stock (*GE13722*), which is presumably a very weak *dASPP* allele, strongly suppresses the *GMRsav,wts* phenotype. This suggests that *GE13722* represented a 'false positive' in my screen and that the suppression of *GMRsav,wts* observed is not due to loss of dASPP function but instead due to secondary mutation(s) on the *GE13722* chromosome. This view is supported by the fact that the precise excision line ($dASPP^{precise}$), which is essentially wild-type for *dASPP*, also strongly suppresses *GMRsav,wts*. Additionally, the *dASPP* null allele ($dASPP^{8}$), which was generated from a different genetic background, does not appreciably suppress *GMRsav,wts* (data not shown).

In summary, it was not possible to firmly conclude whether dASPP plays a role in the Hippo pathway. The fact that heterozygosity for *wts* enhances the eye phenotype of *dASPP* mutants is the strongest argument that dASPP plays a role in the Hippo pathway. However, in the wing, interactions between *dASPP* and *wts* are merely additive rather than synergistic and *dASPP* shows no interaction with *hpo*. Additionally, known targets of the Hippo pathway are not affected by loss of dASPP. Therefore, if dASPP does play a role in the Hippo pathway it is certainly a minor role.

3.4 dASPP genetically interacts with dCsk

3.4.1 The basis for testing interactions between dASPP and dCsk

The lack of convincing evidence suggesting that dASPP functions in the Hippo pathway led me to investigate whether the dASPP growth regulatory functions are mediated through another tumour suppressor pathway. For several reasons a strong candidate pathway was the dCsk/SFK pathway, which has also been shown to negatively regulate the size of tissues (Read et al., 2004). Firstly, *dASPP* phenotypes are highly similar to

dCsk phenotypes. The strength of the *dASPP* overgrowth phenotype is more similar to the *dCsk* phenotype than *hpo* or *wts* phenotypes; *dCsk* mutants die as giant pupae whereas *hpo* and *wts* mutants are lethal at an early larval stage. Also the retinal mis-patterning phenotype observed in *dASPP* mutants is highly reminiscent of the mis-patterning phenotype reported for *dCsk* mutant retinas (Vidal et al., 2006). Secondly, although *dCsk* mutant tissues or animals have overgrowth phenotypes, discrete patches of *dCsk* mutant cells do not overgrow; instead cells delaminate from the epithelial layer and undergo apoptosis (Vidal et al., 2006). The result of this is that *dCsk* mutant clones are eventually eliminated from tissue during the course of development. Similarly, *dASPP* mutant flies are overgrown, however, when *dASPP* clones are generated they do not have any apparent growth advantage over control clones (data not shown). This suggests that loss of *dCsk* or *dASPP* in discrete patches results in a similar phenomenon. However, *dASPP* clones are not completely eliminated during development in the same way as *dCsk* clones are. This may be due to the fact that *dCsk* has a stronger phenotype than *dASPP*. Thirdly, dCsk has been reported to phosphorylate Wts and *dCsk* genetically interacts with *wts* (Stewart et al., 2003). As I have shown, *dASPP* also genetically interacts with *wts* in certain contexts; it is possible that dASPP indirectly regulates Wts through dCsk. For these reasons I decided to address whether *dASPP* and *dCsk* genetically interact and uncovered a strong relationship between these genes, the rest of the characterization of dASPP focused on exploring this relationship.

3.4.2 dASPP-dCsk deficient wing discs show ectopic apoptosis

Reducing *dCsk* function in a *dASPP* mutant background by introducing a strong *dCsk* allele ($dCsk^{1jd8}$) results in a striking notched wing phenotype (see figure 17 C''). This wing notching of $dASPP^{8}$ mutants lacking one copy of *dCsk* is due to ectopic apoptosis. I observed large patches of cell death in the wing pouch of 3rd instar wing discs as visualised using an antibody directed against cleaved (activated) Caspase 3 (see figure 17 C and C'). This wing notching phenotype is only observed when *dASPP* and *dCsk* mutations are combined. Very little apoptosis occurs in wing discs of *dCsk* heterozygotes (see figure 17 A and A') or $dASPP^{8}$ homozygotes (see figure 17 B and B') and adult wings of these genotypes are never notched (see figure 17 A'' and B''). Furthermore, this phenotype is only observed when both copies of *dASPP* are lost;

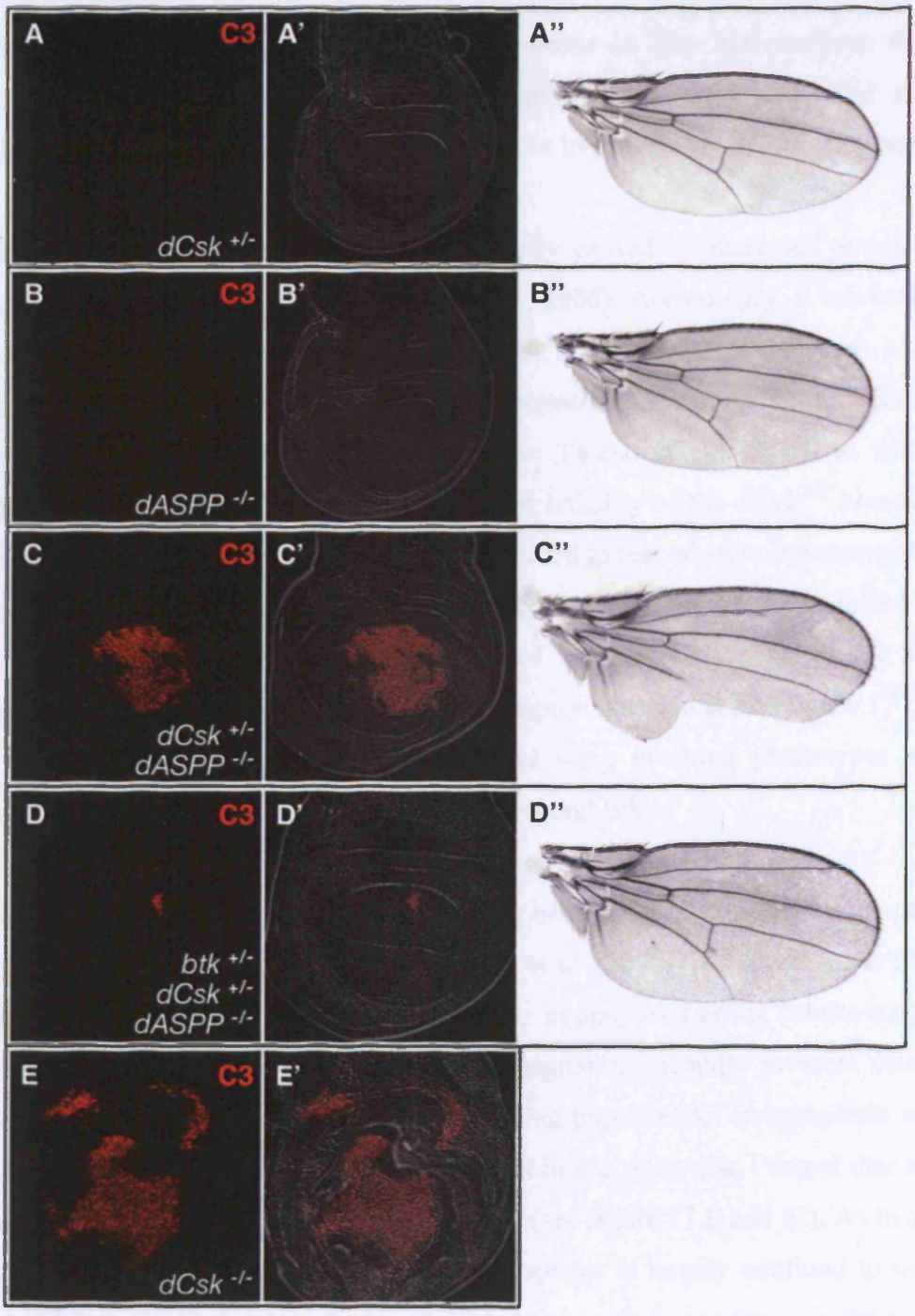

Figure 17: *dASPP* genetically interacts with *dCsk*. (A-E) Cleaved Caspase 3 (C3) (red) immunostainings of third instar wing discs of the indicated genotypes to label apoptotic cells. (A'-E') Overlays of C3 immunostainings and phase contrast images. (A"-D") Adult wings of the corresponding genotypes. (C-C") Halving the *dCsk* gene dosage in a *dASPP* mutant background leads to ectopic apoptosis in the wing disc and notching of adult wings. (D-D") Introducing a *btk* mutation into this genetic background rescues the apoptosis and notching phenotypes. (E-E') Large patches of apoptosis are also observed in *dCsk* homozygous mutant discs, no adult wing is shown as this allele is pupal lethal. Very little apoptosis is observed in control discs, *dCsk* heterozygotes (A-A") or *dASPP* homozygotes (B-B") and adult wings are not notched.

ectopic apoptosis and wing notching does not occur in flies heterozygous for both *dASPP* and *dCsk* (data not shown). This suggests that *dASPP* and *dCsk* strongly genetically interact and may function in the same or in parallel signalling pathways.

It is thought that the *dCsk* phenotype is primarily caused by increased activation of *Drosophila* SFKs (Read et al., 2004; Vidal et al., 2006). Accordingly, it can be largely rescued by reducing the function of Btk (Bruton's tyrosine kinase), which has been shown to function downstream of SFKs in *Drosophila* and mammals (Guarnieri et al., 1998; Roulier et al., 1998; Saouaf et al., 1994; Tateno et al., 2000). In particular, heterozygosity for *btk* can rescue the pupal stage lethality of the $dCsk^{1jd8}$ homozygous mutants (Read et al., 2004). For this reason I decided to test whether heterozygosity for *btk* could rescue the apoptosis phenotype observed in *dASPP-dCsk* compromised wings. Interestingly, I found that removing a copy of *btk* largely suppresses the ectopic apoptosis and wing notching in *dASPP-dCsk* compromised wings (see figure 17 D-D''). This suggests that the observed apoptosis and wing notching phenotypes are the consequence of increased signalling through SFKs and Btk.

Previously, loss of dCsk in discrete patches has been reported to result in apoptosis of cells at the mutant / wild-type boundary (Vidal et al., 2006). However, it has not been previously shown that broad loss of dCsk results in apoptosis as my results suggest. In fact, it has been proposed that loss of dCsk signalling actually protects cells from developmental apoptosis, at least in the developing pupal retina. In agreement with the idea that broad loss of dCsk results in apoptosis in the wing disc I found that $dCsk^{1jd8}$ homozygous wings show considerable apoptosis (see figure 17 E and E'). As in *dASPP-dCsk* compromised wing discs the patch of apoptosis is largely confined to the wing pouch. This suggests that broad loss of *dCsk* does result in apoptosis in the wing and that the phenotype I observe in *dASPP-dCsk* compromised wing discs is indeed due to loss of dCsk function. There is no adult wing shown for $dCsk^{1jd8}$ homozygotes as this allele is lethal at the pupal stage. Taken together, these results suggest that dASPP and dCsk may function in the same signalling pathway. As *dASPP* phenotypes are weaker than *dCsk* phenotypes it is probable that dASPP is required for maximal dCsk signalling.

To check that the genetic interaction observed between *dASPP* and *dCsk* is not due to unspecific effects, for example secondary background mutations present on either chromosome, I tested whether the interaction was still observed when other *dASPP* and *dCsk* alleles are combined. Firstly, I asked whether $dASPP^{d}$ also genetically interacts with $dCsk^{1jd8}$. Introducing one copy of $dCsk^{1jd8}$ into a $dASPP^{d}$ mutant background results in apoptosis in the 3rd instar wing disc and notching of adult wings (see figure 18 A-A''). This interaction is highly similar to the interaction between $dASPP^{8}$ and $dCsk^{1jd8}$ suggesting that the notching phenotype is caused by loss of *dASPP* and not by background mutations on *dASPP* mutant chromosomes. Furthermore, the interaction is not due to background mutations on the $dCsk^{1jd8}$ chromosome as wing notching is observed when $dASPP^{d}$ is combined with other *dCsk* alleles. Introducing a copy of either $dCsk^{S017909}$ (a P-element insertion in the dCsk locus) or $dCsk^{Q156stop}$ (an EMS allele reported to be a *dCsk* null) into a $dASPP^{d}$ mutant background results in notching of adult wings (data not shown). These results suggest that *dASPP* specifically interacts with *dCsk* in the wing disc.

As dCsk has been reported to function upstream of Wts (Stewart et al., 2003) I tested whether the phenotype of *dASPP-dCsk* deficient wing discs was due to loss of signalling through Wts. However, removing a copy of *wts* (using the amorphic wts^{X1} allele) in a $dASPP^{d}$ mutant background does not lead to ectopic apoptosis or wing notching (see figure 18 B-B''). This suggests that the apoptotic phenotype of *dASPP-dCsk* deficient wings is not due to loss of signalling through Wts and may in fact be due to mis-regulation of *Drosophila* SFKs. The *btk* rescue experiment supports this hypothesis.

3.4.3 Apoptosis of *dASPP-dCsk* deficient cells is mediated via the JNK pathway

The JNK pathway has been shown to mediate apoptosis of *dCsk* mutant cells. Firstly, the apoptosis of *dCsk* boundary cells (see below) requires components of the JNK pathway (Vidal et al., 2006). Secondly, the lethality of $dCsk^{1jd8}$ can be rescued by removing a copy of *bsk*, the *Drosophila* JNK ortholog (Stewart et al., 2003). Taken together these results suggest that dCsk functions upstream of SFKs and the JNK pathway in *Drosophila* to protect cells from apoptosis. Indeed, it has been shown that c-

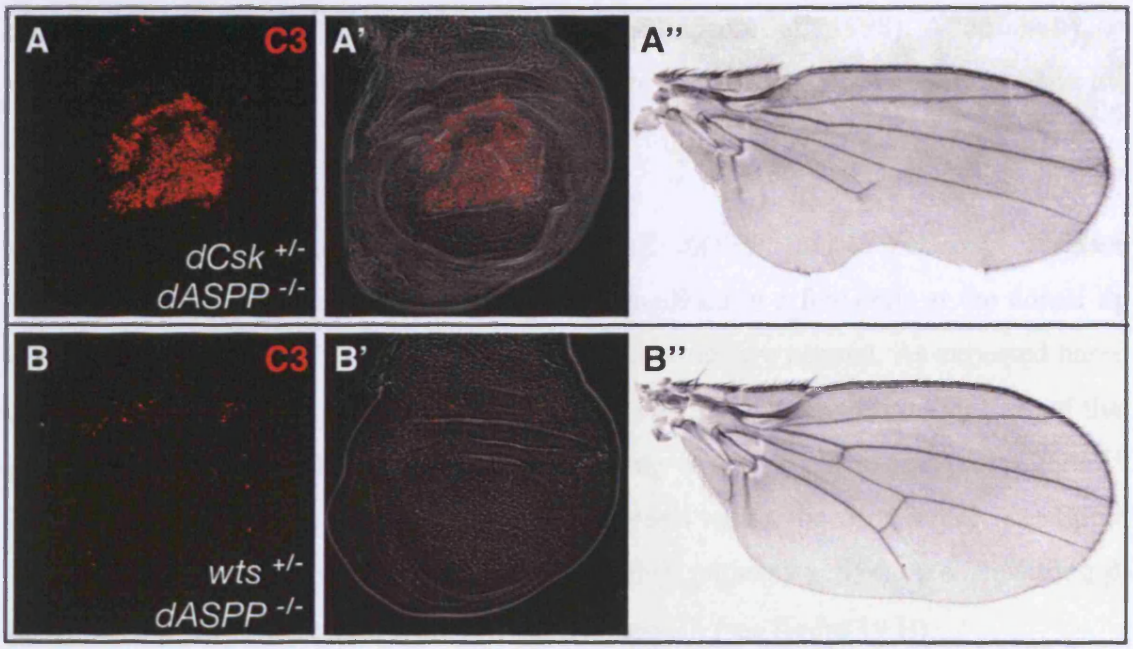

Figure 18: Multiple *dASPP* alleles genetically interact with *dCsk*. (A-A") Removing one copy of *dCsk* in a $dASPP^{d}$ mutant background leads to ectopic wing disc apoptosis, as visualised using a cleaved Caspase 3 antibody (C3) (red), and notching of adult wings. This is highly similar to the phenotype observed when *dCsk* is compromised in a $dASPP^{8}$ mutant background (see Figure 14). (B-B") This phenotype is not seen when a copy of *wts* is removed in a *dASPP* mutant background.

SRC functions upstream of the JNK pathway in mammalian cells (Dolfi et al., 1998; Hauck et al., 2002; Hsia et al., 2003). Therefore, I tested whether the apoptosis observed in *dASPP-dCsk* deficient wings is JNK pathway dependent.

Puckered (Puc) is the phosphatase responsible for shutting down Basket / JNK. *puc* is also transcriptionally activated by the pathway, providing a negative feedback loop (Martin-Blanco et al., 1998). JNK pathway activity can thus be monitored using *puc-LacZ* (*pucZ*) reporter, which is a transposon insertion placing the *LacZ* gene under the control of the endogenous *puc* promoter (Martin-Blanco et al., 1998). Additionally, as *pucZ* is a mutant allele for *puc* and allowed me to test for genetic interactions with the JNK pathway.

In *pucZ* heterozygotes (data not shown) or *pucZ, dASPP*^{8} double heterozygotes (see figure 19 A-A''') *pucZ* reporter expression is visualised in a few cells at the dorsal tip of the wing disc (arrows in figure 19 A), and adult wings are normal. As expected based on published results, *dCsk*^{1jd8} shows a strong genetic interaction with *pucZ*. I found that *dCsk*^{1jd8}, *pucZ* double heterozygotes have a wing notching phenotype (see figure 19 B''') and 3rd instar wing discs show ectopic apoptosis within the wing pouch (see figure 19 B'). This is presumably a result of excessive JNK pathway activation since strong β-Galactosidase expression is detected in the wing pouch (see figure 19 B).

The ectopic apoptosis of *dCsk*^{1jd8}, *pucZ* double heterozygotes is enhanced when animals are also heterozygous for *dASPP*^{8} (see figure 19 C-C'''), leading to a severely reduced adult wing size (see figure 19 C'''). Extensive expression of the *pucZ* reporter is observed (see figure 19 C'). Adult flies of this genotype also have leg deformities (data not shown), which is a phenotype ascribed to JNK pathway activation (Kirchner et al., 2007). Additionally, removing both copies of *dASPP* in a *dCsk*^{1jd8}, *pucZ* double heterozygous background results in lethality before the 3rd instar larval stage (data not shown).

Furthermore, I showed that *dASPP* genetically interacts with *puc* even when *dCsk* is not compromised. Introducing a copy of *pucZ* into a *dASPP*^{8} homozygous mutant background results in moderate patches of apoptosis in 3rd instar wing discs (see figure 19 D-D'''), which are labelled by *pucZ* reporter expression (arrow in figure 19 D). Such

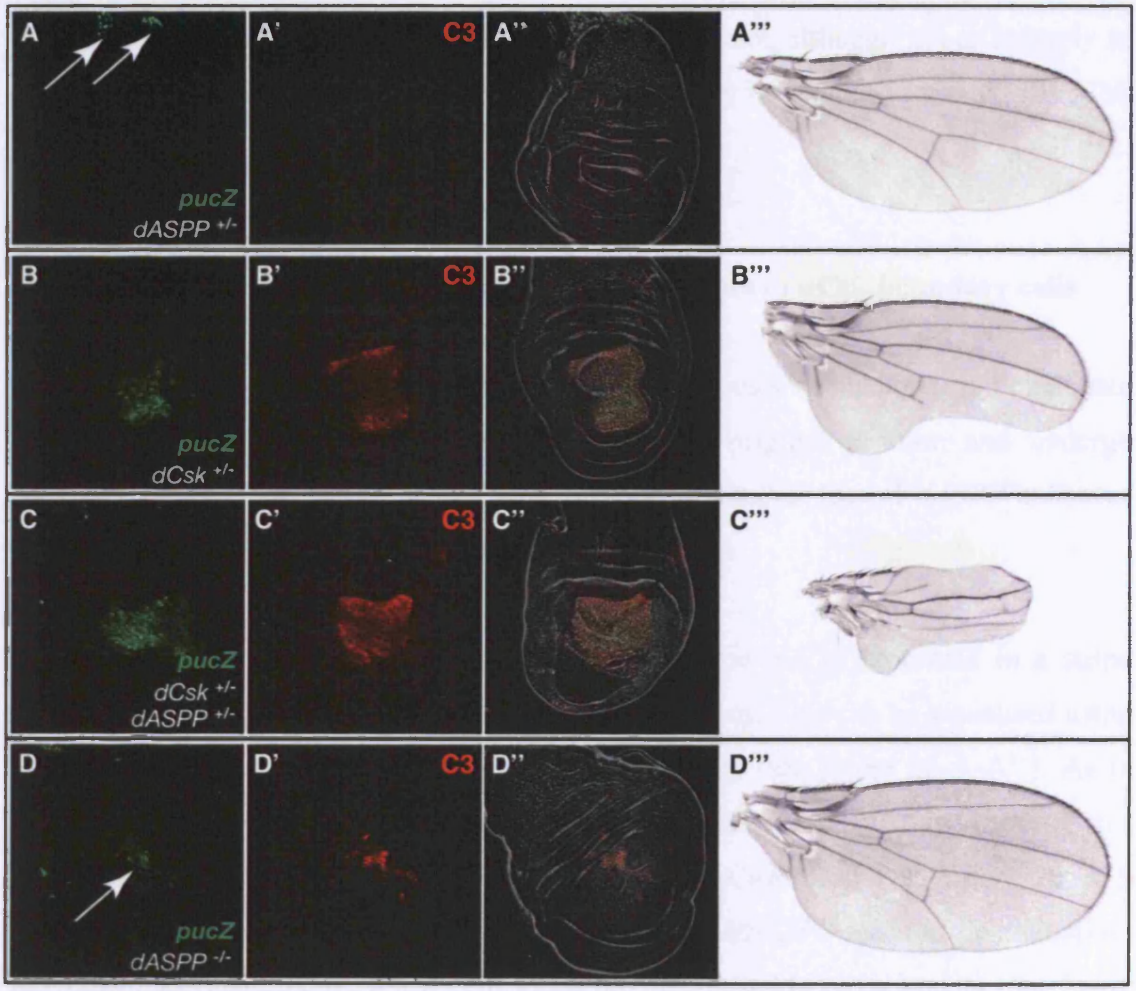

Figure 19: Apoptosis of *dASPP/dCsk* deficient cells is mediated by the JNK pathway. (A-D) Beta-Galactosidase staining (green) to visualise *pucZ* reporter expression in wing discs of the indicated genotypes. (A'-D') Cleaved Caspase 3 staining (C3) (red) to label apoptotic cells. (A''-D'') Overlay of B-Galactosidase staining, Caspase 3 staining and a phase contrast image of the disc. (A'''-B''') Adult wings of the corresponding genotypes.

patches of apoptosis are not observed in *dASPP*^{8} homozygous discs (compare figure 19 D to figure 17 B) or in *pucZ* heterozygotes (data not shown). This moderate level of cell death is not sufficient to induce notching of adult wings (see figure 19 D'''). Taken together, this data suggests that dCsk and, to a lesser extent, dASPP prevent inappropriate JNK pathway activation and thus protect wing pouch epithelial cells from apoptosis. The fact that *dASPP* and *puc* genetically interact, although not as strongly as *dCsk* and *puc*, strengthens the argument that dASPP may be required for maximal dCsk signalling.

3.4.4 dASPP loss of function enhances the phenotypes of dCsk boundary cells

dCsk mutant cells bordering wild-type cells have previously been shown to delaminate from wing disc epithelia, migrate away from their original position and undergo apoptosis (Vidal et al., 2006). Therefore, I examined whether loss of *dASPP* enhances these specific phenotypes of *dCsk* mutant boundary cells.

The *patched* (*ptc*) gene encodes the Hedgehog receptor and is expressed in a stripe along the anteroposterior boundary of wing imaginal discs. This can be visualised using a *ptc-Gal4* driver combined with a *UAS-GFP* transgene (see figure 20 A-A''). As in wild-type wing discs (data not shown), little apoptosis is detected in discs of this genotype using an antibody directed against cleaved Caspase 3 (see figure 20 A'). Driving expression of a *dCsk* RNAi transgene along with *GFP* leads to delamination, movement and apoptosis of a few cells along the mutant/wild-type boundary (see figure 20 B-B''). Cell movement and apoptosis predominately occur at the posterior-most boundary of the *ptc* expression pattern (indicated by the arrow in figure 20 B). Removing *dASPP* leads to a dramatic enhancement of the *dCsk* RNAi phenotype. The number of boundary cells undergoing apoptosis and moving away from the *ptc* domain is greatly increased (see figure 20 C-C''). This result confirms that *dASPP* and *dCsk* genetically interact and suggests that dASPP and dCsk collaborate to maintain epithelial integrity.

As an additional control I examined the effect of removal of *dASPP* in *ptcGal4>UASGFP* wing discs. This was done to be sure that *dASPP* is interacting

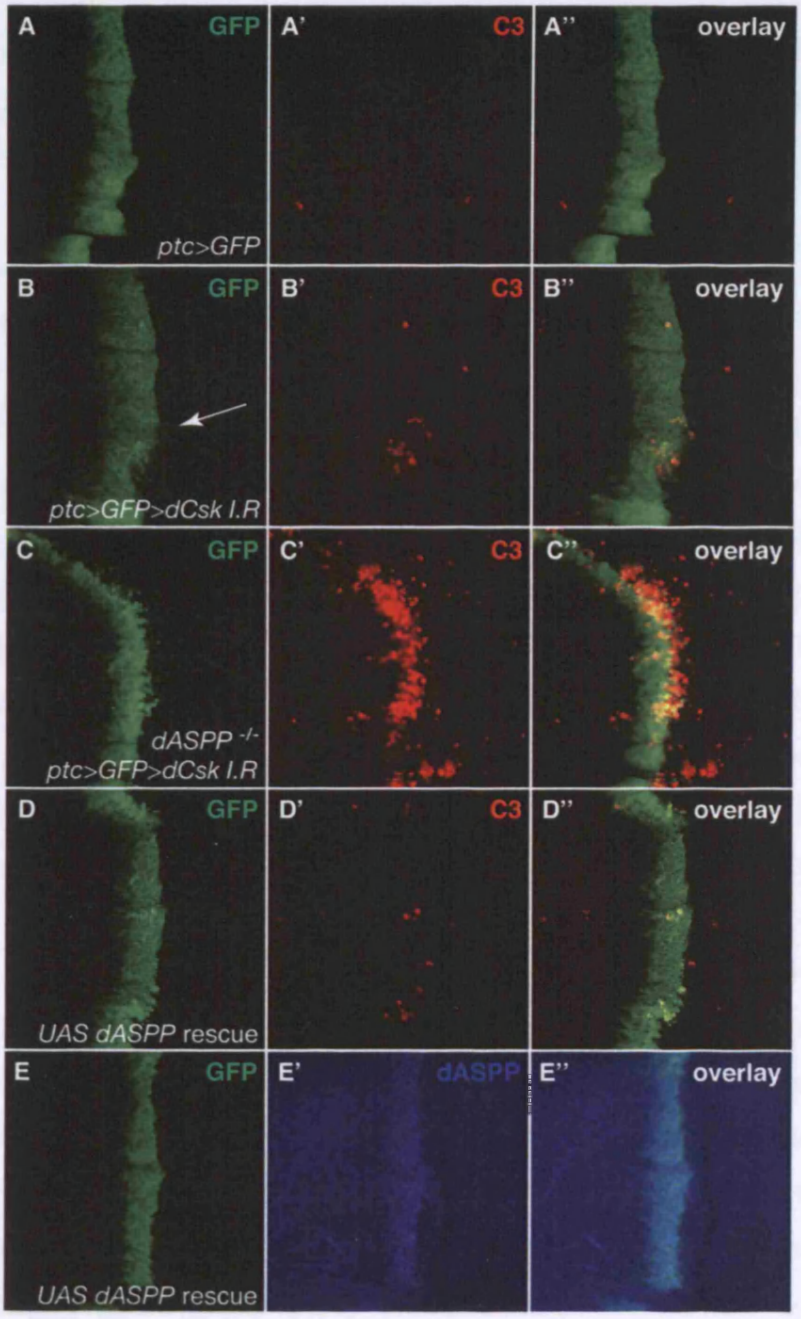

Figure 20: *dASPP* mutants enhance the phenotype of dCsk deficient boundary cells. All images focus on a region within the wing pouch of the 3rd instar wing disc. (A-A'') Patched (Ptc) is expressed along the anterior-posterior boundary of the wing disc as visualised by *ptc-Gal4* driving GFP expression. Cleaved Caspase 3 antibody (C3) (red) is used as a marker of cell death, little apoptosis occurs in control discs (A'). (B-B'') Reducing dCsk function in the *ptc* domain by RNAi leads to apoptosis and migration (arrow in B) of some cells at the mutant-wildtype boundary. (C-C'') These phenotypes are strongly enhanced by loss of *dASPP*, many more boundary cells undergo apoptosis and spread away from the *ptc* domain. (D-D'') Re-expressing *dASPP* in this genetic background largely rescues the apoptosis along the boundary. (E-E'') shows an image of the same disc shown in D-D'' in an apical plane to visualise *dASPP* overexpression using a dASPP antibody (blue).

specifically with *dCsk*. Wing discs of this genotype however show similar levels of apoptosis to *ptcGal4>UASGFP* wing discs (data not shown), suggesting that *dASPP* is specifically interacting with *dCsk*.

The enhanced phenotype when *dASPP* is removed (see figure 20 C-C'') is almost fully rescued if *dASPP* expression is restored by driving a *UAS-dASPP* construct in the *ptc* domain (see figure 20 D-D''). This suggests that the enhancement of the *dCsk* RNAi phenotype is indeed due to loss of dASPP. Due to the nature of the cross scheme used to generate the *dASPP* rescue genotype only 50% of the progeny are expected to have the *UAS-dASPP* transgene. Therefore I also stained the discs with a dASPP antibody (dASPP39, see materials and methods) to distinguish those that over-express *dASPP* (see figure 20 E-E'' – an apical section through the same disc shown in figure 20 D-D''). The enhanced phenotype was clearly rescued in all discs expressing *dASPP* within the *ptc* domain. Furthermore, I found that *dASPP* over-expression rescues the pupal stage lethality caused by *dCsk* RNAi expression in the *ptc* domain. Therefore, the specific phenotypes of *dCsk* RNAi boundary cells are sensitive to dASPP levels.

dCsk RNAi cells move to a basal position within epithelia and spread amongst wild-type cells. This can be visualised by taking transversal (XZ) sections through the wing disc (see figure 21 A). Note that apoptotic cells are observed basally and some cells are migrating away from the *ptc* domain. Loss of *dASPP* enhances both the number of dying cells and the distance those cells move away from the *ptc* domain (see figure 21 B). Interestingly, not all of the migrating cells of this genotype are Caspase 3 labelled (see figure 21 B) suggesting that Caspase activation may not be absolutely required for the migratory phenotype. In an attempt to address this question I co-expressed *DIAP1* in the *ptc* domain and asked whether this rescues the defects observed. Expression of *DIAP1*, as expected, largely blocks the apoptosis induced by *dCsk* RNAi in a *dASPP* mutant background (compare figure 22 A-A'' to figure 22 B-B', the bracket indicates the equivalent region of the disc). Expression of *DIAP1* also seems to largely inhibit the migratory phenotype; the number of individual cells moving away from the *ptc* domain is reduced (compare figure 22 A to figure 22 B). However, the morphology of the boundary is abnormal and appears 'ruffled' compared to wild-type boundaries (compare figure 22 A to figure 20 A). This suggests that these cells may still possess migratory

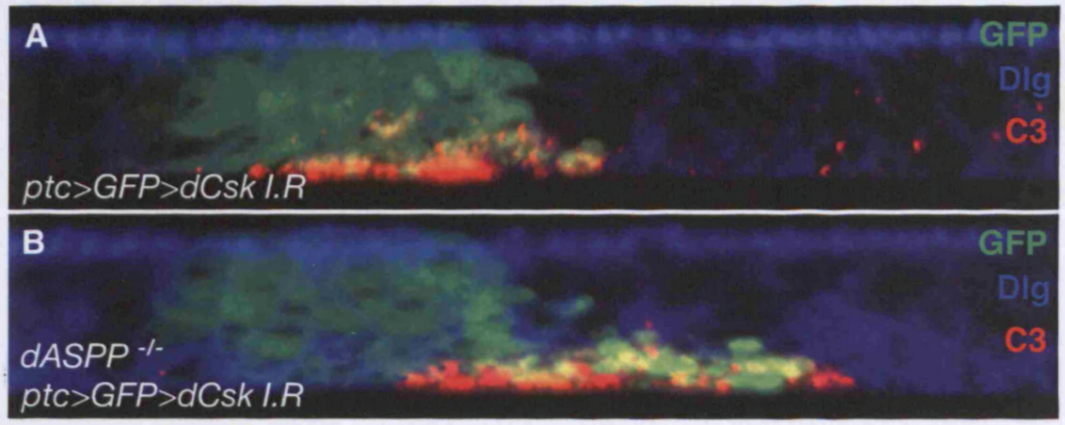

Figure 21: *dASPP/dCsk* deficient boundary cells delaminate and migrate through the basal layer. (A and B) Transversal (XZ) sections through wing discs to show that dCsk deficient cells delaminate, undergo apoptosis and spread through the basal layer. Anti Discs-Large (Dlg) staining (blue) is used to distinguish apical from basal. B shows the enhancement of the phenotype by *dASPP* loss of function.

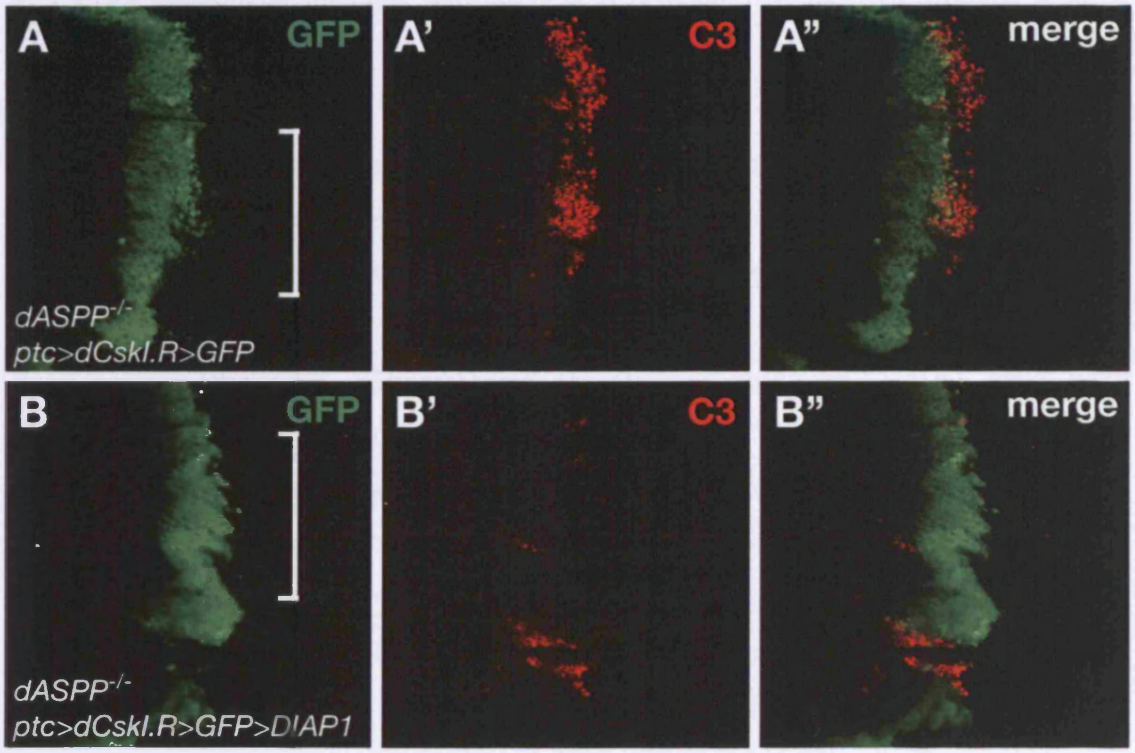

Figure 22: The apoptosis and cell spreading phenotypes of *dASPP/dCsk* deficient boundary cells are largely rescued by *DIAP1* expression. (A-A") The enhanced dCsk boundary phenotype when flies are also mutant for *dASPP*. Cells at the boundary move away from the *ptc* domain whilst simultaneously undergoing apoptosis, as visualised by anti cleaved Caspase 3 staining (C3) (red). (B-B") If *DIAP1* is co-expressed apoptosis and cell spreading are largely blocked, compare the region indicated by the bracket in A and B. However, the interface between the GFP expressing and non-GFP expressing cells is ruffled compared to control discs.

properties but as apoptosis is blocked individual cells are prevented from dissociating from their neighbours and moving away from the *ptc* domain.

3.5 dASPP physically interacts with dCsk

As *dASPP* genetically interacts with *dCsk* it is possible that the two proteins bind to each other. This was tested by Julien Colombani using co-immunoprecipitation and GST-pulldown experiments. HA-tagged dASPP (dASPP-PA) and Myc-tagged dCsk (dCsk-PB) were transfected into cultured *Drosophila* Kc167 cells (a haemocyte derived cell line). dCsk-Myc was detected in HA but not control (GFP) immunoprecipitates suggesting that dASPP and dCsk physically interact (see figure 23 A).

To carry out the GST (Glutathione-S-Transferase) pulldown, Kc167 cells were transfected with HA-tagged dASPP and cell lysates were used for pull-down experiments using bacterially produced GST or GST-dCsk. dASPP-HA is pulled down by GST-dCsk but not GST (see figure 23 B), which is in agreement with the co-immunoprecipitation result suggesting that dASPP and dCsk physically interact. Subsequent GST pulldown experiments using truncated forms of dASPP (GST-dASPP N-term (amino acids 1-484 of dASPP-PA) or GST dASPP C-term) and bacterially expressed dCsk suggest than dASPP and dCsk directly bind to each other and that the dASPP N-terminal region mediates binding to dCsk (data not shown). These biochemical results strongly suggest the dASPP binds to dCsk and support our view based on the genetic data that dASPP and dCsk function in the same signalling pathway.

3.6 dASPP promotes dCsk kinase activity on its target dSrc42A

As dASPP and dCsk physically interact and dCsk is a tyrosine kinase, it was possible that dASPP functions as a regulator of dCsk kinase activity. This hypothesis was tested by Julien Colombani using *in vitro* kinase assays to determine dCsk activity either in the presence or absence of transfected dASPP. First, a kinase-dead form of dSrc42A ($dSrc^{K276R}$) was produced as a GST fusion protein in *E.coli*. This form of dSrc42A contains a mutation within the ATP-binding site and thus prevents autophosphorylation.

Figure 23: dASPP physically interacts with and enhances the kinase activity of dCsk. (A) Co-immunoprecipitations between dASPP and dCsk. Drosophila Kc167 cells were transfected with pAc5.1-dCsk-Myc and pAc5.1-dASPP-HA. HA and control (GFP) immunoprecipitates and input (1/10) were probed with anti-Myc (top) and anti-HA (bottom) antibodies. dCsk-Myc is detected in HA but not control immunoprecipitates. (B) Drosophila Kc167 cells were transfected with pAc5.1-dASPP-HA. Cell lysates were used for pull-down experiments using GST and GST-dCsk. Precipitated fractions and input (1/10) were probed with anti-HA. dASPP is pulled down by GST-dCsk but not GST suggesting that dASPP and dCsk physically interact. The coomassie blue-stained gel shows the immunoprecipitated fusion proteins. (C) Immunoprecipitations followed by kinase assays were used to monitor the kinase activity of a tagged form of dCsk (dCsk-Myc) on a bacterial dSrc substrate (GST-dSrc42A^{K276R}). dCsk-alone and a negative control (mock immunoprecipitation with GFP antibody, marked by the asterisk) are shown (lanes 1-2 respectively). Input (1/5) and immunoprecipitated protein levels are shown by Western blots. GSTdSrc^{K276R} levels are shown after coomassie blue staining. dCsk phosphorylation activity was quantified on a phosphorimager. Signals were normalized according to immunoprecipitated kinase levels (see experimental procedures) and fold changes are indicated at the top of each lane. As expected, dASPP was detected in dCsk immunoprecipitates. Cotransfection of Kc167 cells with dCsk-Myc and increasing quantity of dASPP-HA results in an enhancement of dCsk activity (lanes 3-5, 125, 250 and 375µg transfected DNA respectively). The data and figure were generated by Julien Colombani.

This makes $dSrc^{K267R}$ a suitable substrate for dCsk in kinase assays as the phosphorylation status of this substrate is influenced only by dCsk kinase activity and not by autophosphorylation. Myc-tagged dCsk was immunoprecipitated from *Drosophila* Kc167 cells and an *in vitro* kinase assay was performed using GST-$dSrc^{K267R}$ as a substrate.

The kinase activity of dCsk immunoprecipitated from Kc167 cells is potentiated by co-transfection of dASPP in a dose dependent manner (see figure 23 C, compare lane 1 to lanes 3, 4 and 5). The values given above each ^{32}-P band represent the fold increase in dCsk activity in the presence of dASPP (see figure 23 C). The values were obtained by quantifying the phosphorylation signal and normalising according to the efficiency of dCsk immunoprecipitation (see materials and methods for further details). Therefore, in the presence of dASPP the kinase activity of dCsk may be increased by up to 1.7 fold. Although this is a modest increase, the result is highly reproducible as it was observed in five independent experiments (data not shown). Furthermore, dCsk phosphorylates a single dSrc42A tyrosine residue, which may limit the dynamic range of the assay. In further experiments in *Drosophila* D16 cells it was shown that dASPP RNAi reduces the kinase activity of dCsk by 2-fold (data not shown) (Langton et al., 2007).

Taken together these results suggest that dASPP binds to and enhances the kinase activity of dCsk. The positive regulation of dCsk by dASPP in the *in vitro* kinase assays is supported by the genetic data, which shows that *dASPP* and *dCsk* have similar LOF phenotypes. Furthermore, the result showing that dASPP RNAi reduces dCsk kinase activity by 2-fold suggests that dASPP is not absolutely required for dCsk kinase activity. This is probably the reason why *dASPP* mutants have a considerably weaker phenotype than *dCsk* mutants. Overall, our data suggest that dASPP is an important regulator of dCsk activity.

Although the biochemical data suggest that dASPP enhances the kinase activity of dCsk, the mechanism by which this is achieved is not known. One tempting possibility is that dASPP regulates dCsk by controlling its sub-cellular localization. Unfortunately, without a dCsk antibody that recognises dCsk in fixed tissues, this theory is difficult to test. However, I checked whether dCsk regulates dASPP localisation/levels by staining eye-antennal imaginal discs bearing *dCsk* mutant clones with the dASPP38 antibody.

dASPP expression appears normal in *dCsk*^{ljd8} clones (see figure 24 A-A'') indicating that dCsk does not control the levels or localization of dASPP.

3.7 dASPP is epistatic to dSrc64B

The *in vitro* kinase assays suggest that dASPP functions as a positive dCsk regulator, implying that dASPP functions upstream of the dCsk targets dSrc42A and dSrc64B. Therefore, mutations in *dSrc42A* and *dSrc64B* should rescue *dASPP* phenotypes. This was tested in the eye where loss of *dASPP* results in a large, rough eye phenotype (see figure 25 B-B') compared to control eyes (see figure 25 A-A'). I have already shown that removing one copy of the *Drosophila* SFK target, *btk*, suppresses the apoptotic phenotype observed in *dASPP/dCsk* deficient wing discs. Therefore I asked whether compromising *btk* also rescued the eye phenotype of *dASPP* mutants. Introducing a *btk* mutation into the *dASPP* mutant background partially suppressed the eye phenotype (see figure 25 C-C'), further suggesting that Btk functions downstream of dASPP.

Complete loss of *dSrc64B* is not lethal; *dSrc64B*^{KO} (O'Reilly et al., 2006) is a viable, null allele and homozygous flies have normal sized eyes (see figure 25 D-D'), although the shape of the eye seems slightly affected (compare figure 25 D-D' to figure 25 A-A'). Having a null allele for both *dSrc64B* and *dASPP* allowed me to perform epistasis experiments. Complete removal of *dSrc64B* strongly suppresses the *dASPP* eye phenotype and rescues the size and bristle patterning defects (see figure 25 E-E'). The *dSrc64B-dASPP* double mutant eye is phenotypically very similar to the *dSrc64B* mutant eye suggesting that *dSrc64B* is epistatic to *dASPP*. This is clear evidence that dASPP functions upstream of or in parallel to dSrc64B during eye development and that the observed phenotypes are due to increased *Drosophila* SFK signalling.

It has been shown that dCsk functions upstream of both dSrc42A and dSrc64B (Pedraza et al., 2004), therefore it is maybe surprising that removal of *dSrc64B* suppresses the *dASPP* eye phenotype so strongly. One likely explanation is that inhibition of dSrc64B by dCsk is important for normal eye development whereas inhibition of dSrc42A is less important in this context. The extent to which dSrc42A mutations suppress the dASPP eye phenotype was not tested.

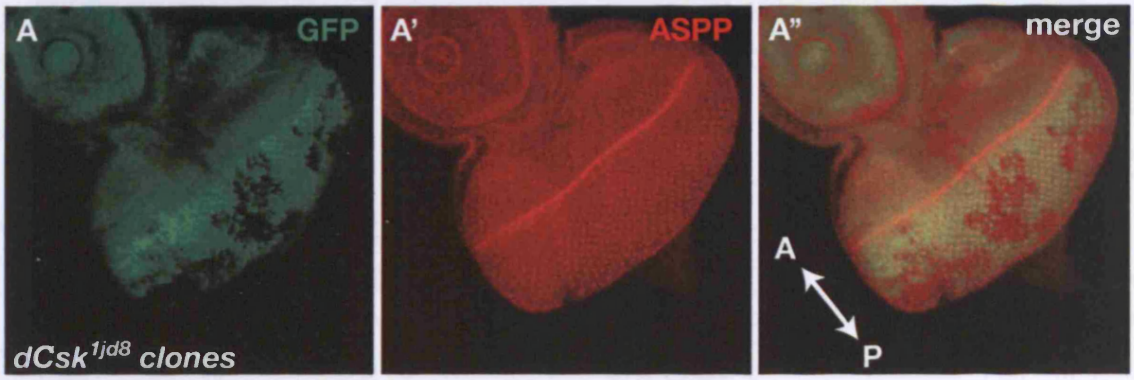

Figure 24: dCsk does not regulate dASPP expression or localization. (A-A") A 3rd instar eye-antennal imaginal disc with *dCsk*^{1jd8} clones, marked by absence of GFP (A). dASPP protein staining (red) is normal within the clones (A'). The orientation of the disc is indicated in A" (A is anterior, P is posterior).

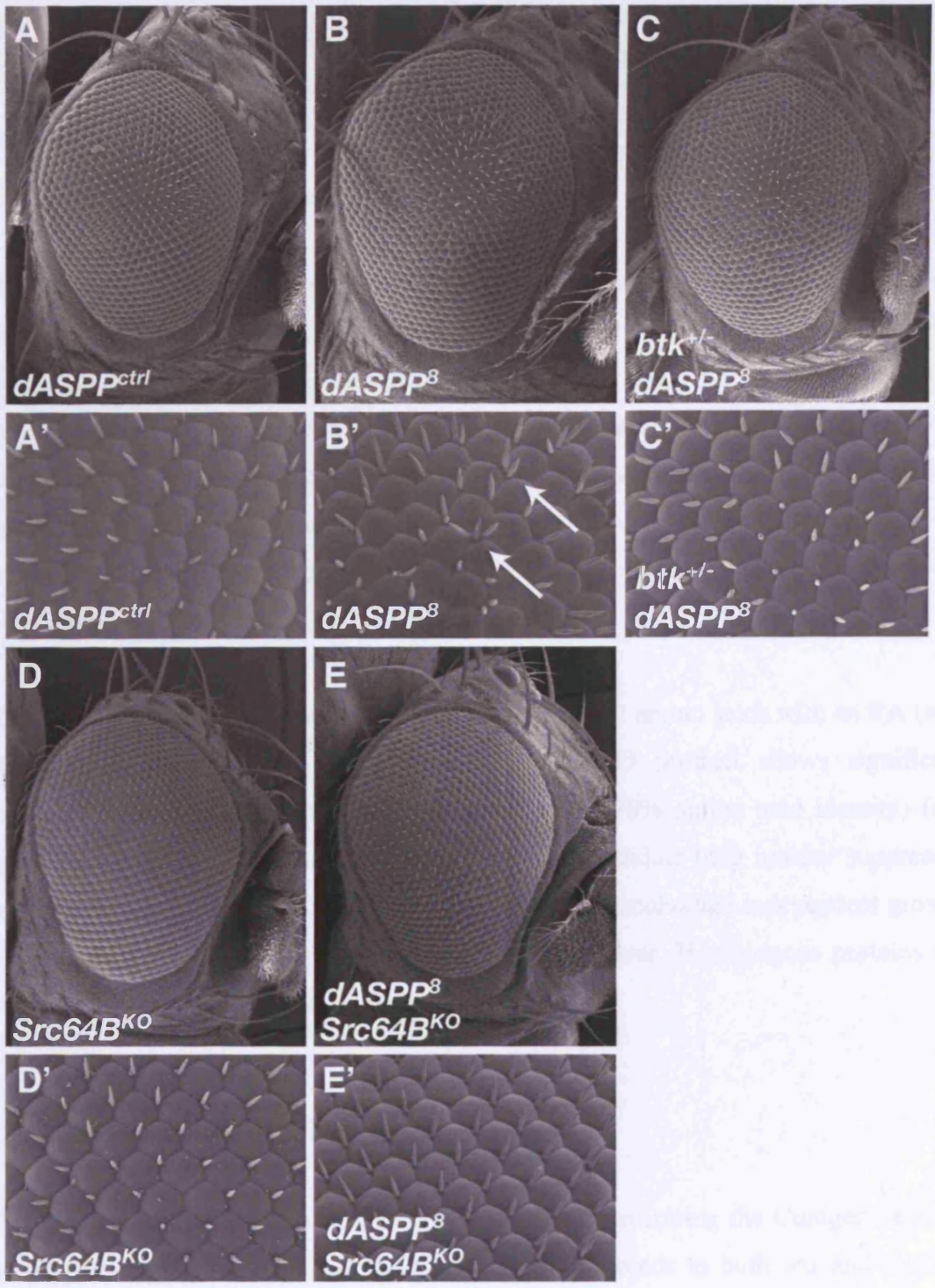

Figure 25: The *dASPP* eye phenotypes are rescued by *btk* or *dSrc64B* mutations. Scanning electron micrographs (SEMs) of adult eyes of the indicated genotypes. *dASPP*^{8} eyes (B) are large and rough compared to control eyes (A). (A' and B') High magnification SEMs, bristle clustering is evident in *dASPP*^{8} eyes (arrows in B'). (C and C') The *dASPP*^{8} eye phenotype is partially rescued by halving the *btk* gene dosage. (E and E') The *dASPP*^{8} eye phenotype is almost fully suppressed by removal of *dSrc64B*. The *dASPP-dSrc64B* double mutant eye (E and E') is highly similar to the *dSrc64B* mutant eye (D and D') suggesting that *dSrc64B* is epistatic to *dASPP*.

CHAPTER 4 Characterization of Boa

4.1 Introduction to Boa (Binder of dASPP)

CG5053 is the gene that links *CG18375/dASPP* to *wts* in the Curagen yeast 2-hybrid data set (see figure 9A). A P-element insertion (*GE27409*) within the *CG5053* locus dominantly suppresses the *GMRsav,wts* eye phenotype (data not shown), suggesting that *CG5053* may function as a negative regulator of tissue size. By this stage of the project, *dASPP* mutants had been generated and I had shown that *dASPP* is a negative regulator of tissue size. Therefore I was interested in characterizing *CG5053* to determine whether it also functions in organ size control and if so whether it plays a role in the Hippo pathway and/or in a dASPP pathway.

CG5053 is a conserved gene and encodes a protein of 607 amino acids with an RA (Ras Association) domain at the N-terminus. The *CG5053* product shows significant homology to RASSF8/HOJ-1 within the RA domain (70% amino acid identity) (see figure 26). *RASSF8/HOJ-1* has been identified as a candidate lung tumour suppressor gene and its expression in A459 cells led to inhibition of anchorage-independent growth (Falvella et al., 2006), though its function remains unclear. Homologous proteins are also found in *A.gambiae* and *C.elegans* (see figure 26).

4.2 Boa binds to dASPP

The initial characterization of *CG5053* was aimed at confirming the Curagen yeast 2-hybrid data, which suggests that the *CG5053* product binds to both *wts* and *dASPP*. Julien Colombani carried out this work. Despite numerous attempts it was not possible to confirm the interaction between the *CG5053* product and *wts* by co-immunoprecipitation suggesting that these two proteins do not bind to each other. Additionally, the 'score' given for this interaction, which represents the probability that the interaction is genuine, is only just above the cut-off value of 0.3. Therefore the predicted CG5053-Wts interaction may represent a false positive within the yeast 2-hybrid data. However, the interaction between the *CG5053* product and dASPP was

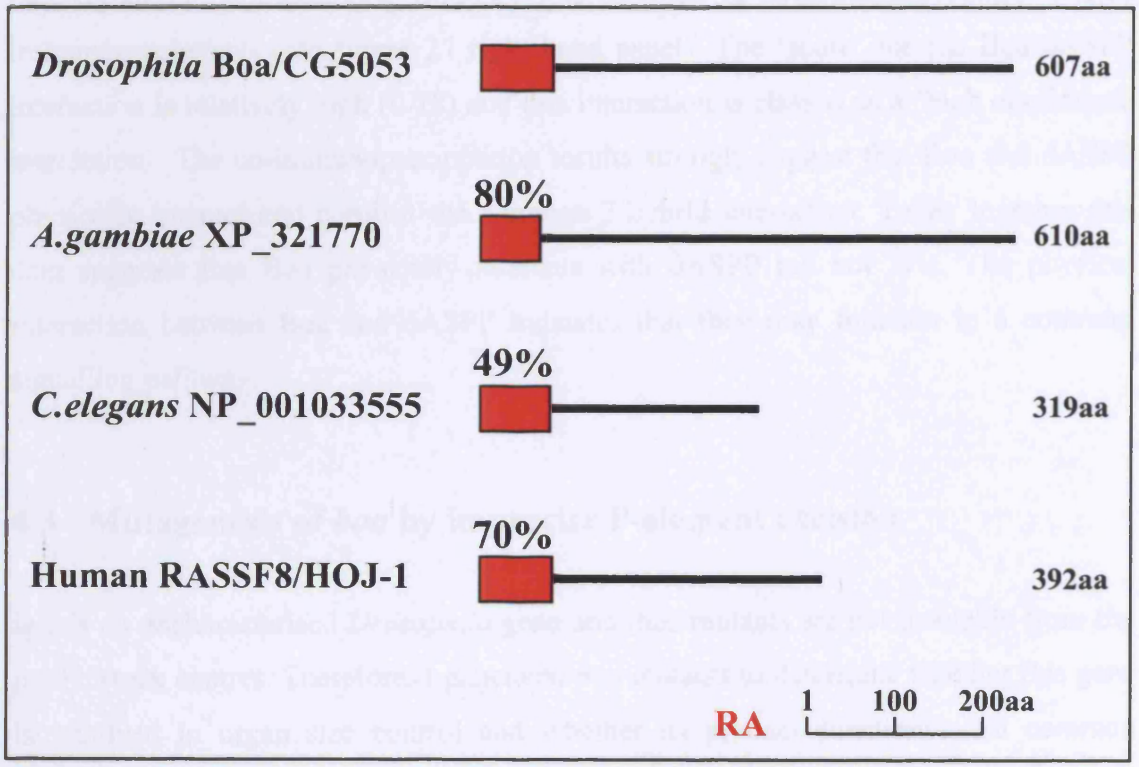

Figure 26: Domain structure of Boa and alignment with homologs from other species. Alignment of Boa with *A.gambiae* (XP_321770), *C.elegans* (NP_001033555) and human (RASSF8/HOJ-1) homologs. Boa/CG5053 has a conserved N-terminal RA (Ras Association) domain. Percentage amino acid identity within the RA domain is indicated.

confirmed by co-immunoprecipitation in *Drosophila* Kc167 cells (see below). Therefore the *CG5053* product was renamed Boa (for binder of dASPP) and the *CG5053* gene will be referred to as *boa* in the following text. Myc-tagged dASPP and HA-tagged Boa were transfected into cultured *Drosophila* Kc167 cells. dASPP-Myc was detected in HA immunoprecipitates but not in control (GFP) immunoprecipitates (see figure 27). Furthermore, Boa-HA was detected in Myc but not control (GFP) immunoprecipitates (see figure 27 right hand panel). The 'score' for the Boa-dASPP interaction is relatively high (0.78) and this interaction is classed as a 'high confidence interaction'. The co-immunoprecipitation results strongly suggest that Boa and dASPP physically interact and confirm the Curagen 2-hybrid interaction. Taken together this data suggests that Boa physically interacts with dASPP but not Wts. The physical interaction between Boa and dASPP indicates that they may function in a common signalling pathway.

4.3 Mutagenesis of *boa* by imprecise P-element excision

boa is an uncharacterised *Drosophila* gene and thus mutants are not available from the public stock centres. Therefore, I generated *boa* mutants to determine whether this gene is involved in organ size control and whether its product functions in a common pathway to its binding partner dASPP. In addition to the P-element insertion (*GE27409*) identified as a suppressor of *GMRsav,wts*, I was able to obtain an additional P-element line (*G15974*) with an insertion 2bp upstream of the *boa* transcription start site (see figure 28 A).

G15974 is homozygous viable and fertile and adults show no obvious phenotype. This transposon was imprecisely excised to generate *boa* mutants. First, the P-element insertion site was confirmed by sequencing a PCR product amplified using a P-element specific primer and a genomic primer close to the reported insertion site (data not shown). A similar strategy to the one used for *dASPP* mutagenesis was employed, which involved initially screening by PCR, followed by screening for phenotype (see chapter 3.2.2). The cross scheme to excise *G15974* was carried out (see materials and methods for cross scheme) and individual putative mutant males were crossed to third chromosome balancer virgins (*TM3/TM6B*). After a few days the males were lifted from

Figure 27: dASPP and Boa physically interact. Co-immunoprecipitation between dASPP and Boa. *Drosophila* Kc167 cells were transfected with pAc5.1-dASPP-Myc and pAc5.1-Boa-HA. HA, Myc and control (GFP) immunoprecipitates and inputs (1/10) were probed with anti-HA (top) and anti-Myc (bottom). dASPP-Myc is detected in HA but not control immunoprecipitates (left hand panels). Boa-HA is detected in Myc but not control immunoprecipitates (right hand panels). The data and figure were generated by Julien Colombani.

the cross and screened by PCR for genomic deletions in the *boa* locus using the primers Boa-5'a and Boa-3'a, which flank the insertion site (see primers table).

4.4 Description of the *boa* alleles generated

100 putative mutant chromosomes were screened by PCR, leading to the identification of boa^2, which is an 823bp deletion that removes the *boa* 5'UTR, the start codon and the first coding exon (see figure 28 A). This deletion results in a downward shift when amplifying a PCR product using primers spanning the excision site. boa^2 is a homozygous viable mutation and adults present a visible rough eye phenotype (data not shown).

As boa^2 is a small deletion and only removes the first exon of the gene it may not a null allele. Although only one transcript is predicted (RA) for *boa* it is possible that a second translation initiation codon exists that is not deleted by boa^2. Indeed, there are two methionine residues (amino acids 60 and 107) in the second *boa* exon that may be utilised as alternative translation start sites. This seems likely as *boa* transcript was detected following RT-PCR on boa^2 templates (see figure 28 C). For this reason I screened more putative *boa* mutant chromosomes with the aim of obtaining an allele likely to be null. As boa^2 has a rough eye phenotype, this could be used to screen for further alleles by crossing putative mutants to boa^2 and screening for the rough eye phenotype.

Roughly 300 putative mutant males were crossed to boa^2 and the most useful alleles identified were boa^4 and boa^6. boa^4 is a re-insertion of *G15974* into the boa 5'UTR (see figure 28 A). This allele is also homozygous viable and results in a slightly stronger eye phenotype than boa^2. During this reinsertion event, deletion of P-element sequence must have occurred; boa^4 mutants have white eyes and thus the *mini-white* gene within the P-element sequence has been disrupted or deleted. The exact nature of this allele has not been determined and it is not known how much of the P-element sequence was deleted. For this reason boa^4 was not used for the characterisation of the *boa* phenotype.

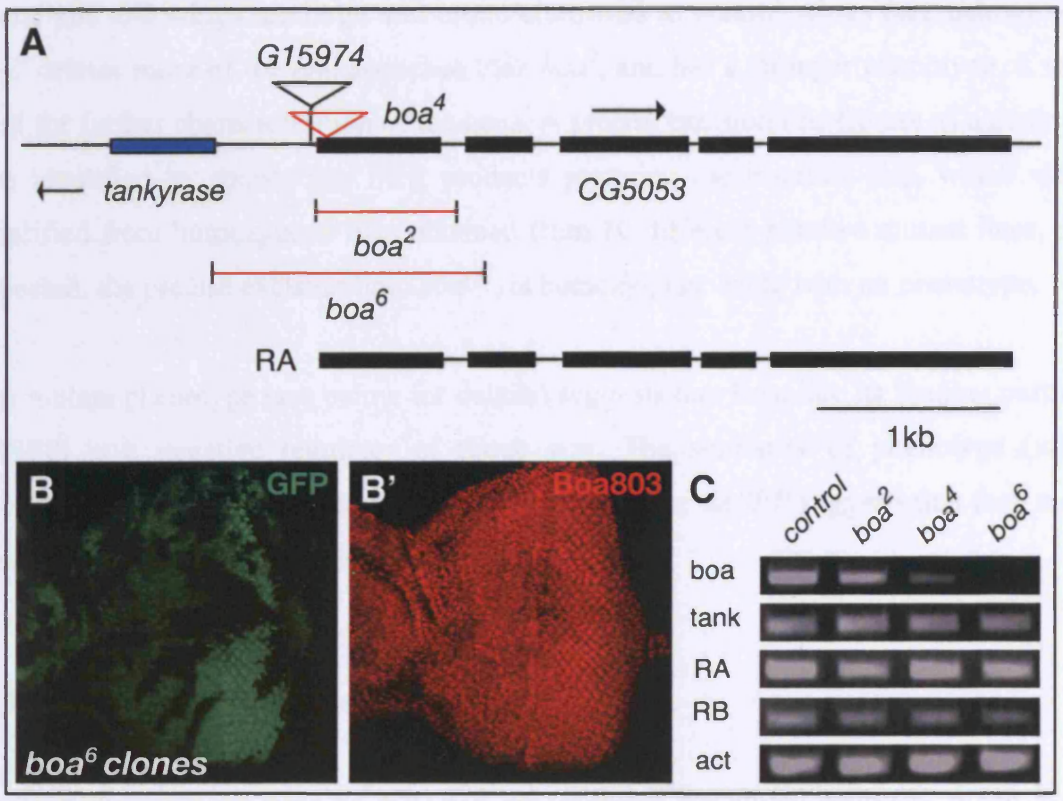

Figure 28: *boa* mutagenesis by imprecise P-element excision. (A) An illustration showing the *boa* locus and the alleles generated. *G15974* is inserted 2bp upstream of the *boa* transcription start site. This P-element was excised to generate boa^2, boa^4 and boa^6. boa^2 and boa^6 are deletions, boa^2 removes the first exon and boa^6 removes the first exon and part of the second. boa^4 is a reinsertion of part of the P-element sequence into the *boa* 5'UTR. (B-B') An eye-antennal disc with boa^6 clones, marked by absence of GFP. A reduction in Boa antibody staining (red) is observed within boa^6 clones. (C) RT-PCR analysis of *boa*, *tankyrase*, *dASPP* (RA and RB) and *actin* (act) transcript levels in *boa* mutants and controls (precise excision). The amount of *boa* transcript is reduced in all *boa* alleles and is not detected in boa^6 samples (last lane). *dASPP* and *tankyrase* transcript levels are unaffected. *actin* transcript levels provide a positive control for the samples.

boa^{6} is a deletion of 1.4kb, which removes genomic sequence on both sides of the P-element (see figure 28 A). *boa*^{6} deletes the first *boa* exon and part of the second exon. *boa*^{6} is a homozygous viable allele and the eye phenotype (see below) is stronger than observed for either *boa*^{2} or *boa*^{4} (data not shown). *boa*^{6} homozygotes also have a wing phenotype and wings are large and broad compared to control wings (see below). As *boa*^{6} deletes more of the *boa* sequence than *boa*^{2}, and has a stronger phenotype, it was used for further characterisation of the gene. A precise excision line (to use as a control) was identified by sequencing PCR products spanning the insertion site, which were amplified from homozygous flies obtained from 10 different putative mutant lines. As expected, the precise excision line, *boa*^{ctrl}, is homozygous viable with no phenotype.

The mutant phenotype (see below for details) suggests that Boa, like its binding partner dASPP, is a negative regulator of tissue size. The similarity of phenotype (mild overgrowth and rough eye) resulting from loss of *boa* or *dASPP* suggests that they may function in the same signalling pathway.

4.5 Confirmation of the *boa* alleles

boa^{6} was recombined onto an *FRT82B* chromosome for clonal analysis. When *boa*^{6} mutant clones are generated in the eye-antennal imaginal disc a reduction in Boa protein is detected within the clones (see figure 28 B-B') using an antibody directed against Boa (Boa803, see materials and methods). The Boa803 antibody was generated by Eurogentec and raised in Guinea pigs against a peptide corresponding to amino acids 218-232 of Boa. The Boa antibody is probably not as specific as the dASPP antibody as considerable staining is still detected in *boa*^{6} clones. The alternative explanation is that *boa*^{6} is not a protein null, however this is probably not the case as no *boa* transcript is detected in *boa*^{6} mutant samples (see figure 28 C and below). Recently, we have generated a highly specific Boa antibody, and Boa protein is completely absent in *boa*^{6} mutant tissues following Western blotting (Julien Colombani, personal communication), confirming that *boa*^{6} is likely to be a null allele.

RT-PCR analysis using cDNA prepared from whole fly extract templates revealed that *boa* transcript levels are reduced in all excision alleles generated. Interestingly, the

reduction in transcript observed for each allele corresponds to the strength of the phenotype of that allele. For example, *boa*^{2} has the weakest phenotype and also the weakest reduction in transcript levels, whereas *boa*^{6} has the strongest phenotype and the strongest reduction in transcript levels (see figure 28 C). Although this method of RT-PCR analysis is only semi-quantitative (see materials and methods for description) this result was observed in several independent experiments. In fact, *boa* transcript is completely absent from *boa*^{6} samples suggesting that *boa*^{6} is a null allele.

boa^{6} deletes roughly 100bp of the 5'UTR of the neighbouring gene, *tankyrase* (see figure 28 A). This raises the possibility that *boa*^{6} is a double mutant for *boa* and *tankyrase*. To address this concern I examined the levels of *tankyrase* transcript in the *boa* mutants by RT-PCR (see figure 28 C). However, the level of *tankyrase* transcript is unaffected by the *boa*^{6} deletion suggesting that *boa*^{6} does not strongly affect *tankyrase* expression. Furthermore, a lethal P-element insertion within the *tankyrase* locus is viable when crossed to *boa*^{6} and progeny have no discernable phenotype (data not shown). Taken together, this data suggests that *boa*^{6} is not a strong *tankyrase* allele however, it cannot be ruled out that *tankyrase* expression may be mildly affected in *boa*^{6} mutants. What is clear is that the observed *boa* phenotypes are due to deletion of *boa* and not *tankyrase* because they are fully rescued by ubiquitous *boa* expression using the Gal4-UAS system (Julien Colombani, personal communication). *dASPP* transcript (RA and RB) levels were also examined in samples from *boa* mutants (see figure 28 C) but no difference was observed between control and mutants. This indicates that Boa does not regulate dASPP at the transcriptional level.

4.6 Boa loss of function results in a rough eye phenotype

boa^{6} homozygous mutant have large, rough eyes compared to controls (see figure 29 A and B). The observed eye phenotype is similar but not identical to the eye phenotype of *dASPP* mutants (compare figure 29 B to figure 13 B and C). *boa* mutant eyes are not as enlarged as *dASPP* mutant eyes but are rougher in appearance. High magnification SEMs of *boa*^{6} eyes reveal a strong patterning defect and the ommatidial lattice is disrupted (see figure 29 A' and B'). As observed in *dASPP* mutant eyes, *boa* mutant eyes have a bristle clustering phenotype (arrow in figure 29 B').

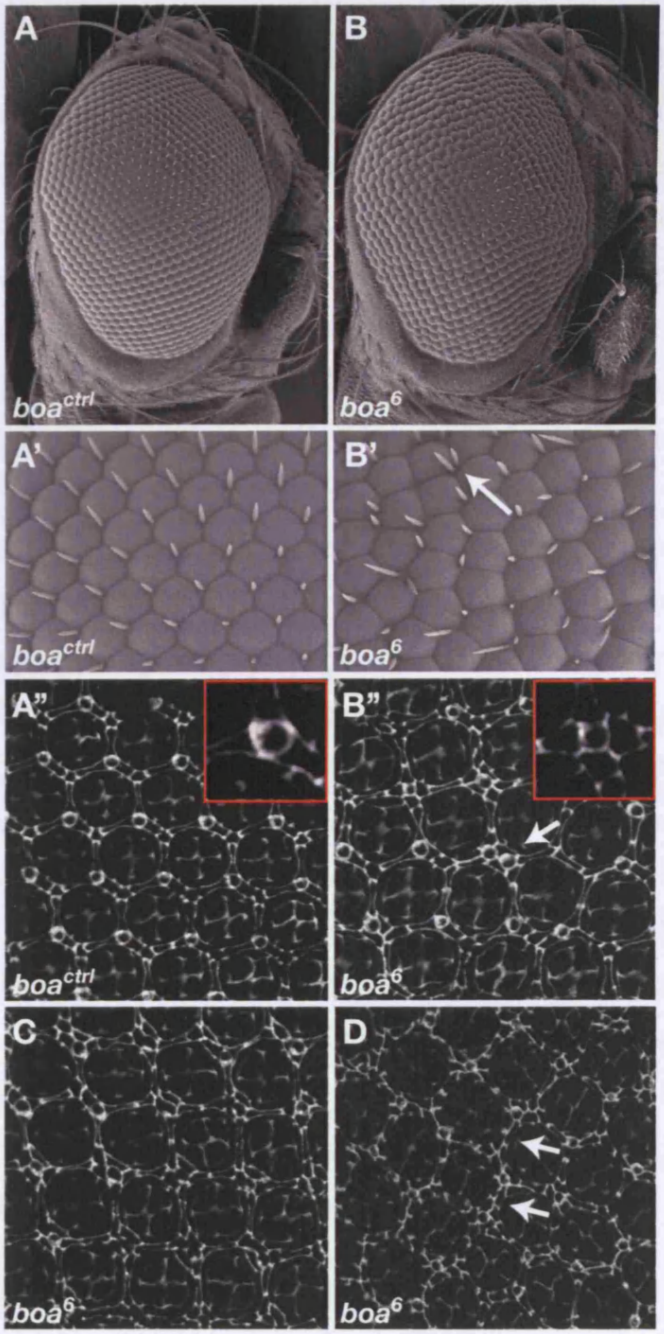

Figure 29: *boa* mutants have enlarged, rough eyes and mispatterned retinas. (A and B) Scanning electron micrographs (SEMs) of boa^{ctrl} (precise excision) (A) and boa^{6} (B) adult eyes. *boa* mutant eyes are large and rough compared to controls. (A' and B') High magnification SEMs of adult eyes, in boa^{6} mutant eyes the hexagonal lattice of ommatidia is disrupted and bristle clustering is observed. (A" and B") boa^{ctrl} and boa^{6} pupal retinas at 40h after puparium formation (APF) stained with anti-Dlg to mark cell outlines. In control retinas (A") the interommatidial cells form a regular hexagonal lattice and bristle cells always contact three secondary interommatidial cells (inset). In boa^{6} retinas (B") the lattice is disrupted. The inset shows a bristle cell contacted by four interommatidial cells and the arrow indicates bristle clustering. (C and D) Further examples of the phenotypes seen in boa^{6} mutant retinas. (C) shows a retina where each ommatidia has 4 vertices instead of 6 and (D) shows a retina where a double layer of interommatidial cells is observed (arrows).

The phenotype of *boa*^{6} eyes was also examined at the pupal stage using an anti-Discs large antibody to mark cell membranes. *boa*^{ctrl} retinas at 40-44h APF show the regular crystalline arrangement of hexagonal units (see figure 29 A''). The bristle cells are evenly spaced and each one always contacts three secondary pigment cells (inset in figure 29 A''). *boa*^{6} retinas at 40-44h APF are mis-patterned (see figure 29 B'', C and D). Ommatidia may have four or five vertices instead of six leading to a disruption of the hexagonal lattice. Bristle clustering is commonly observed (arrow in figure 29 B'') and bristle cells may contact four or more inter-ommatidial cells (inset in figure 29 B'').

A striking phenotype is commonly observed in *boa*^{6} mutant retinas where the organization of the lattice is severely altered and the ommatidia arrange into square rather than hexagonal lattice (see figure 29 C). It is not currently known why loss of *boa* can result in the formation of a square lattice although it is probably not due to dASPP mis-regulation as this phenotype is not observed in *dASPP* mutant retinas. Another striking phenotype of *boa*^{6} retinas is an increase in the number of inter-ommatidial cells, which can lead to the formation of a double layer of inter-ommatidial cells separating each ommatidium (see figure 29 D, arrows indicate double layer). An increase in the number of inter-ommatidial cells suggests either a delay in cell cycle exit after the MF and/or a defect in developmental apoptosis, which removes excess inter-ommatidial cells from the retina between 24h and 40h APF. These possibilities have not yet been tested. Although a few excess inter-ommatidial cells are detected in *dASPP* mutant retinas a double layer was never observed. This suggests that Boa could function to control the number of inter-ommatidial cells independently of dASPP.

4.7 Boa functions as a tumour suppressor

boa^{6} homozygous mutants, and to a lesser extent *boa*^{4} homozygous mutants, show a characteristic broad wing phenotype. *boa*^{6} mutant wings are shorter along the proximodistal axis and broader along the anteroposterior axis compared to *boa*^{ctrl} wings (see figure 30 A-C). Julien Colombani quantified the adult wing size and body weight of *boa*^{6} mutants and controls (see figure 30 D). In density-controlled crosses the average wing area of *boa*^{6} homozygotes (n=20) is 9.8% larger than *boa*^{ctrl} wings (n=15). Importantly, the wing hair density of *boa*^{6} mutants (n=12) is comparable to control

Figure 30: Boa is a negative regulator of tissue size. Density controlled crosses were performed at 25°C to obtain the genotypes indicated and adult wing area was determined. (A-C) *boa*^{6} mutant wings (B) are larger than *boa*^{ctrl} wings (A). (D) Quantification of body weight, wing area and wing hair density of *boa*^{ctrl} and *boa*^{6} flies. *boa*^{6} flies are heavier than controls and have larger wings (** indicates the $p<0.01$, using a student's t-test), the hair density is similar to controls suggesting that *boa*^{6} wings contain more cells rather than larger cells. The data and figure were done by Julien Colombani.

wings (n=12) indicating that *boa*^{6} mutant wings are larger because they contain more cells rather than larger cells (see figure 30 D). This suggests that proliferation is increased in *boa*^{6} mutant wings and that Boa does indeed function as a tumour suppressor to negatively regulate the size of developing organs. Accordingly, the adult body weight of *boa*^{6} mutants (n=80) is higher than the weight of control flies (n=120) by 9.9%. Both the increased wing size and body weight was rescued by ubiquitous *UAS-boa* expression, indicating that the observed phenotypes are indeed specific to loss of *boa* (Julien Colombani, personal communication).

4.8 The relationship between Boa and dASPP

By carefully quantifying the adult wing area and body weight of mutants and their appropriate controls we have shown that both dASPP and Boa are negative regulators of tissue size. As dASPP and Boa bind to each other and have similar mutant phenotypes it is highly likely that they function in the same cellular process. However, there are subtle differences between the phenotypes, for example *boa* mutant wings are large and broad and *dASPP* mutant wings are large but the shape is not affected. *boa* mutants also have a more severe rough eye phenotype. These differences suggest that although Boa and dASPP likely function together in some processes, they may also have independent functions.

Boa binding to dASPP raises the possibility that Boa functions to regulate the stability or localization of dASPP. This was tested by generating *boa*^{6} clones in eye-antennal imaginal discs and examining dASPP protein using the dASPP38 antibody. Interestingly, a reduction in dASPP protein was observed within *boa*^{6} clones (see figure 31 A-A'', arrows indicate examples), indicating that Boa regulates either the stability or localization of dASPP. These possibilities cannot be distinguished from this result as both would cause a reduction of apical dASPP staining. Ideally, the level of dASPP protein would be examined in *boa* mutant discs compared to controls by Western blotting. Unfortunately, this experiment was not possible as the dASPP antibodies generated do not recognise endogenous dASPP in protein extracts from either tissues or cultured cells (data not shown). However, it is possible to conclude that Boa is required to maintain high levels of dASPP at the apical membrane by controlling its stability or

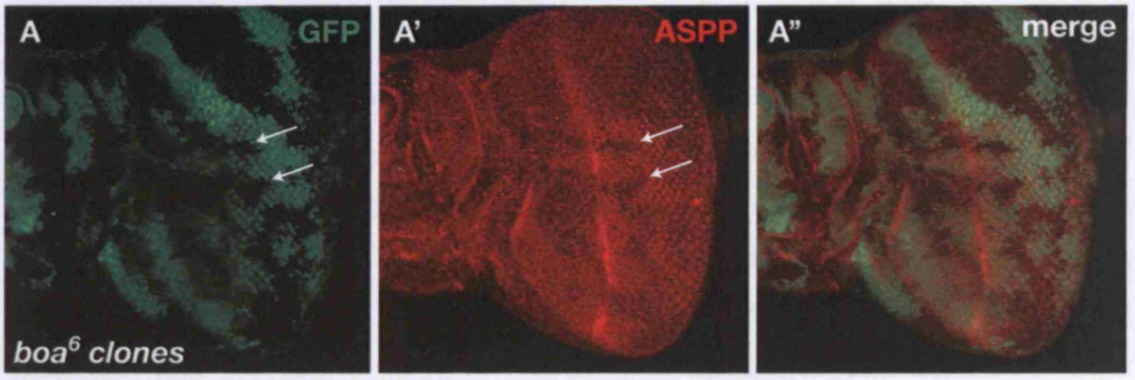

Figure 31: Boa regulates the levels or localization of dASPP. (A-A") A third instar eye-antennal disc with *boa*^{6} clones, marked by absence of GFP. A reduction in dASPP antibody staining (red) is observed in *boa*^{6} clones (arrows). This suggests that Boa regulates dASPP protein levels or dASPP sub-cellular localization.

localization. This implies that Boa is required for dASPP function and that the *boa* phenotype is at least partly due to de-regulation of dASPP. In support of this idea, the boa^6 phenotype can be partially rescued by ubiquitous expression of *dASPP* using the Gal4-UAS system. For example, *dASPP* expression in a boa^6 mutant background somewhat rescues the rough eye phenotype. The boa^6 eye phenotype is only partially rescued by *dASPP* expression whereas the $dASPP^8$ eye phenotype is completely rescued by *dASPP* expression (Julien Colombani, unpublished observation). Therefore it is likely that Boa has functions that are independent of dASPP.

4.9 *boa* genetically interacts with *dCsk*

As Boa is partially required for dASPP function and dASPP is required for maximal dCsk activity it is likely that dCsk activity is reduced in *boa* mutants. Therefore one would expect *boa* to genetically interact with *dCsk*, although more weakly than *dASPP* interacts with *dCsk*. To address this I compromised dCsk function in a boa^6 mutant background by introducing a copy of the strong $dCsk^{1jd8}$ allele. This resulted in moderate patches of ectopic apoptosis in wing discs (see figure 32 B-B') indicating that *dCsk* and *boa* genetically interact. The level of apoptosis occurring in *boa-dCsk* compromised wing discs is considerably lower than the level of apoptosis occurring in *dASPP-dCsk* compromised wing discs and accordingly notching of adult wings is not observed (see figure 32 B''). However, removing one copy of *dCsk* does enhance the large wing phenotype of boa^6 mutants (compare figure 32 A' to B' and A'' to B'') although the enhancement of wing area is yet to be quantified. This suggests that the proliferation defect observed in boa^6 wings is at least partially caused by a reduction in dCsk activity.

4.10 Boa, dASPP and dCSk – three proteins functioning in a common pathway?

Taken together these results suggest a model whereby Boa and dASPP function upstream of dCsk and SFKs to negatively regulate the organ size. Boa is required to maintain high levels of dASPP at the apical membrane and dASPP is required for maximal dCsk activity. The phenotypes observed suggest that minor increases in SFK

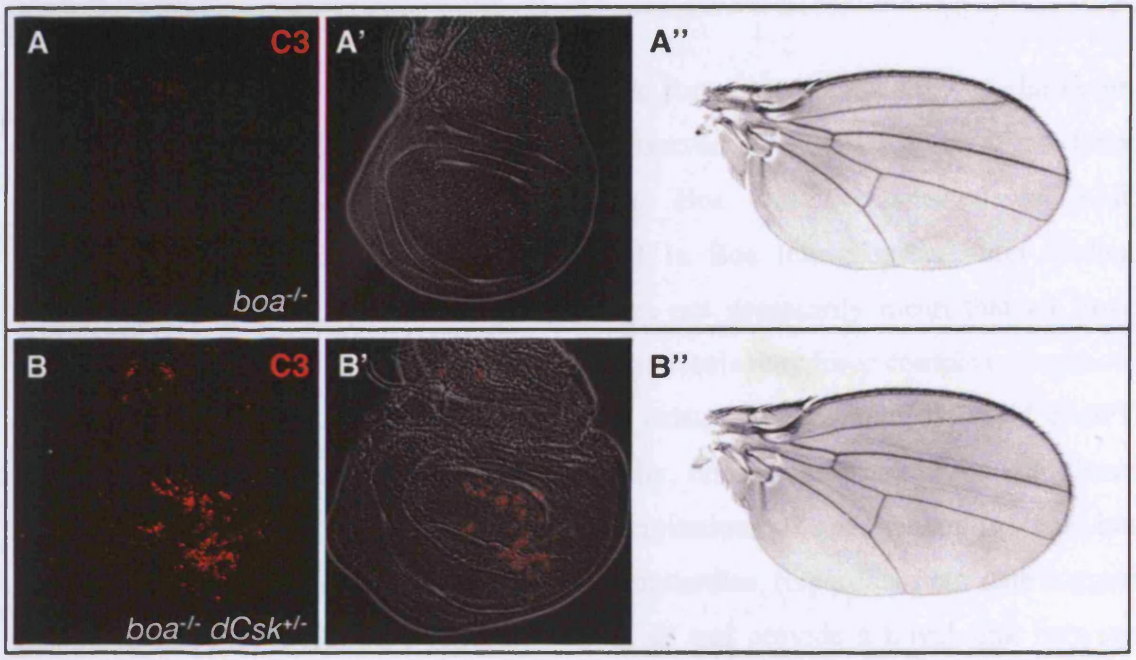

Figure 32: Genetic interactions between *boa* and *dCsk*. Cleaved Caspase 3 immunostainings (C3) (red) of third instar wing imaginal discs and the corresponding adult wings of the indicated genotypes. (B-B") Reducing dCsk function in a *boa* mutant background leads to ectopic apoptosis in wing discs. This level of apoptosis does not however result in notched adult wings (B"). (A-A") Little apoptosis is observed in boa^{6} mutant wings or in *dCsk* heterozygous wings (see figure 14).

activity (for example, in a *boa* or *dASPP* mutant) results in organ overgrowth as a consequence of increased proliferation and possibly reduced cell death. The data generated in this work also suggest that high levels of SFK signalling (for example in *dCsk* mutants or *dASPP-dCsk* compromised wings) lead to induction of apoptosis. This is in agreement with previous work showing that mild over-expression of *dSrc42A* or *dSrc64B* results in overgrowth and strong over-expression of *dSrc42A* or *dSrc64B* leads to apoptosis (Pedraza et al., 2004; Vidal et al., 2007).

It is not clear whether Boa, dASPP and dCsk form a complex *in vivo*, however, complexes containing all three proteins are observed in cultured cells. If all three proteins are overexpressed in Kc167 cells, Boa can be detected in dCsk immunoprecipitates and dCsk can be detected in Boa immunoprecipitates (Julien Colombani, personal communication). This does not necessarily mean that all three proteins form a complex *in vivo* as high expression levels may force complex formation. It is equally possible that 2 separate complexes exist, one containing Boa and dASPP and the other containing dASPP and dCsk. Ideally, one would examine the complexes formed in cultured cells following immunoprecipitations of endogenous proteins but this was not possible due to the lack of suitable antibodies. Regardless, our data suggest that both Boa and dASPP are regulators of dCsk and provide a novel link between previously unrelated tumour suppressor genes. It will be interesting to discover whether mammalian RASSF8 interacts with ASPP1 and/or ASPP2 and whether ASPP proteins also regulate CSK in mammals.

CHAPTER 5 The *DIAP-LacZ* project

5.1 Does the EGF/Ras/ERK pathway control DIAP1 at the transcriptional level ?

The EGF/Ras/ERK signalling pathway (the Ras pathway) carries out several important functions in the developing *Drosophila* eye. The Ras pathway promotes cell proliferation and cell survival and is re-iteratively utilised to control the differentiation of neuronal cells posterior to the MF, which become the light sensing photoreceptor cells (Raabe, 2000).

The Ras signalling pathway is known to promote cell survival in *Drosophila* by specifically inhibiting the activity of the pro-apoptotic protein, Hid (head involution defective) (Bergmann et al., 1998; Kurada and White, 1998). Hid is believed to be a phosphorylation target of MAPK/ERK and contains several MAPK consensus phosphorylation sites (Bergmann et al., 1998). Hid induces apoptosis by promoting the polyubiquitination and degradation of DIAP1, consequently relieving inhibition of Caspases (Yoo et al., 2002). Therefore Ras signalling promotes cell survival by indirectly increasing DIAP1 protein levels via Hid inhibition. Conversely, the Hippo signalling pathway promotes apoptosis by decreasing DIAP1 levels and this regulation occurs at both the post-translational and transcriptional level (Harvey and Tapon, 2007). Therefore, I was interested in examining the possibility that the Ras signalling pathway promotes cell survival by regulating DIAP1 at the transcriptional level.

5.2 The basis for examining whether Ras signalling upregulates DIAP1 transcription

In the third instar eye imaginal disc the Ras signalling pathway is highly active in the ommatidial preclusters, which are specified as cells exit the MF. This can be visualised using an antibody that recognises active ERK/MAPK (see figure 33 A'). This pattern of ERK activation is highly reminiscent of the observed pattern of *DIAP1* expression in eye discs following in-situ hybridization (Nic Tapon, personal communication). *DIAP1*

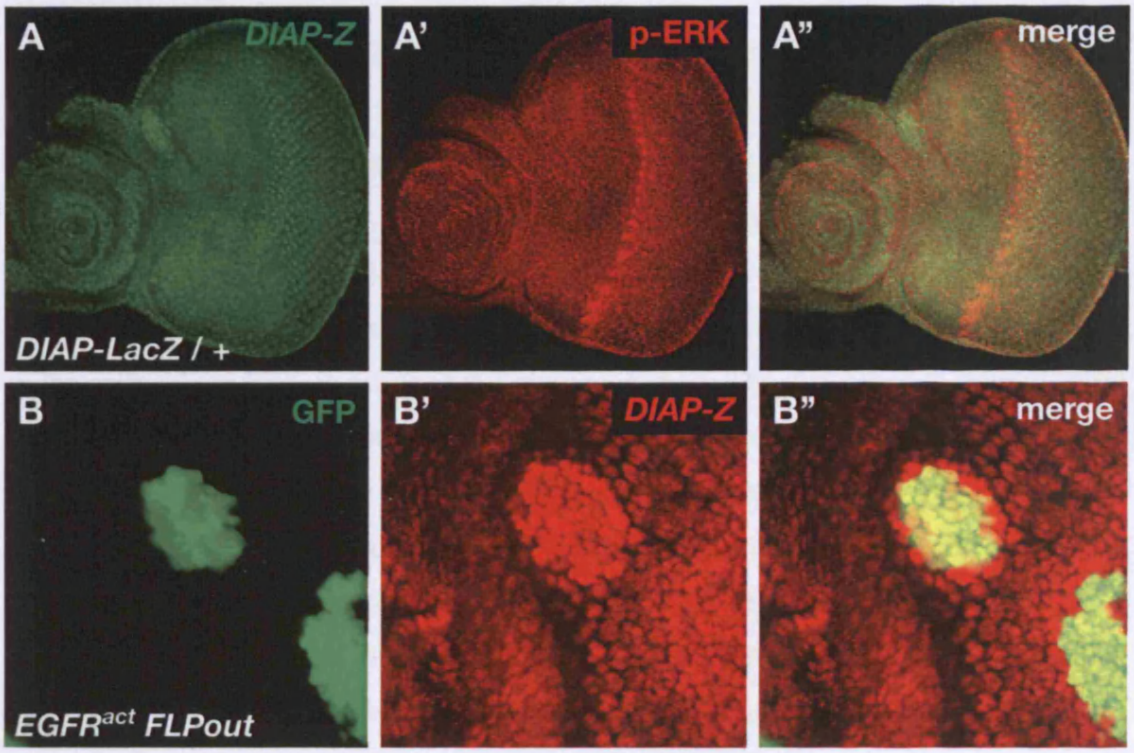

Figure 33: Transcriptional control of *DIAP1* by the EGF/Ras/ERK pathway. (A-A") A wildtype (*w*) eye-antennal disc immunostained with p-ERK (red) and Beta-Gal (green) (to visualise *DIAP-LacZ* reporter expression) antibodies. p-ERK is detected in ommatidial preclusters as cells exit the morphogenetic furrow (MF). *DIAP-LacZ* expression is highest in the photoreceptor clusters posterior to the MF and is first detected in the row of cells directly posterior to p-ERK expressing cells suggesting that DIAP1 may be transcriptionally regulated by the EGF/Ras/ERK pathway. (B-B") A eye-antennal disc bearing activated EGF receptor ($EGFR^{act}$) FLPout clones, labelled by GFP expression. *DIAP-LacZ* (red) is elevated within the EGFR overexpressing clones and within cells neighbouring the clone.

transcript is observed in 'tufts' of cells directly posterior to the MF corresponding to the preclusters. ERK activation and DIAP1 transcription therefore occur concurrently in a spatial and temporal manner suggesting that DIAP1 may be a direct transcriptional target of the Ras pathway. This observation led me to examine this potential regulation mechanism in detail.

DIAP-LacZ is a transposon insertion into the first *DIAP1* intron that places the *LacZ* gene under the control of the endogenous *DIAP1* promoter. *DIAP-LacZ* can therefore be used to monitor levels of *DIAP1* transcription. *DIAP-LacZ* expression is observed in all differentiating photoreceptor cells and is highest in the first few rows of cells posterior to the MF (see figure 33 A). *DIAP-LacZ* is not detected in the 'tufts' of cells where ERK is active; its expression is first detected in the row of cells immediately posterior to the cells where ERK is active (see figure 33 A-A''). The difference in time of onset of *DIAP1* transcription as visualised by in-situ hybridization or by using *DIAP-LacZ* is likely to be due to the time taken to accumulate LacZ and produce β-Galactosidase. Therefore the earliest induction of *DIAP1* transcription, directly posterior to the MF, may not be seen when using the *DIAP-LacZ* reporter. However, *DIAP-LacZ* is expressed at high levels directly posterior to the region of high Ras signalling suggesting that *DIAP1* may be a transcriptional target of the Ras pathway.

5.3 Analysis of *DIAP-LacZ* in Ras pathway gain of function clones

To address whether *DIAP1* is a transcriptional target of the Ras pathway I used mosaic analysis and examined the expression of *DIAP-LacZ* in clones that were either gain or LOF for various Ras pathway components. Ras signalling is known to be activated following ligand binding and activation of the EGF receptor (EGFR). Therefore, I overexpressed an activated form of EGFR ($EGFR^{act}$) in FLPout clones and asked whether the transcription of *DIAP1* is affected. I observed a strong induction of *DIAP-LacZ* expression in $EGFR^{act}$ expressing clones (see figure 33 B-B''). This was the first indication that *DIAP1* may be a transcriptional target of the Ras pathway. Interestingly, the induction of *DIAP* transcription was observed within the clone and also in a ring of cells around the clone suggesting that the Ras pathway can non-autonomously regulate *DIAP1* transcription over a short distance. Next, I overexpressed an activated form of

Ras (Ras^{V12}) in FLPout clones. Like $EGFR^{act}$ expressing clones, Ras^{V12} expressing clones showed an upregulation of *DIAP1* (data not shown) suggesting that the *DIAP-LacZ* expression observed in $EGFR^{act}$ FLPout clones is likely due to Ras activation.

Next, I wanted to determine which of the transcription factors known to function downstream of Ras could be responsible for regulating *DIAP1* expression. Pointed (Pnt), Yan and Tramtrack (Ttk) are transcription factors known to function downstream of Ras and MAPK to control photoreceptor differentiation (Brunner et al., 1994; Lai and Rubin, 1992; Li et al., 1997; O'Neill et al., 1994; Tang et al., 1997). Therefore, I tested whether gain or LOF for these transcription factors affected *DIAP-LacZ* expression. The *pnt* locus encodes 2 transcriptional activator proteins, PntP1 and PntP2 (O'Neill et al., 1994). The *yan* locus is encodes a single transcriptional repressor protein (Lai and Rubin, 1992; O'Neill et al., 1994). The *ttk* locus codes for 2 repressor proteins, Ttk69 and Ttk88 (Harrison and Travers, 1990; Read and Manley, 1992).

For gain of function analysis I was able to acquire *UAS-pntP1*, *UAS-pntP2*, *UAS-ttk69* and *UAS-ttk88* transgenes and generated FLPout clones to examine their effects on *DIAP1* transcription. Unfortunately, I was not able to acquire a *UAS-yan* transgene. Over-expression of *pntP1* or *pntP2* did not affect expression of *DIAP-LacZ* (see figure 34 A-A''' and B-B''') suggesting that the transcriptional upregulation of DIAP1 by the Ras signalling pathway does not occur via PntP1or PntP2. However, when I generated *ttk69* overexpressing clones I observed a strong induction of *DIAP-LacZ* expression (see figure 34 C-C'''). This effect was specific to Ttk69 as over-expression of *ttk88* had no effect on *DIAP-LacZ* expression (see figure 34 D-D''').

As Ttk69 is a transcriptional repressor it was surprising that its over-expression resulted in an upregulation of *DIAP1* transcription. One possibility is that Ttk69 regulates *DIAP1* transcription indirectly, for example Ttk69 may represses expression of a protein that itself represses *DIAP1* transcription. If this were the case then Ttk69 over-expression would alleviate *DIAP1* repression. Another possibility is that over-expression of *ttk69* has dominant negative effects. For example, excessive Ttk69 may titrate a co-repressor leading to a derepression of *DIAP1* transcription. In order to distinguish between these possibilities it would be necessary to firstly determine whether Ttk69 is able to bind to the *DIAP1* promoter.

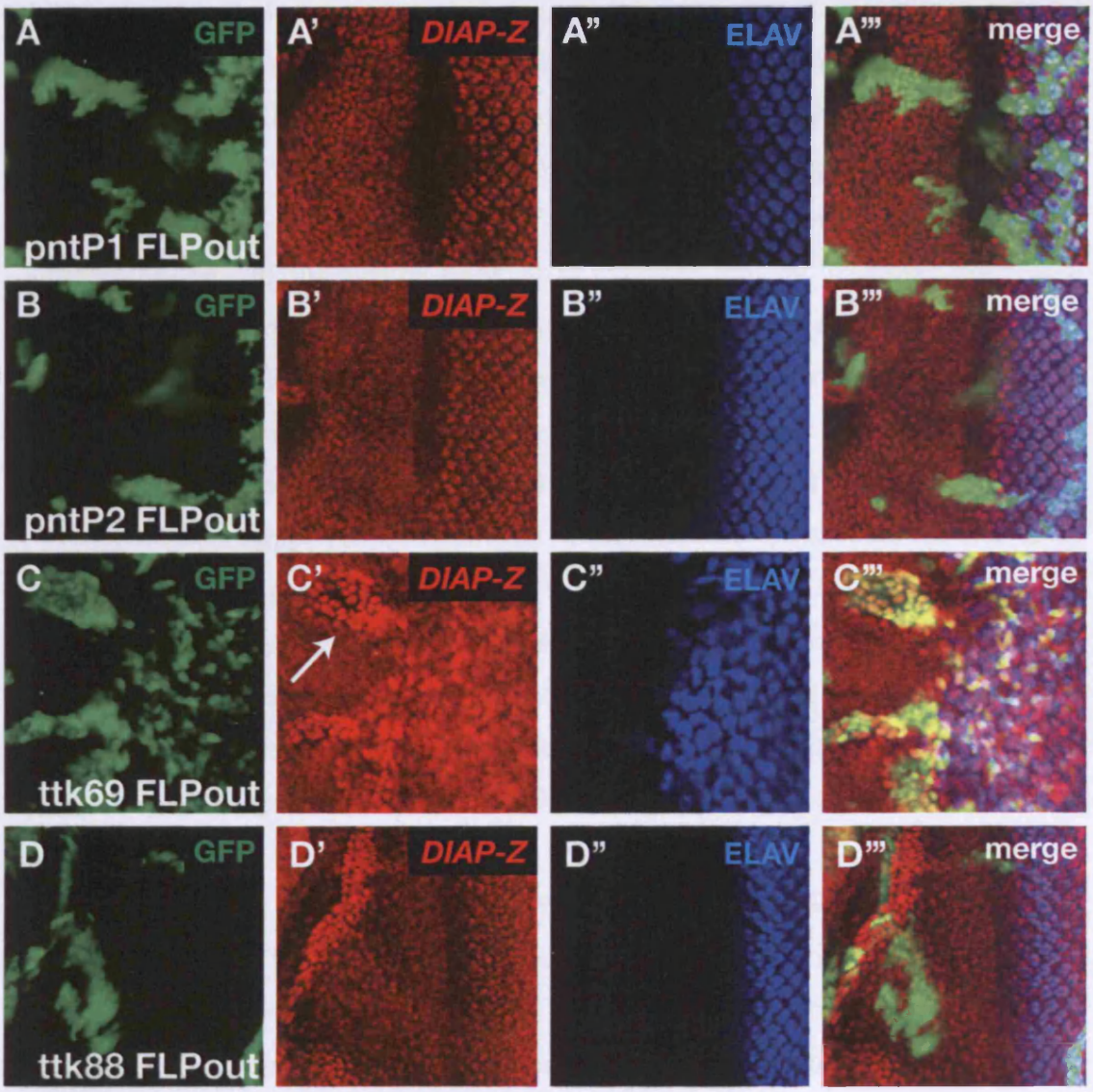

Figure 34: The effect of overexpressing transcription factors functioning downstream of the Ras pathway on *DIAP-LacZ* expression. (A, B, C, D) FLPout clones, marked by GFP expression, overexpressing either *pntP1*, *pntP2*, *ttk69* or *ttk88* were generated in eye-antennal discs. (A', B', C', D') The level of *DIAP-LacZ* reporter expression (red) within the clones was examined. Elevated *DIAP-LacZ* was observed in *ttk69* overexpressing clones (C') but not in *pntP1*, *pntP2* or *ttk88* overexpressing clones. (A", B", C", D") ELAV staining (blue) is used a marker of neuronal differentiation, *ttk69* over-expression (C") resulted in abnormal neuronal differentiation posterior to the morphogenetic furrow.

5.4 Analysis of *DIAP-LacZ* in Ras pathway loss of function clones

Ttk69 was identified as a transcription factor downstream of Ras that might be responsible for promoting *DIAP1* transcription. Therefore I generated LOF *ttk* clones and asked whether DIAP1 levels are reduced within the clones. ttk^{lel1} is a mutation that disrupts expression of both Ttk isoforms and ttk^{l} specifically disrupts the Ttk88 isoform (Xiong and Montell, 1993). Therefore, if Ttk69 promotes *DIAP1* transcription, as suggested by gain of function analysis, it is expected that ttk^{lel1} clones will show reduced DIAP protein and ttk^{l} clones will not affect DIAP1 protein levels. However I observed no change in DIAP1 staining in either ttk^{lel1} clones (see figure 35 A-A''') or in ttk^{l} clones (see figure 35 B-B'''). This result conflicts with the gain of function data and suggests that Ttk69 may not regulate DIAP1 levels. Neither of the models proposed in the previous paragraph based on the gain of function data can account for this result. If the first model, suggesting that Ttk69 indirectly regulates *DIAP1* at the transcriptional level is true, then one would still expect to see reduced DIAP1 protein in Ttk^{lel1} clones. The second model suggested that Ttk69 actually did repress *DIAP1* transcriptionally and that *UAS-ttk69* acts as a dominant negative by titrating a co-repressor. If this is true then one expects to see an upregulation of DIAP1 in ttk^{lel1} clones as repression is lost.

One explanation that may reconcile the LOF and gain of function data is that Ttk69 does upregulate *DIAP1* transcriptionally but acts redundantly with other transcription factors. In other words Ttk69 may be sufficient but not necessary for *DIAP1* transcription, which would explain the observed upregulation in gain-of-function clones and lack of effect in loss-of-function clones. Therefore, whether Ttk69 regulates *DIAP1* transcriptionally downstream of Ras remains and open question and further experiments would be needed to address this.

I was not able to obtain *UAS-yan*, which prevented gain of function analysis, but I was able to obtain a *yan* mutation (yan^{ex1}) recombined onto an FRT chromosome for LOF analysis. In *yan* clones I observed a reduction in DIAP1 protein levels (see figure 35 C-C''') suggesting that Yan may regulate DIAP1. Yan is a transcriptional repressor so direct targets are expected to be elevated in mutant clones. The fact that I observed reduced DIAP1 levels suggests that Yan may regulate DIAP1 indirectly. Alternatively, the downregulation of DIAP1 observed may be due to very indirect effects as a

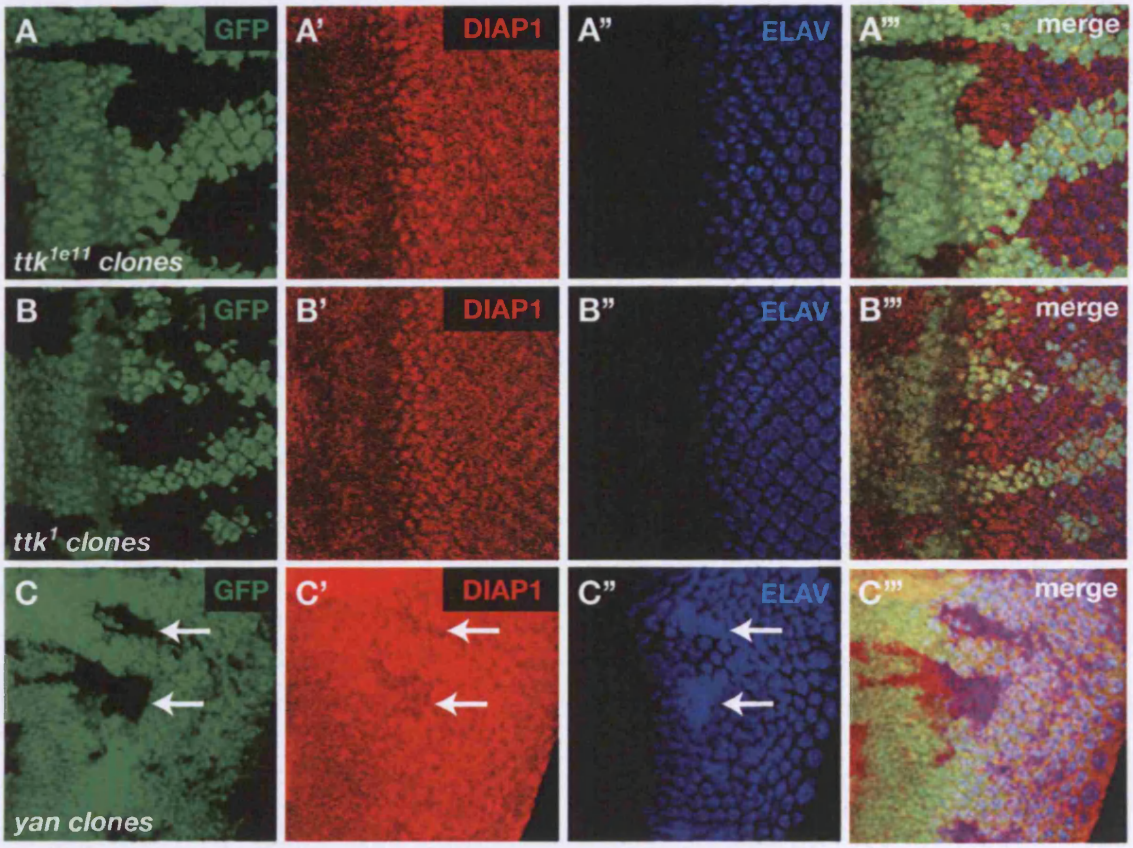

Figure 35: DIAP1 levels in *ttk* and *yan* loss of function clones. 3rd instar eye-antennal discs with *ttk* or *yan* mutant clones marked by absence of GFP were immunostained with an anti-DIAP1 antibody (red) and the neuronal marker ELAV (blue). (A and B) DIAP1 levels are normal in *ttk1e11* (A-A"') and *ttk1* (B-B"') clones and neuronal differentiation is unaffected. (C) A reduction in DIAP1 protein is observed in *yan* clones (arrows in C'). Excessive neuronal differentiation is observed in *yan* clones (arrows in C").

consequence of abnormal cell behaviours induced by loss of Yan. Yan is a general inhibitor of differentiation and, as expected, I observed overproduction of neuronal cells in *yan* mutant clones as visualised using an antibody against the neuronal marker, ELAV (see figure 35 C'', arrows indicate position of clones). The level of *DIAP-LacZ* in *yan* loss-of-function clones has not been examined.

CHAPTER 6 Discussion

6.1 dASPP regulates dCsk activity

6.1.1 Summary of findings

The work presented provides evidence that dASPP, the homolog of the human ASPP proteins, has a previously uncharacterized role as a regulator of SFKs in *Drosophila*, by binding to and potentiating the kinase activity of the SFK inhibitor, dCsk. The genetic and biochemical data complement each other and suggest that dASPP is a positive regulator of dCsk (Langton et al., 2007).

Firstly, *dASPP* and *dCsk* mutants show similar phenotypes. They both function as tumour suppressors and LOF mutations lead to increased proliferation, which results in an increase in the size of organs and animals. *dASPP* and *dCsk* mutants also show developmental delay, which is approximately one day for *dASPP* mutant adults. The developmental delay is more prolonged in *dCsk* mutants; the emergence of wandering larvae is delayed by about four days. *dASPP* and *dCsk* mutants show an alteration in cell-cell adhesion properties, which results in mis-patterning of the retina and compromises epithelial integrity in the wing. The similarity of phenotype suggests that dASPP and dCsk may function in the same signalling pathway. *dCsk* has a stronger phenotype than *dASPP*. For example, *dCsk* hypomorphic mutants die as giant pupae, whereas *dASPP* mutants are homozygous viable and show a more modest increase in organ and animal size. This suggests that dASPP is not absolutely required for dCsk function but rather it is necessary for maximal signalling.

Secondly, *dASPP* mutants enhance the *dCsk* RNAi phenotype, as would be expected for a positive regulator of dCsk. It is likely that dCsk function is partially compromised in *dASPP* mutant flies and therefore this genetic background confers extreme sensitivity to further loss of dCsk function. For example, reducing the gene dosage of *dCsk* in a *dASPP* mutant background leads to considerable apoptosis in the developing wing, which results in notched adult wings. Importantly, the wing disc apoptosis phenotype is observed for *dCsk* homozygous mutants suggesting that it is indeed the result of

reduced dCsk function. Furthermore, the interaction was specific to dASPP and dCsk as the phenotype is not observed when a null allele for *wts*, another tumour suppressor, is introduced into a *dASPP* mutant background. The fact that multiple *dASPP* alleles (*dASPP*^{d} and *dASPP*^{8}) show this genetic interaction with multiple *dCsk* alleles (*dCsk*^{1jd8} and *dCsk*^{SO17909}), strengthens the argument that *dASPP* and *dCsk* genetically interact and that the phenotype observed is not due to secondary mutations on either chromosome. In addition *dASPP* mutants strongly enhance the specific phenotypes of *dCsk* RNAi boundary cells providing further evidence that dASPP positively regulates dCsk. The enhanced phenotype is rescued by expressing *dASPP* transgenically showing that the enhancement is specifically caused by loss of dASPP. Taken together the genetic data for dASPP and dCsk strongly suggests that dASPP has a positive role in a dCsk-signalling pathway that acts to maintain epithelial integrity.

Thirdly, dASPP and dCsk physically interact as shown by co-immunoprecipitation and GST-pulldown experiments, which supports the hypothesis that dASPP functions in a dCsk-signalling pathway. Furthermore, dASPP is able to enhance the kinase activity of dCsk on one of its physiological substrates, dSrc42A. Taken together with the genetic data this provides compelling evidence that dASPP functions as a positive regulator of dCsk and hence, a negative regulator of SFKs in *Drosophila*. Genetic epistasis experiments also suggest that dASPP functions upstream of SFKs. The *dASPP* null phenotype (*dASPP*^{8}) is almost completely suppressed by loss of *dSrc64B* (using the *dSrc64B*^{KO} null allele) showing that *dSrc64B* is required for the *dASPP* phenotype.

6.1.2 dASPP and p53

Human ASPP proteins have been shown to directly bind to and regulate the apoptotic function of p53 (Samuels-Lev et al., 2001). However, several lines of evidence suggest that dASPP does not function as a regulator of Dmp53. Firstly, *dASPP* mutants show overgrowth phenotypes and Dmp53 is not implicated in the control of tissue growth. This does not exclude the possibility that dASPP regulates Dmp53 but does suggest that the overgrowth phenotype of dASPP mutants is not due to Dmp53 mis-regulation. Secondly, dASPP and Dmp53 do not physically interact in co-immunoprecipitation experiments (Julien Colombani, personal communication). Additionally, neither the

four human p53 residues (His^{178}, Arg^{181}, Met^{243} and Asn^{247}) shown in crystallography studies to contact ASPP2 (Gorina and Pavletich, 1996) nor the proline-rich region shown to be a second site for binding between the two proteins (Bergamaschi et al., 2006) are conserved in Dmp53. Thirdly, dASPP is not required for radiation-induced cell death; *dASPP* clones in the wing disc show similar levels of apoptosis to wild-type tissue following irradiation (Julien Colombani, personal communication). Radiation-induced apoptosis is known to require Dmp53 (Brodsky et al., 2000; Ollmann et al., 2000), suggesting that dASPP is not required for Dmp53 to induce apoptosis in response to DNA damage. Taken together this suggests that p53 activating function of ASPP proteins is not conserved in *Drosophila* and may have evolved later. It will be interesting to see whether human ASPP proteins function as regulators of CSK as this work on *Drosophila ASPP* suggests; one possibility is that human ASPP regulates both p53 and CSK.

6.1.3 dASPP largely functions to regulate dCsk rather than the Hippo pathway

The aim at the start of this project was to identify novel components of the Hippo pathway by conducting a candidate-based genetic screen for modifiers of a Hippo pathway over-expression phenotype (*GMRsav,wts*). The strongest suppressor (*dASPP*) identified did have the expected overgrowth phenotype, however I subsequently showed that this is probably largely attributable to increased SFK signalling rather that reduced Hippo signalling. Combining *dASPP* mutations with Hippo pathway mutations either results in no enhancement of the large wing phenotype (in the case of $hpo^{42\text{-}47}$) or additive effects (in the case of wts^{X1}). However, combining *dASPP* mutations with *dCsk* mutations results in a synergistic interaction that gives rise to ectopic apoptosis in the developing wing. Therefore, the strong genetic interaction suggests that dASPP functions to negatively regulate growth in a dCsk-SFK pathway rather than in the Hippo pathway.

6.1.4 Caveats of the genetic modifier screen

The *dASPP* mutants I generated did not show a convincing genetic interaction with the Hippo pathway. This was surprising as *GE13722*, which presumably represents a very

weak *dASPP* allele, strongly suppresses the *GMRsav,wts* phenotype. This suggests that *GE13722* represented a 'false positive' in my screen and that the suppression of *GMRsav,wts* observed is not due to loss of dASPP function but instead due to secondary mutation(s) on the *GE13722* chromosome. This highlights the importance of following up modifier screens with secondary screens to confirm hits and eliminate false positives arising from background effects.

Another potential caveat of the screen was that the majority of P-element insertions tested likely constituted weak LOF alleles as they were inserted either within the promoter region or within introns of genes of interest. This reduced the sensitivity of the screen since I was searching for dominant modifiers of the *GMRsav,wts* phenotype. Thus, the false negative rate of the screen was probably high. Furthermore, the intrinsic variability of the *GMRsav,wts* phenotype makes assessing the extent of suppression or enhancement difficult.

6.1.5 dASPP may have a minor and indirect role in the Hippo pathway

Despite the fact that merely additive effects on wing growth are observed when *dASPP* and *wts* mutations are combined, it is still possible the dASPP has some input to the Hippo pathway. Firstly, some of the genetic data presented suggests that in fact *dASPP* does genetically interact with the Hippo pathway. For example, *wts* mutations convincingly enhance the eye phenotype of *dASPP* mutants. In this case it cannot be said that the interaction is additive as heterozygosity for *wts* does not result in an eye phenotype. In addition, a deficiency for *dASPP* does partially suppress *GMRsav,wts*.

One possibility is that dASPP indirectly regulates the Hippo pathway via dCsk and *Drosophila* SFKs. Indeed, Wts was shown to be a phosphorylation target of dCsk and *dCsk* mutants are partially rescued by *wts* expression suggesting that dCsk functions upstream of Wts (Stewart et al., 2003). Another group recently showed that the rough eye induced by mild *dSrc64B* expression is suppressed by *wts* mutation (Vidal et al., 2007). This result indicates that the effects dCsk has on Wts are mediated indirectly via the SFKs and that Wts may not be a direct target of dCsk. Therefore, the relationship between dCsk and the Wts is not clear at present. It is unlikely to be a straightforward as

Hippo pathway readouts are not affected in *dCsk* clones. However, the Hippo and dCsk/SFK pathways genetically interact suggesting that there is crosstalk between the two. Regardless of whether dCsk regulates Wts directly or indirectly, this data, along with my own, suggests that the overgrowth phenotype of *dASPP* mutants is primarily due to decreased dCsk function, which may indirectly result in mild reductions in Hippo pathway activity.

6.1.6 dASPP, dCsk and epithelial integrity

dCsk mutant cells have been shown to be only susceptible to apoptosis when in contact with wild-type tissue (Vidal et al., 2006). I confirmed this result and found that *dCsk* LOF in discrete areas of the wing disc (using *ptcGal4>dCskIR*) does induce apoptosis of mutant cells. However, I found that broad loss of dCsk in wing discs also results in considerable apoptosis (for example in *dCsk* homozygous discs). This has not been previously described for *dCsk* mutant wing discs and suggests that epithelial extrusion and cell death may not only occur at mutant/wild-type boundaries but instead is a more general phenotype of *dCsk* mutant cells. This idea is supported by results from a recent paper, which shows that different levels of *Drosophila* SFK signalling have different outcomes; mild increases in SFK signalling lead to overgrowth and inhibit apoptosis, whereas strong increases in SFK signalling leads to apoptosis. The authors used a *dCsk* null allele to completely remove dCsk function in the eye and found that this leads to eye ablation by apoptosis (Vidal et al., 2007). Therefore, broad loss of dCsk can either protect against or induce apoptosis depending on the strength of the allele in question.

It has been suggested that specific interactions occur at mutant/wild-type boundaries that lead to the exclusion and death of *dCsk* mutant cells (Vidal et al., 2006). However, this conclusion was based on the effects of driving a *dCsk* RNAi construct using Gal4 drivers that express in the whole wing (Eg. *765-Gal4*) or in discrete areas of the wing (Eg. *ptc-Gal4*) (Vidal et al., 2006). One possibility is that the *ptc-Gal4* driver simply expresses more strongly than the *756-Gal4* driver, leading to apoptosis only when the former controls *dCsk* RNAi expression. The fact that apoptosis largely occurs at the posterior boundary of the *ptc* expression domain may not be due to the presence of a sharp boundary between mutant and wild-type cells as suggested, but instead because

ptc is expressed more strongly towards the posterior side of its expression domain. Additionally, the authors could not explain why apoptosis occurs several cell diameters away from the boundary when the strongly expressing *sd-Gal4* driver was used (Vidal et al., 2006).

Vidal et al showed that the *ptcGal4>dCskIR* phenotype (discrete loss, leading apoptosis) but not the *GMRGal4>dCskIR* phenyotype (broad loss, leading to overgrowth) is suppressed by heterozygosity for *p120-catenin.* This suggests that p120-catenin is specifically required for the boundary phenotype. However, I believe that the phenotype of *dCsk* in the eye and wing should not be compared. For example, d*ASPP-dCsk* compromised animals show a strong apoptotic wing phenotype and only a mild enhancement of the rough eye phenotype (data not shown), suggesting that the wing epithelium is more sensitive to loss of *dCsk* than the eye epithelium. It is not understood at present why the wing is more sensitive to loss of *dCsk-dASPP.*

Therefore, I speculate that broad loss of dCsk can result in apoptosis depending on the strength of LOF and the tissue examined. An interesting question arises from this study: is the extrusion and cell death caused by either discrete or broad loss of dCsk the result of the same phenomenon? The fact that broad loss and discrete loss result in a similar phenotype suggests that this is the case. However, clones of hypomorphic *dCsk* mutations in the eye do not survive to adulthood, whereas when the whole eye is mutant, the adult eye is often overgrown (Vidal et al., 2006). This cannot be easily explained unless there is a boundary-specific effect caused by loss of *dCsk*, which eliminates clonal tissue. One possibility is that *dCsk* mutant clones are eliminated by cell competition, which could be tested by examining the survival of *dCsk* clones in a *minute* background. More work will be needed to address whether there is indeed a specific boundary effect induced by loss of dCsk and to identify the responsible cellular components and behaviours.

6.1.7 Loss of dASPP / dCsk promotes extrusion, apoptosis and migration

dASPP-dCsk deficient wing disc cells undergo apoptosis, move to a basal position within the epithelium and adopt a 'migratory' like behaviour. These events are likely to

be the consequence of ectopic SFK activation, which has been shown to induce apoptosis in *Drosophila* imaginal discs (Pedraza et al., 2004; Tateno et al., 2000; Vidal et al., 2007), and is known to disrupt cell adhesions and promote migratory behaviour in mammalian cells (Yeatman, 2004).

6.1.7.1 Apoptosis of *dASPP-dCsk* mutant cells

I have shown that the ectopic apoptosis in *dASPP-dCsk* compromised wings is sensitive to the dosage of Btk, which is known to function downstream of SFKs in *Drosophila* and mammals (Guarnieri et al., 1998; Roulier et al., 1998; Saouaf et al., 1994; Tateno et al., 2000). Furthermore, I have shown that the cell death is mediated via the JNK signalling pathway, which induces cell death in many contexts, and is known to function downstream of SFKs in *Drosophila* and mammals (Dolfi et al., 1998; Read et al., 2004; Tateno et al., 2000). Therefore, it is highly likely that the apoptosis phenotype is the result of abnormal SFK activation. Indeed, over-expression of constitutively active *dSrc42A* has been shown to induce apoptosis in the wing disc via the JNK pathway (Tateno et al., 2000) and over-expression of activated forms of either *Drosophila* SFK in the eye leads to its ablation (Pedraza et al., 2004).

Since *btk* is required for the *dCsk* apoptosis phenotype, it is possible that SFKs activate Btk, which in turn directly or indirectly activates the JNK pathway, leading to cell death. It would be interesting to examine this possibility, as Btk has not previously been implicated in the induction of cell death by *Drosophila* or mammalian SFKs. Firstly, it would be necessary to confirm that *btk* LOF rescues the apoptosis phenotype using other *dCsk* and *btk* alleles. For, example it has recently been shown that *dCsk* null eyes are ablated by apoptosis; one could test whether *btk* mutants rescue this phenotype. *UAS-btk* transgenic lines could be generated to assess whether *btk* over-expression, like SFK over-expression, induces apoptosis. Once the result is confirmed it would be interesting to delineate the pathway responsible for inducing apoptosis. For example, it is not known whether Btk is regulated by both *Drosophila* SFKs. This could be addressed by assessing whether *btk* mutations suppress phenotypes resulting from over-expression of either of the *Drosophila* SFKs. Also, if Btk is responsible for inducing JNK signalling, then how is this achieved? One could examine which known

components of the JNK cascade are required for SFK/Btk induced apoptosis; this may provide clues as to where Btk functions within the JNK pathway.

In mammals active c-SRC has been shown to activate the JNK pathway in collaboration with FAK (Hauck et al., 2002; Hsia et al., 2003). The role of dFAK in SFK signalling is not well characterized and it would be interesting to test whether it is required for SFKs to activate the JNK pathway in *Drosophila*.

6.1.7.2 Loss of cell adhesions in *dASPP-dCsk* mutant cells

Mammalian c-SRC is known to have dramatic effects on both adherens junctions and focal adhesions (Yeatman, 2004). Therefore, it seems likely that *dASPP-dCsk* compromised wing disc cells move to a basal position within the epithelium as a result of altered adhesion properties induced by SFK activation. However, this is purely speculative, and was not directly examined in this work. Loss of cell-cell adhesions probably also contributes to the migratory phenotype as cells must detach from their neighbours to spread through the basal layer.

Interestingly, the phenotype of *dCsk* deficient boundary cells is suppressed by reducing the gene dosage of *shg* (*Drosophila E-Cadherin*) (Vidal et al., 2006), implying that an alteration in cell-cell adhesion properties is important for both basal extrusion and cell migration following SFK activation. However, this is a surprising result; it is expected that reducing *shg* levels would enhance rather than suppress the phenotype, as SFK activation is known to inhibit E-Cadherin function in mammals. One proposed explanation is that Shg has an autonomous role in the pathway responsible for promoting the removal of dCsk boundary cells; Shg may be required for JNK activation by SFKs. It would be interesting to see whether Shg is also required for the basal extrusion and apoptosis resulting from broad loss of dCsk in wing discs. Such experiments may reveal whether the phenotypes resulting from broad or discrete loss of dCsk are the result of the same cellular response.

6.1.7.3 Migration of *dASPP-dCsk* mutant cells

Activated c-SRC is implicated in the metastasis of tumour cells and has been shown to induce migratory behaviour using *in vitro* metastasis models (Hauck et al., 2002). Therefore, it is likely that the movement of dCsk boundary cells away from their original position occurs by active migration. In support of this view the migratory phenotype is sensitive to modulations in JNK pathway activity and is suppressed by heterozygosity for *matrix-metalloprotease 2* (*MMP-2*) (Vidal et al., 2006). The JNK pathway is known to induce expression of *MMPs* in mammals (Hauck et al., 2002), which are required to degrade the ECM, allowing cells to become migratory. The fact that *dASPP* mutations enhance the distance that *dCsk* RNAi cells migrate suggests that human *ASPP* LOF may contribute to tumour cell metastasis. Interestingly, ASPP2 has been reported to be downregulated in invasive and metastatic breast carcinoma cells (Sgroi et al., 1999). The results presented in this work provide a potential mechanism for ASPP's role in tumour cell invasion.

An alternative explanation for the movement of *dCsk* RNAi cells away from the *ptc* domain is that they are simply diffusing within the basal layer. However, *dCsk* null clones that also express Ras^{V12} are highly invasive and mutant cells metastasize to distant secondary locations; a diffusion model cannot explain this result. Ras^{V12} also rescues the apoptosis of dCsk mutant cells suggesting that the movement of such cells is not simply the result of apoptosis and basal extrusion (Vidal et al., 2007).

6.1.7.4 Does loss of polarity lead to apoptosis or vice versa?

Previous work has shown that loss of polarity precedes JNK activation and cell death. For example, mutants for apico-basal polarity genes such as *scribble* lead to E-Cadherin down-regulation and JNK dependent apoptosis (Bilder and Perrimon, 2000; Brumby and Richardson, 2003). In fact *scribble* and *dCsk* phenotypes are highly similar; both result in overgrowth in a homotypic environment whereas clones are eliminated by JNK dependent apoptosis (Brumby and Richardson, 2003; Vidal et al., 2006). Therefore, it is possible that SFK activation in *dCsk* mutant cells disrupts apico-basal polarity complexes, leading to mis-localization of adherens junction components, JNK

activation and cell death. Alternatively, SFK activation may directly affect adherens junctions, leading to JNK activation and cell death. Both of these possible models suggest that loss of polarity / adhesion precedes apoptosis.

Interestingly, my results indicate that cell death may contribute to extrusion and migration of *dCsk* RNAi cells. I found that blocking cell death in *dCsk* RNAi cells by over-expressing *DIAP1* largely prevents the migration of individual cells away from the *ptc* domain. One possibility is that Caspase activation may be required for disruption of cell-cell adhesions, which is likely to be necessary for *dCsk* mutant cells to detach from their neighbours and migrate. An alternative possibility is that Caspases have a more direct role in promoting migration. Interestingly, DIAP1 and the apical Caspase DRONC have been previously implicated in cell migration of the border cells during oogenesis (Geisbrecht and Montell, 2004). However, conversely to my result, it was shown that *DIAP1* over-expression promoted rather than prevented cell migration. Therefore, whereas it seems likely that loss of polarity and / or cell-cell adhesions induces JNK signalling and apoptosis, it is also possible that cell death pathways contribute to loss of cell-cell adhesion and migration. The *dCsk* RNAi phenotype is likely to be a complex phenomenon involving numerous SFK targets.

6.1.8 Mechanism of activation of dCsk by dASPP

This study of dASPP has shown that dASPP is a positive regulator of dCsk and this is achieved through binding and enhancement of dCsk kinase activity. However, it is still not clear exactly by which mechanism this regulation is achieved. For example, dASPP binding may induce a conformational change, which renders dCsk more active. Alternatively, dASPP may function as a scaffold to mediate the recruitment of other proteins to dCsk (possibly binding to the dASPP C-terminal region), which act to increase its activity. A third possibility is that dASPP regulates dCsk activity by controlling its sub-cellular localization and/or binding to substrates. Mammalian CSK's ability to inhibit SFKs is believed to be primarily determined by its translocation to lipid rafts, where c-SRC is tethered by virtue of its myristylated N-terminus (Cole et al., 2003). The transmembrane protein Cbp (CSK binding protein or PAG) has been reported to recruit dCsk to lipid rafts (Kawabuchi et al., 2000), but there is not a clear

Cbp homolog in flies. Therefore, it is possible that dASPP carries out an analogous function and regulates dCsk activity by causing its re-localization to parts of the cell where SFKs are active. Indeed, dASPP has a specific sub-cellular localization and is found at the apical membrane of epithelial cells, just above the adherens junction (data not shown). Therefore, dASPP may be important for localizing dCsk to the apical membrane either to promote its activation or to bring it in proximity to substrates. Ideally dCsk antibodies would be used to examine the sub-cellular localization of dCsk in *dASPP* mutant clones. We have not managed to produce a dCsk antibody that recognises dCsk in fixed tissues but experiments are currently underway to examine the localization of a dCsk-GFP fusion protein in *dASPP* clones. It will be important in the future to determine exactly how dASPP regulates dCsk.

6.2 Boa (Binder of dASPP) - a novel regulator of tissue growth

6.2.1 Boa and dASPP function in the same signalling pathway

In this work the initial characterization of another tumour suppressor, Boa (Binder of dASPP), was carried out. Boa is the *Drosophila* homolog of RASSF8, a member of the RASSF family, which all possess an RA (Ras Association) domain. Boa was identified as a suppressor in the *GMRsav,wts* modifier screen and links dASPP to Wts in the Curagen 2-hybrid data. The predicted interactions were tested by co-immunoprecipitation and this showed that Boa binds to dASPP but not Wts. As the characterization of dASPP suggests that it primarily regulates dCsk and not the Hippo pathway, it is likely that Boa also functions upstream of SFKs, rather than as a component of the Hippo pathway. Several lines of evidence suggest that Boa is a positive regulator of its binding partner, dASPP. Firstly, *boa* and *dASPP* phenotypes are similar; homozygous mutants are viable and show an increase in organ size and body size, suggesting that both genes are tumour suppressors. Also, *boa* and *dASPP* mutations result in mis-patterning of the ommatidial lattice, presumably as a consequence of altered cell-cell adhesion properties. Secondly, Boa is required to maintain high levels of dASPP at the apical membrane by either regulating its stability or localization. This is likely to be achieved through post-transcriptional mechanisms, as

dASPP transcript levels are not affected by loss of Boa. Thirdly, knockdown of endogenous Boa in cultured cells by RNAi prevents dASPP from enhancing the kinase activity of dCsk (Julien Colombani, personal communication). Taken together, this data suggests that Boa is a positive dASPP regulator and is important for dASPP to enhance the kinase activity of dCsk.

6.2.2 Boa is not absolutely required for dASPP function

Several pieces of data suggest that dASPP function is compromised but not abolished by Boa LOF. Boa maintains high levels of dASPP at the apical membrane but is not absolutely required for dASPP localization as small amounts of dASPP protein still detectable at the apical membrane in *boa* mutant clones. Additionally, *boa* shows a weak genetic interaction with *dCsk*. Reducing the *dCsk* gene dosage by 50% in a *boa* mutant background results in ectopic apoptosis in the wing disc. However, the level of apoptosis observed is considerably less than is observed in *dASPP-dCsk* compromised wing discs, and does not result in notching of adult wings. These results suggest that Boa is partially required for dASPP function, by regulating dASPP protein stability or dASPP localization. In agreement with this model, the boa^6 rough eye phenotype is partially rescued by ubiquitous expression of *dASPP* under the control of the *daughterless* promoter (Julien Colombani, unpublished observation). The rescue is incomplete suggesting that Boa has other functions during eye development that are independent of dASPP.

6.2.3 Boa has other roles besides maintaining dASPP regulation

Although *dASPP* and *boa* mutant phenotypes are similar, there are important differences suggesting that Boa has other functions besides dASPP regulation. For example, *dASPP* mutant wings are large but of normal shape, whereas *boa* mutant wings are large and broadened. Also, *boa* has a stronger eye phenotype than *dASPP*; loss of *boa* can severely disrupt retinal patterning leading to the formation of a square, rather than hexagonal lattice, a phenotype not observed in *dASPP* mutant retinas. *boa* but not *dASPP* mutant retinas frequently show a double layer of inter-ommatidial cells, indicating that they contain considerably more inter-ommatidial cells. The number of

excess cells in *boa* mutant retinas has not been quantified yet. It will be important to determine whether this is a result of delayed cell cycle exit after the MF or reduced apoptosis between 24h and 40h APF, as this may give clues as to the 'other' function(s) of Boa. Therefore, while Boa is a regulator of dASPP it is likely to have additional, independent functions. Accordingly, while *dASPP* over-expression in the eye has no phenotype, *boa* over-expression results in a rough eye (data not shown). Furthermore, the *dASPP-boa* double mutant overgrowth phenotype is stronger than the *dASPP* overgrowth phenotype (Julien Colombani, personal communication). These two pieces of data strongly suggest that Boa has dASPP-independent functions.

The other function(s) of Boa may be related to its conserved RA domain. RA domain containing proteins are known to bind to Ras super-family proteins, raising the intriguing possibility the Boa may regulate the Ras pathway. However, heterozygosity for a *Ras1* null allele does not obviously affect the *boa* phenotype (data not shown). One explanation is that Boa regulates another member of the Ras family. Alternatively, Boa may have a minor role in the Hippo pathway; as Boa and Wts do not co-immunoprecipitate it is unlikely to function at the level of Wts. Over-expression of *fat* results in a broad wing phenotype, which is highly reminiscent of *boa* mutant wings, raising the possibility that Fat regulates Boa or vice versa. These possibilities remain to be tested.

In summary Boa has been identified as a tumour suppressor gene in *Drosophila*, which acts to maintain high levels of dASPP at the apical membrane. This appears to be important for dASPP to carry out its role as a positive regulator of dCsk.

6.3 Potential impact of the work on dASPP and Boa

This work has provided the initial characterization if two *Drosophila* genes of previously unknown function. We have shown that dASPP and Boa function as tumour suppressors *in vivo* and are likely to function upstream of SFKs. The discovery that dASPP regulates dCsk suggests that ASPP proteins could be regulators of CSK, and hence SFKs in mammals.

As c-SRC activation is associated with metastasis, which is frequently the cause of death in cancer patients, it is important to fully understand how SFKs are regulated. The discovery that dASPP and Boa are positive regulators of dCsk broadens our understanding of SFK regulation. If the interactions between these proteins are conserved in mammals and RASSF8 and ASPP proteins function upstream of SFKs, this work could have implications for the development of novel cancer treatments.

6.4 Future directions

The next stage of this project will involve completing the characterisation of the *boa* phenotype, confirming interactions between *boa* and *dASPP / dCsk* and attempting to pinpoint the 'other' functions of Boa. Careful analysis of the phenotypes resulting from both over-expression and loss of *boa* in the eye will be carried out. I plan to quantify the number of excess inter-ommmatidial cells per ommatidium in *dASPP* and *boa* mutant retinas. If, as expected, there are excess inter-ommatidial cells in *dASPP* and *boa* mutant retinas I will examine whether this is due to delayed cell cycle exit (using BrdU labelling of discs with *boa* clones) or reduced apoptosis at 40h AFP (using TUNEL staining of pupal retinas with *boa* clones).

I also plan to make sections of *boa* adult eyes to examine whether there are defects in planar cell polarity (PCP), which regulates ommatidial rotation, or in photoreceptor differentiation. Additionally, live imaging of developing pupal retinas will be carried out for control, boa^{6} mutant, and *boa* over-expressing retinas to try and understand the cell-sorting defect that leads to the severe patterning defects. A useful tool for this will be *E-Cadherin-GFP* and *p120-catenenin-GFP*, which have been previously used for live imaging of the developing retina (Vidal et al., 2006). Irregular Chiasm / Roughest is known to be important for inter-ommatidial cell-sorting in the pupal retina, and mutant eye phenotypes are similar to *boa* eye phenotypes. Early in pupal development (~20h APF) Roughest accumulates at the membrane of primary pigment cells where they contact inter-ommatidial cells (Reiter et al., 1996). I plan to examine the localization of Roughest in *boa* clones in pupal retina to see whether the observed cell-sorting defect is due to Roughest mis-localization. Hopefully, this analysis of the *boa* eye phenotype will give clues as the other role(s) of Boa.

In the future it will be interesting to carry out genetic or cell based screens for novel interactors of Boa, dASPP and dCsk. In particular, as *boa* and *dASPP* are viable mutations, they provide sensitized backgrounds to screen for novel genes involved in SFK signalling. This may reveal other factors functioning in the dASPP-dCsk-SFK pathway or identify new components of Boa signalling pathways.

It will be important to map the region of Boa required for binding dASPP and vice versa. The co-immunoprecipitation experiments suggest that Boa binds to dASPP and dASPP binds to dCsk. Boa does not bind to dCsk unless dASPP is also expressed (Julien Colombani, personal communication). This suggests that all three proteins may form a complex *in vivo*. However, this is based on experiments where proteins are over-expressed and binding between endogenous proteins would need to be examined to address this possibility. Alternatively, two separate complexes may exist, one containing Boa and dASPP and the other containing dASPP and dCsk. The N-terminus of dASPP is required for binding to dCsk but it has not been determined which region of dCsk bind dASPP.

Future experiments will also include further analysis of the mechanism of regulation of dASPP by Boa. It will be interesting to determine whether Boa regulates dASPP protein stability or regulates it localization. Ideally, antibodies that recognize endogenous dASPP on Western blots would be used to examine levels of dASPP protein in *boa* mutant versus control wing discs. This will reveal whether Boa regulates dASPP stability or localization. Additionally, the mechanism by which dASPP regulates dCsk will be investigated.

6.5 *DIAP-LacZ* project discussion

In addition to characterizing dASPP and Boa, I have also examined the transcriptional regulation of *DIAP1* by the Ras pathway. The onset of Ras pathway signalling in the ommatidial preclusters posterior to the MF, as visualized using a phospho-MAPK antibody, is accompanied by the onset of *DIAP1* transcription, as visualised by in-situ hybridization (Nic Tapon, personal communication). I have presented results that suggest that the Ras pathway transcriptionally regulates DIAP1 to promote cell survival.

This has not been described before and is likely to be independent of the posttranslational regulation of DIAP1 by the Ras pathway via Hid. Therefore, although this study is incomplete due to lack of time, it could potentially provide a novel mechanism of survival signalling by the Ras pathway.

I have shown that DIAP1 is transcriptionally upregulated by the Ras pathway. The EGF receptor and Ras are likely to be involved and Ttk69 may be the downstream transcription factor responsible for controlling *DIAP1* transcription. EGFR and Ras are known to regulate a wide variety of cellular processes, so it can be argued that the effect on *DIAP1* transcription may be very indirect. However, Ttk69 over-expression upregulates *DIAP1* transcription suggesting that the mechanism may be more direct, as Ttk69 is targeted for degradation by the Ras pathway.

Ttk69 is known to function as a transcriptional repressor (Harrison and Travers, 1990; Read and Manley, 1992); therefore it was surprising that its over-expression led to an upregulation of *DIAP-LacZ*. One possibility is that high levels of Ttk69 titrate a co-repressor required for DIAP1 repression, and in this way act like a dominant negative. If this is true then it is expected that *ttk69* LOF clones would show the same phenotype. However, I observed no modification of DIAP1 protein levels in LOF clones. Another possibility is that Ttk69 can function as a transcriptional activator is some circumstances. Interestingly, whereas the literature mainly describes Ttk69 as a transcriptional repressor, it has been shown to strongly activate transcription of a *ftz* reporter when expressed in yeast cells (Yu et al., 1999). This is proposed to be due to the fact that yeast cells lack a necessary *Drosophila* co-repressor but nevertheless suggests that Ttk has the potential to activate transcription. However, if Ttk69 does function as an activator of *DIAP1* transcription it is not easy to explain why I did not observe less DIAP1 protein in ttk^{lel1} clones. It is plausible that Ttk69 regulates *DIAP1* transcription redundantly with another transcription factor, which can compensate for loss of Ttk69. A third possible explanation is that Ttk69 indirectly upregulates *DIAP1* transcription by repressing expression of a negative regulator. However, if this model were correct, I would expect loss of Ttk69 to reduce DIAP1 protein levels, which was not the case. Therefore, preliminary results suggest that Ttk69 may regulate transcription of *DIAP1* downstream of Ras, but how this is achieved is not yet clear.

Further work will be required to distinguish what effect Ttk69 has on *DIAP1* transcription.

I have also shown that DIAP1 protein levels are reduced in *yan* LOF clones suggesting that Yan may play a role in regulating DIAP levels. However, DIAP1 levels may be downregulated very indirectly as a consequence of apoptosis occurring in response to loss of Yan. This is likely to be the case for two reasons. Firstly, Yan is a transcriptional repressor (O'Neill et al., 1994). Therefore direct transcriptional targets are expected to be elevated rather than reduced in mutant clones. Secondly, the result suggests that Yan promotes cell survival (as there is less DIAP1 in clones). This does not make sense with respect to its role in the Ras pathway, as Ras signalling is known to promote survival and inhibit Yan.

Yan is a general inhibitor of differentiation and, as expected, excess photoreceptor differentiation was observed in *yan* clones. As *yan* clones have less DIAP1 protein this suggests that DIAP1 is not upregulated posterior to the MF simply as a consequence of photoreceptor differentiation. In order to address whether Yan regulates *DIAP1* transcription it would be necessary to examine the level of *DIAP-LacZ* in *yan* over-expression and LOF clones.

In order to determine whether Ttk69 regulates the *DIAP1* promoter it will be necessary to first confirm that Ttk69 regulates *DIAP1* using another system, for example a cell-based reporter assay. If this reveals that Ttk69 regulates DIAP1 transcription (either positively or negatively), the next step will be to search for Ttk69 consensus binding site(s) within the *DIAP1* promoter. Mutation of these sites should clarify the effect of Ttk69 on *DIAP1* transcription. If Ttk69 is a regulator of *DIAP1* transcription it will be interesting to determine whether this only occurs in the eye or whether it is a general mechanism of survival signalling by the Ras pathway. Future work would also include further analysis of the effect of Yan on *DIAP1* levels.

REFERENCES

Abdelwahid, E., Yokokura, T., Krieser, R. J., Balasundaram, S., Fowle, W. H., and White, K. (2007). Mitochondrial disruption in Drosophila apoptosis. Dev Cell *12*, 793-806.

Adachi-Yamada, T., Fujimura-Kamada, K., Nishida, Y., and Matsumoto, K. (1999). Distortion of proximodistal information causes JNK-dependent apoptosis in Drosophila wing. Nature *400*, 166-169.

Agirre, X., Roman-Gomez, J., Jimenez-Velasco, A., Garate, L., Montiel-Duarte, C., Navarro, G., Vazquez, I., Zalacain, M., Calasanz, M. J., Heiniger, A., *et al.* (2006). ASPP1, a common activator of TP53, is inactivated by aberrant methylation of its promoter in acute lymphoblastic leukemia. Oncogene *25*, 1862-1870.

Arama, E., Bader, M., Srivastava, M., Bergmann, A., and Steller, H. (2006). The two Drosophila cytochrome C proteins can function in both respiration and caspase activation. Embo J *25*, 232-243.

Baker, N. E., and Yu, S. Y. (2001). The EGF receptor defines domains of cell cycle progression and survival to regulate cell number in the developing Drosophila eye. Cell *104*, 699-708.

Baonza, A., Murawsky, C. M., Travers, A. A., and Freeman, M. (2002). Pointed and Tramtrack69 establish an EGFR-dependent transcriptional switch to regulate mitosis. Nat Cell Biol *4*, 976-980.

Basler, K., Christen, B., and Hafen, E. (1991). Ligand-independent activation of the sevenless receptor tyrosine kinase changes the fate of cells in the developing Drosophila eye. Cell *64*, 1069-1081.

Bellen, H. J., Levis, R. W., Liao, G., He, Y., Carlson, J. W., Tsang, G., Evans-Holm, M., Hiesinger, P. R., Schulze, K. L., Rubin, G. M., *et al.* (2004). The BDGP gene disruption project: single transposon insertions associated with 40% of Drosophila genes. Genetics *167*, 761-781.

Bennett, F. C., and Harvey, K. F. (2006). Fat cadherin modulates organ size in Drosophila via the Salvador/Warts/Hippo signaling pathway. Curr Biol *16*, 2101-2110.

Bergamaschi, D., Samuels, Y., Jin, B., Duraisingham, S., Crook, T., and Lu, X. (2004). ASPP1 and ASPP2: common activators of p53 family members. Mol Cell Biol *24*, 1341-1350.

Bergamaschi, D., Samuels, Y., O'Neil, N. J., Trigiante, G., Crook, T., Hsieh, J. K., O'Connor, D. J., Zhong, S., Campargue, I., Tomlinson, M. L., *et al.* (2003). iASPP oncoprotein is a key inhibitor of p53 conserved from worm to human. Nat Genet *33*, 162-167.

Bergamaschi, D., Samuels, Y., Sullivan, A., Zvelebil, M., Breyssens, H., Bisso, A., Del Sal, G., Syed, N., Smith, P., Gasco, M., *et al.* (2006). iASPP preferentially binds p53 proline-rich region and modulates apoptotic function of codon 72-polymorphic p53. Nat Genet *38*, 1133-1141.

Bergamaschi, D., Samuels, Y., Zhong, S., and Lu, X. (2005). Mdm2 and mdmX prevent ASPP1 and ASPP2 from stimulating p53 without targeting p53 for degradation. Oncogene *24*, 3836-3841.

Bergmann, A., Agapite, J., McCall, K., and Steller, H. (1998). The Drosophila gene hid is a direct molecular target of Ras-dependent survival signaling. Cell *95*, 331-341.

Bilder, D., and Perrimon, N. (2000). Localization of apical epithelial determinants by the basolateral PDZ protein Scribble. Nature *403*, 676-680.

Blair, S. S. (2003). Genetic mosaic techniques for studying Drosophila development. Development *130*, 5065-5072.

Brand, A. H., and Perrimon, N. (1993). Targeted gene expression as a means of altering cell fates and generating dominant phenotypes. Development *118*, 401-415.

Brennecke, J., Hipfner, D. R., Stark, A., Russell, R. B., and Cohen, S. M. (2003). bantam encodes a developmentally regulated microRNA that controls cell proliferation and regulates the proapoptotic gene hid in Drosophila. Cell *113*, 25-36.

Brodsky, M. H., Nordstrom, W., Tsang, G., Kwan, E., Rubin, G. M., and Abrams, J. M. (2000). Drosophila p53 binds a damage response element at the reaper locus. Cell *101*, 103-113.

Bromberg, J. F., Horvath, C. M., Besser, D., Lathem, W. W., and Darnell, J. E., Jr. (1998). Stat3 activation is required for cellular transformation by v-src. Mol Cell Biol *18*, 2553-2558.

Brumby, A. M., and Richardson, H. E. (2003). scribble mutants cooperate with oncogenic Ras or Notch to cause neoplastic overgrowth in Drosophila. Embo J *22*, 5769-5779.

Brunner, D., Ducker, K., Oellers, N., Hafen, E., Scholz, H., and Klambt, C. (1994). The ETS domain protein pointed-P2 is a target of MAP kinase in the sevenless signal transduction pathway. Nature *370*, 386-389.

Burnham, M. R., Bruce-Staskal, P. J., Harte, M. T., Weidow, C. L., Ma, A., Weed, S. A., and Bouton, A. H. (2000). Regulation of c-SRC activity and function by the adapter protein CAS. Mol Cell Biol *20*, 5865-5878.

Butler, M. J., Jacobsen, T. L., Cain, D. M., Jarman, M. G., Hubank, M., Whittle, J. R., Phillips, R., and Simcox, A. (2003). Discovery of genes with highly restricted expression patterns in the Drosophila wing disc using DNA oligonucleotide microarrays. Development *130*, 659-670.

Cam, W. R., Masaki, T., Shiratori, Y., Kato, N., Ikenoue, T., Okamoto, M., Igarashi, K., Sano, T., and Omata, M. (2001). Reduced C-terminal Src kinase activity is correlated inversely with pp60(c-src) activity in colorectal carcinoma. Cancer *92*, 61-70.

Chan, E. H., Nousiainen, M., Chalamalasetty, R. B., Schafer, A., Nigg, E. A., and Sillje, H. H. (2005). The Ste20-like kinase Mst2 activates the human large tumor suppressor kinase Lats1. Oncogene *24*, 2076-2086.

Chang, J. H., Gill, S., Settleman, J., and Parsons, S. J. (1995). c-Src regulates the simultaneous rearrangement of actin cytoskeleton, p190RhoGAP, and p120RasGAP following epidermal growth factor stimulation. J Cell Biol *130*, 355-368.

Cheung, W. L., Ajiro, K., Samejima, K., Kloc, M., Cheung, P., Mizzen, C. A., Beeser, A., Etkin, L. D., Chernoff, J., Earnshaw, W. C., and Allis, C. D. (2003). Apoptotic phosphorylation of histone H2B is mediated by mammalian sterile twenty kinase. Cell *113*, 507-517.

Chipuk, J. E., Kuwana, T., Bouchier-Hayes, L., Droin, N. M., Newmeyer, D. D., Schuler, M., and Green, D. R. (2004). Direct activation of Bax by p53 mediates mitochondrial membrane permeabilization and apoptosis. Science *303*, 1010-1014.

Cho, E., Feng, Y., Rauskolb, C., Maitra, S., Fehon, R., and Irvine, K. D. (2006). Delineation of a Fat tumor suppressor pathway. Nat Genet *38*, 1142-1150.

Chong, Y. P., Chan, A. S., Chan, K. C., Williamson, N. A., Lerner, E. C., Smithgall, T. E., Bjorge, J. D., Fujita, D. J., Purcell, A. W., Scholz, G., *et al.* (2006). C-terminal Src kinase-homologous kinase (CHK), a unique inhibitor inactivating multiple active conformations of Src family tyrosine kinases. J Biol Chem *281*, 32988-32999.

Chong, Y. P., Mulhern, T. D., Zhu, H. J., Fujita, D. J., Bjorge, J. D., Tantiongco, J. P., Sotirellis, N., Lio, D. S., Scholz, G., and Cheng, H. C. (2004). A novel non-catalytic mechanism employed by the C-terminal Src-homologous kinase to inhibit Src-family kinase activity. J Biol Chem *279*, 20752-20766.

Cole, P. A., Shen, K., Qiao, Y., and Wang, D. (2003). Protein tyrosine kinases Src and Csk: a tail's tale. Curr Opin Chem Biol *7*, 580-585.

Colombani, J., Bianchini, L., Layalle, S., Pondeville, E., Dauphin-Villemant, C., Antoniewski, C., Carre, C., Noselli, S., and Leopold, P. (2005). Antagonistic actions of ecdysone and insulins determine final size in Drosophila. Science *310*, 667-670.

Colombani, J., Polesello, C., Josue, F., and Tapon, N. (2006). Dmp53 activates the Hippo pathway to promote cell death in response to DNA damage. Curr Biol *16*, 1453-1458.

Colombani, J., Raisin, S., Pantalacci, S., Radimerski, T., Montagne, J., and Leopold, P. (2003). A nutrient sensor mechanism controls Drosophila growth. Cell *114*, 739-749.

Conlon, I., and Raff, M. (1999). Size control in animal development. Cell *96*, 235-244.

Cooley, L. (1998). Drosophila ring canal growth requires Src and Tec kinases. Cell *93*, 913-915.

Cooley, L., Thompson, D., and Spradling, A. C. (1990). Constructing deletions with defined endpoints in Drosophila. Proc Natl Acad Sci U S A *87*, 3170-3173.

Coutts, A. S., and La Thangue, N. B. (2005). The p53 response: emerging levels of co-factor complexity. Biochem Biophys Res Commun *331*, 778-785.

Daksis, J. I., Lu, R. Y., Facchini, L. M., Marhin, W. W., and Penn, L. J. (1994). Myc induces cyclin D1 expression in the absence of de novo protein synthesis and links mitogen-stimulated signal transduction to the cell cycle. Oncogene *9*, 3635-3645.

Datta, A., Huber, F., and Boettiger, D. (2002). Phosphorylation of beta3 integrin controls ligand binding strength. J Biol Chem *277*, 3943-3949.

Dickson, B. J. (1998). Photoreceptor development: breaking down the barriers. Curr Biol *8*, R90-92.

Dickson, B. J., van der Straten, A., Dominguez, M., and Hafen, E. (1996). Mutations Modulating Raf signaling in Drosophila eye development. Genetics *142*, 163-171.

Dietzl, G., Chen, D., Schnorrer, F., Su, K. C., Barinova, Y., Fellner, M., Gasser, B., Kinsey, K., Oppel, S., Scheiblauer, S., *et al.* (2007). A genome-wide transgenic RNAi library for conditional gene inactivation in Drosophila. Nature *448*, 151-156.

Ditzel, M., Wilson, R., Tenev, T., Zachariou, A., Paul, A., Deas, E., and Meier, P. (2003). Degradation of DIAP1 by the N-end rule pathway is essential for regulating apoptosis. Nat Cell Biol *5*, 467-473.

Dolfi, F., Garcia-Guzman, M., Ojaniemi, M., Nakamura, H., Matsuda, M., and Vuori, K. (1998). The adaptor protein Crk connects multiple cellular stimuli to the JNK signaling pathway. Proc Natl Acad Sci U S A *95*, 15394-15399.

Dong, J., Feldmann, G., Huang, J., Wu, S., Zhang, N., Comerford, S. A., Gayyed, M. F., Anders, R. A., Maitra, A., and Pan, D. (2007). Elucidation of a universal size-control mechanism in Drosophila and mammals. Cell *130*, 1120-1133.

Dorstyn, L., Mills, K., Lazebnik, Y., and Kumar, S. (2004). The two cytochrome c species, DC3 and DC4, are not required for caspase activation and apoptosis in Drosophila cells. J Cell Biol *167*, 405-410.

Emoto, K., He, Y., Ye, B., Grueber, W. B., Adler, P. N., Jan, L. Y., and Jan, Y. N. (2004). Control of dendritic branching and tiling by the Tricornered-kinase/Furry signaling pathway in Drosophila sensory neurons. Cell *119*, 245-256.

Emoto, K., Parrish, J. Z., Jan, L. Y., and Jan, Y. N. (2006). The tumour suppressor Hippo acts with the NDR kinases in dendritic tiling and maintenance. Nature *443*, 210-213.

Engels, W. R. (1992). The origin of P elements in Drosophila melanogaster. Bioessays *14*, 681-686.

Espanel, X., and Sudol, M. (2001). Yes-associated protein and p53-binding protein-2 interact through their WW and SH3 domains. J Biol Chem *276*, 14514-14523.

Falvella, F. S., Manenti, G., Spinola, M., Pignatiello, C., Conti, B., Pastorino, U., and Dragani, T. A. (2006). Identification of RASSF8 as a candidate lung tumor suppressor gene. Oncogene *25*, 3934-3938.

Fincham, V. J., Chudleigh, A., and Frame, M. C. (1999). Regulation of p190 Rho-GAP by v-Src is linked to cytoskeletal disruption during transformation. J Cell Sci *112 (Pt 6)*, 947-956.

Fogal, V., Kartasheva, N. N., Trigiante, G., Llanos, S., Yap, D., Vousden, K. H., and Lu, X. (2005). ASPP1 and ASPP2 are new transcriptional targets of E2F. Cell Death Differ *12*, 369-376.

Fox, D. T., and Peifer, M. (2007). Cell adhesion: separation of p120's powers? Curr Biol *17*, R24-27.

Frame, M. C. (2004). Newest findings on the oldest oncogene; how activated src does it. J Cell Sci *117*, 989-998.

Freeman, M. (1996). Reiterative use of the EGF receptor triggers differentiation of all cell types in the Drosophila eye. Cell *87*, 651-660.

Friedler, A., Hansson, L. O., Veprintsev, D. B., Freund, S. M., Rippin, T. M., Nikolova, P. V., Proctor, M. R., Rudiger, S., and Fersht, A. R. (2002). A peptide that binds and stabilizes p53 core domain: chaperone strategy for rescue of oncogenic mutants. Proc Natl Acad Sci U S A *99*, 937-942.

Fujita, Y., Krause, G., Scheffner, M., Zechner, D., Leddy, H. E., Behrens, J., Sommer, T., and Birchmeier, W. (2002). Hakai, a c-Cbl-like protein, ubiquitinates and induces endocytosis of the E-cadherin complex. Nat Cell Biol *4*, 222-231.

Geisbrecht, E. R., and Montell, D. J. (2004). A role for Drosophila IAP1-mediated caspase inhibition in Rac-dependent cell migration Cell *118*, 111-125.

Giot, L., Bader, J. S., Brouwer, C., Chaudhuri, A., Kuang, B., Li, Y., Hao, Y. L., Ooi, C. E., Godwin, B., Vitols, E., *et al.* (2003). A protein interaction map of Drosophila melanogaster. Science *302*, 1727-1736.

Golic, K. G., and Lindquist, S. (1989). The FLP recombinase of yeast catalyzes site-specific recombination in the Drosophila genome. Cell *59*, 499-509.

Good, A. G., Meister, G. A., Brock, H. W., Grigliatti, T. A., and Hickey, D. A. (1989). Rapid Spread of Transposable P Elements in Experimental Populations of Drosophila Melanogaster. Genetics *122*, 387-396.

Gorina, S., and Pavletich, N. P. (1996). Structure of the p53 tumor suppressor bound to the ankyrin and SH3 domains of 53BP2. Science *274*, 1001-1005.

Guarnieri, D. J., Dodson, G. S., and Simon, M. A. (1998). SRC64 regulates the localization of a Tec-family kinase required for Drosophila ring canal growth. Mol Cell *1*, 831-840.

Hamaratoglu, F., Willecke, M., Kango-Singh, M., Nolo, R., Hyun, E., Tao, C., Jafar-Nejad, H., and Halder, G. (2006). The tumour-suppressor genes NF2/Merlin and Expanded act through Hippo signalling to regulate cell proliferation and apoptosis. Nat Cell Biol *8*, 27-36.

Harrison, S. D., and Travers, A. A. (1990). The tramtrack gene encodes a Drosophila finger protein that interacts with the ftz transcriptional regulatory region and shows a novel embryonic expression pattern. Embo J *9*, 207-216.

Harvey, K., and Tapon, N. (2007). The Salvador-Warts-Hippo pathway - an emerging tumour-suppressor network. Nat Rev Cancer *7*, 182-191.

Harvey, K. F., Pfleger, C. M., and Hariharan, I. K. (2003). The Drosophila Mst ortholog, hippo, restricts growth and cell proliferation and promotes apoptosis. Cell *114*, 457-467.

Hauck, C. R., Hsia, D. A., Puente, X. S., Cheresh, D. A., and Schlaepfer, D. D. (2002). FRNK blocks v-Src-stimulated invasion and experimental metastases without effects on cell motility or growth. Embo J *21*, 6289-6302.

Haupt, S., Berger, M., Goldberg, Z., and Haupt, Y. (2003). Apoptosis - the p53 network. J Cell Sci *116*, 4077-4085.

Hay, B. A., and Guo, M. (2006). Caspase-dependent cell death in Drosophila. Annu Rev Cell Dev Biol *22*, 623-650.

Hay, B. A., Huh, J. R., and Guo, M. (2004). The genetics of cell death: approaches, insights and opportunities in Drosophila. Nat Rev Genet *5*, 911-922.

He, Y., Fang, X., Emoto, K., Jan, Y. N., and Adler, P. N. (2005). The tricornered Ser/Thr protein kinase is regulated by phosphorylation and interacts with furry during Drosophila wing hair development. Mol Biol Cell *16*, 689-700.

Held, L. I. J. (2002). Imaginal Discs - The Genetics and Cellular Logic of Pattern formation. (Cambridge, UK: Cambridge University Press).

Helps, N. R., Barker, H. M., Elledge, S. J., and Cohen, P. T. (1995). Protein phosphatase 1 interacts with p53BP2, a protein which binds to the tumour suppressor p53. FEBS Lett *377*, 295-300.

Hergovich, A., Stegert, M. R., Schmitz, D., and Hemmings, B. A. (2006). NDR kinases regulate essential cell processes from yeast to humans. Nat Rev Mol Cell Biol *7*, 253-264.

Howell, B. W., and Cooper, J. A. (1994). Csk suppression of Src involves movement of Csk to sites of Src activity. Mol Cell Biol *14*, 5402-5411.

Hsia, D. A., Mitra, S. K., Hauck, C. R., Streblow, D. N., Nelson, J. A., Ilic, D., Huang, S., Li, E., Nemerow, G. R., Leng, J., *et al.* (2003). Differential regulation of cell motility and invasion by FAK. J Cell Biol *160*, 753-767.

Huang, J., Wu, S., Barrera, J., Matthews, K., and Pan, D. (2005). The Hippo Signaling Pathway Coordinately Regulates Cell Proliferation and Apoptosis by Inactivating Yorkie, the Drosophila Homolog of YAP. Cell *122*, 421-434.

Huh, J. R., Guo, M., and Hay, B. A. (2004). Compensatory proliferation induced by cell death in the Drosophila wing disc requires activity of the apical cell death caspase Dronc in a nonapoptotic role. Curr Biol *14*, 1262-1266.

Imamoto, A., and Soriano, P. (1993). Disruption of the csk gene, encoding a negative regulator of Src family tyrosine kinases, leads to neural tube defects and embryonic lethality in mice. Cell *73*, 1117-1124.

Irby, R. B., and Yeatman, T. J. (2000). Role of Src expression and activation in human cancer. Oncogene *19*, 5636-5642.

Iwabuchi, K., Bartel, P. L., Li, B., Marraccino, R., and Fields, S. (1994). Two cellular proteins that bind to wild-type but not mutant p53. Proc Natl Acad Sci U S A *91*, 6098-6102.

Jones, L., Richardson, H., and Saint, R. (2000). Tissue-specific regulation of cyclin E transcription during Drosophila melanogaster embryogenesis. Development *127*, 4619-4630.

Jung, E. J., and Kim, C. W. (2002). Interaction between chicken protein tyrosine phosphatase 1 (CPTP1)-like rat protein phosphatase 1 (PTP1) and p60(v-src) in v-src-transformed Rat-1 fibroblasts. Exp Mol Med *34*, 476-480.

Justice, R. W., Zilian, O., Woods, D. F., Noll, M., and Bryant, P. J. (1995). The Drosophila tumor suppressor gene warts encodes a homolog of human myotonic dystrophy kinase and is required for the control of cell shape and proliferation. Genes Dev *9*, 534-546.

Kango-Singh, M., Nolo, R., Tao, C., Verstreken, P., Hiesinger, P. R., Bellen, H. J., and Halder, G. (2002). Shar-pei mediates cell proliferation arrest during imaginal disc growth in Drosophila. Development *129*, 5719-5730.

Kanuka, H., Kuranaga, E., Takemoto, K., Hiratou, T., Okano, H., and Miura, M. (2005). Drosophila caspase transduces Shaggy/GSK-3beta kinase activity in neural precursor development. Embo J *24*, 3793-3806.

Karim, F. D., Chang, H. C., Therrien, M., Wassarman, D. A., Laverty, T., and Rubin, G. M. (1996). A screen for genes that function downstream of Ras1 during Drosophila eye development. Genetics *143*, 315-329.

Kawabuchi, M., Satomi, Y., Takao, T., Shimonishi, Y., Nada, S., Nagai, K., Tarakhovsky, A., and Okada, M. (2000). Transmembrane phosphoprotein Cbp regulates the activities of Src-family tyrosine kinases. Nature *404*, 999-1003.

Kelso, R. J., Hudson, A. M., and Cooley, L. (2002). Drosophila Kelch regulates actin organization via Src64-dependent tyrosine phosphorylation. J Cell Biol *156*, 703-713.

Kim, M., Tezuka, T., Tanaka, K., and Yamamoto, T. (2004a). Cbl-c suppresses v-Src-induced transformation through ubiquitin-dependent protein degradation. Oncogene *23*, 1645-1655.

Kim, S. O., Avraham, S., Jiang, S., Zagozdzon, R., Fu, Y., and Avraham, H. K. (2004b). Differential expression of Csk homologous kinase (CHK) in normal brain and brain tumors. Cancer *101*, 1018-1027.

Kirchner, J., Gross, S., Bennett, D., and Alphey, L. (2007). The nonmuscle myosin phosphatase PP1beta (flapwing) negatively regulates Jun N-terminal kinase in wing imaginal discs of Drosophila. Genetics *175*, 1741-1749.

Klages, S., Adam, D., Class, K., Fargnoli, J., Bolen, J. B., and Penhallow, R. C. (1994). Ctk: a protein-tyrosine kinase related to Csk that defines an enzyme family. Proc Natl Acad Sci U S A *91*, 2597-2601.

Kmiecik, T. E., and Shalloway, D. (1987). Activation and suppression of pp60c-src transforming ability by mutation of its primary sites of tyrosine phosphorylation. Cell *49*, 65-73.

Kunte, D. P., Wali, R. K., Koetsier, J. L., Hart, J., Kostjukova, M. N., Kilimnik, A. Y., Pyatkin, I. G., Strelnikova, S. R., and Roy, H. K. (2005). Down-regulation of the tumor suppressor gene C-terminal Src kinase: an early event during premalignant colonic epithelial hyperproliferation. FEBS Lett *579*, 3497-3502.

Kurada, P., and White, K. (1998). Ras promotes cell survival in Drosophila by downregulating hid expression. Cell *95*, 319-329.

Lai, Z. C., and Li, Y. (1999). Tramtrack69 is positively and autonomously required for Drosophila photoreceptor development. Genetics *152*, 299-305.

Lai, Z. C., and Rubin, G. M. (1992). Negative control of photoreceptor development in Drosophila by the product of the yan gene, an ETS domain protein. Cell *70*, 609-620.

Lai, Z. C., Wei, X., Shimizu, T., Ramos, E., Rohrbaugh, M., Nikolaidis, N., Ho, L. L., and Li, Y. (2005). Control of cell proliferation and apoptosis by mob as tumor suppressor, mats. Cell *120*, 675-685.

Landgren, E., Blume-Jensen, P., Courtneidge, S. A., and Claesson-Welsh, L. (1995). Fibroblast growth factor receptor-1 regulation of Src family kinases. Oncogene *10*, 2027-2035.

Langton, P. F., Colombani, J., Aerne, B. L., and Tapon, N. (2007). Drosophila ASPP Regulates C-Terminal Src Kinase Activity. Dev Cell *13*, 773-782.

Lawrence, P. A., and Green, S. M. (1979). Cell lineage in the developing retina of Drosophila. Dev Biol *71*, 142-152.

Lee, T., and Luo, L. (1999). Mosaic analysis with a repressible cell marker for studies of gene function in neuronal morphogenesis. Neuron *22*, 451-461.

Lehtinen, M. K., Yuan, Z., Boag, P. R., Yang, Y., Villen, J., Becker, E. B., DiBacco, S., de la Iglesia, N., Gygi, S., Blackwell, T. K., and Bonni, A. (2006). A conserved MST-FOXO signaling pathway mediates oxidative-stress responses and extends life span. Cell *125*, 987-1001.

Li, S., Li, Y., Carthew, R. W., and Lai, Z. C. (1997). Photoreceptor cell differentiation requires regulated proteolysis of the transcriptional repressor Tramtrack. Cell *90*, 469-478.

Liu, Z. J., Zhang, Y., Zhang, X. B., and Yang, X. (2004). Abnormal mRNA expression of ASPP members in leukemia cell lines. Leukemia *18*, 880.

Lu, N., Guarnieri, D. J., and Simon, M. A. (2004). Localization of Tec29 to ring canals is mediated by Src64 and PtdIns(3,4,5)P3-dependent mechanisms. Embo J *23*, 1089-1100.

Ludwig, R. L., Bates, S., and Vousden, K. H. (1996). Differential activation of target cellular promoters by p53 mutants with impaired apoptotic function. Mol Cell Biol *16*, 4952-4960.

Maitra, S., Kulikauskas, R. M., Gavilan, H., and Fehon, R. G. (2006). The tumor suppressors Merlin and Expanded function cooperatively to modulate receptor endocytosis and signaling. Curr Biol *16*, 702-709.

Malek, R. L., Irby, R. B., Guo, Q. M., Lee, K., Wong, S., He, M., Tsai, J., Frank, B., Liu, E. T., Quackenbush, J., *et al.* (2002). Identification of Src transformation fingerprint in human colon cancer. Oncogene *21*, 7256-7265.

Malumbres, M., and Barbacid, M. (2001). To cycle or not to cycle: a critical decision in cancer. Nat Rev Cancer *1*, 222-231.

Malumbres, M., and Barbacid, M. (2005). Mammalian cyclin-dependent kinases. Trends Biochem Sci *30*, 630-641.

Martin-Blanco, E., Gampel, A., Ring, J., Virdee, K., Kirov, N., Tolkovsky, A. M., and Martinez-Arias, A. (1998). puckered encodes a phosphatase that mediates a feedback loop regulating JNK activity during dorsal closure in Drosophila. Genes Dev *12*, 557-570.

McCartney, B. M., Kulikauskas, R. M., LaJeunesse, D. R., and Fehon, R. G. (2000). The neurofibromatosis-2 homologue, Merlin, and the tumor suppressor expanded function together in Drosophila to regulate cell proliferation and differentiation. Development *127*, 1315-1324.

Meier, P., Finch, A., and Evan, G. (2000a). Apoptosis in development. Nature *407*, 796-801.

Meier, P., Silke, J., Leevers, S. J., and Evan, G. I. (2000b). The Drosophila caspase DRONC is regulated by DIAP1. Embo J *19*, 598-611.

Meignin, C., Alvarez-Garcia, I., Davis, I., and Palacios, I. M. (2007). The salvador-warts-hippo pathway is required for epithelial proliferation and axis specification in Drosophila. Curr Biol *17*, 1871-1878.

Mendes, C. S., Arama, E., Brown, S., Scherr, H., Srivastava, M., Bergmann, A., Steller, H., and Mollereau, B. (2006). Cytochrome c-d regulates developmental apoptosis in the Drosophila retina. EMBO Rep *7*, 933-939.

Mikeladze-Dvali, T., Wernet, M. F., Pistillo, D., Mazzoni, E. O., Teleman, A. A., Chen, Y. W., Cohen, S., and Desplan, C. (2005). The growth regulators warts/lats and melted interact in a bistable loop to specify opposite fates in drosophila R8 photoreceptors. Cell *122*, 775-787.

Mitra, S. K., and Schlaepfer, D. D. (2006). Integrin-regulated FAK-Src signaling in normal and cancer cells. Curr Opin Cell Biol *18*, 516-523.

Moreno, E., Yan, M., and Basler, K. (2002). Evolution of TNF signaling mechanisms: JNK-dependent apoptosis triggered by Eiger, the Drosophila homolog of the TNF superfamily. Curr Biol *12*, 1263-1268.

Morgan, D. O. (1997). Cyclin-dependent kinases: engines, clocks, and microprocessors. Annu Rev Cell Dev Biol *13*, 261-291.

Nagata, S. (2005). DNA degradation in development and programmed cell death. Annu Rev Immunol *23*, 853-875.

Nakagawa, T., Tanaka, S., Suzuki, H., Takayanagi, H., Miyazaki, T., Nakamura, K., and Tsuruo, T. (2000). Overexpression of the csk gene suppresses tumor metastasis in vivo. Int J Cancer *88*, 384-391.

Naumovski, L., and Cleary, M. L. (1996). The p53-binding protein 53BP2 also interacts with Bc12 and impedes cell cycle progression at G2/M. Mol Cell Biol *16*, 3884-3892.

Neufeld, T. P., de la Cruz, A. F., Johnston, L. A., and Edgar, B. A. (1998). Coordination of growth and cell division in the Drosophila wing. Cell *93*, 1183-1193.

Newsome, T. P., Asling, B., and Dickson, B. J. (2000). Analysis of Drosophila photoreceptor axon guidance in eye-specific mosaics. Development *127*, 851-860.

Nolo, R., Morrison, C. M., Tao, C., Zhang, X., and Halder, G. (2006). The bantam microRNA is a target of the hippo tumor-suppressor pathway. Curr Biol *16*, 1895-1904.

O'Hagan, R. C., Ohh, M., David, G., de Alboran, I. M., Alt, F. W., Kaelin, W. G., Jr., and DePinho, R. A. (2000). Myc-enhanced expression of Cul1 promotes ubiquitin-dependent proteolysis and cell cycle progression. Genes Dev *14*, 2185-2191.

O'Kane, C. J., and Gehring, W. J. (1987). Detection in situ of genomic regulatory elements in Drosophila. Proc Natl Acad Sci U S A *84*, 9123-9127.

O'Neill, E. M., Rebay, I., Tjian, R., and Rubin, G. M. (1994). The activities of two Ets-related transcription factors required for Drosophila eye development are modulated by the Ras/MAPK pathway. Cell *78*, 137-147.

O'Reilly, A. M., Ballew, A. C., Miyazawa, B., Stocker, H., Hafen, E., and Simon, M. A. (2006). Csk differentially regulates Src64 during distinct morphological events in Drosophila germ cells. Development *133*, 2627-2638.

Ogawa, A., Takayama, Y., Sakai, H., Chong, K. T., Takeuchi, S., Nakagawa, A., Nada, S., Okada, M., and Tsukihara, T. (2002). Structure of the carboxyl-terminal Src kinase, Csk. J Biol Chem *277*, 14351-14354.

Okada, M., Nada, S., Yamanashi, Y., Yamamoto, T., and Nakagawa, H. (1991). CSK: a protein-tyrosine kinase involved in regulation of src family kinases. J Biol Chem *266*, 24249-24252.

Olivier, J. P., Raabe, T., Henkemeyer, M., Dickson, B., Mbamalu, G., Margolis, B., Schlessinger, J., Hafen, E., and Pawson, T. (1993). A Drosophila SH2-SH3 adaptor protein implicated in coupling the sevenless tyrosine kinase to an activator of Ras guanine nucleotide exchange, Sos. Cell *73*, 179-191.

Ollmann, M., Young, L. M., Di Como, C. J., Karim, F., Belvin, M., Robertson, S., Whittaker, K., Demsky, M., Fisher, W. W., Buchman, A., *et al.* (2000). Drosophila p53 is a structural and functional homolog of the tumor suppressor p53. Cell *101*, 91-101.

Overholtzer, M., Zhang, J., Smolen, G. A., Muir, B., Li, W., Sgroi, D. C., Deng, C. X., Brugge, J. S., and Haber, D. A. (2006). Transforming properties of YAP, a candidate oncogene on the chromosome 11q22 amplicon. Proc Natl Acad Sci U S A *103*, 12405-12410.

Pagliarini, R. A., and Xu, T. (2003). A genetic screen in Drosophila for metastatic behavior. Science *302*, 1227-1231.

Palacios, E. H., and Weiss, A. (2004). Function of the Src-family kinases, Lck and Fyn, in T-cell development and activation. Oncogene *23*, 7990-8000.

Palacios, F., Tushir, J. S., Fujita, Y., and D'Souza-Schorey, C. (2005). Lysosomal targeting of E-cadherin: a unique mechanism for the down-regulation of cell-cell adhesion during epithelial to mesenchymal transitions. Mol Cell Biol *25*, 389-402.

Pantalacci, S., Tapon, N., and Leopold, P. (2003). The Salvador partner Hippo promotes apoptosis and cell-cycle exit in Drosophila. Nat Cell Biol *5*, 921-927.

Pawson, T. (1997). New impressions of Src and Hck. Nature *385*, 582-583, 585.

Pedraza, L. G., Stewart, R. A., Li, D. M., and Xu, T. (2004). Drosophila Src-family kinases function with Csk to regulate cell proliferation and apoptosis. Oncogene *23*, 4754-4762.

Perez-Garijo, A., Martin, F. A., and Morata, G. (2004). Caspase inhibition during apoptosis causes abnormal signalling and developmental aberrations in Drosophila. Development *131*, 5591-5598.

Perrimon, N. (1998). Creating mosaics in Drosophila. Int J Dev Biol *42*, 243-247.

Polesello, C., Huelsmann, S., Brown, N. H., and Tapon, N. (2006). The Drosophila RASSF homolog antagonizes the hippo pathway. Curr Biol *16*, 2459-2465.

Polesello, C., and Tapon, N. (2007). Salvador-warts-hippo signaling promotes Drosophila posterior follicle cell maturation downstream of notch. Curr Biol *17*, 1864-1870.

Prober, D. A., and Edgar, B. A. (2002). Interactions between Ras1, dMyc, and dPI3K signaling in the developing Drosophila wing. Genes Dev *16*, 2286-2299.

Raabe, T. (2000). The sevenless signaling pathway: variations of a common theme. Biochim Biophys Acta *1496*, 151-163.

Read, D., and Manley, J. L. (1992). Alternatively spliced transcripts of the Drosophila tramtrack gene encode zinc finger proteins with distinct DNA binding specificities. Embo J *11*, 1035-1044.

Read, R. D., Bach, E. A., and Cagan, R. L. (2004). Drosophila C-terminal Src kinase negatively regulates organ growth and cell proliferation through inhibition of the Src, Jun N-terminal kinase, and STAT pathways. Mol Cell Biol *24*, 6676-6689.

Rebay, I., and Rubin, G. M. (1995). Yan functions as a general inhibitor of differentiation and is negatively regulated by activation of the Ras1/MAPK pathway. Cell *81*, 857-866.

Reinke, R., and Zipursky, S. L. (1988). Cell-cell interaction in the Drosophila retina: the bride of sevenless gene is required in photoreceptor cell R8 for R7 cell development. Cell *55*, 321-330.

Reiter, C., Schimansky, T., Nie, Z., and Fischbach, K. F. (1996). Reorganization of membrane contacts prior to apoptosis in the Drosophila retina: the role of the IrreC-rst protein. Development *122*, 1931-1940.

Rengifo-Cam, W., Konishi, A., Morishita, N., Matsuoka, H., Yamori, T., Nada, S., and Okada, M. (2004). Csk defines the ability of integrin-mediated cell adhesion and migration in human colon cancer cells: implication for a potential role in cancer metastasis. Oncogene *23*, 289-297.

Robertson, H. M., Preston, C. R., Phillis, R. W., Johnson-Schlitz, D. M., Benz, W. K., and Engels, W. R. (1988). A stable genomic source of P element transposase in Drosophila melanogaster. Genetics *118*, 461-470.

Rorth, P. (1996). A modular misexpression screen in Drosophila detecting tissue-specific phenotypes. Proc Natl Acad Sci U S A *93*, 12418-12422.

Roulier, E. M., Panzer, S., and Beckendorf, S. K. (1998). The Tec29 tyrosine kinase is required during Drosophila embryogenesis and interacts with Src64 in ring canal development. Mol Cell *1*, 819-829.

Rubin, G. M., and Spradling, A. C. (1982). Genetic transformation of Drosophila with transposable element vectors. Science *218*, 348-353.

Rubin, G. M., Yandell, M. D., Wortman, J. R., Gabor Miklos, G. L., Nelson, C. R., Hariharan, I. K., Fortini, M. E., Li, P. W., Apweiler, R., Fleischmann, W., *et al.* (2000). Comparative genomics of the eukaryotes. Science *287*, 2204-2215.

Ryoo, H. D., Gorenc, T., and Steller, H. (2004). Apoptotic cells can induce compensatory proliferation through the JNK and the Wingless signaling pathways. Dev Cell *7*, 491-501.

Sakai, T., Jove, R., Fassler, R., and Mosher, D. F. (2001). Role of the cytoplasmic tyrosines of beta 1A integrins in transformation by v-src. Proc Natl Acad Sci U S A *98*, 3808-3813.

Salz, H. K., Cline, T. W., and Schedl, P. (1987). Functional changes associated with structural alterations induced by mobilization of a P element inserted in the Sex-lethal gene of Drosophila. Genetics *117*, 221-231.

Samuels-Lev, Y., O'Connor, D. J., Bergamaschi, D., Trigiante, G., Hsieh, J. K., Zhong, S., Campargue, I., Naumovski, L., Crook, T., and Lu, X. (2001). ASPP proteins specifically stimulate the apoptotic function of p53. Mol Cell *8*, 781-794.

Saouaf, S. J., Mahajan, S., Rowley, R. B., Kut, S. A., Fargnoli, J., Burkhardt, A. L., Tsukada, S., Witte, O. N., and Bolen, J. B. (1994). Temporal differences in the activation of three classes of non-transmembrane protein tyrosine kinases following B-cell antigen receptor surface engagement. Proc Natl Acad Sci U S A *91*, 9524-9528.

Schaller, M. D., Hildebrand, J. D., Shannon, J. D., Fox, J. W., Vines, R. R., and Parsons, J. T. (1994). Autophosphorylation of the focal adhesion kinase, pp125FAK, directs SH2-dependent binding of pp60src. Mol Cell Biol *14*, 1680-1688.

Scheel, H., and Hofmann, K. (2003). A novel interaction motif, SARAH, connects three classes of tumor suppressor. Curr Biol *13*, R899-900.

Sentry, J. W., and Kaiser, K. (1994). Application of inverse PCR to site-selected mutagenesis of Drosophila. Nucleic Acids Res *22*, 3429-3430.

Sgroi, D. C., Teng, S., Robinson, G., LeVangie, R., Hudson, J. R., Jr., and Elkahloun, A. G. (1999). In vivo gene expression profile analysis of human breast cancer progression. Cancer Res *59*, 5656-5661.

Silva, E., Tsatskis, Y., Gardano, L., Tapon, N., and McNeill, H. (2006). The tumor-suppressor gene fat controls tissue growth upstream of expanded in the hippo signaling pathway. Curr Biol *16*, 2081-2089.

Simon, M. A., Dodson, G. S., and Rubin, G. M. (1993). An SH3-SH2-SH3 protein is required for p21Ras1 activation and binds to sevenless and Sos proteins in vitro. Cell *73*, 169-177.

Slee, E. A., Gillotin, S., Bergamaschi, D., Royer, C., Llanos, S., Ali, S., Jin, B., Trigiante, G., and Lu, X. (2004). The N-terminus of a novel isoform of human iASPP is required for its cytoplasmic localization. Oncogene *23*, 9007-9016.

Sondhi, D., and Cole, P. A. (1999). Domain interactions in protein tyrosine kinase Csk. Biochemistry *38*, 11147-11155.

Soriano, P., Montgomery, C., Geske, R., and Bradley, A. (1991). Targeted disruption of the c-src proto-oncogene leads to osteopetrosis in mice. Cell *64*, 693-702.

Spradling, A. C., and Rubin, G. M. (1982). Transposition of cloned P elements into Drosophila germ line chromosomes. Science *218*, 341-347.

St John, M. A., Tao, W., Fei, X., Fukumoto, R., Carcangiu, M. L., Brownstein, D. G., Parlow, A. F., McGrath, J., and Xu, T. (1999). Mice deficient of Lats1 develop soft-tissue sarcomas, ovarian tumours and pituitary dysfunction. Nat Genet *21*, 182-186.

Stein, P. L., Vogel, H., and Soriano, P. (1994). Combined deficiencies of Src, Fyn, and Yes tyrosine kinases in mutant mice. Genes Dev *8*, 1999-2007.

Stewart, R. A., Li, D. M., Huang, H., and Xu, T. (2003). A genetic screen for modifiers of the lats tumor suppressor gene identifies C-terminal Src kinase as a regulator of cell proliferation in Drosophila. Oncogene *22*, 6436-6444.

Stowers, R. S., and Schwarz, T. L. (1999). A genetic method for generating Drosophila eyes composed exclusively of mitotic clones of a single genotype. Genetics *152*, 1631-1639.

Sun, G., Sharma, A. K., and Budde, R. J. (1998). Autophosphorylation of Src and Yes blocks their inactivation by Csk phosphorylation. Oncogene *17*, 1587-1595.

Takahashi, M., Takahashi, F., Ui-Tei, K., Kojima, T., and Saigo, K. (2005). Requirements of genetic interactions between Src42A, armadillo and shotgun, a gene encoding E-cadherin, for normal development in Drosophila. Development *132*, 2547-2559.

Takeda, H., Nagafuchi, A., Yonemura, S., Tsukita, S., Behrens, J., Birchmeier, W., and Tsukita, S. (1995). V-src kinase shifts the cadherin-based cell adhesion from the strong to the weak state and beta catenin is not required for the shift. J Cell Biol *131*, 1839-1847.

Takeuchi, S., Takayama, Y., Ogawa, A., Tamura, K., and Okada, M. (2000). Transmembrane phosphoprotein Cbp positively regulates the activity of the carboxyl-terminal Src kinase, Csk. J Biol Chem *275*, 29183-29186.

Talamonti, M. S., Roh, M. S., Curley, S. A., and Gallick, G. E. (1993). Increase in activity and level of pp60c-src in progressive stages of human colorectal cancer. J Clin Invest *91*, 53-60.

Tang, A. H., Neufeld, T. P., Kwan, E., and Rubin, G. M. (1997). PHYL acts to down-regulate TTK88, a transcriptional repressor of neuronal cell fates, by a SINA-dependent mechanism. Cell *90*, 459-467.

Tapon, N., Harvey, K. F., Bell, D. W., Wahrer, D. C., Schiripo, T. A., Haber, D. A., and Hariharan, I. K. (2002). salvador Promotes both cell cycle exit and apoptosis in Drosophila and is mutated in human cancer cell lines. Cell *110*, 467-478.

Tateno, M., Nishida, Y., and Adachi-Yamada, T. (2000). Regulation of JNK by Src during Drosophila development. Science *287*, 324-327.

Thomas, J. W., Ellis, B., Boerner, R. J., Knight, W. B., White, G. C., 2nd, and Schaller, M. D. (1998). SH2- and SH3-mediated interactions between focal adhesion kinase and Src. J Biol Chem *273*, 577-583.

Thomas, S. M., and Brugge, J. S. (1997). Cellular functions regulated by Src family kinases. Annu Rev Cell Dev Biol *13*, 513-609.

Thomas, S. M., Soriano, P., and Imamoto, A. (1995). Specific and redundant roles of Src and Fyn in organizing the cytoskeleton. Nature *376*, 267-271.

Thompson, B. J., and Cohen, S. M. (2006). The Hippo pathway regulates the bantam microRNA to control cell proliferation and apoptosis in Drosophila. Cell *126*, 767-774.

Tice, D. A., Biscardi, J. S., Nickles, A. L., and Parsons, S. J. (1999). Mechanism of biological synergy between cellular Src and epidermal growth factor receptor. Proc Natl Acad Sci U S A *96*, 1415-1420.

Trigiante, G., and Lu, X. (2006). ASPP [corrected] and cancer. Nat Rev Cancer *6*, 217-226.

Tsubota, S., and Schedl, P. (1986). Hybrid dysgenesis-induced revertants of insertions at the 5' end of the rudimentary gene in Drosophila melanogaster: transposon-induced control mutations. Genetics *114*, 165-182.

Udan, R. S., Kango-Singh, M., Nolo, R., Tao, C., and Halder, G. (2003). Hippo promotes proliferation arrest and apoptosis in the Salvador/Warts pathway. Nat Cell Biol *5*, 914-920.

Van de Craen, M., Berx, G., Van den Brande, I., Fiers, W., Declercq, W., and Vandenabeele, P. (1999). Proteolytic cleavage of beta-catenin by caspases: an in vitro analysis. FEBS Lett *458*, 167-170.

van der Weyden, L., and Adams, D. J. (2007). The Ras-association domain family (RASSF) members and their role in human tumourigenesis. Biochim Biophys Acta *1776*, 58-85.

Vidal, M., Larson, D. E., and Cagan, R. L. (2006). Csk-deficient boundary cells are eliminated from normal Drosophila epithelia by exclusion, migration, and apoptosis. Dev Cell *10*, 33-44.

Vidal, M., Warner, S., Read, R., and Cagan, R. L. (2007). Differing Src signaling levels have distinct outcomes in Drosophila. Cancer Res *67*, 10278-10285.

Vives, V., Su, J., Zhong, S., Ratnayaka, I., Slee, E., Goldin, R., and Lu, X. (2006). ASPP2 is a haploinsufficient tumor suppressor that cooperates with p53 to suppress tumor growth. Genes Dev *20*, 1262-1267.

Vogelstein, B., Lane, D., and Levine, A. J. (2000). Surfing the p53 network. Nature *408*, 307-310.

Wei, X., Shimizu, T., and Lai, Z. C. (2007). Mob as tumor suppressor is activated by Hippo kinase for growth inhibition in Drosophila. Embo J *26*, 1772-1781.

Wen, Y., Nguyen, D., Li, Y., and Lai, Z. C. (2000). The N-terminal BTB/POZ domain and C-terminal sequences are essential for Tramtrack69 to specify cell fate in the developing Drosophila eye. Genetics *156*, 195-203.

White, K., Grether, M. E., Abrams, J. M., Young, L., Farrell, K., and Steller, H. (1994). Genetic control of programmed cell death in Drosophila. Science *264*, 677-683.

Willecke, M., Hamaratoglu, F., Kango-Singh, M., Udan, R., Chen, C. L., Tao, C., Zhang, X., and Halder, G. (2006). The fat cadherin acts through the hippo tumor-suppressor pathway to regulate tissue size. Curr Biol *16*, 2090-2100.

Wilson, R., Goyal, L., Ditzel, M., Zachariou, A., Baker, D. A., Agapite, J., Steller, H., and Meier, P. (2002). The DIAP1 RING finger mediates ubiquitination of Dronc and is indispensable for regulating apoptosis. Nat Cell Biol *4*, 445-450.

Wu, S., Huang, J., Dong, J., and Pan, D. (2003). hippo encodes a Ste-20 family protein kinase that restricts cell proliferation and promotes apoptosis in conjunction with salvador and warts. Cell *114*, 445-456.

Xiong, W. C., and Montell, C. (1993). tramtrack is a transcriptional repressor required for cell fate determination in the Drosophila eye. Genes Dev *7*, 1085-1096.

Xu, T., and Rubin, G. M. (1993). Analysis of genetic mosaics in developing and adult Drosophila tissues. Development *117*, 1223-1237.

Xu, T., Wang, W., Zhang, S., Stewart, R. A., and Yu, W. (1995). Identifying tumor suppressors in genetic mosaics: the Drosophila lats gene encodes a putative protein kinase. Development *121*, 1053-1063.

Yagi, R., Waguri, S., Sumikawa, Y., Nada, S., Oneyama, C., Itami, S., Schmedt, C., Uchiyama, Y., and Okada, M. (2007). C-terminal Src kinase controls development and maintenance of mouse squamous epithelia. Embo J *26*, 1234-1244.

Yang, J. P., Hori, M., Sanda, T., and Okamoto, T. (1999). Identification of a novel inhibitor of nuclear factor-kappaB, RelA-associated inhibitor. J Biol Chem *274*, 15662-15670.

Yeatman, T. J. (2004). A renaissance for SRC. Nat Rev Cancer *4*, 470-480.

Yoo, S. J., Huh, J. R., Muro, I., Yu, H., Wang, L., Wang, S. L., Feldman, R. M., Clem, R. J., Muller, H. A., and Hay, B. A. (2002). Hid, Rpr and Grim negatively regulate DIAP1 levels through distinct mechanisms. Nat Cell Biol *4*, 416-424.

Yu, Y., Yussa, M., Song, J., Hirsch, J., and Pick, L. (1999). A double interaction screen identifies positive and negative ftz gene regulators and ftz-interacting proteins. Mech Dev *83*, 95-105.

Zender, L., Spector, M. S., Xue, W., Flemming, P., Cordon-Cardo, C., Silke, J., Fan, S. T., Luk, J. M., Wigler, M., Hannon, G. J., *et al.* (2006). Identification and validation of

oncogenes in liver cancer using an integrative oncogenomic approach. Cell *125*, 1253-1267.

Zhang, S. Q., Yang, W., Kontaridis, M. I., Bivona, T. G., Wen, G., Araki, T., Luo, J., Thompson, J. A., Schraven, B. L., Philips, M. R., and Neel, B. G. (2004). Shp2 regulates SRC family kinase activity and Ras/Erk activation by controlling Csk recruitment. Mol Cell *13*, 341-355.

Zhao, B., Wei, X., Li, W., Udan, R. S., Yang, Q., Kim, J., Xie, J., Ikenoue, T., Yu, J., Li, L., *et al.* (2007). Inactivation of YAP oncoprotein by the Hippo pathway is involved in cell contact inhibition and tissue growth control. Genes Dev *21*, 2747-2761.

Zheng, X. M., Wang, Y., and Pallen, C. J. (1992). Cell transformation and activation of pp60c-src by overexpression of a protein tyrosine phosphatase. Nature *359*, 336-339.

Zornig, M., and Evan, G. I. (1996). Cell cycle: on target with Myc. Curr Biol *6*, 1553-1556.

Zou, J. X., Liu, Y., Pasquale, E. B., and Ruoslahti, E. (2002). Activated SRC oncogene phosphorylates R-ras and suppresses integrin activity. J Biol Chem *277*, 1824-1827.

Zuzarte-Luis, V., and Hurle, J. M. (2002). Programmed cell death in the developing limb. Int J Dev Biol *46*, 871-876.